UNIVERSITY OF ADELAIDE LIBRARY 16/6/87

Diffusion, Boundary Layers and the Uptake of Nutrients by Aquatic Macrophytes

Jeffrey Julius MacFarlane B.Sc.(Hons.)

Botany Department

The University of Adelaide.

Submitted for the Degree of

Doctor of Philosophy, June, 1985.

Awarded 7/3/86

To my Father : Friend

and Master Teacher

CONTENTS

SUMMARY

Diffusion limitations on the influxes of [^{14}C] methylamine and [^{32}P] phosphate, and on the respiratory uptake of O_2, have been examined in the marine macroalga Ulva rigida and the freshwater angiosperm Vallisneria spiralis; photosynthetic O_2 evolution (and fixation of ^{14}C-labelled inorganic carbon) has also been studied in these two plants and in the marine angiosperm Amphibolis antarctica. In Ulva, the influx of methylamine and the apparent "K_M" of the process are greatly affected by the rate of stirring of the bulk medium. The kinetics of the influx are directly predicted by an equation of the Michaelis-Menten form which includes a term for the rate of transport of methylamine through the boundary layer (the Briggs-Maskell equation). Transport coefficients range from 3.6 μm s^{-1} in a barely-moving solution to nearly 40 μm s^{-1} in a well stirred one, with a corresponding change in K_M from 20 to 80 μM. The equation is also directly applicable to the photosynthesis of the alga at low pH provided that O_2 inhibition can be neglected. The equation is not directly applicable to $H_2PO_4^-$ influx, respiratory O_2 uptake or photosynthetic CO_2 fixation at high pH. $H_2PO_4^-$ influx is complicated by the concomitant flux of HPO_4^{2-} which effectively increases the concentration of $H_2PO_4^-$ at the plasmalemma. O_2 uptake in dark respiration has a complex relationship with the bulk concentration of O_2,

and the kinetics are not necessarily first-order Michaelis-Menten; consequently the Briggs-Maskell equation is invalid. Rates of photosynthesis that are observed at high pH could not be attained if CO_2 was the only inorganic carbon species transporting carbon through the unstirred layer. The alga probably uses HCO_3^- ions directly from the bulk solution as a carbon source and so again the Briggs-Maskell equation, in terms of CO_2 fixation, does not hold. The photosynthesis of Amphibolis has a similar response to CO_2 and pH as that of Ulva - again the Briggs-Maskell equation is not directly applicable. Vallisneria leaves have a cuticle which has such a high resistance to the movement of solutes that boundary layer limitations are negligible. The leaves also have a substantial supply of endogenous CO_2. Here the cuticle is a distinct advantage because it increases the probability of a CO_2 molecule being assimilated rather than escaping into the bulk medium; this source of CO_2 (originally derived from the sediment?) is probably much more important than the CO_2 in the surrounding water.

DECLARATION

This thesis contains no material which has been accepted for the award of any other degree or diploma in any University. To the best of my knowledge and belief this thesis contains no material previously published or written by any other person except where due reference is made in the text.

Jeffrey J. MacFarlane.

ACKNOWLEDGEMENTS

This work was carried out under the supervision of Dr. F.A. Smith, who was the ever-encouraging driving force for this rather unsteady flux. I should also like to thank others in the Botany Department - Drs. J.T. Wiskich and G.G. Ganf for many varied and stimulating discussions, Prof. H.B.S. Womersley, Dr R. Sinclair and B.C. Rowland for advice, Dr. E. Robertson for culture room space, Ian Dry and Patrick Hone for some good talks, and Jane Gibson and Anthony Fox for company. Outwith the Botany Department, I acknowledge the help given by B.C. van Wageningen in translating some German scientific papers, the computer time allowed by Prof. N.A. Walker and the patience of Prof. J.A. Raven. Finally, to my wife, Carol, for typing the manuscript, for numerous calculations, for support and for a small portion of her indomitable spirit.

UNIVERSITY OF ADELAIDE LIBRARY

INTRODUCTION

The growth of a plant involves a host of chemical reactions, the reactants which sustain them being substances that occur in the plant's environment; I shall refer to these as nutrients. This thesis has to do with the transport of these nutrients up to and into the cells of aquatic plants. (The word transport is used merely in the sense of movement from A to B, regardless of the energetics of the movement.) Transport is intimately linked with chemical reaction (and vice versa), simply because reactants must first meet before they can hope to become a product, or products. This applies at the microscopic level (for reactions between individual atoms or molecules) but is much more obvious at the macroscopic level, i.e. when reactants are in distinct phases. A living plant in its environment constitutes such a heterogeneous system - as does, at a much lower level of complexity, a lead plate in a car battery.

For these sorts of reactions, transport by diffusion may play a crucial, rate-limiting role. Although a number of reports imply that this is the case for plants (e.g. instances of increased growth or nutrient uptake accompanying the stirring of the medium around the plant) there have been few quantitative studies. Such studies are important, however, as there are several

instances in plant physiology where major conclusions have been called into question because of "unstirred layer" effects. Examples are the presence of pores in the plasmalemma for water transport (see Dainty, 1963) and the presence of C_4 photosynthesis in aquatic macrophytes (see Smith and Walker, 1980).

In this thesis, the aim is to quantify the diffusional limitations to reactions involving a variety of nutrients in a variety of aquatic macrophytes. However, before considering the relationship between transport and reaction kinetics in plants, it is useful to start on a simpler level with heterogeneous reactions of the car battery type.

I. The Kinetics of Heterogeneous Reactions

(i) Nernst's theory

In 1900 Walther Nernst, in the third edition of his text book on theoretical chemistry (see Nernst, 1916), suggested that in certain circumstances the rates of heterogeneous chemical reactions were entirely due to the rates at which reactants could diffuse to the interface and the products diffuse away. To a certain extent, the idea was based on some earlier work by Schükarev (1891), Noyes and Whitney (1897) and Bruner and St. Tolloczko (1900) on the dissolution of various solid bodies in water. Noyes and Whitney (1897) suggested that a layer of saturated solution rapidly

formed around the surface of the solid, from which the solute particles diffused into the bulk solution. The rate of this diffusion at any one time (t) would be proportional to the difference between the concentration of the solute in the saturated layer (c_s) and that in the bulk solution (c_b). (This follows from Fick's first law which is discussed in Appendix I). Hence, the rate equation could be written

$$\frac{dc}{dt} = k(c_s - c_b) \qquad (1)$$

which was verified experimentally. Bruner and St.Tolloczko (1900) showed that the velocity constant, k, was dependent upon the surface area of the solid, as would be expected.

Nernst (1904) extended these ideas to heterogeneous chemical reactions. He assumed that at every boundary between two phases, equilibrium is established with a practically infinite velocity.* For example, in the case of magnesia (MgO) in acid, the solution adjacent to the magnesia would be saturated by Mg^{2+} and therefore weakly alkaline and the acid at the interface would be completely neutralized. Granted this assumption, the rate of dissolution of the magnesia will simply depend on the rate at which the acid reaches the interface by diffusion. For well-stirred systems, the bulk of the

* Incorrectly based on the fact that the difference in chemical potential at the interface is extremely large.

solution may be considered as practically homogeneous and the diffusion zone will be confined to a thin layer (thickness δ) adhering to the surface of the solid.

Nernst assumed that the concentration of the acid varied linearly across the thin layer, i.e. the concentration gradient was given by $(c_b - c_s)/\delta$ where c_b is the concentration of the acid in the bulk solution and c_s that at the surface of the magnesia (Nernst assumed c_s was zero in this particular case). From Fick's first law (Appendix I) the equation for the flux, J, of acid across the thin layer could be written

$$J = - D \frac{c_b - c_s}{\delta} \qquad (2)$$

where D is the diffusion coefficient of the acid. In terms of the rate of change of the concentration of acid in the bulk solution, equation (2) becomes

$$- \frac{dc}{dt} = \frac{D\ A}{vol} \frac{c_b - c_s}{\delta} \qquad (3)$$

where A is the surface area of the magnesia and "vol" is the volume of the solution. This is of the same form as equation (1), with

$$k = \frac{D\ A}{vol} \quad . \qquad (4)$$

If k is measured per unit area at unit volume, then we may write

$$k_T = \frac{k \text{ vol}}{A} = \frac{D}{\delta} \qquad (5)$$

which has the dimensions of a velocity.

Bircumshaw and Riddiford (1952), in their review, show that Nernst's theory has been confirmed for many heterogeneous reactions. Thus, many different reactions carried out under the same stirring conditions yield the same values for k_T and δ. Reaction rates have also been shown to increase with increasing D, although it would appear the relationship is <u>not</u> a direct one - Eucken (1932) found $k_T \propto D^{0.66}$ and King and Cathcart (1937) found $k_T \propto D^{0.7}$, while under turbulent flow conditions the suggested power on the diffusion coefficient is 0.75 (King, 1948). k_T frequently, but by no means always, has a similar temperature coefficient to D. Increased stirring, which would decrease the thickness, δ, of the Nernst layer, has also been shown to increase reaction rates. Most workers find δ proportional to $1/U^q$ where U is the velocity of the moving liquid. Values for the exponent q usually range from 0.5 to 1.

Nevertheless, it is now well known that there are heterogeneous reactions which are chemically controlled,

i.e. the rate of the reaction does not depend on diffusion rates but on the physico-chemical properties of the reactants. Nernst's basic assumption that equilibrium is always attained virtually instantaneously at the interface of two phases is, then, not valid for all heterogeneous systems; for the particular cases where the assumption holds, the reaction rate will almost certainly be transport limited by diffusion.

The in-between case is where the concentration of reactant at the interface is neither the equilibrium concentration (pure transport control) nor that of the bulk solution (pure chemical control). Nernst's theory must be modified to take into account such cases.

(ii) Modifications of Nernst's theory

The rate equation for the chemical process may be written

$$-\frac{dc}{dt} = k_C \frac{A_C}{vol}(c_s)^n \qquad (6)$$

where k_C is the velocity constant for the chemical process and A_C the true surface area of the solid available for chemical reaction. The rate equation for the transport process, from equations (3) and (5), can be written

$$-\frac{dc}{dt} = k_T \frac{A}{vol}(c_b - c_s) \qquad (7)$$

where A is the apparent surface area. In the steady state, equations (6) and (7) are equal, i.e. $k_T A (c_b - c_s) = k_C A_C (c_s)^n$ and for first order reactions (n = 1), $c_s = k_T A c_b/(k_T A + k_C A_C) = k_T c_b/(k_T + k_C (A_C/A))$. Substituting in equation (7) we obtain

$$-\frac{dc}{dt} = \frac{k_C k_T}{k_C + k_T (A/A_C)} \frac{A}{vol} c_b \qquad (8)$$

and

$$k_{app} = \frac{k_C k_T}{k_C + k_T (A/A_C)} \qquad (9)$$

where k_{app} is the apparent velocity constant for the reaction per unit (apparent) area at unit volume. When $k_C >> k_T (A/A_C)$ the system is transport controlled; with $k_C << k_T (A/A_C)$, chemically controlled. For any given reaction, there may be a change in control if the experimental conditions change such that k_C, k_T or the ratio A/A_C are affected.

For many enzyme-catalysed reactions, the rate equation for the chemical process can be written

$$v_C = V \frac{c_s}{K_M + c_s} \qquad (10)^*$$

where v_C is the overall velocity of the chemical reaction, V the maximum possible velocity and K_M the Michaelis constant. If v has the units of a flux

(e.g. mol m^{-2} s^{-1}) then the rate of the transport process, v_T, will be $v_T = k_T (c_b - c_s)$, i.e.

$$c_s = c_b \frac{v_T}{k_T} . \qquad (11)$$

In the steady state, $v_T = v_C = v$ and substituting equation (11) into equation (10) leads to a quadratic equation in v for which the solution is

$$v = \tfrac{1}{2}\{ K_M k_T + c_b k_T + V - \sqrt{(K_M k_T + c_b k_T + V)^2 - 4 c_b k_T V} \} . \qquad (12)$$

This equation was first derived by G. E. Briggs (pers. comm. to F. A. Smith and N. A. Walker; see Appendix II)

---

* Strictly, this equation should be written in terms of the activity, rather than the concentration, at the surface of the enzyme, i.e.

$$v_C = V \frac{y c_s}{K_M + y c_s}$$

where y is the molar activity coefficient of the substrate. For a number of substances (ions in particular) y is often significantly different from unity, even in quite dilute solutions. In sea water, the term may be very important. The effect on the Michaelis-Menten equation is to change the meaning of K_M since

$$v_C = V \frac{y c_s}{K_M + y c_s} = V \frac{c_s}{(K_M/y) + c_s} .$$

I shall simply refer to K_M, which can be regarded as the true K_M expressed in terms of activity; this quantity may be significantly different from the K_M measured in a solution of different ionic strength.

and E. J. Maskell (1928). It has been rederived many times (e.g. Lommen, Schwintzer, Yocum and Gates, 1971; Winne, 1973; Wilson and Dietschy, 1974; Märkl, 1977; Dromgoole, 1978; Wheeler, 1980; Lívanský, 1982). It can be shown that when $k_T >> V/2K_M$, the kinetics are enzymically controlled and $v = V\, c_b/(K_M + c_b)$. When $k_T << V/2K_M$, the kinetics are transport controlled up to saturation and either $v = k_T c_b$ or $v = V$ (Appendices II and III, Hill and Whittingham, 1955). Figure 1 shows some kinetic curves for various values of k_T.

The modified model for heterogeneous reaction kinetics includes both the chemically and transport controlled cases; although Nernst's predictions with regard to the latter have been verified on the whole, there are deficiencies. The relationship between k_T and D (page 5) is not predicted by Nernst's theory and the relationship between k_T and the fluid velocity is not well defined. The next two sections are an outline of a more quantitative definition of k_T.

(iii) Physical basis for k_T

Nernst assumed that the diffusion of solute from the bulk phase to the interface (and back) was via a thin, stationary layer (thickness 30 μm or more) adhering to the surface of the solid. Does this hypothetical "unstirred layer" have any physical basis?

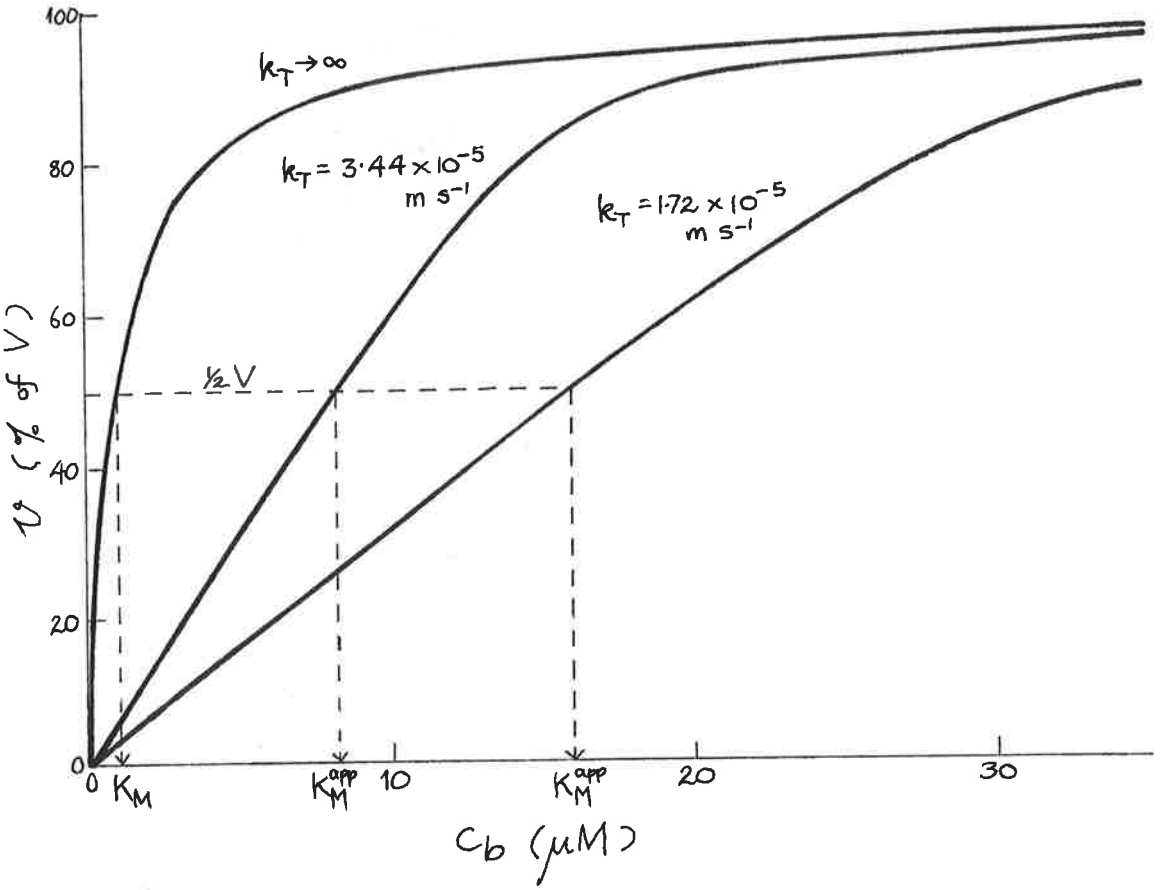

FIGURE 1. Velocity versus concentration curves for the Briggs-Maskell equation (equation 12), with various values of k_T, $K_M = 1\,\mu M$ and $V = 517$ nmol m^{-2} s^{-1}; for small k_T, the initial slope is approximately k_T. $K_M^{app} = K_M + \frac{1}{2}V/k_T$ (see Appendix III).

By studying the dynamics of fluid flow through pipes and around solid objects it has been found that fluid motion persists down to at least 0.6 μm from the surface (Fage and Townend, 1932) if not closer (Roller, 1935). Nernst´s stationary layer is, therefore, a fiction. However, another fact which emerges from the study of fluid flow around solid bodies is that, even in very turbulent systems, there is a region adjacent to the solid surface where the flow is laminar (Schlichting, 1968). In laminar flow, the viscous forces of the fluid are important, so that slower moving layers of the fluid can be thought of as retarding the flow of faster moving layers. When the fluid is flowing over a surface, the fluid in contact with the surface is stationary which retards the fluid in contact with it, which in turn retards the next layer and so on. The essential feature of laminar flow is that the component of the fluid velocity normal to the surface (i.e. between the laminae) is very small. The tangential component of the fluid velocity, as we have seen, depends on the distance from the surface. Figure 2a shows the velocity profile of pure laminar flow over a flat plate.

When the flow in the bulk medium is turbulent (Fig. 2b) the fluid motion is irregular; the arrows therefore represent the <u>average</u> fluid velocity. Compared with Fig. 2a, this velocity remains quite large as the surface of the plate is approached and the region of

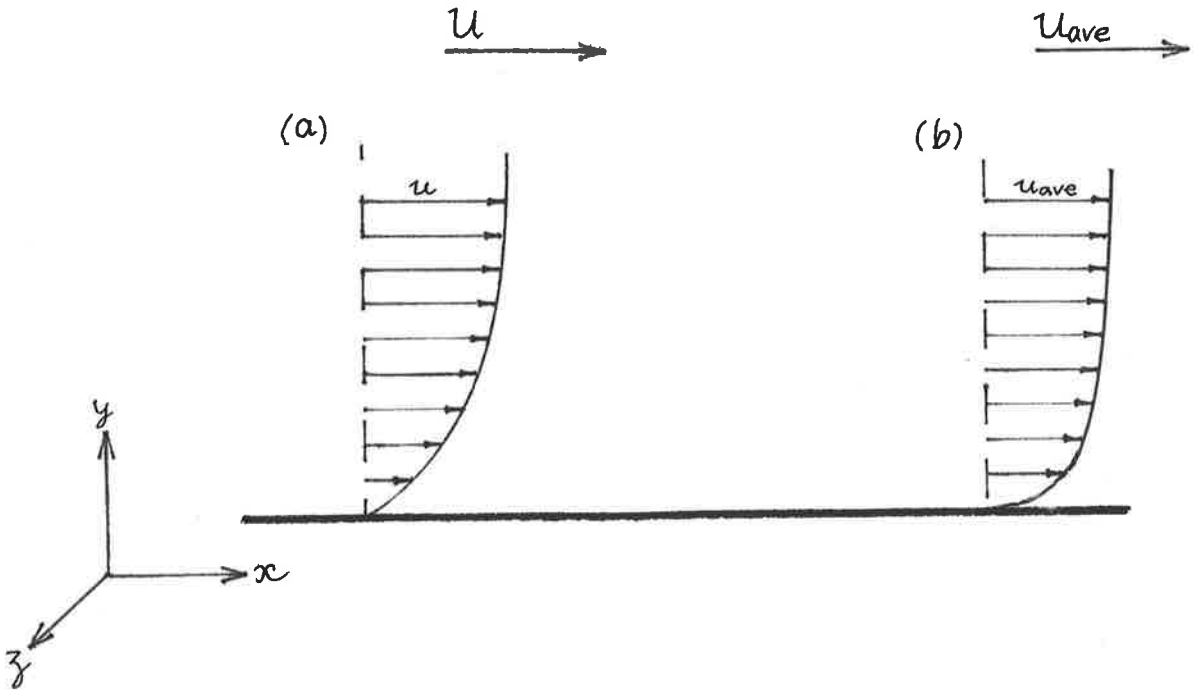

FIGURE 2. Velocity (u) profiles for (a) laminar and (b) turbulent flow along a flat plate. U is the fluid velocity in the bulk medium.

laminar flow is much thinner.

Where the surface is reacting with substances dissolved in the fluid, the fluid dynamics have important implications. For a solution flowing over a flat plate, at the leading edge the concentration of solute will be the same as that in the bulk solution. As the solution flows over the plate, however, solute will be used up from the layers immediately adjacent to the surface. Since convection between these layers is extremely small (laminar flow), diffusion is virtually the only means by which fresh solute can be supplied to the surface. It is clear, then, that there is a region (the extent of which depends on the flow conditions) where diffusive transport is important. This is the essential part of Nernst's theory, and in this respect his ideas are supported.

Before going on to discuss the hydrodynamic/mass-transport relationships more fully, I will briefly mention relaxation of the diffusion process. This phenomenon illustrates the chief difference between the hydrodynamic description of the diffusion region and that of Nernst; namely that the fluid in the diffusion region is not an "unstirred layer", but is in fact continually mixing with the bulk solution.

Again using the reacting flat plate as an example, suppose the average flux of reactant to the surface is

$\bar{J}_1$. Now part of the leading section is coated so that it can no longer react, and the average flux of the substance (per unit area of the uncoated surface) is again measured. It is found that the new average flux, $\bar{J}_2$, is significantly larger than the original. It can be shown (Appendix IV) that the ratio of $\bar{J}_2$ to $\bar{J}_1$ is given by

$$\frac{\bar{J}_2}{\bar{J}_1} = \frac{1}{(1 - X_o/X)} \left[1 - (X_o/X)^{3/4} \right]^{2/3} \qquad (13)$$

where X_o/X is the ratio of the length of the coated section (X_o) to the length of the whole plate (X). $\bar{J}_2$ is nearly twice $\bar{J}_1$ when 90% of the plate is coated. If 99% of the plate is coated, $\bar{J}_2$ is nearly four times $\bar{J}_1$.

The enhancement occurs because the solution streaming over the coated plate is not depleted of reactant; hence for a considerable distance downstream of this section the flux is greater than it would have been were the plate not coated. At large distances from the coated region, the two fluxes are similar. The extent of the relaxation region (i.e. where the new flux is significantly larger than the original) is of the order of X_o (Levich, 1962, p 106). By comparison, the Nernst picture of the diffusion zone would predict a relaxation area (due to diffusion from points tangential, as well as normal, to the surface) of much smaller dimensions,

and the area would not be affected by changes in X_o. The hydrodynamic picture shows that the tangential velocity component of the liquid is very important for mass transport.

(iv) Fluid mechanical description of k_T

The quantitative interaction between the momentum transfer occuring in fluid flow and transfer of matter due to chemical reaction involves solving the diffusion-convection equation

$$\frac{\partial c}{\partial t} = D\left(\frac{\partial^2 c}{\partial x^2} + \frac{\partial^2 c}{\partial y^2} + \frac{\partial^2 c}{\partial z^2}\right) - \left(u_x \frac{\partial c}{\partial x} + u_y \frac{\partial c}{\partial y} + u_z \frac{\partial c}{\partial z}\right) \tag{14}$$

where u_x, u_y and u_z are the velocity components parallel to the x, y, and z axes at a particular point in the fluid. The first part of equation (14) is the rate of change of concentration ($\frac{\partial c}{\partial t}$) due to diffusion (Fick's second law for the three-dimensional case) while the second part deals with changes in concentration due to convection. Equation (14) can only be solved exactly where the equations for the fluid motion have been worked out, which is usually in systems of fairly simple geometry. However, a number of initial approximations can be made.

The thickness of the hydrodynamic boundary layer, δ_o, can be defined as the distance from the surface of the

solid to the point where the tangential velocity component is 99% of the velocity of the main stream (Schlichting, 1968). For liquids, δ_o is <u>not</u> equivalent to the thickness of the <u>diffusion</u> boundary layer. This is because diffusion is so slow in liquids that even relatively slow rates of convection are able to transport mass faster than diffusion. For gases, in which diffusion is comparatively fast, δ_o and δ are similar. In non-turbulent systems, Levich (1962) has shown that $\delta \sim \frac{\delta o}{Pr^{1/3}}$ where Pr (the Prandtl number) is equal to $\frac{\nu}{D}$, ν being the kinematic viscosity of the solvent. (For gases, Pr $\sim$ 1. For water, $\nu \sim 10^{-6}$ m^2 s^{-1} and D for small molecules in water is about 10^{-9} m^2 s^{-1}; Pr is therefore about 10^3, i.e. $\delta \sim 0.1\ \delta_o$). In the case of laminar flow over a semi-infinite plate, $\delta_o \sim 5\sqrt{\frac{x\nu}{U}}$ (Blasius, 1908; Schlichting, 1968) where x is the distance along the plate from the leading edge; we can therefore write

$$\delta \sim 5\ D^{1/3}\ \nu^{1/6}\ \sqrt{\frac{x}{U}}\ . \qquad (15)$$

Levich (1942) has solved equation (14) exactly for the case of a rotating disk electrode, based on Cochran's (1934) solution of the hydrodynamic equations. In this instance the flux of mass, J, to the surface of the disk rotating with an angular velocity of ω (radians per unit time) is given by

$$J = (0.62\ D^{2/3} \nu^{-1/6} \omega^{1/2}) c_b . \qquad (16)$$

(The concentration gradient is simply given by c_b, as c_s is assumed to be zero. J is therefore the limiting flux.) Comparing equation (16) with equation (2), it is readily seen that the thickness of the Nernst diffusion layer must be

$$\delta = 1.62\ D^{1/3} \nu^{1/6} \omega^{-1/2} \qquad (17)$$

which is comparable with equation (15). The term "x" does not appear because in this particular case the diffusion boundary layer is the same thickness over the surface of the disk. Levich's equation has been tested (Hogge and Kraichman, 1954; Kraichman and Hogge, 1955; Gregory and Riddiford, 1956) with very good agreement between theory and experiment.

For flat plates, where the length and width are large compared with δ_o, Levich found that the flux is given by

$$J \sim 0.34\ D^{2/3} \nu^{-1/6} \sqrt{\frac{U}{x}}\ c_b \qquad (18)$$

again with $c_s = 0$. Hence

$$\delta = \frac{D\ c_b}{J} \sim 3\ D^{1/3} \nu^{1/6} \sqrt{\frac{x}{U}} \quad . \qquad (19)$$

In this case δ, and the flux J, are a function of the distance from the leading edge of the plate. δ increases and the flux, therefore, decreases, proportionally with $\sqrt{x}$. It can be easily shown that the average unstirred layer thickness over a plate of length X is simply one half of δ_X , where δ_X is the value of equation (19) at x = X.

The preceding expressions for δ apply where the flow of fluid throughout is laminar. Where flow is turbulent, the diffusion-convection equation usually cannot be solved; in this case, dimensional analysis is useful (Bircumshaw and Riddiford, 1952). For the rotating disk and for laminar flow over a flat plate, the flux of reactant, J, depends on the diffusion coefficient, D, the relative fluid velocity, U, the kinematic viscosity, ν ,the concentration difference, $(c_b - c_s) = \Delta c$ and, where applicable, the distance from the leading edge of the plate, x. It is reasonable, therefore, to write for the flux in turbulent flow $J = f(D,U,x,\nu,\Delta c)$; we could further assume that f is a power function of the form

$$J = B\ D^p\ U^q\ x^r\ \nu^s\ \Delta c^t \qquad (20)$$

where B is a number. Because the dimensions of J ($M\ L^{-2}\ T^{-1}$) must equal the overall dimensions of the right hand side of equation (20), the powers p, q, r, s and t can be

expressed in terms of any two of them, e.g.

$$J = B\, D^{p}\, U^{q}\, x^{(q-1)}\, \nu^{(1-p-q)}\, \Delta c \quad . \qquad (21)$$

By comparison of this equation with that of Nernst ($J = (D/\delta)\Delta c$) it can be shown that

$$\delta = \frac{1}{B}\, D^{1-p}\, U^{-q}\, x^{1-q}\, \nu^{q-(1-p)} \quad . \qquad (22)$$

The power on U may be evaluated by the variation of J with the fluid velocity. As was mentioned on page 5, q usually varies between 0.5 and 1; for the rotating disk and laminar flow over a plate, q = 0.5. As a rule, q increases with increasing turbulence. The other power, p, can be determined by the variation of J with ν or D, assuming the interdependence of D and ν is known. The theoretical value of 1 - p is $\frac{1}{4}$ to $\frac{1}{3}$, probably dependent on the degree of turbulence (Levich, 1962), and this is generally found to be the case experimentally (cf. p 5). From the empirical relationship between J, D, U, x and ν, the value of B can be found. Using this sort of analysis, many workers have derived an expression of the form

$$\delta = 1/B\, x^{0.2}\, U^{-0.8}\, \nu^{0.5}\, D^{0.3} \qquad (23)$$

for turbulent flow over a flat plate, with B about 0.03

(Rohsenow and Choi, 1961). The thickness of the Nernst layer depends on x to only the 0.2th power, i.e. it is similar over most of the length of the plate. The average effective Nernst layer thickness ($\bar{\delta}$) for the whole plate is given by

$$\bar{\delta} = 0.8\ \delta_X \qquad (24)$$

where δ_X is the layer thickness at the trailing edge of the plate. In fact the power on U (and hence on x) may be even smaller. Vielstich (1953) suggested δ proportional to $x^{0.1}\ U^{-0.9}$, in which case $\bar{\delta}$ would be $0.9\delta_X$ (Vetter, 1967, p 193). As already mentioned, there is also uncertainty as to the power on D (and hence on ν); it is difficult to distinguish experimentally between the theoretical "limits" of 0.25 and 0.333.

Figures 3a and b (from Vielstich, 1953) summarize the relationship between the fluid dynamics and mass transport in laminar and turbulent flow. The purely operational nature of the value of δ is clearly seen; it is only an approximation to the actual thickness of the region of changing concentration which is decidedly larger (Dainty, 1963). Generally it is a useful approximation because the concentration gradient is mostly linear and of the same form for a range of systems.

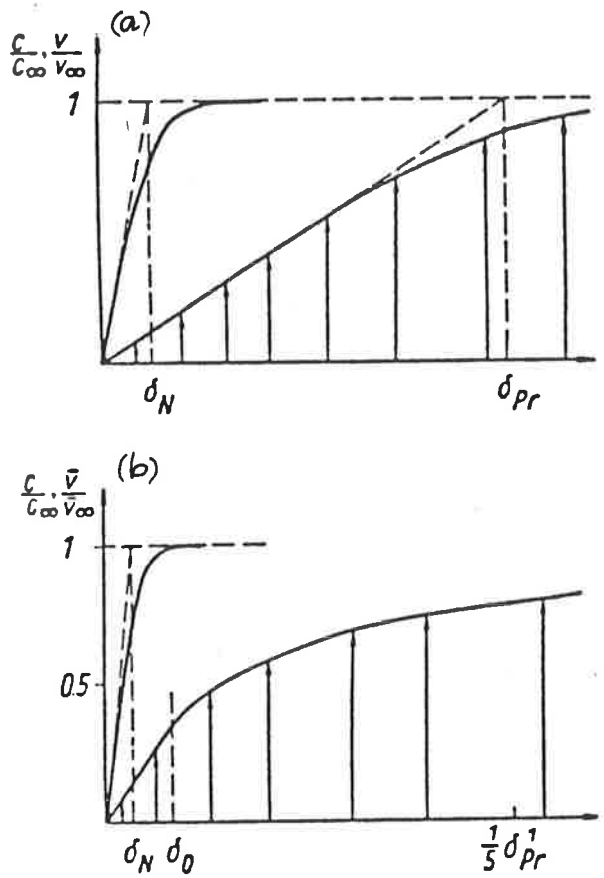

FIGURE 3. Concentration (c) and velocity (v) gradients for (a) laminar and (b) turbulent flow over a flat plate. The abscissa is the distance normal to the surface of the plate. δ_N refers to the thickness of the Nernst layer, δ_o the "laminar sub-layer" and δ_{Pr} the thickness of the Prandtl (hydrodynamic) boundary layer. For laminar flow, $\delta_{Pr} = \delta_o$ (see pp 13 - 14).
From Vielstich (1953).

Finally, the transport of mass to a surface in a completely stagnant solution will be considered. In theory this is the simplest case, but in practice a perfectly stagnant solution is not normally attained. The main reason is the density changes which occur close to the surface due to the reaction itself. This results in natural convection currents, equivalent to slow stirring (Karaoglanoff, 1906). The concentration gradient that develops with natural convection has been photographed by Ibl and Muller (1955) using an interferometric method. The flow conditions were also photographed and it is clearly seen that, while the bulk of the solution is still, there is a net flow near the reacting surface. This is shown diagrammatically in Fig. 4 (see also Skelland, 1974, Fig. 5.2).

Numerous workers (see Vetter, 1967, p 194) have derived equations to describe the Nernst layer thickness in stagnant solutions for a vertical plate. The equations are all of the form

$$\delta = \frac{1}{B}\left(\frac{D \nu x}{\alpha g \Delta c}\right)^{1/4} \qquad (25)$$

where α is the density coefficient ($\frac{1}{\rho}\frac{\partial \rho}{\partial C}$, ρ being the density) and g the acceleration due to gravity. Estimates of the constant B lie between 0.51 and 0.73. The value of δ thus depends on $\Delta c^{-1/4}$. From equation (2), the flux of reactant, J, is then proportional to $\Delta c^{\frac{5}{4}}$

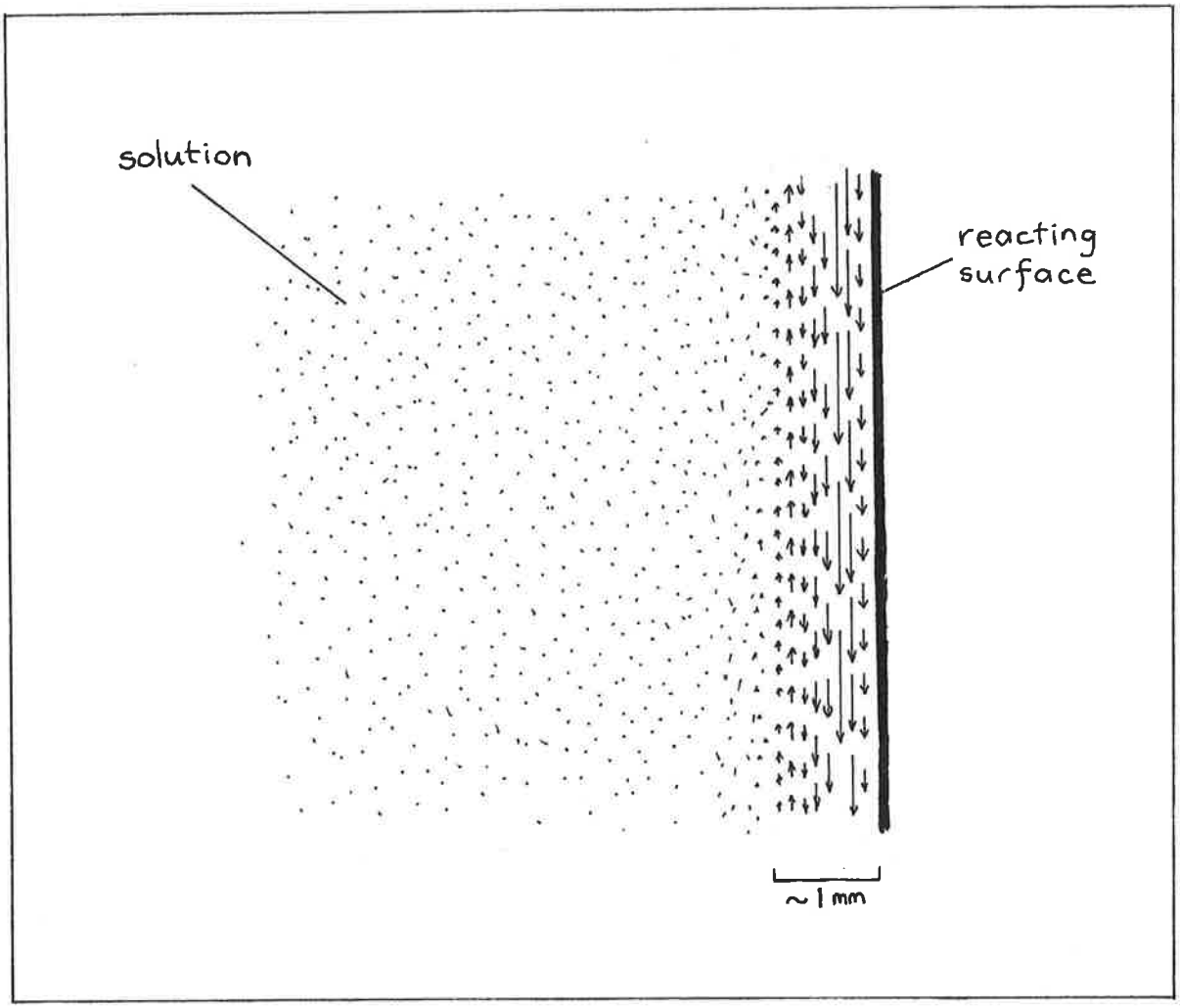

FIGURE 4. Natural convection near the surface of a reacting, vertical plate. Arrows illustrate flow velocity. (At the surface, flow is zero.) After Ibl and Muller (1955).

(not directly proportional to Δc) and δ is proportional to $1/J^{0.2}$. The interesting result, therefore, is that the larger the flux, the thinner is the Nernst diffusion layer. This has been verified experimentally (Ibl, Barrada and Trümpler, 1954).

In closing, it should be noted that the hydrodynamical descriptions of k_T which I have considered are for relatively simple systems, i.e. a rotating disk or a flat plate, in a flow of fluid which is either laminar or turbulent. More complex systems are intractable theoretically; besides irregular geometry, the flow may be laminar in some places and turbulent in others and even the scale and intensity of turbulence may differ in space (and time). However, dimensional analysis is still useful in these situations and it is usually possible to assign an average unstirred layer thickness (based on an average flux) to the object in question, using a "characteristic" dimension which becomes "x" in equation (22). Thus, equations of the form of (19) and (23) can be constructed.

(v) Conclusions

Transport processes can be important in determining heterogeneous reaction kinetics. In these cases, the kinetics can be treated by the simple Nernst theory, provided the real nature of the region represented by "δ" is kept in mind. Where the flux can be predicted

exactly from the hydrodynamics, δ represents the thickness of an hypothetical, stationary unstirred layer through which an equivalent flux would occur, assuming a linear concentration gradient throughout. When δ is determined experimentally (from a measured flux, concentration gradient and diffusion coefficient) it must be realized that the value is at best only an approximation to the real extent of the region of concentration change. At worst, in complicated hydrodynamic systems δ may be, physically, quite meaningless.

It must also be remembered that δ depends on the diffusion coefficient, so that in the same system there can be several different Nernst layers for different solutes and that, in stagnant solutions, δ also depends on the concentration gradient itself.

In this section I have only discussed reactions on a solid surface. The question of what happens when the solid is permeable to the reactants is relevant to living systems and will be briefly considered in the next section.

II. Diffusion and Simultaneous Chemical Reaction

(i) Equations for diffusion-reaction

In section I, transport and chemical reaction were linked in series. Here they will also be considered in

parallel, with substance diffusing through a solid body and being consumed at the same time. Such problems have been tackled from two quite different points of view: that of the physiologist and that of the chemical engineer (Weisz, 1973).

The physiologists were interested in the O_2 supply to respiring tissues. Krogh (1919), with the mathematician Erlang, developed an equation relating the respiration of tissue to the supply of oxygen from a capillary. Warburg (1923) examined respiration and oxygen diffusion in tissue slices and similar equations were worked out for cylinders of tissue (Fenn, 1927; Gerard, 1927; Hill, 1929) and for spheres (Gerard,1931).

The same question was of great interest to chemical engineers with regard to optimizing yields from catalytic reactors, and it led to the concept of catalyst "effectiveness". The effectiveness factor, η , was defined as the ratio of the actual reaction rate to that which would occur if all the surface throughout the inside of the porous catalyst particle were exposed to reactant of the same concentration as that existing in the bulk medium (Satterfield, 1981, p 130).

In solving the equations that describe reaction rates under these conditions, it is found that the solutions are functions of a characteristic dimension, R, of the (porous) solid body (e.g. the radius of a sphere or the

thickness of a plate), the rate constant for the reaction, k', and the effective diffusion coefficient of the reactants within the solid, D_{eff}. These three quantities can be combined into a dimensionless parameter of the form $R\sqrt{\frac{k'}{D_{eff}}}$ which became known, among chemical engineers, as the Thiele modulus, ϕ (after E.W. Thiele (1939) and see Aris (1975), p. 40).

The importance of the Thiele modulus becomes clear in Appendix V, where expression for η are derived for reactions having first-order and zeroth-order kinetics. These η's set lower and upper bounds on the effectiveness factor for reactions with Michaelis-Menten (Briggs-Haldane) kinetics.

For a first-order reaction, the expression for the effectiveness factor is

$$\eta_1 = \frac{\tanh \phi}{\phi} \qquad (26)$$

if the boundary layer resistance is negligible. If this is not the case,

$$\eta_1 = \left\{ \frac{\phi}{\tanh \phi} + \frac{\phi^2}{Bi} \right\}^{-1} \qquad (27)$$

where k_T has been expressed in terms of the dimensionless Biot number, $Bi = \frac{R\, k_T}{D_{eff}}$.

For a zeroth-order reaction,

$$\eta_0 = \begin{cases} 1 & (\phi \leqslant \sqrt{2}) \\ \dfrac{\sqrt{2}}{\phi} & (\phi \geqslant \sqrt{2}) \end{cases} \qquad (V.17)$$

for $k_T \rightarrow \infty$. When the external resistance is important

$$\eta_0 = \begin{cases} 1 & \left(\phi \leqslant \sqrt{\dfrac{2}{1 + 2/Bi}}\right) \\ \sqrt{\dfrac{1}{Bi^2} + \dfrac{2}{\phi^2}} - \dfrac{1}{Bi} & \left(\phi \geqslant \sqrt{\dfrac{2}{1 + 2/Bi}}\right) . \end{cases} \qquad (V.18)$$

Yamané (1981) developed an empirical equation for η for the full range of Michaelis-Menten kinetics, which is a weighted arithmetic mean of η_1 and η_0

$$\eta = \frac{\eta_0 + (2.6\,\kappa^{0.8})\,\eta_1}{1 + 2.6\,\kappa^{0.8}} \; . \qquad (V.21)$$

κ is the dimensionless Michaelis constant, K_M/c_b. The Thiele modulus to be used in calculating η_0 and η_1 is

$$\phi = R\sqrt{\frac{V}{D_{eff}\,(K_M + c_b)}} . \qquad (V.22)$$

This is an "overall" modulus, since k' for the strictly first-order process is V/K_M while for the zeroth-order process it is V/c_b (V is the maximum rate of the reaction).

Fig. 5 shows some rate versus concentration curves based on Yamané's expression for η, with various values of k_T. The curves are for a permeable flat plate, of a definite thickness, containing enzyme. Note that when internal transport limitations are insignificant compared with external ones, the kinetics approximate to the Briggs-Maskell type.

(ii) Determination of the extent of internal diffusion limitations

The extent of internal resistances to mass transfer (e.g. within a piece of plant tissue) can be gauged by repeatedly subdividing the tissue until there is no change in the rate (assuming the damage due to cut cells is accounted for). This method is not appropriate for plants sensitive to being cut into little pieces nor, of course, to single plant cells (e.g. Characean internodal cells). The best method would be to isolate the enzyme catalysing the reaction in question. This assumes the kinetics of the enzyme *in vivo* match those found *in vitro*, which may not be the case (e.g. Jensen and Bahr, 1977).

If no data are available about the variation of rate with the size of the tissue section, or about the kinetic properties of the enzyme, it may still be possible to estimate the effectiveness factor. If the flow conditions are known, k_T can be estimated by the theory outlined in section I. If there are other

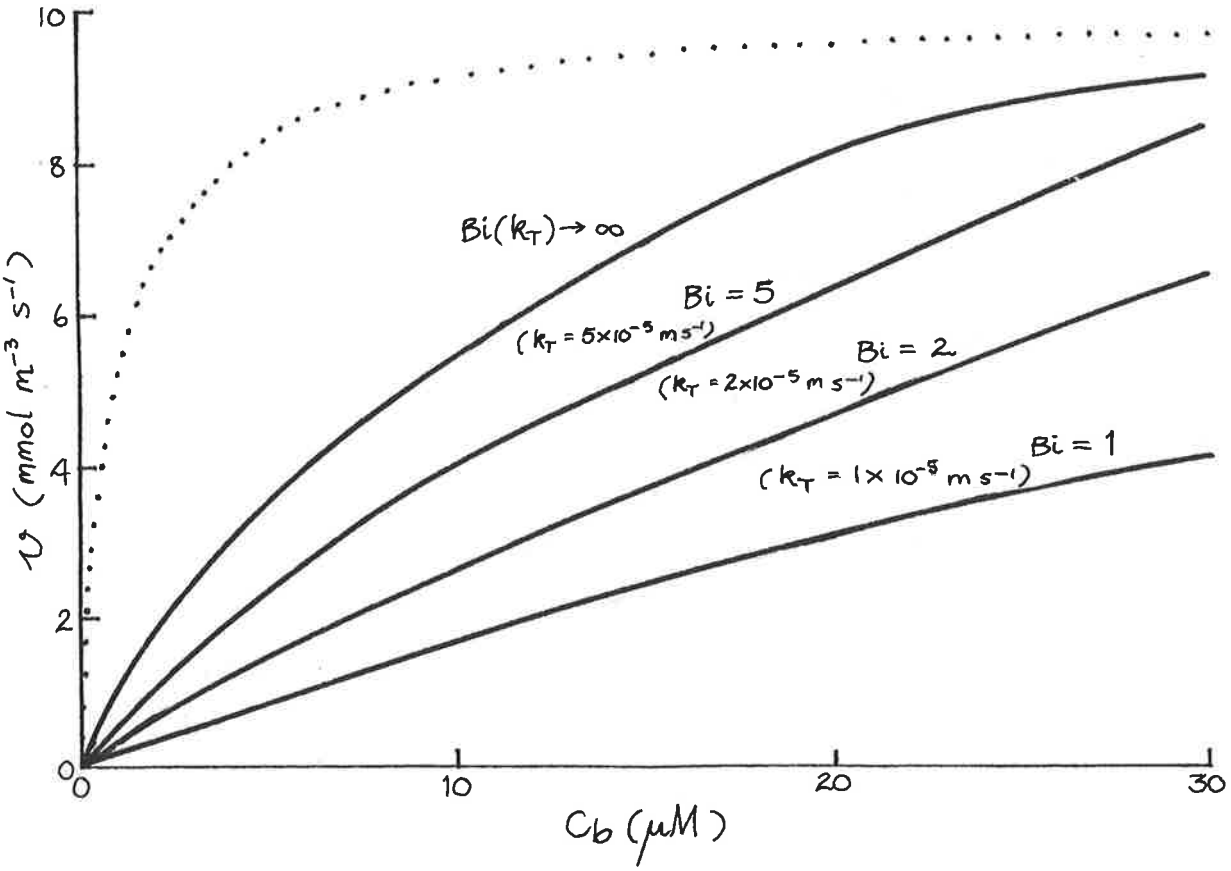

FIGURE 5. Concentration curves for the rate of an enzyme-catalysed reaction in a slab, 100 μm thick. $D_{eff} = 5 \times 10^{-10}$ m^2 s^{-1}, $K_M = 1$ μM, $V = 10$ mmol m^{-3} s^{-1}. Dotted line - Michaelis-Menten kinetics with no transport limitations (i.e. D_{eff}, $k_T \to \infty$).

significant external resistances, then these must be included in k_T to form an effective mass transfer coefficient, e.g.

$$\frac{1}{k_{T(eff)}} = \frac{1}{k_{T(dbl)}} + \frac{1}{k_{T(cut)}} + \frac{1}{k_{T(wall)}} \qquad (28)$$

where the abbreviations in brackets refer to the diffusion boundary layer, a cuticle (if present) and an outer cell wall.

The only other parameter needed to determine the extent of diffusion limitations is the Thiele modulus. This contains K_M, and the measurement of K_M is subject to the very diffusion limitations whose extent we wish to ascertain. A way out of this quandary was first proposed by Wagner (1943) and developed by Weisz and his school (see Weisz and Hicks, 1962). They defined a new modulus, Φ , based on the actual, observed reaction rate, defined by

$$\Phi = \frac{R^2}{D_{eff}} \left(\frac{1}{vol} \frac{dn}{dt}\right) \frac{1}{c_b} \qquad (29)$$

in which $\frac{1}{vol} \frac{dn}{dt}$ is the actual reaction rate (amount of substrate or product, n, per unit time, t) measured per unit volume, at a substrate concentration of c_b. R is the ratio of the volume to the surface area of the body (cf. Figs V.1 and V.2). Graphs of η against Φ are of the same shape as those of η against the Thiele modulus

(Fig. V.8) and, while the curves vary depending on K_M, all fall between the limits set by a first-order ($K_M/c_b \rightarrow \infty$) and zeroth-order ($K_M/c_b \rightarrow 0$) reaction. Hence even if K_M is unknown, η can be estimated to good accuracy for Φ less than 1 or greater than 10. For $1 < \Phi < 10$, the estimate of η will be uncertain by no more than 33%. Graphs of η versus Φ are given in Roberts and Satterfield (1965) and Knudsen, Roberts and Satterfield (1966). From these graphs it can be seen that for all values of K_M, if Φ is less than 0.1, catalyst effectiveness is nearly 100% while for $\Phi > 5$, there are very significant internal diffusion limitations ($\eta < 0.5$). These values assume there is no external resistance; if this is significant, the limits are all decreased in proportion to k_T (cf. Fig. V.4).

III. Diffusion Boundary Layers and Nutrient Uptake in Aquatic Plants

A plant living and growing in its environment represents a heterogeneous reaction system, albeit a highly complex one. It is reasonable to suppose, then, that diffusion may be important in limiting the rates of various reactions in the plant, where the reactants are supplied from the environment or where the products are expelled thereto. Compared with terrestrial plants, boundary layer restrictions may be quite severe for aquatic plants because diffusion coefficients in water

are reduced some 10,000-fold compared with those in air. (That is not to say the problems are 10,000 times worse; δ itself depends on D (equation (15)) and also there is a dependence on the kinematic viscosity of the fluid, ν, which is 10 times smaller in water cf. air).

Internal diffusion limitations are of a similar nature for plants in either habitat. A considerable amount of work has been done on the gas exchange of leaves of terrestrial plants, where internal diffusion has generally been assigned a fixed resistance in an "electrical analogue" model (Gaastra, 1959; Lommen et al., 1971; Jones and Slatyer, 1972). In other cases, the diffusion-reaction equation has been solved as in Appendix V, making various assumptions (e.g. Briggs and Robertson, 1948; Briggs, 1959; Parkhurst, 1977).

(i) Previous studies

There is a large body of evidence which gives qualitative support to the idea that transport restrictions due to boundary layers can be significant for the uptake of nutrients by aquatic plants. Increasing fluid velocity, whether by shaking, stirring or increased flow down a channel, has been found to increase growth rates and nutrient fluxes of single-celled algae (Myers, 1944; Falco, Kerr, Barron and Brockway, 1975; Pasciak and Gavis, 1975), colonies or compacted communities of microalgae and bacteria

(McIntire, 1966 a,b; Roff, Rough, Cummins and Coffman, 1966; Hartmann, 1967; Sperling and Grunewald, 1969; Sperling and Hale, 1973), marine macroalgae (Gessner, 1940; Printz, 1942; Matsumoto, 1959; Jones, 1959; Conover, 1968; Doty, 1971; Dromgoole, 1978; Littler, 1979; Wheeler, 1980; Parker, 1981; Gerard, 1982) freshwater macroalgae (Whitford and Schumacher, 1961,1964; Schumacher and Whitford, 1965; Pfeifer and McDiffet, 1975; Thirb and Benson-Evans, 1982) and aquatic bryophytes (James, 1928; Bain, 1982) and angiosperms (Darwin and Pertz, 1896; Gessner, 1938; Owens and Maris, 1964; Westlake, 1967; Buesa, 1977; Werner and Weise, 1982; Madsen and Søndergaard, 1983).

Some of the increases have been quite spectacular; for example, Schumacher and Whitford (1965) observed a 43-fold stimulation in the rate of ^{32}P uptake by the freshwater red alga Audouinella violacea in stirred (180 mm s^{-1}) versus unstirred solutions. The effect of water velocity is greatest when the maximum rate of the metabolic process is high - for instance, stirring has only a minor effect on photosynthesis at low light intensities (Wheeler, 1980) or where maximum rates are reduced by seasonal or genetic variation (McIntire, 1966a; Westlake, 1967). Such a result is in line with the predictions of the Briggs-Maskell equation.

The increased metabolic rates accompanying stirring also appear to be dependent upon the form of the plant

or plant part in question. Gessner (1938) found that stirring increased photosynthesis of entire leaves of Proserpinaca palustris by 22% (i.e. compared with photosynthesis in stagnant water), but that the increase was only 5% for the featherlike leaves of the same plant. Similar results have been found when different species of plants, having either entire or highly dissected leaves, are compared (see Hutchinson, 1975).

Some workers have plotted rate versus velocity curves (James, 1928; Pasciak and Gavis, 1975; Wheeeler, 1980; Bain, 1982; Madsen and Søndergaard, 1983) which usually show some saturation of rate with water velocity, U. The hydrodynamic description of k_T in laminar flow predicts $k_T \propto \sqrt{U}$ (p 15) which resembles the beginning of a saturation type curve; generally, however, the experimental curves have been taken to denote increasing rate control by the biochemical reaction itself. It has sometimes been found that there is an adverse effect of water velocity when this is too high.

Rate versus concentration curves of the type expected for Michaelis-Menten kinetics in series with a thick unstirred layer (i.e. virtually linear at first with a sharp transition to the saturated rate, Fig. 1) also frequently occur in the literature (e.g. Hanisak and Harlin, 1978; Kautsky, 1982) and are suggestive of diffusional limitations (Smith and Walker, 1980; Madsen,

1984). Indeed McIntire and Phinney (1965) found that photosynthetic oxygen evolution increased linearly with $[CO_2]$ up to the highest concentration studied (~ 1 mM), and Werner and Weise (1982), found the same result for phosphate uptake by Ranunculus penicillatus. Phosphate and sulphate absorption by Elodea densa leaves was found to have a complex relationship to concentration by Jeschke and Simonis (1965); however it was linear from 0.01 to 3.2 μM and the authors concluded that absorption was limited by the boundary layer in this region. Similarly, respiratory oxygen consumption by various aquatic plants has been studied by Gessner and Pannier (1958a,b) in relation to the external oxygen concentration and in many plants (including phytoplankton) respiration rates varied linearly with concentration and were stimulated by stirring. In other plants respiration seemed to depend on $[O_2]$ raised to some power (<1): this may have reflected internal diffusion limitations to oxygen transport (Owens and Maris, 1964, and see Longmuir, 1966). Dromgoole (1978) observed a hyperbolic relationship between respiration rate and oxygen concentration in a number of marine macro-algae and showed how the curves became more oblique as the water velocity decreased.

Studies of a more quantitative nature on the relationship between transport through boundary layers and the absorption or loss of matter by plants are few

and far between. Apart from Wheeler (1980), they have been mainly concerned with phytoplankton. Munk and Riley (1952) used heat transfer theory to predict the effect of fluid velocity on mass transfer (i.e. nutrient absorption). Apart from changes in the meaning (and value) of the symbols, the equations for heat and mass transfer are virtually identical (Bird, Stewart and Lightfoot 1960; Thom, 1968). Munk and Riley took phosphate to be the limiting nutrient for phytoplankton growth, and its absorption rate to be completely diffusion limited (i.e. $c_s = 0$). Their calculations point out the advantages of small size for mass transfer, the importance of sinking as a means of increasing it and the relative effects for cylinders, spheres, disks and plates. Some of their predictions are borne out in natural phytoplankton assemblages. They also give an equation for the effect of water velocity on mass transfer to an attached plant in the form of a plate, which is analogous to Levich's equation (equation (18)). Based on this equation, using reasonable values of the inorganic P concentration of sea water and rates of P uptake by plants, Munk and Riley concluded that attached plants would need to inhabit regions of quite high water velocity. The calculated water velocity depends upon the phosphate influx squared, so that a somewhat lower influx would make a considerable difference to the answer. Munk and Riley used an influx of some 300 nmol m^{-2} s^{-1} which is

large.

Pasciak and Gavis (1974) derived the quadratic equation relating c_s in the Michaelis-Menten equation to c_b for a sphere in an infinite, perfectly stagnant continuum. Under these conditions, $k_T = D/R$ where R is the radius of the sphere and D the diffusion coefficient (see Appendix V, p156). They then incorporated motion by employing the expression for k_T used by Munk and Riley (1952) for sinking spheres, $k_T = D/R\ (1 + \frac{1}{2}(R/D)\ U)$ where U is the relative water velocity of the bulk medium and the sphere. They showed how the familiar Michaelis-Menten hyperbolic kinetic curve became more and more oblique depending on the value of a dimensionless parameter, P′, equivalent to $k_T\ K_M/V$. (Pasciak and Gavis (1974) actually defined $P' = (14.4\ R^2)k_T\ K_M/V$; however, if consistent units are used and V is expressed as a flux (e.g. nmol $m^{-2}\ s^{-1}$), the parameter becomes simply $k_T\ K_M/V$.) This dependence on P′ follows directly from the Briggs-Maskell equation, which predicts severe transport limitations through the boundary layer if $k_T << V/2K_M$, i.e. $k_T\ K_M/V << 0.5$. Pasciak and Gavis (1974) arbitrarily chose $k_T\ K_M/V < 0.56$ as indicative of limitations imposed by the diffusion boundary layer, and concluded that a number of species of phytoplankton (both motile and non-motile) could suffer unstirred layer problems.

For shapes other than spheres, Pasciak and Gavis

(1975) incorporated a shape factor into the equation for P′. They predicted P′ values for nitrate and nitrite uptake by the marine diatom Ditylum brightwellii (roughly cylindrical cells, about 150 μm long and 50 μm in diameter) in a stagnant solution and found reasonable agreement between theory and experiment. They demonstrated that diffusional constraints were lessened in shaking solutions, or in solutions subjected to known rates of shear; however, they did not compare observed with predicted P′ values under these conditions.

The effect of transport through the boundary layer of a macrophyte (Macrocystis pyrifera) was examined by Wheeler(1980). In this case, the fluid velocity was carefully measured and it was also deduced that flow became turbulent at quite low velocities (10 mm s^{-1}) because of the roughness of the Macrocystis blade. Based on calculated average unstirred layer thicknesses (see p 20) and using another variation on the Briggs-Maskell equation, Wheeler obtained reasonable agreement between predicted rates of photosynthsis and those actually observed.

Diffusion boundary layers are also important in animal physiology and in the study of membrane permeability, but these aspects will not be discussed in detail. The many articles by Sallee, Thomson and Dietschy (see Thomson, 1979b) illustrate the point for uptake in the intestine. Barry and Diamond (1984)

have recently reviewed many of the studies on membrane permeability where unstirred layers are critical.

(ii) This work

This thesis is an attempt to quantify the limitations imposed by mass transport from the bulk medium to reactions involving phosphate, methylamine*, O_2 and CO_2 in a few aquatic macrophytes. In all cases, the geometry is that of a more or less flat plate, which conveniently gives rise to the simplest equations. For phosphate and methylamine, the "reaction" step will be assumed to be the membrane transport reaction $R_{out} \rightleftharpoons R_{in}$, in which the rate of the forward (and back) reaction can be studied at equilibrium using tracers. Such reactions frequently display first-order Michaelis-Menten kinetics, although this gives little information about the mechanism of the process (Stein, 1981). Each mechanism gives rise to its own definition of "K_M"; here it will simply be taken to mean the intrinsic half-saturation constant for transport across the membrane in the absence of other transport limitations. In the case of O_2 and CO_2, the reactions (of respiration and photosynthesis respectively) are more complicated and the kinetics may not be simple first-order, or even

---

*Methylamine is not a nutrient, as defined on p.1, but it is an analogue of ammonia in so far as it probably shares the membrane porter for ammonia (see MacFarlane and Smith, 1982).

pseudo first-order, Michaelis-Menten. These bridges, however, will be crossed later, as the need arises.

MATERIALS AND METHODS

(i) Plants

A number of aquatic plants, both marine and freshwater, were studied. Many of the experiments were done using the marine alga *Ulva rigida* C. Agardh (Fig.6) collected from pontoons at West Lakes, South Australia. The plants were stored in natural, aerated sea water in a constant temperature room (16°C) with four cool white fluorescent tubes for illumination. These provided a photon flux density at the surface of the sea water of 70 μmol (400 - 700 nm) m^{-2} s^{-1} and were set on a 12h on/ 12h off cycle. Under these conditions the plants remained healthy for six weeks or longer. Clumps of the sea grass *Amphibolis antarctica* (Labill.) Sond. & Aschers ex Aschers (Fig.7) were stored in a similar way but were generally used soon after collecting. These were clumps that had been washed up on beaches at Grange and Semaphore, South Australia, after storms. The freshwater macrophyte *Vallisneria spiralis* L. (Fig.8) was grown in large plastic tanks in the Botany Department. The tanks contained about 50 l of deionized water, to which was added KCl, $CaSO_4$, KH_2PO_4 and $NaHCO_3$ to give final concentrations of 1 mM, 0.05 mM, 0.6 mM and 1 mM respectively. The plants were rooted in a 70 - 80 mm layer of mud, collected from the River Torrens. Light was provided by two "Gro-Lux" fluorescent tubes giving a photon flux density of about 40 μmol (400 - 700

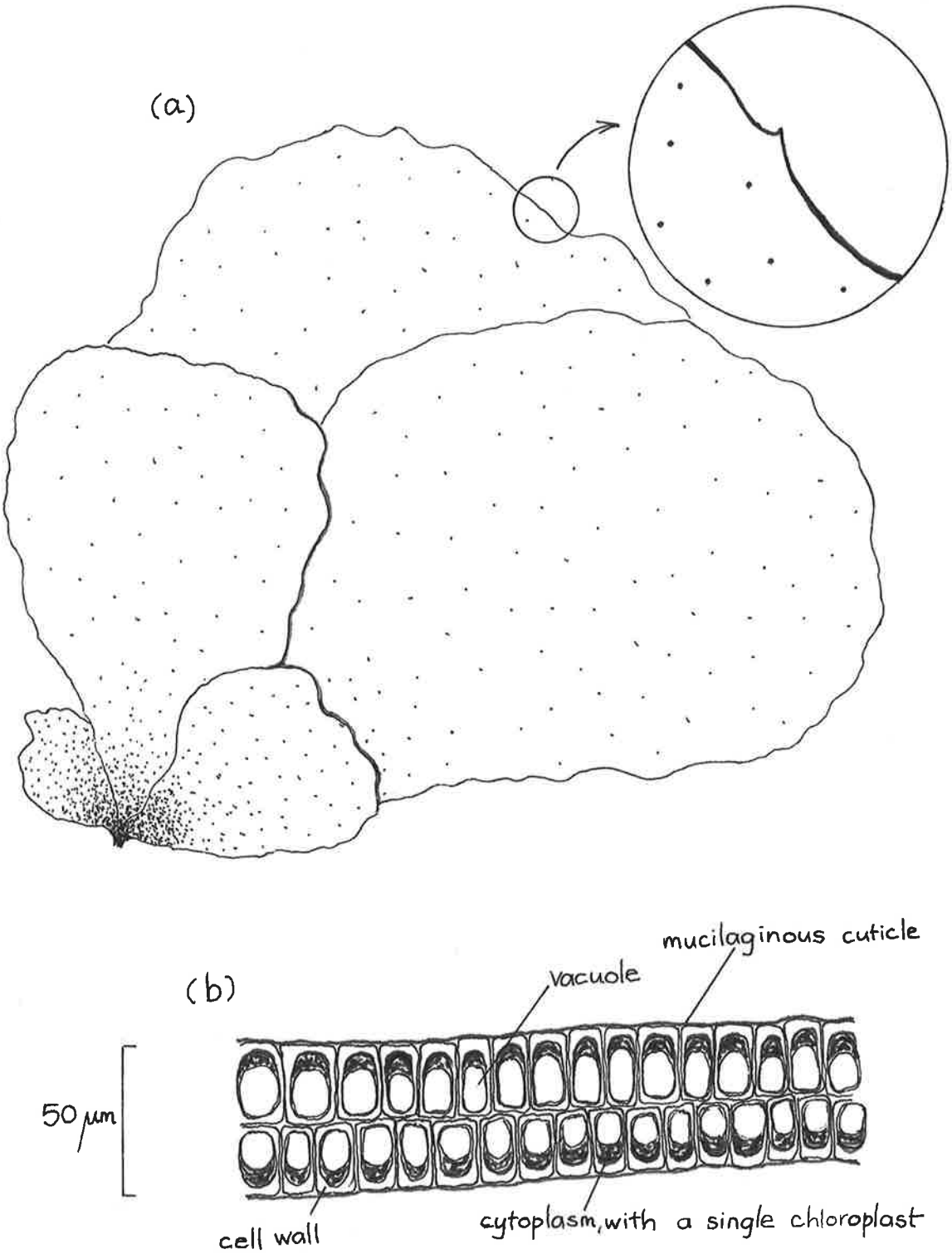

FIGURE 6. (a) Sketch of habit of U.rigida, about half natural size. At intervals along the margin of the intact thallus there are microscopic spines.

(b) T.S. of thallus (diagramatic). The chloroplasts are convoluted and so appear in several places in each cell in transverse section.

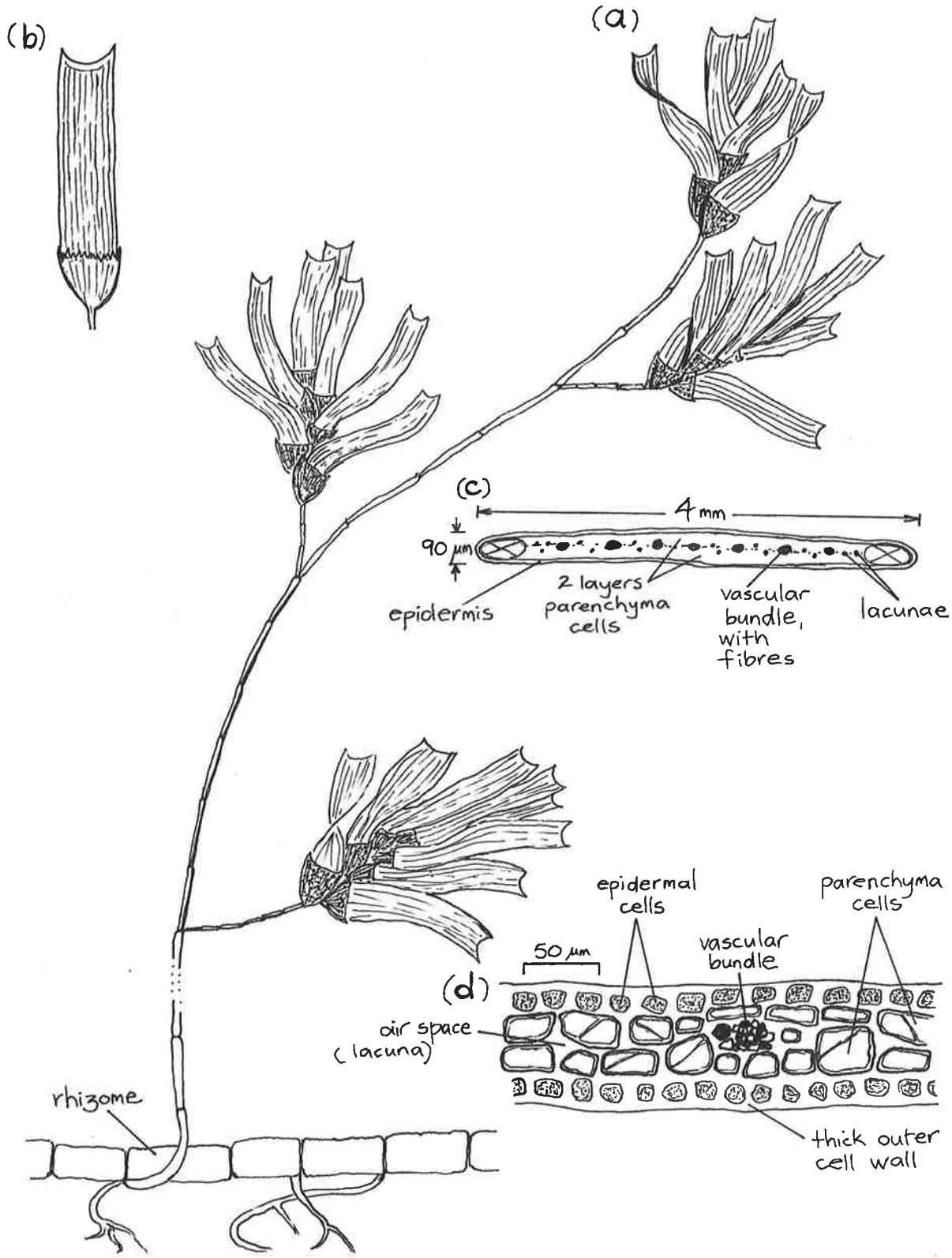

FIGURE 7. (a) Sketch of habit of A.antarctica, ~ natural size.

(b) A single leaf, ~ twice natural size.

(c) T.S. of leaf; zone diagramme.

(d) T.S. of leaf showing cell detail. The epidermal cells are densely cytoplasmic with many chloroplasts. The parenchyma cells have a very thin layer of cytoplasm, containing chloroplasts, and have thin walls.

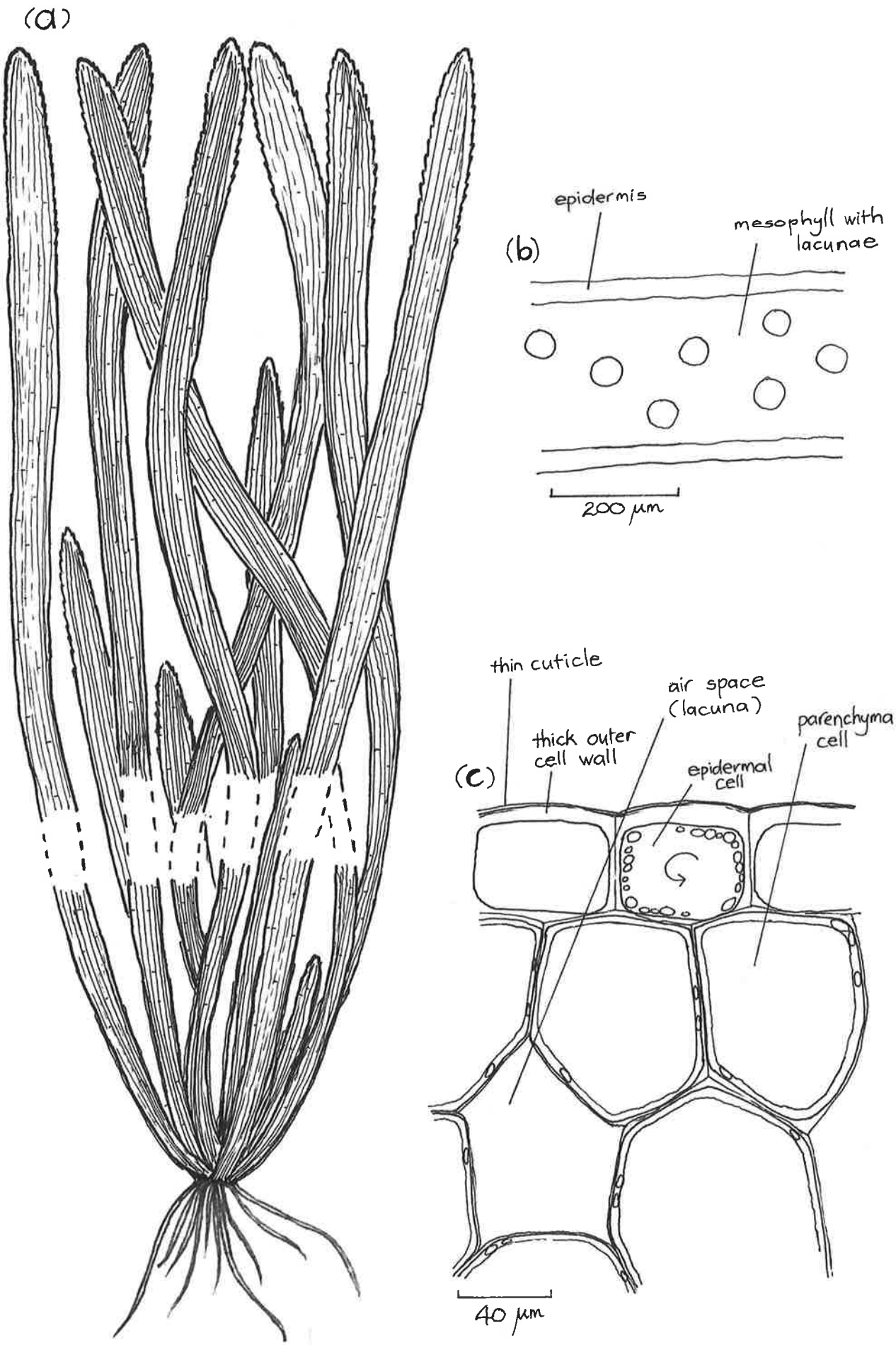

FIGURE 8. (a) Habit sketch of V.spiralis. Leaves grew 1 - 1·5 m long in the culture tanks and upto 20 mm broad.

(b) T.S. of leaf; zone diagramme.

(c) Cell detail (T.S.). The epidermal cells contain dense, streaming cytoplasm and many chloroplasts.

nm) m^{-2} s^{-1} at the surface of the water. The lights were again set on a 12h on/ 12h off cycle.

In the experiments with Vallisneria, segments or disks were cut from the mid-section of healthy leaves, i.e. avoiding the region near the base or the apex. When the leaves were in poor condition, the bathing solution infiltrated the air spaces of the leaf when it was cut (van Lookeren Campagne, 1955); these leaves were discarded. In Ulva, tissue was also cut from the mid-region of the frond, avoiding the margin and the rhizoidal region at the base of the thallus. Individual leaves were used in experiments with Amphibolis; younger leaves were usually chosen as older leaves were often covered with epiphytes.

(ii) Solutions

Experiments with marine plants were done using either natural, filtered sea water (FSW) or an artificial sea water (ASW). FSW was prepared by filtering sea water collected at Grange, S.A., through a Whatman GF/C filter. This removed any particles larger than 1.2 μm which includes all but the smallest bacteria. The FSW was stored at 4°C in the dark. Chlorinity was 22.8‰, determined by the Mohr titration (Strickland and Parsons, 1965). Total inorganic carbon was estimated from the alkalinity (Strickland and Parsons, 1965) to be 2.2 mM. ASW was deionized water containing 490 mM NaCl,

10 mM KCl, 11.5 mM $CaCl_2$, 25 mM $MgCl_2$, 25 mM $MgSO_4$ and 2.5 mM $NaHCO_3$ (Findlay, Hope, Pitman, Smith and Walker, 1971). The chlorinity is 20.3‰. The medium for Vallisneria was an artificial pond water (APW) as used by Smith (1980) in his experiments with Elodea (and Chara). It contained 1 mM NaCl, 0.1 mM K_2SO_4 and 0.5 mM $CaSO_4$, plus $NaHCO_3$ to give a final concentration of 2 mM. Usually the ASW or APW was buffered with a zwitterionic buffer, at a pH no more than 0.6 pH units away from the pK_a value of the buffer.

For measurements of photosynthesis and its relationship to the inorganic carbon concentration, ASW or APW was made up with no $NaHCO_3$. To ensure that the solution was completely carbon-free, the pH of the solution was taken down to 4 or lower where virtually all of the inorganic carbon is in the form of CO_2. The solution was then flushed for at least 30 minutes with CO_2-free nitrogen after which the pH of the solution (still under nitrogen) was adjusted to its proper value with a freshly prepared NaOH solution. The nitrogen was scrubbed of CO_2 by passing it through soda lime, concentrated NaOH and deionized water in that order. The solution was kept under nitrogen until it was ready to be used; sometimes this was with the solution illuminated and containing pieces of plant material, a system which proved to be a very effective "CO_2 - scrubber".

(iii) Respiration

The uptake of O_2 during dark respiration was measured polarographically using a Rank Bros. O_2 electrode connected to a Rikadenki chart recorder. A full scale deflection from zero on the chart recorder corresponded to a solution in equilibrium with air i.e., at 25°C, 236 μM O_2 for fresh water, 193 μM for ASW and 188 μM for FSW (Table 6 in Riley and Skirrow, 1975). Zero O_2 was obtained by adding a small amount of sodium dithionite to the solution. Temperature was controlled (usually at 25°C) by pumping water from a thermostatted water bath through the water jacket around the electrode.

Plant tissue was placed in the electrode chamber as slices, small pieces or in special holders (see Fig.9). When small pieces of plant material, or slices of Vallisneria, were used, a disk of coarse nylon mesh was positioned inside the chamber to prevent the pieces touching the stirring flea.

The holders, shown in Fig.9, allowed large (about 20 x 15 mm) "slabs" of leaf or thallus to be placed vertically in the electrode chamber. For the type A holder, the tissue was simply cut to size and placed between the wire supports. In type B holders, the tissue was cut to a size slightly smaller than that of the holder, sandwiched between the two sides and the edges sealed with stop-cock grease or dental wax. The

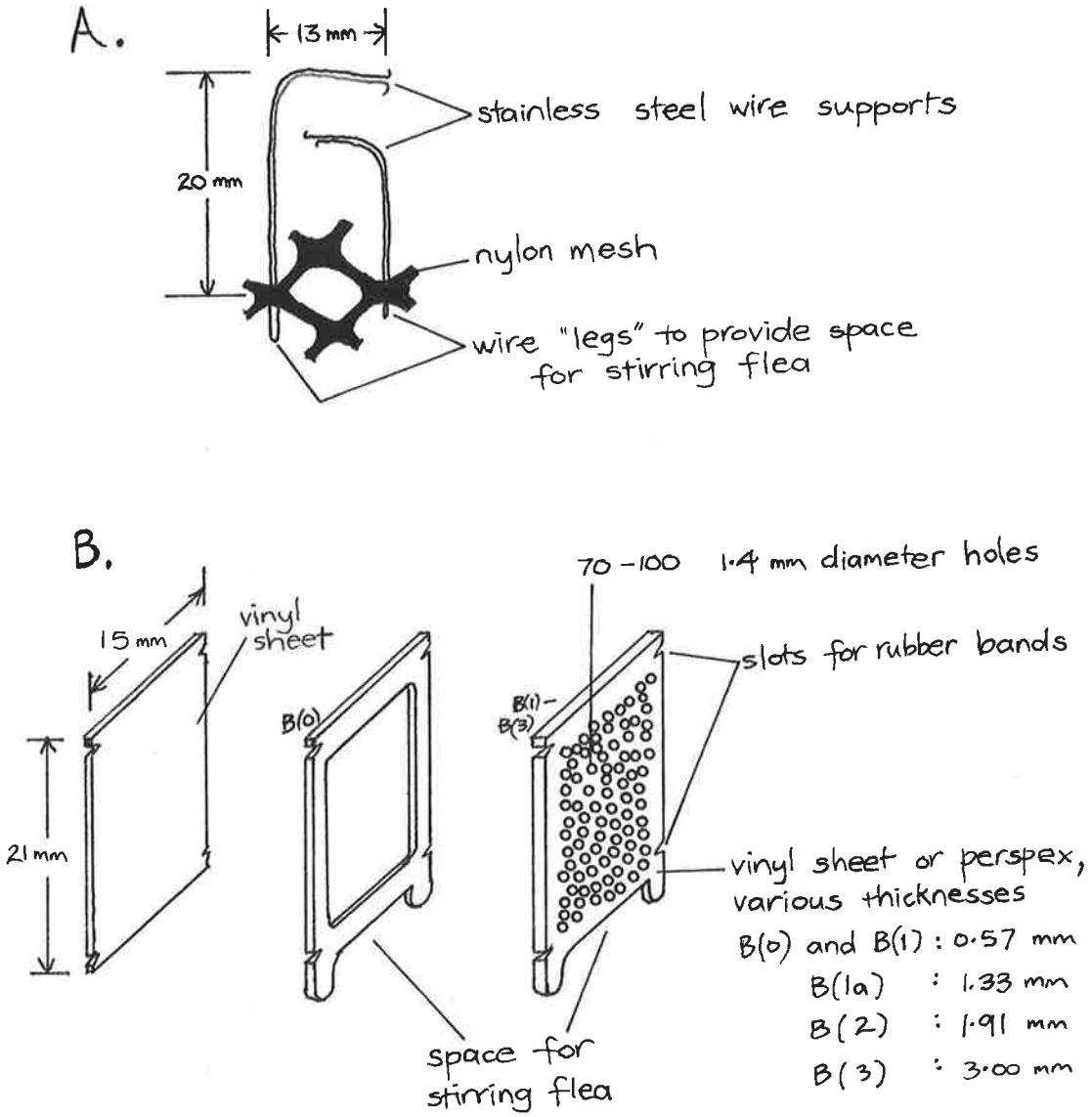

FIGURE 9. Holders for plant tissue in the oxygen electrode chamber.

whole assembly was held firmly together by two small rubber bands. Usually one side of the holder consisted of a greased piece of solid vinyl sheet; in some experiments the two sides were identical. For type B holders, the surface area available for diffusion in the boundary layer is less than that of the piece of tissue. In the type A holder, they are assumed to be the same. Type B holders were a means of varying the thickness of the hydrodynamic (and diffusion) boundary layer without changing the stirring conditions for the O_2 electrode.

The thickness of the unstirred layer was also varied by laying sheets of lens tissue or filter paper over both faces of a piece of Ulva. The assembly was held together using two type B(O) holders. The thickness of the layer was estimated by adding together the thicknesses of the single sheets, as measured under the microscope. The value agreed tolerably well with the thickness obtained using outside calipers and/or the displacement of water. The actual length of the diffusion pathway will be longer than the thickness of the layer(s) because of tortuosity. The diffusional flux will also be decreased because the pathway is not entirely aqueous.

To measure respiration as a function of the external O_2 concentration, the solution in the O_2 electrode chamber was allowed to equilibrate with air and then the plant tissue was added. The chamber was sealed, and the

oxygen concentration recorded as a function of time. The flux of oxygen was determined from the slope of the recorder trace at various points.

Sometimes bacteria contaminated the solution in the chamber, and their respiration could be quite significant at the end of prolonged runs. To correct for this, at various stages the plant tissue was removed and the respiration of the solution alone was measured. Then the solution was replaced with fresh solution which was bubbled with N_2 gas to lower the O_2 concentration to the required level. The plant tissue was then replaced and the run continued. The respiration of bacteria on the surface of the tissue itself, however, would not be corrected for by this method. The results, after correcting for O_2 uptake by the solution alone, are expressed as nmol O_2 m^{-2} (tissue) s^{-1}.

(iv) Photosynthesis

Photosynthesis was measured both by O_2 evolution, using an O_2 electrode, and by ^{14}C fixation. For the O_2 evolution measurements, the set-up was the same as for respiration. Light was from a slide projector fitted with a 150 W quartz iodide bulb and the plant tissue was either oriented face-on or edge-on to the light beam with a curved aluminium reflector placed behind the electrode chamber. In all cases bar one, the light intensity was saturating for photosynthesis; the

exception was the thickest perspex holder, B(3), which did shade the tissue quite markedly.

To measure photosynthesis as a function of the inorganic carbon concentration, the experimental solution was scrubbed of CO_2 by the method described and an aliquot (3 - 5 ml) pipetted into the O_2 electrode chamber. The plant tissue was added and the chamber sealed. Usually a 5 - 10 min equilibration time in the dark was allowed before the light was switched on. In the light there was often a burst of photosynthesis probably due to inorganic carbon remaining in the free space of the plant tissue. The rate of O_2 evolution then, usually, declined to zero, corresponding to the inorganic carbon compensation point.

There were a number of exceptions. Sections of Vallisneria leaf continued to evolve O_2 in the chamber for six hours or longer, the rate decreasing only slightly with time. In some experiments with Ulva, which were carried out in buffered ASW containing sulphanilamide, (an inhibitor of carbonic anhydrase- Mann and Keilin, 1940) and para-amino benzoic acid (PABA), there was net O_2 uptake in the light. Otherwise, O_2 uptake in the light was never observed with Ulva, but it sometimes occurred with pieces of Vallisneria epidermis and Amphibolis leaves. The only other exception was in one experiment with Ulva swarmers. These were zoospores

or gametes (not identified) that were released in the aquarium sea water two days after collecting the alga. Batches totalling about 250 ml of sea water were centrifuged in a bench centrifuge at 3,000 r.p.m. for 5 min. The pellets were gently resuspended and combined, giving 3 ml of "swarmer concentrate". 400 µl of this concentrate was added to 3 ml of buffered ASW (pH~5.5) in the O_2 electrode chamber; under these conditions photosynthesis was completely saturated by inorganic carbon because of its high concentration in the sea water of the swarmer concentrate. Subsequently the concentrate was purged of CO_2 by taking the pH down to 5.5 and bubbling with CO_2-free N_2 under light. Samples of this suspension then behaved as described in the previous paragraph, even though rates of respiration were extremely high (cf. Haxo and Clendenning, 1953) averaging nearly 70% of net photosynthesis.

With net photosynthesis at zero (or below) a small volume of fresh $NaHCO_3$ solution (1, 10 or 100 mM) was added using an automatic pipette, and O_2 evolution quickly reached a steady rate. The concentration of O_2 in the solution in the electrode chamber was not allowed to go much above 60% of the air equilibrated value; for any particular run this generally enabled two photosynthesis measurements to be made at two different inorganic carbon concentrations.

After the photosynthesis measurements, the light was switched off so that respiration could be measured. Respiratory O_2 uptake in Ulva sometimes showed a post - illumination burst while Vallisneria displayed the opposite effect - O_2 uptake after switching off the light was zero at first but gradually increased to a steady (low) value. In the type B holders there was a slow (depending on the thickness of the holder) transition to net O_2 uptake, i.e. net O_2 evolution continued for some time after switching off the light. For these last two cases, then, the respiration rate immediately upon switching off the light was impossible to determine because of the slow transition to a steady rate; this was probably because of the large volume of stagnant solution associated with the holders or the thicker tissue of Vallisneria, compared with Ulva.

It is important, however, to know the rate of O_2 uptake during net O_2 evolution so that it can be corrected for (i.e. so that true, or gross, photosynthesis can be determined as opposed to the apparent, or net, rate). It is a matter of debate as to whether or not mitochondrial respiration is affected by the events surrounding photosynthesis (Graham, 1979; Singh and Naik, 1984). The problem is also complicated by the fact that there may be recycling of the CO_2 produced in respiration (and photorespiration). The efficiency of recycling will itself depend on the

unstirred layer thickness. Complete recycling of respired and photorespired CO_2 would mean a CO_2 compensation point of zero and net and gross photosynthesis, for all intents and purposes, would be the same. Partial recycling would mean a net rate of photosynthesis somewhat smaller than the true rate, but not as small as one would expect, based on the rate of dark respiration, photorespiration, and no recycling.

In the results, I have assumed that the initial, steady rate of O_2 exchange in the light is indeed for a $[CO_2]$ of zero. Where net O_2 exchange was zero (the majority of cases) complete recycling of respired and photorespired CO_2 is implied.

The pH of the solution was determined at the beginning and end of a run, using a Philips CA11 combination glass electrode connected to an Orion 701A digital pH meter. The pH change was generally small and mainly due to the $NaHCO_3$ additions. The final pH was therefore the best measure of the pH during the period of photosynthesis.

Results are expressed as nmol O_2 evolved m^{-2} (tissue) s^{-1} or as mol O_2 (g chlorophyll)$^{-1}$ s^{-1} or, in some experiments with slices where neither surface area nor chlorophyll were measured, as a percentage of the maximum rate. Normally only one photosynthesis

measurement was done at any one inorganic carbon concentration. Sometimes more than one determination was made and error bars represent maximum and minimum values if the number of measurements was two, or the standard error of the mean if the number was greater.

Photosynthesis was also measured by the fixation of ^{14}C-labelled inorganic carbon. For experiments involving the "stirring gradient tower" (see later), disks of Ulva were used, 7.5 mm in diameter cut with a cork borer. With Vallisneria, oblong pieces 15 x 8 mm were used. The disks or pieces were left aerating overnight in ASW or APW. The following day, a solution with the required concentration of inorganic carbon was prepared and gently decanted into the tower which was then loaded up with the sieves and plant tissue. There were 12 disks of Ulva or six pieces of Vallisneria to each level. The tower was sealed and the whole allowed to equilibrate in the light for 50 - 60 min. After this pretreatment, the solution was poured off and replaced by a solution labelled with ^{14}C (~ 0.1 μCi ml^{-1}; $NaH^{14}CO_3$ supplied by Amersham). This was done as quickly and gently as possible, to minimise exposure to atmospheric CO_2. The plant tissue was allowed to fix the ^{14}C-labelled inorganic carbon for 10 min, and then the sieves were taken out and placed immediately in 100 mM nitric acid to prevent further carbon fixation. Batches of four disks (or two Vallisneria pieces) were

subsequently removed to scintillation vials containing 1 ml of 100 mM HNO_3. A sample of the experimental solution was taken for a final pH measurement, and then the whole apparatus was thoroughly rinsed and the experiment repeated at a different inorganic carbon concentration or pH.

The scintillation vials containing the plant material were left open in a fume hood overnight to allow the release of volatile carbon. The next day, 10 ml of scintillation cocktail (PPO/POPOP/toluene/detergent) was added and the vials counted in a Packard Tri-Carb Scintillation Spectrometer. Quenching by chlorophyll was corrected for by the channels-ratio method (Herberg,1965). After each experiment, 50 µl samples were taken from the radioactive solutions so that specific activities (cts min^{-1}/mol) could be calculated.

Results are expressed as nmol carbon fixed m^{-2} (tissue surface area) s^{-1}. Error bars in the figures represent the standard error of the mean of three samples. Usually, tissue of known surface area was also weighed so that results could be expressed in terms of fresh weight. Sometimes, chlorophyll was also extracted (Arnon, 1949).

(v) Uptake of methylamine and phosphate

Influxes of [^{14}C]methylamine and [^{32}P]phosphate were determined in the "stirring gradient tower" (see later)

in a similar way to inorganic [^{14}C]carbon fixation. Methylamine was added as CH_3NH_3Cl and phosphate as KH_2PO_4. At the end of a 10 - 15 min period in radioactive solution ($\sim$ 0.1 μCi/ml), the plant tissue was washed for 2 - 5 min in non-radioactive solution to remove label from the free space. After rinsing, the tissue was lightly blotted, divided into subsamples and placed into scintillation vials containing 10 ml of scintillation cocktail, plus 1 ml 100 mM HNO_3. Radio - nuclides were supplied by Amersham.

In some cases, slices of plant material were used. These were treated in the same way as disks or leaves and were divided into three subsamples at the end of the experiment. The subsamples were placed into weighed scintillation vials and the results expressed as nmol g^{-1} (fresh weight) s^{-1}. Knowing the weight of a piece of tissue of known surface area, the results could be converted to nmol m^{-2} s^{-1}.

(vi) Stirring gradient tower

This is illustrated in Fig.10. The different levels of the "tower" had different rates of water movement due to the stainless steel mesh sieves which decreased the water velocity of the section immediately above them.

Fig.11 shows the stirring gradient that is set up in the tower, with the magnetic stirrer on its maximum

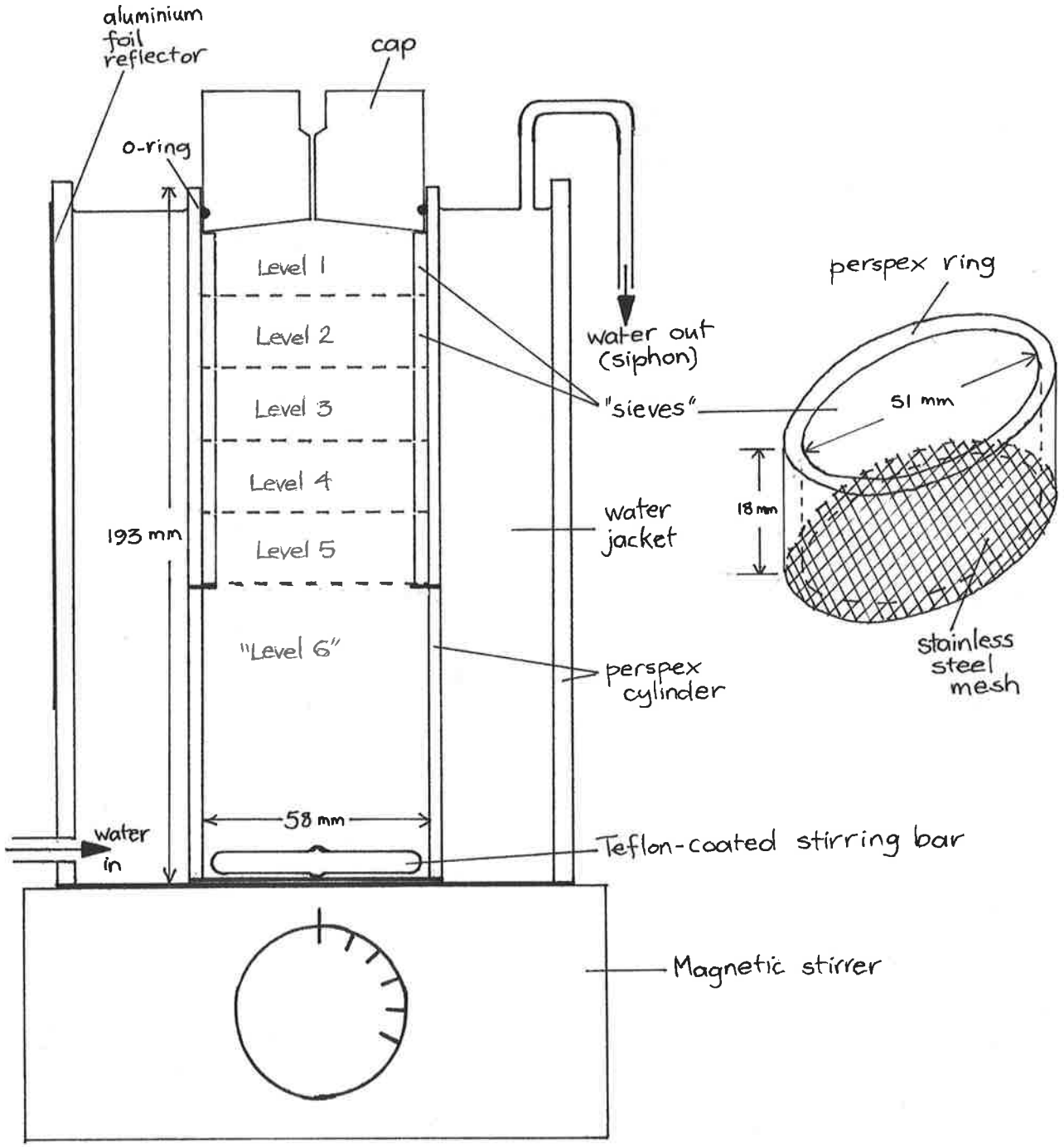

FIGURE 10. Apparatus for obtaining a stirring gradient in a solution. Light was provided from the side by a slide projector with a 150 W quartz iodide bulb, giving a photon flux density of ~670 μmol (400-700 nm) m^{-2} s^{-1} at the centre of the tower.

setting ("8.4"). The measurements were made by timing the rotation of a match, using a stop watch for levels 3 and 4 and a stroboscope for 5 and 6. The water velocity in levels 1 and 2 was too low to be measured. As a check on the accuracy of the method, the angular velocity of the vortex was also measured for each level when there were no other sieves above it. This produced a curve of the same shape as that shown in Fig.11a although all the velocities were about 1/3 again higher.

Fig.11b is a plot of log (r.p.m.) against log (level). The points are a good fit to a straight line which suggests the empirical relationship

$$r.p.m. = 0.113\ L^{4.5} \qquad (29)$$

where L is the level number. This equation is represented by the lines in Figs.11a and 11b.

In the Introduction (section I), it was shown that δ is related to the inverse of the fluid velocity raised to some power, usually between 0.5 and 1. To get an idea of the actual values of δ in the various levels, 13 mm diameter disks were punched from zinc foil (380 μm thick) and their rate of dissolution in HCl was measured at each level of the tower (3 disks/level). The acid solution also contained 50 mM KNO_3 to act as a depolarizer and prevent H_2 evolution. King and Braverman (1932) showed that the dissolution of rotating

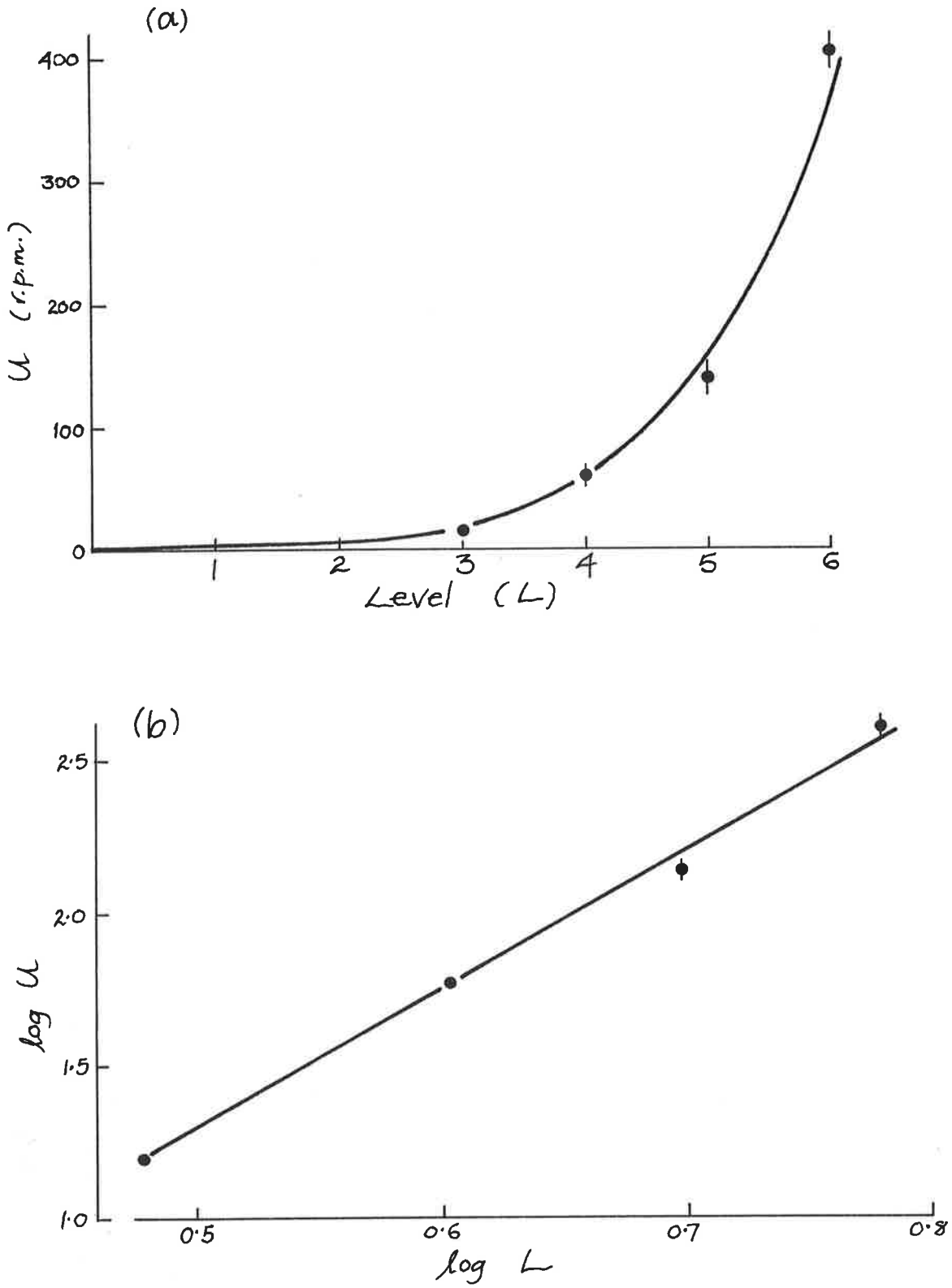

FIGURE 11. (a) Angular velocity, U, of water in different levels, L, of the stirring gradient tower.

(b) Plot of log U against log L. The slope of the line is 4·5.

zinc cylinders in HCl solutions is rate limited by the diffusion of HCl in the boundary layer at speeds upto 5,600 r.p.m. Before the experiment, the disks were etched for 10 s in 5 M HCl, washed in deionized water, then in ethanol and finally blotted and weighed. Batches of disks not being weighed were kept in deionized water; the rate of dissolution was immeasurably small under these conditions. The disks were removed at various intervals and the change in weight plotted against time. The change in surface area was negligible.

Results are shown in Fig.12 a, b and c. The weight changes were non-linear with time, which may have been due to impurities in the zinc foil reacting with the HCl/KNO_3 solutions and producing an impervious coating. However, the initial rates allow k_T to be calculated for each level of the tower, for the three concentrations of HCl used. These calculations are shown in Table 1, together with the inferred unstirred layer thicknesses (both sides of the disk). Fig.13 shows a plot of log k_T against the log of the water velocity, U (calculated from equation (29) for levels 1 and 2). The points fit well to a straight line of slope 0.35, which suggests $k_T \propto U^{0.35}$. Low powers on U (i.e.< 0.5) have been found by some workers (Sackur, 1906; Eucken, 1932; Trümpler and Zeller, 1951); they would appear to indicate "sub-laminar" flow. Perhaps in my case the interstices of

the stainless steel mesh trap pockets of fluid which do not mix with the bulk solution, giving rise to a weaker dependence of k_T on fluid velocity than is predicted for pure laminar flow.

TABLE 1

Values of the transport coefficient, k_T, from the initial slopes of Figs. 12a, b and c. The last entry in each column is the mean value, ± the standard error of the mean. Also shown are the thicknesses of the equivalent Nernst layers for HCl assuming, at the ionic strength of these experiments, a mean ionic diffusion coefficient for HCl of 3.07×10^{-9} m^2 s^{-1} (Robinson and Stokes, 1959).

$k_T \times 10^5$ (m s^{-1})

[HCl](mM)	Level 1	Level 2	Level 3	Level 4	Level 5
5	0.275	1.92	3.75	5.17	7.40
10	1.35	2.63	5.28	8.39	10.5
20	1.16	1.94	3.97	4.89	7.61
	0.928 ± 0.27	2.16 ± 0.19	4.33 ± 0.39	6.15 ± 0.92	8.50 ±0.82

δ (each side of the disk) for HCl (μm)

331 ± 75	142 ± 11	70.9 ± 5.9	49.9 ± 6.5	36.1 ± 3.2

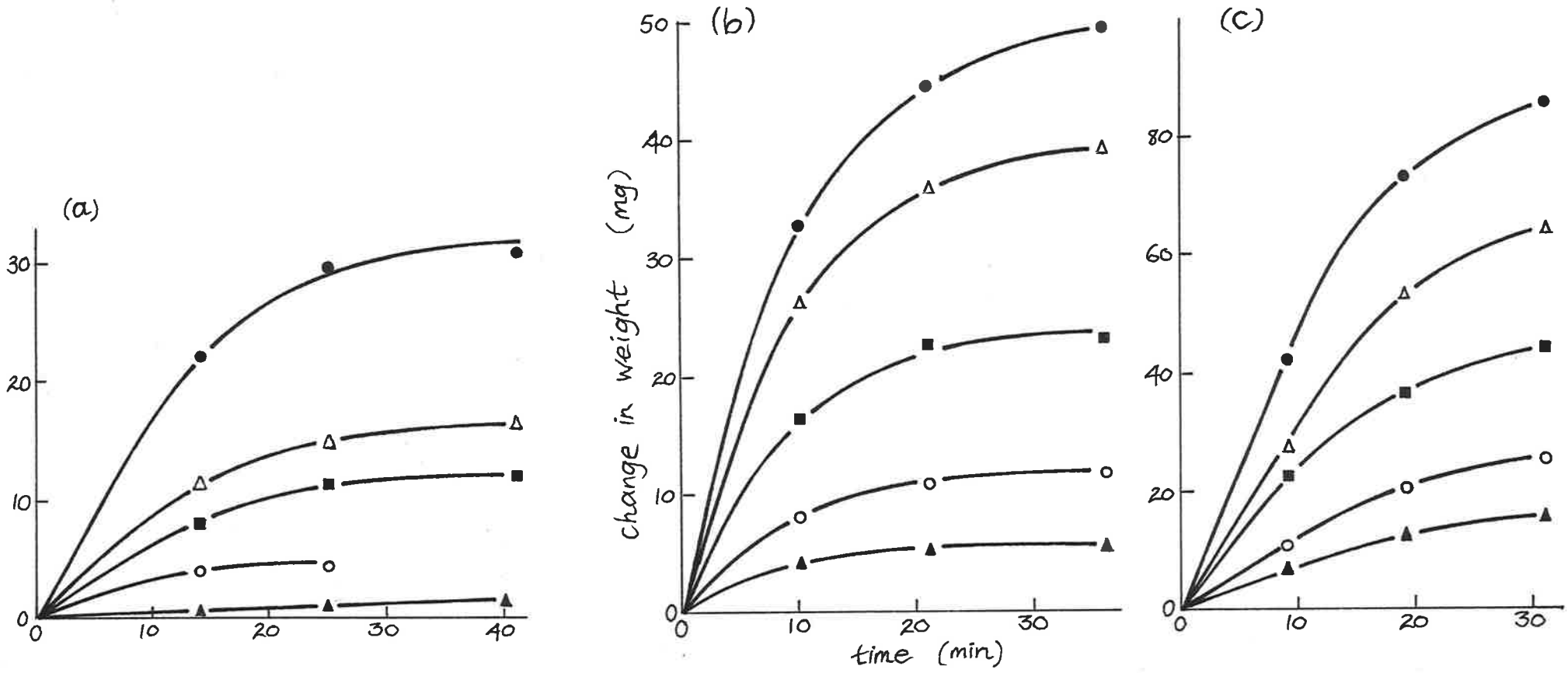

FIGURE 12. Rate of dissolution of zinc disks in the five levels of the stirring gradient tower, (▲) level 1, (o) level 2, (■) level 3, (Δ) level 4 and (●) level 5, in (a) 5 mM, (b) 10 mM and (c) 20 mM HCl. 25°C.

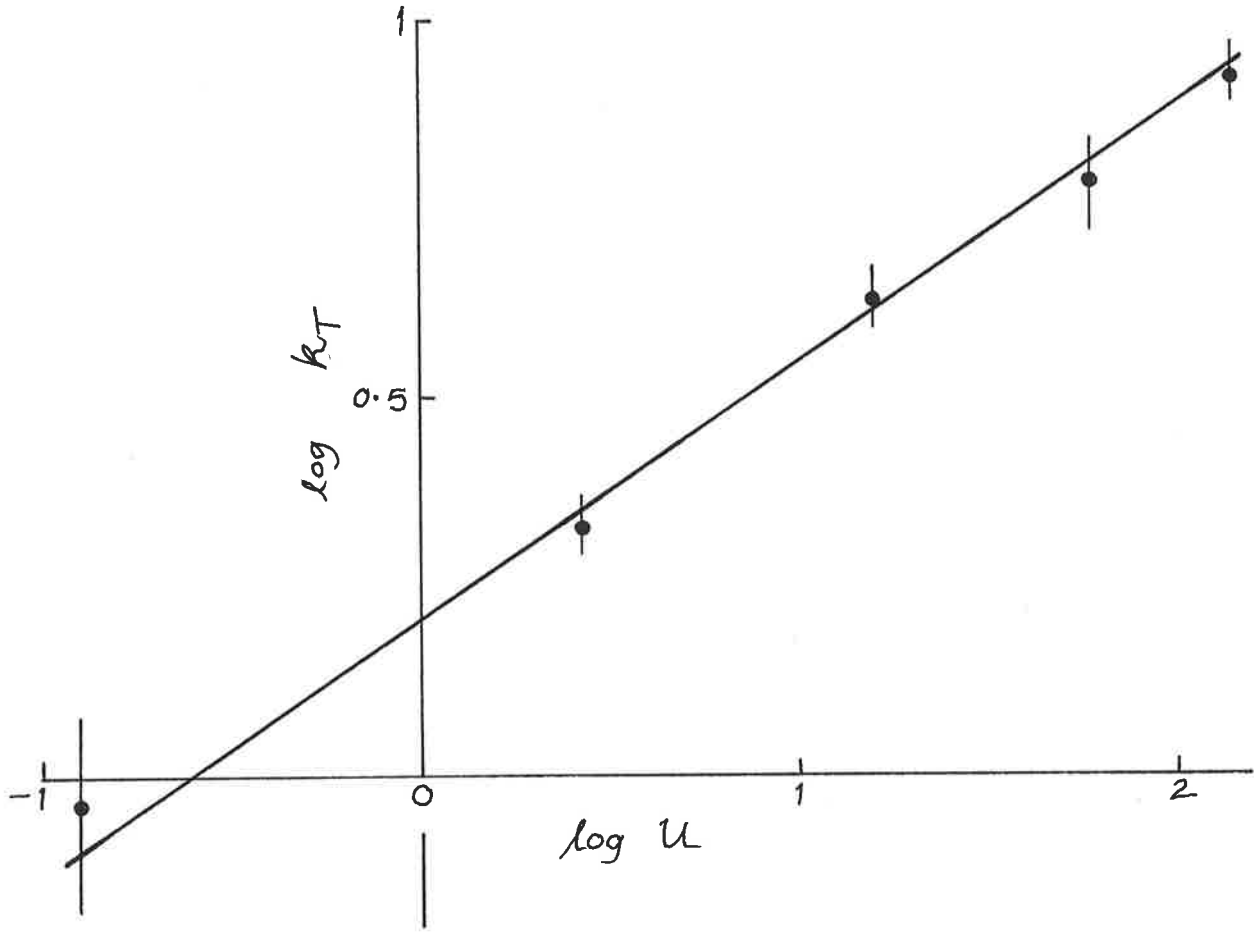

FIGURE 13. Relationship between k_T (Table 1) and U (Fig. 11) in the stirring gradient tower; the slope of the line is 0·35.

I. Uptake of [^{14}C] Methylamine by Ulva rigida

(i) Results

Figures 14 - 17 present the results of a number of experiments on the kinetics of [^{14}C]methylamine* influx and the effects of stirring. In Fig. 14a, the experiment was conducted by the method described in MacFarlane and Smith (1982), with and without shaking. For comparison, Fig. 7 of MacFarlane (1979) is shown in an inset. The shaking rate was such that additional hand swirling made little difference to the rates of uptake. In Fig. 14b the second, linear phase of the "stirred" curve (shown in Fig. 14a as a dashed line) has been subtracted; the solid line represents the Michaelis-Menten equation with $K_M = 20\ \mu M$ and $V = 70$ nmol $m^{-2}\ s^{-1}$.

Figures 15, 16 and 17 represent a number of experiments using the stirring gradient tower. These experiments were done at pH 7.3 - 7.4 so that CH_3NH_2 influx would be negligible. At high concentrations of methylamine it appears that stirring sometimes reduces the rate of uptake. At low concentrations, $CH_3NH_3^+$ influx is markedly greater from a stirred compared with

---

*"Methylamine" refers non - specifically to both free base (CH_3NH_2) and conjugate acid ($CH_3NH_3^+$). Where the distinction is important, chemical formulae will be written.

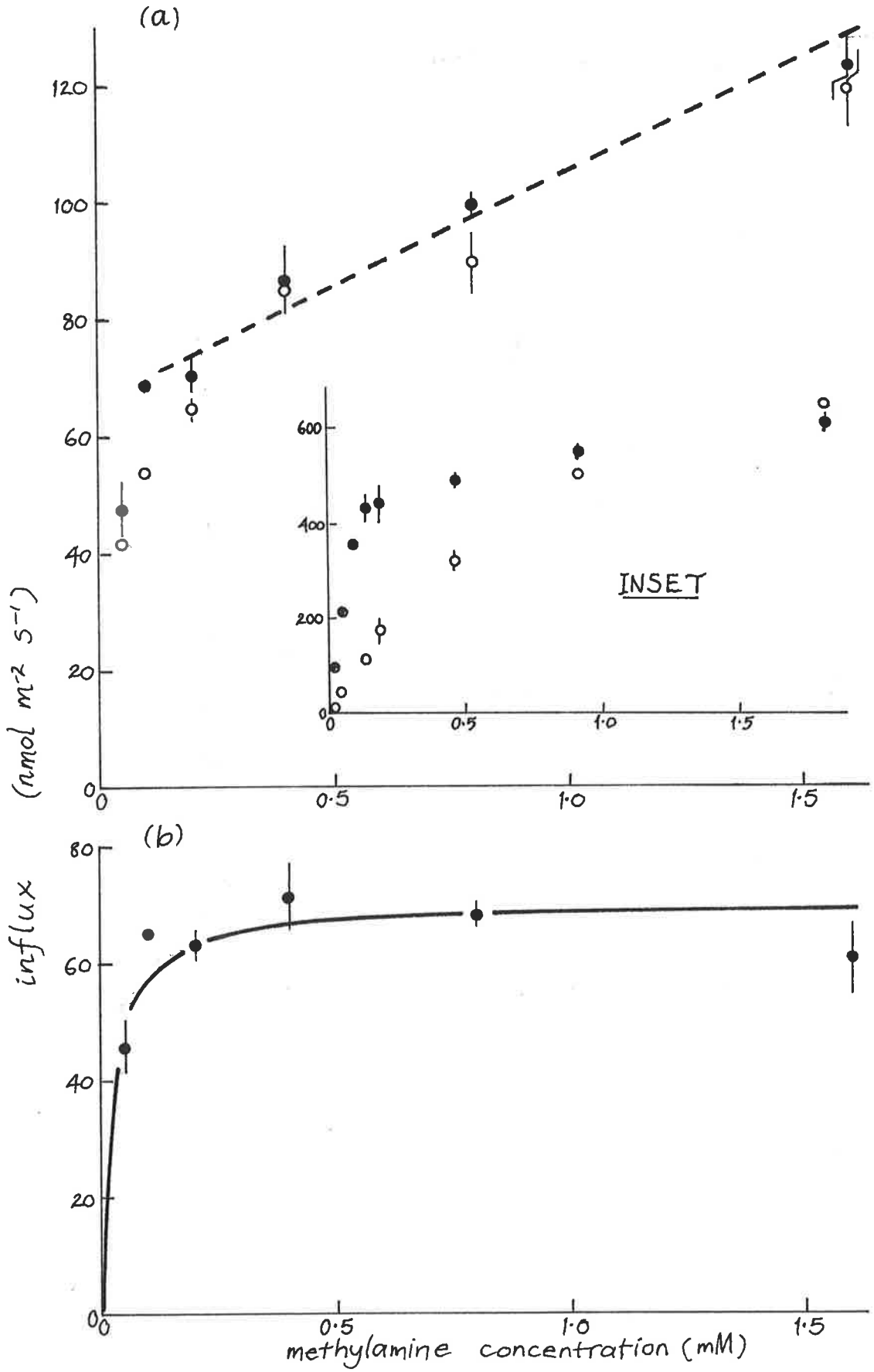

FIGURE 14a and Inset: Methylamine influx in U.rigida from stirred (●) and unstirred (○) ASW (pH 8·2 - 8·3, TAPS) at various concentrations of methylamine.

b: The "stirred" curve above with the second, linear, phase subtracted. T = 27°C. (T = 20°C for results shown in Inset.)

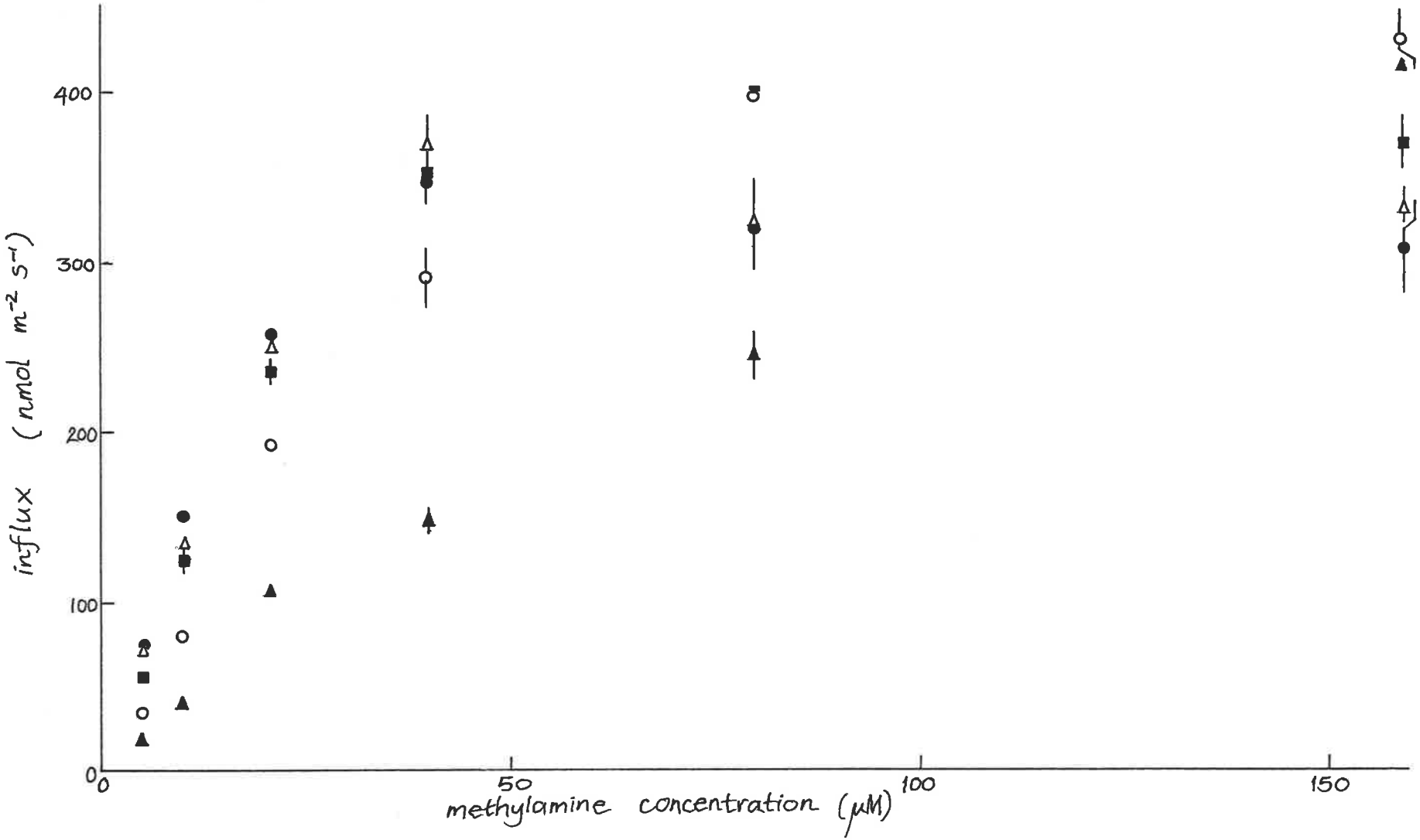

FIGURE 15. $[^{14}C]$methylamine influx versus the methylamine concentration for U.rigida disks (31•3 = 1•9 g fresh weight m^{-2}) in levels 1 (▲), 2 (o), 3 (■), 4 (△) and 5 (●) of the stirring gradient tower. ASW + 10 mM TES, pH 7.30, 25°C. Stirrer on no. 7.

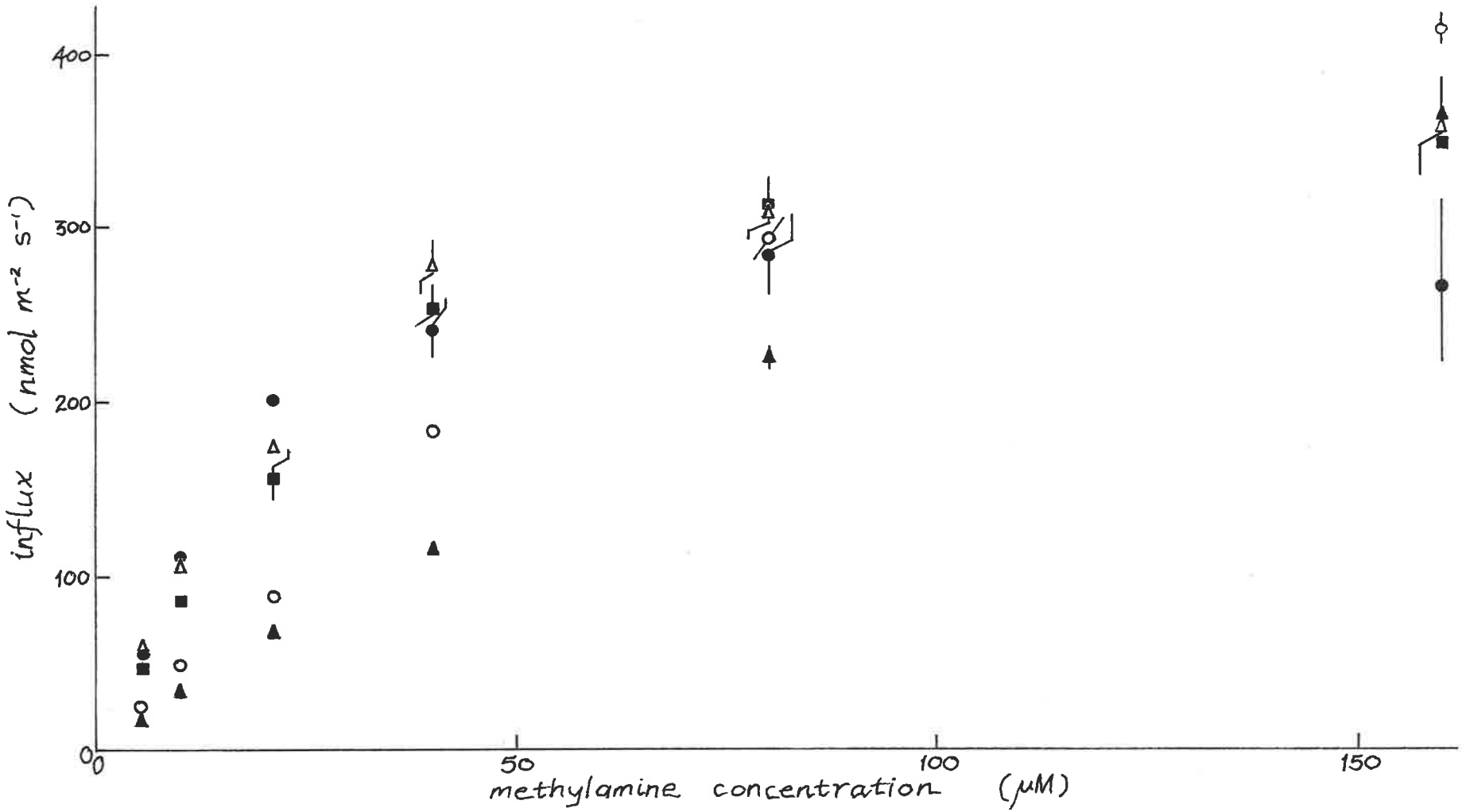

FIGURE 16. [^{14}C]methylamine influx vs. concentration for U.rigida disks (25·0 ± 2·1 g fresh weight m^{-2}) in the five levels of the stirring gradient tower (symbols as in Fig. 15). ASW + 10 mM TES, pH 7.30, 25°C, stirrer on no. 5.

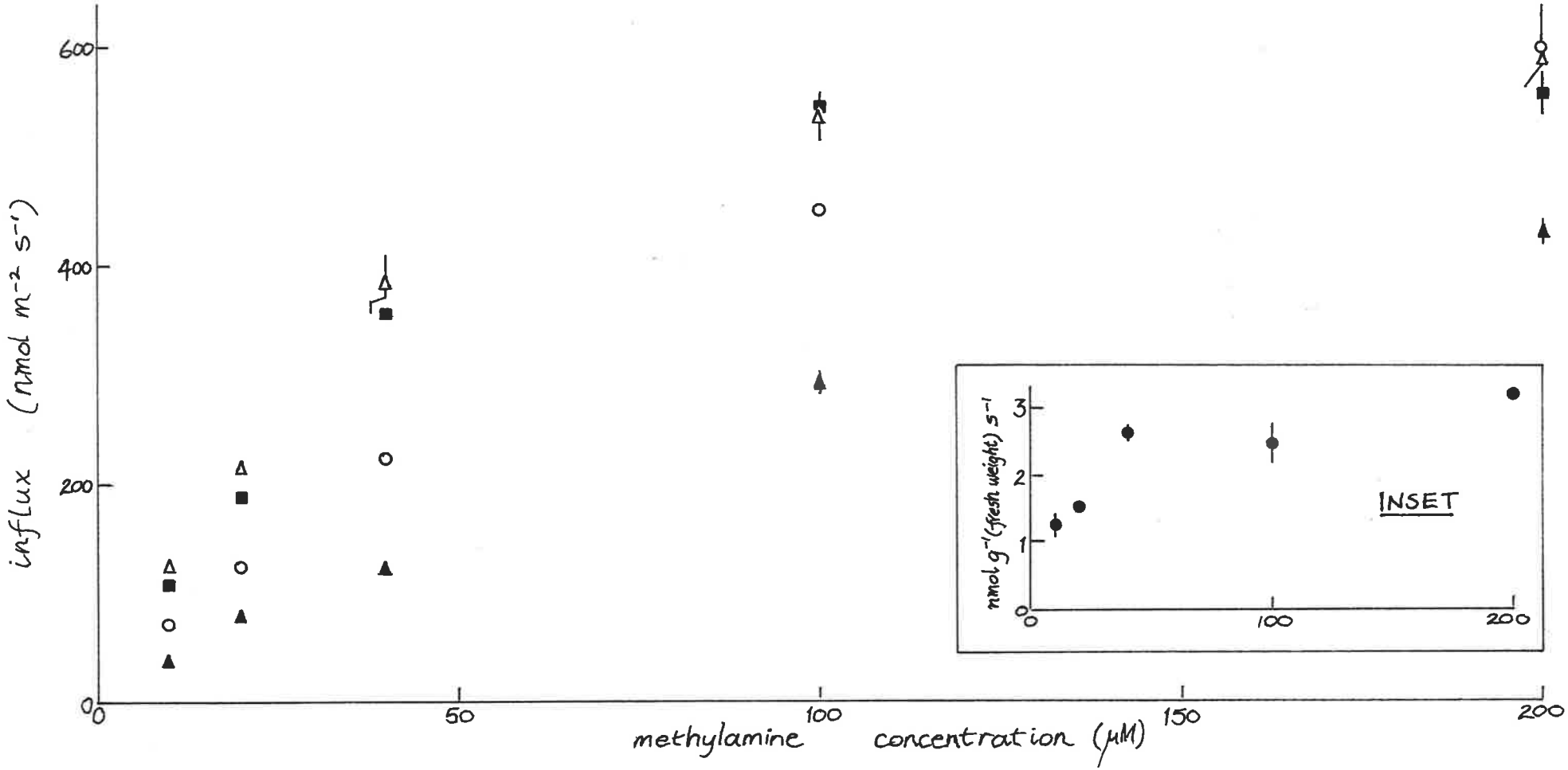

FIGURE 17. [^{14}C]methylamine influx vs. concentration for U.rigida disks (38·4 ± 3·1 g fresh weight m^{-2}) and slices in the stirring gradient tower (symbols as in Fig. 15). Disks were in levels 1 - 4, slices (Inset) in level 5. ASW + 10 mM TES, pH 7.41, 25°C, stirrer on no. 7.

a nearly stagnant solution. The difference in the influx between levels 3, 4 and 5 is comparatively slight.

For the experiments shown in Fig. 15 and 17 the magnetic stirrer was set on "7" ($\sim$ 420 r.p.m.). In Fig. 16 it was set on "5" ($\sim$ 250 r.p.m.).

(ii) Boundary layer limitations and V

Maximum rates of $CH_3NH_3^+$ uptake by U. rigida were found to be quite variable by MacFarlane and Smith (1982), and possibly affected by the overall nitrogen status of the tissue (cf.Wallentinus, 1984). In Fig. 14a if the second, linear phase of the curve represents CH_3NH_2 influx then the maximum rate of $CH_3NH_3^+$ uptake is very low (cf. inset and Figs. 15,16 and 17). Influx is scarcely affected by stirring in this case which is in agreement with the Briggs-Maskell equation. This equation predicts that the extent of diffusion limitations in the boundary layer depends on the relative size of V/K_M and $2k_T$ (p 9); these two are presumably similar in this case. If diffusion limitations are slight, then Fig. 14a allows an initial estimate of 20 μM for the true K_M of $CH_3NH_3^+$ transport (see Fig. 14b).

(iii) The effect of stirring at high methylamine concentrations

Fig. 15 in particular implies that $CH_3NH_3^+$ influx is

adversely affected by stirring at high methylamine concentrations. MacFarlane and Smith (1984) suggested that this reflected a decrease in the observed V due to CH_3NH_2 efflux, which would become more rapid as the unstirred layer thickness decreased. They corrected for this by bringing all estimated V's to the V estimated for the least-well-stirred solution (level 1).

In Fig. 17 increased stirring does not lower influx at high external concentrations which suggests that the effect may be associated with my experimental technique. This probably has to do with the order in which the disks were placed into their scintillation vials. After the five minute rinse in non-radioactive solution, the disks were left in their sieves resting on damp paper towelling, and removed thence to their vials. In Fig. 15, the disks from level 1 were removed first and those from level 5 last. In Fig. 17 the order was reversed for all concentrations, i.e. disks from level 5 were removed first, level 1 disks last. Also in this experiment the sieves were <u>not</u> left resting on the damp towelling. In Fig. 16, the order of removal varied. The time delay between first and last was of the order of five minutes and so a significant amount of intracellular tracer could have been lost to the paper towelling in that time. If the amount lost were a constant fraction of the amount of tracer present, then it could be corrected for by assuming that the true V in

Fig. 15 is the same for each level and that this V is given by the disks which were first removed to their vials. This correction would be the same as the one carried out by MacFarlane and Smith (1984), but for a different reason. However, in view of the uncertainty associated with these results, I will tend to ignore them in subsequent discussion.

(iv) The saturation of influx with stirring

$CH_3NH_3^+$ influx is not greatly increased in level 5 as compared with level 4 or even level 3 (Fig. 16, 17), yet the experiment with zinc disks (Materials and Methods) shows that the thickness of the unstirred layer is significantly reduced. The saturation must be due to rate limitation by some factor other than transport through the external boundary layer. The obvious candidate is transport through the membrane, and this is suggested by Fig. 16 where the K_M^{app} for the most well stirred solution is about 20 μM (cf. the estimate from Fig. 14b). In Fig. 17 however, K_M^{app} in level 4 is 30 μM or more and influx still appears to be linearly dependent on concentration up to near saturation values, when there is a sharp transition to the maximum rate. It is possible, then, that transport through the cell walls, which also will not be affected by stirring, is limiting here. This idea is supported by the data for $CH_3NH_3^+$ uptake by slices (inset, Fig. 17) in which K_M^{app}

is significantly reduced ($K_M^{app} \sim 18\ \mu M$:inset, Fig 19). Compared with Fig. 16, V is some 50% larger in Fig. 17, and the fresh weight per unit area (which quantitatively is related to thallus thickness) is higher by 54%; both of these would lead to more significant diffusional limitations due to cell wall.

(v) Comparison of observed with predicted kinetics

The experiment with zinc disks (Materials and Methods) gives values for the mass transfer coefficient, k_T, with the magnetic stirrer on its maximum setting ("8.4" ≡ 610 r.p.m.). For the experiments shown in Figs. 15 and 17, the stirrer was on "7" (≡ 420 r.p.m.). Since $k_T \propto U^{0.35}$, all the values for k_T will be decreased by $(420/610)^{0.35} = 0.878$. In Fig. 16, the stirrer was set on 5 (≡ 250 r.p.m.), giving predicted k_T's 0.732 times their value in the zinc disk experiment. k_T will be further decreased because of its dependence on the diffusion coefficient. For the ionic strengths used in the zinc disk experiment, D for HCl is about 3.07×10^{-9} m^2 s^{-1} (Robinson and Stokes, 1959) while $D^{CH_3NH_3^+}$ in sea water is about 1.16×10^{-9} m^2 s^{-1} (Tanaka and Hashitani, 1971, and using $D \propto$ molecular weight $^{-\frac{1}{2}}$). Thus, k_T will be reduced in proportion to $(1.16 \times 10^{-9}/3.07 \times 10^{-9})^{\frac{2}{3}}$ (equations (16) and (18)) which is equal to 0.523. The predicted k_T's for Fig. 15 and 17 are then 0.426, 0.992, 1.99, 2.82 and 3.90×10^{-5} m s^{-1} and for Fig. 16, 0.355, 0.827, 1.66, 2.35 and

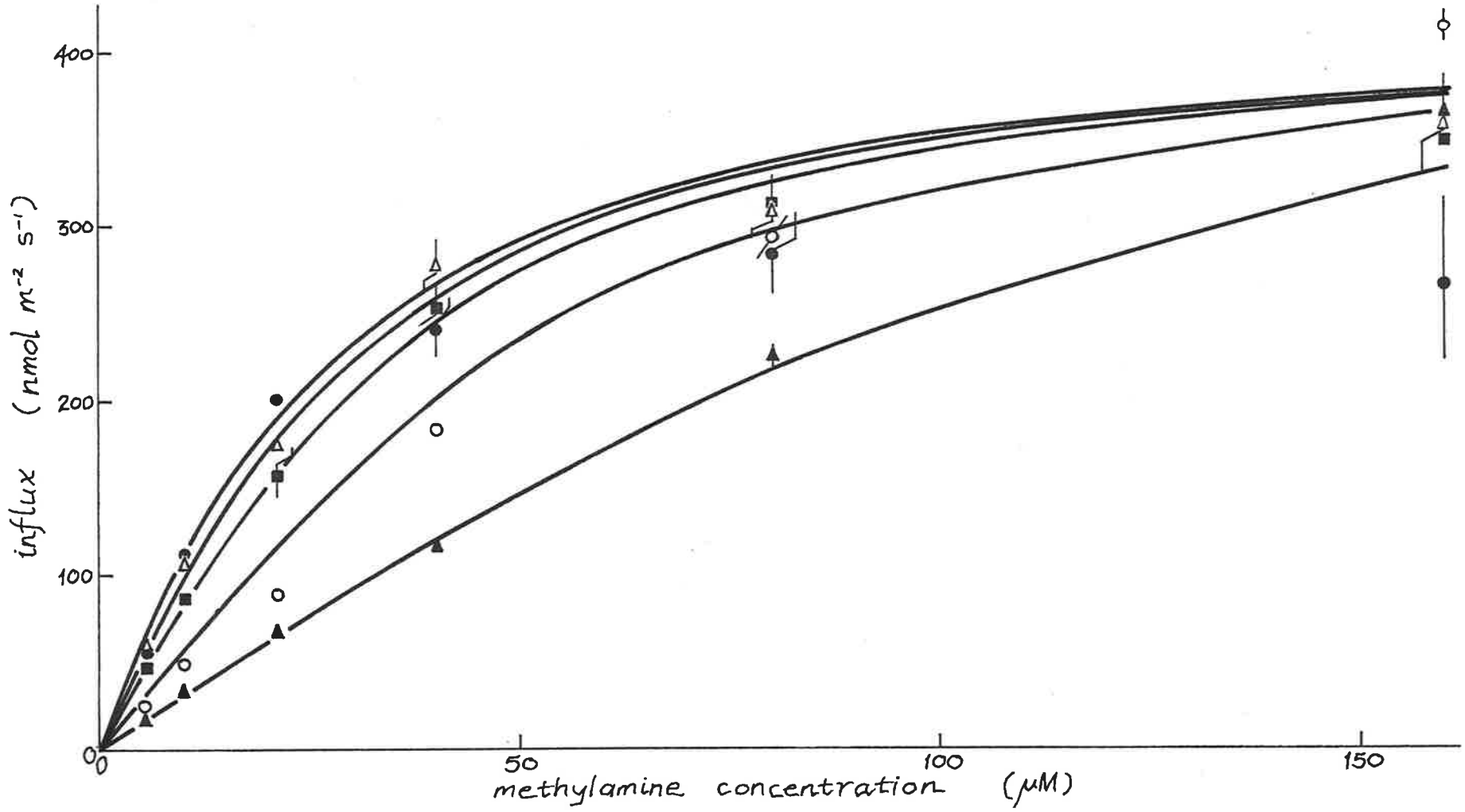

FIGURE 18. Influx against concentration curves for the Briggs-Maskell equation (equation 12). From left to right, values of k_T are: 3.25, 2.35, 1.66, 0.827 and 0.355 x 10^{-5} m s^{-1}. K_M = 18 μM, V = 420 nmol m^{-2} s^{-1}. The symbols are the data of Fig. 16.

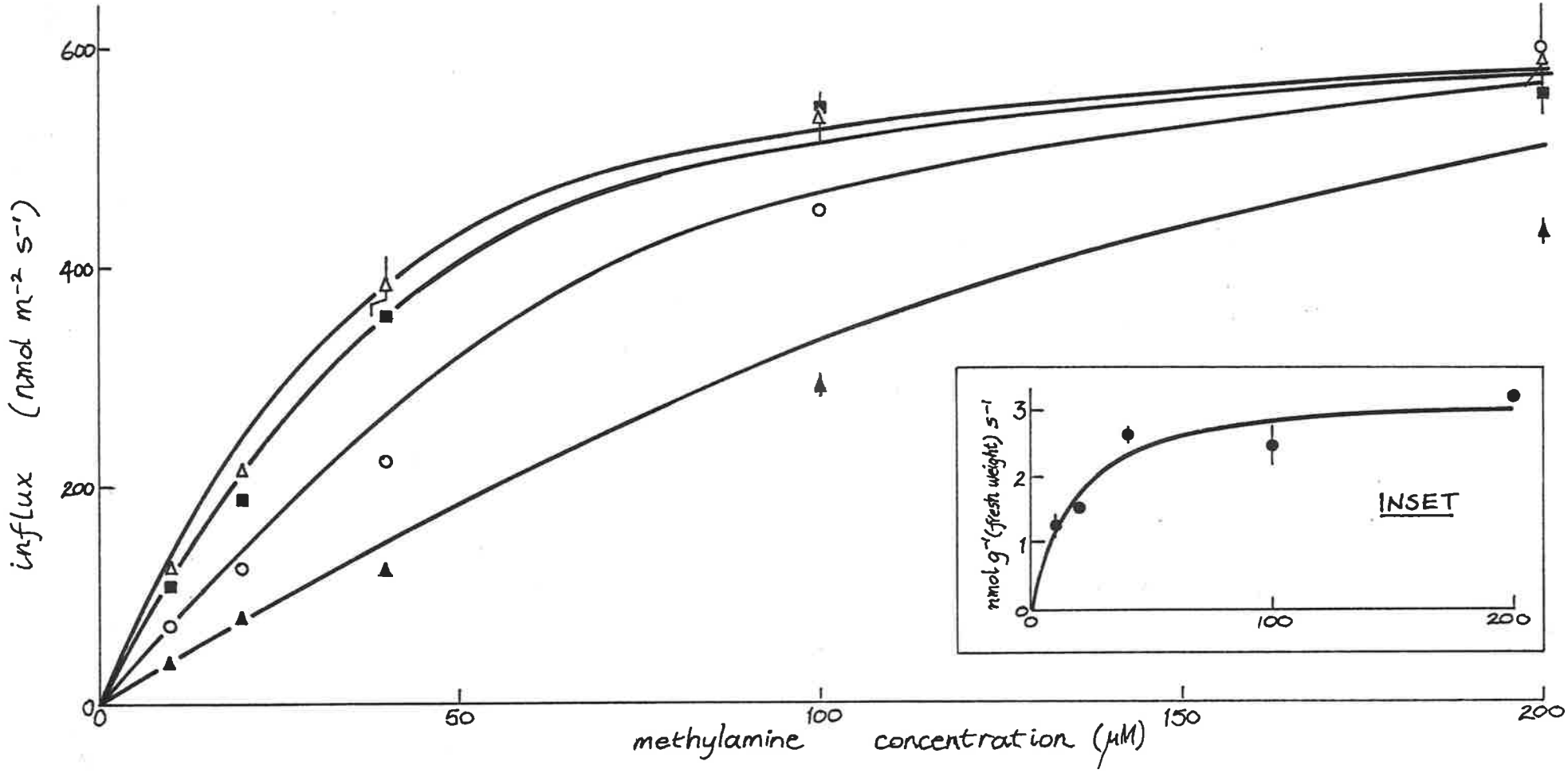

FIGURE 19. Influx against concentration curves for the Briggs-Maskell equation using k_T's of 3.90, 2.82, 1.99, 0.992 and 0.426×10^{-5} m s^{-1}, K_M = 18 μM and V = 636 nmol m^{-2} s^{-1}. Inset: $k_T \rightarrow \infty$, K_M = 18 μM, V = 3.25 nmol $g^{-1}_{fresh\ wt.}$ s^{-1}. The symbols are those of Fig. 17.

3.25×10^{-5} m s^{-1} (levels 1 to 5 respectively).

Plots of the Briggs-Maskell equation using these values of k_T and K_M = 18 μM are shown in Figs. 18 and 19 with the corresponding data of Figs. 16 and 17. In Fig. 18 there is good agreement between theory and experiment. Fig. 19 shows that the Briggs-Maskell equation tends to over-estimate the influx at low methylamine concentrations, which might be due to transport restrictions in the cell wall.

If $CH_3NH_3^+$ porters are distributed evenly over the surface of the membrane then transport through the cell wall will be not only in series with membrane transport, but also in parallel with it. The two situations are illustrated in Fig. 20. The thallus can be thought of as a reacting slab of the thickness of region II surrounded by the unstirred layer of outer cell wall and thin mucilaginous cuticle (region I).

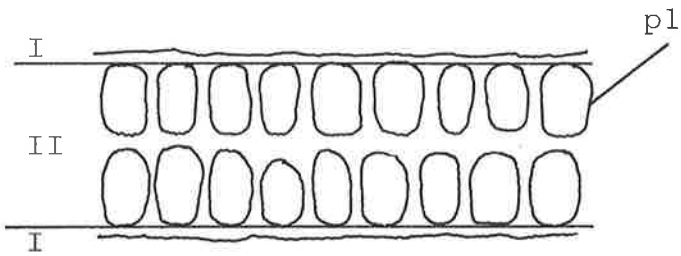

Fig. 20. T.S. Ulva thallus, diagramatic. I - region where transport is in series with reaction. II - transport in parallel with reaction. Reaction is membrane transport $R_{in} \rightleftharpoons R_{out}$

The thallus thickness was not measured for the results shown in Figs. 16 and 17. However, if the thickness is linearly related to the fresh weight (and they are certainly related qualitatively), then the thickness can be estimated. This gives 51 μm for the results shown in Fig. 17 and 33 μm for Fig. 16. 5 - 7% of this consists of outer cell wall. In Fig. 17 then, region II is about 48 μm thick, and region I about 1.5 μm. Using a K_M for $CH_3NH_3^+$ influx of 18 μM, V equal to 27.5 mmol $\underline{m^{-3}}$ s^{-1} (660 nmol m^{-2} s^{-1}) and D_{eff} in cell wall (and mucilage) half its value in sea water*, it is possible to use Yamané's equation (equation V.21) to calculate η and thence the expected influx for various concentrations of methylamine. This graph is shown in Fig. 21 with the data of Fig. 17. Biot numbers have been calculated by combining the k_T's predicted from the zinc disk experiment with k_T for transport through the two outer cell walls (1.93×10^{-4} m s^{-1}) in the manner of equation (28). The agreement between theory and experiment is much better when internal resistances to mass-transport are taken into account. Yamané's equation is also a good fit to the

* Good measurements of diffusion coefficients in cell walls are scarce (Walker and Pitman (1976). Self diffusion coefficients will be reduced because of the tortuosity of the diffusion pathway and because only a fraction of the cell wall is aqueous. A number of workers have found a reduction of about 50% for the effective D in the cell wall cf. the bulk medium (Kohn and Dainty, 1966; Tyree, 1968; Pitman, Luttge, Kramer and Ball, 1974; Smith and Fox, 1975). There are, however, reports of greater reductions (see Walker and Pitman, 1976). My estimate of D_{eff} may then be too high.

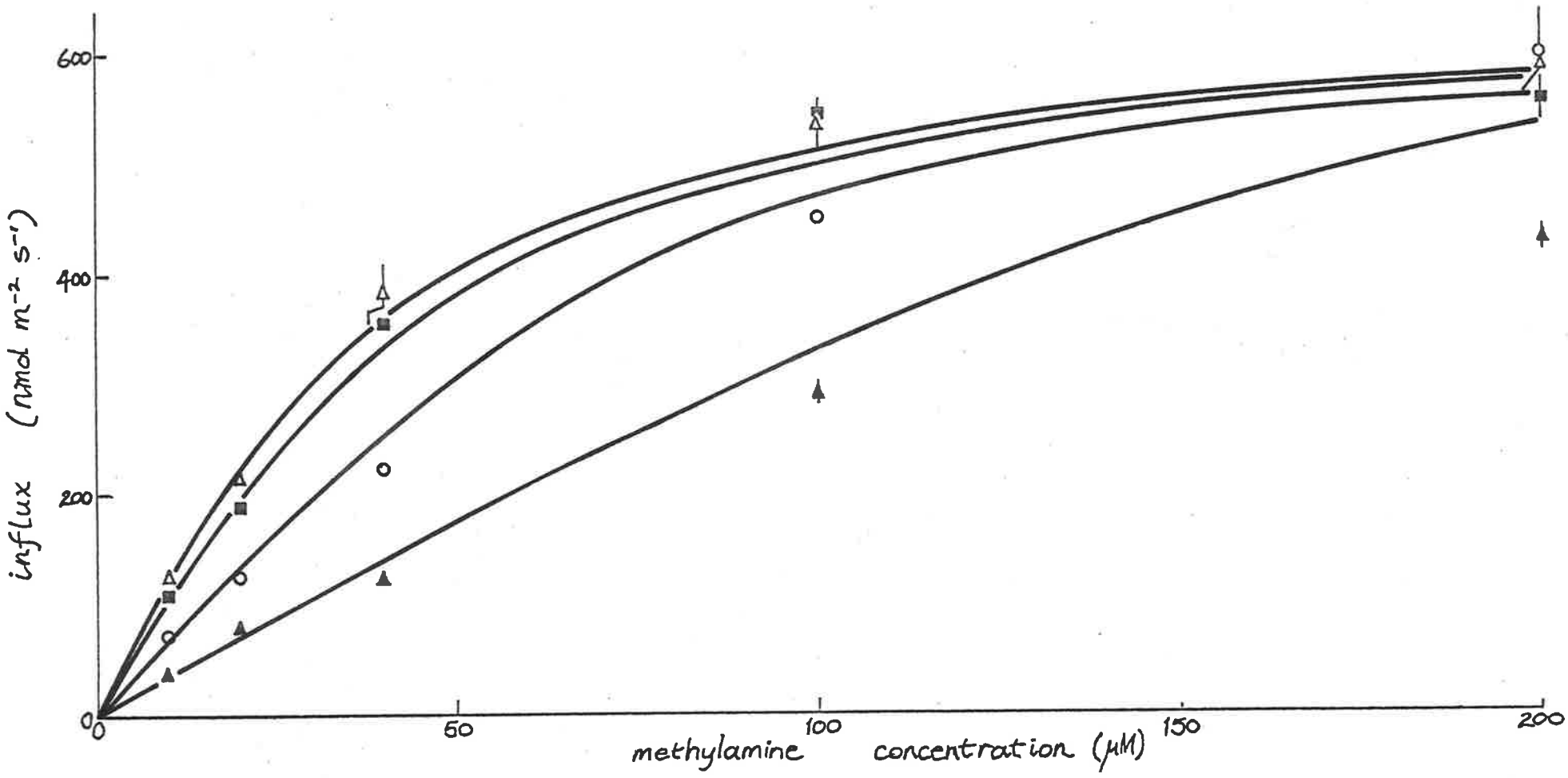

FIGURE 21. Influx versus concentration curves based on Yamané's equation for Biot numbers of 1.02, 0.745, 0.391 and 0.173 (left to right), D_{eff} = 5.80 x 10^{-10} m^2 s^{-1}, R = 24 μm, K_M = 18 μM and V = 27.5 mmol m^{-3} s^{-1}. Symbols are the data of Fig. 17.

data of Fig. 16 (again using a slightly higher V than the Briggs-Maskell equation predicts); in this case, internal diffusion limitations are not as severe mainly because of the thinner tissue.

(vi) Other analyses

Some of the data was analysed using the computer programme FVKUP developed by N.A. Walker (see Smith and Walker, 1980; cf. Märkl, 1977). This programme fits the Briggs-Maskell equation to the data by adjusting the three variables V, K_M and k_T from initial, guessed values. A good fit means that the sum of (weighted) squared differences between observed and calculated values is very low - this is indicated by a regression coefficient close to one.

TABLE 2

Parameters in the Briggs-Maskell equation predicted by FVKUP, and regression coefficients, for the data of Fig. 17.

	Level 1	Level 2	Level 3	Level 4
V (nmol m^{-2} s^{-1})	847	1040	617	706
K_M (μM)	176	126	10.6	31.8
k_T (m s^{-1} x 10^{-5})	2.19	6.00	1.39	3.75
Regression coefficient	0.999	1.000	1.000	1.000

Table 2 shows some results for the data of Fig. 17; each of the data points was weighted according to the inverse of its variance. Calculated K_M's vary considerably and the k_T's do not follow the order expected in the different levels. In levels 3 and 4, however, the calculated k_T's are close to those predicted by the zinc disk experiment and the K_M values are either side of the 18 μM estimated from the experiment with slices. In levels 1 and 2, the computer programme has opted for a relatively low boundary layer resistance and a high K_M, whereas the opposite is likely to be the case.

Fig. 22 shows the graphical analysis of Gains (1980). Fig 22a is simply an Eadie-Hofstee plot of the data of Fig. 17, with the estimated V for slices made equal to that for disks. The deviations from linearity brought about by the unstirred layer are clearly seen (Thomson, 1979a; cf. Winne, 1973). The intercepts on the J/c_b axis are referred to as $(J/c_b)_{c_b=0}$; they are the initial slopes of the J versus c_b hyperbolae (c_b refers to the bulk concentration of methylamine). The intercepts of the curves in Fig. 22a with various values of J have been divided by their respective $(J/c_b)_{c_b=0}$ values to yield the set of lines shown in Fig. 22b. Eight values of J were chosen, ranging from 444 (the lowest line), to 55.6 (the uppermost line) nmol m^{-2} s^{-1}, in steps of 55.6 nmol m^{-2} s^{-1}. The points are very

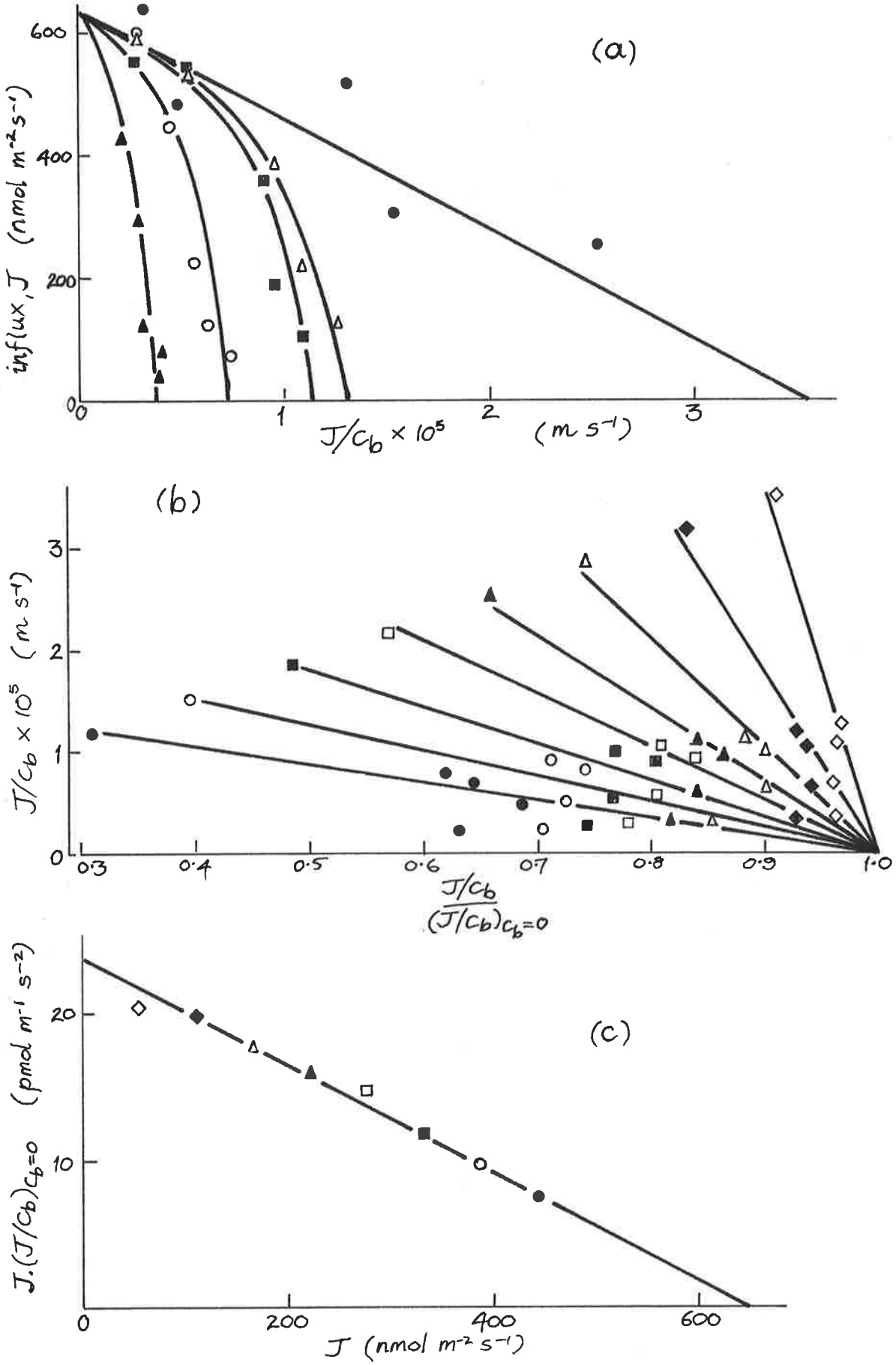

FIGURE 22. Analysis of the data of Fig. 17 by the method of Gains (1980); the symbols in (a) have the same meaning as in Fig. 17, but in (b) and (c) they represent different values of J. For further explanation, see text.

scattered, and the straight lines drawn in Fig. 22b are hardly justified; they are based almost exclusively on the data for slices and the two most well stirred levels of the tower, besides the fact that the quotient of J/c_b and $(J/c_b)_{c_b=0}$ at $J/c_b = 0$ should be unity. The slopes of the lines have been multiplied by their respective J's and plotted against J to generate Fig. 22c. The intercept on the abscissa is V (653 nmol m^{-2} s^{-1}) while that on the ordinate (23.7 pmol m^{-1} s^{-2}) is V^2/K_M. The predicted K_M is then 18 μM. The reciprocal of k_T (the boundary layer "resistance") is obtained by subtracting K_M/V from the reciprocal of the intercepts on the J/c_b axis (Fig 22a). This procedure predicts k_T's of 0.418, 0.880, 1.63 and 2.04 x 10^{-5} m s^{-1} for levels 1 to 4 respectively (the predicted k_T for slices is infinity). There is, therefore, very good agreement with the k_T's derived from the zinc disk experiment. However, for the analysis to be at all reliable when k_T's are small (i.e. when the apparent K_M is far removed from the true K_M), one would require a lot of very good data, particularly at c_b's less than the K_M^{app}. In Fig. 22b, if the data for slices were absent, any justification for the straight lines drawn would practically disappear.

II. Uptake of [^{32}P] Phosphate by Ulva rigida

Phosphate uptake by plants is generally considered to be via, and rate-limited by, a membrane porter

(Schwoerbel and Tillmans, 1964; Loneragen and Asher, 1967; Raven, 1980; Falkner, Horner and Simonis, 1980). Over a large range of phosphate concentrations, the influx versus concentration curve is often complex and could represent two (or more) separate porters having different values of K_M and V (Laties, 1969); it is also possible that the simple diffusion of phosphate across the plasmalemma becomes important at high concentrations (Laties, 1969; Edwards, 1970; Barber, 1972; cf. Maynard and Lucas, 1982). At low external phosphate concentrations, however, it appears that the influx is due to the operation of a membrane porter and the kinetics of influx are of the Michaelis-Menten (Briggs-Haldane) type (Bieleski, 1973; Falkner, Werden, Horner and Heldt, 1974).

Fig. 23 supports this notion showing that ^{32}P-phosphate influx into disks of Ulva rigida in the five levels of the stirring gradient tower has a typical hyperbolic response to concentration. However, even though stirring can increase the phosphate influx by nearly 2·5 fold at low concentrations, influx is much less affected by stirring than methylamine influx.

In this experiment, the stirrer was on its maximum setting; therefore the k_T values from the zinc disk experiment are directly applicable, allowing for the dependence on the diffusion coefficient. Measurements of phosphate diffusion coefficients are scarce, and

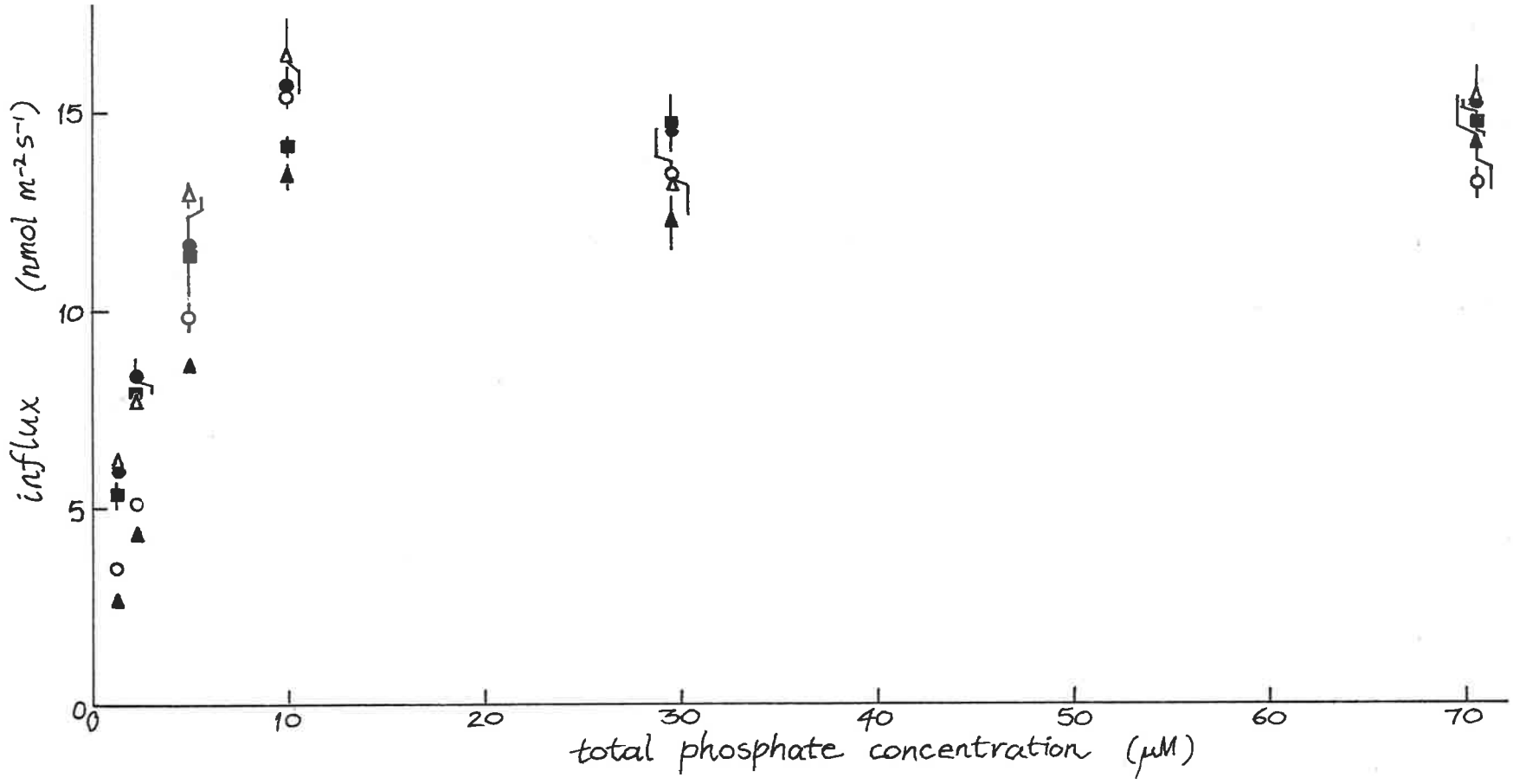

FIGURE 23. [^{32}P]phosphate influx versus phosphate concentration for U.rigida disks (36.3 ± 5.9 g fresh weight m^{-2}) in the five levels of the stirring gradient tower (symbols as in Fig. 15). ASW + 10 mM TES, pH 7.42 - 7.52, 25°C, stirrer on "8.4".

differ depending on the ion species in question (i.e. $H_2PO_4^-$, HPO_4^{2-} or PO_4^{3-}). Relatively meagre evidence suggests that, for the same ion concentration, $H_2PO_4^-$ is taken up much faster by plants than HPO_4^{2-} if the latter is taken up at all (Bieleski, 1973). $H_2PO_4^-$ uptake would certainly be the least expensive energetically for plant cells with a more negative electrical potential than the bathing medium. In U. rigida, phosphate influx from sea water with a high phosphate concentration is relatively constant from pH 5.6 to 7.9 (Fig. 24); however, both $[H_2PO_4^-]$ and $[HPO_4^{2-}]$ may have been high enough over this range of pH to saturate an $H_2PO_4^-$ or HPO_4^{2-} porter. Although $[H_2PO_4^-]$ is decreasing continually, it is still about 5 μM at pH 7.9. $[HPO_4^{2-}]$, on the other hand, is increasing to about pH 7.3 and thereafter decreasing; however there would always be enough HPO_4^{2-} to saturate any HPO_4^{2-} membrane porter over the entire range of pH. At pH 8.4 there is a sharp rise in the phosphate influx. It is very unlikely that this merely reflects the increase in $[PO_4^{3-}]$ since one would then have to assume that PO_4^{3-} influx is much greater than HPO_4^{2-} influx under conditions of a much steeper uphill gradient in electrical potential for the triply charged ion. The effect of pH is probably more indirect, such as a change in the driving force across the membrane or in the degree of phosphate binding in cell walls.

If $H_2PO_4^-$ is the species taken up by U. rigida, the

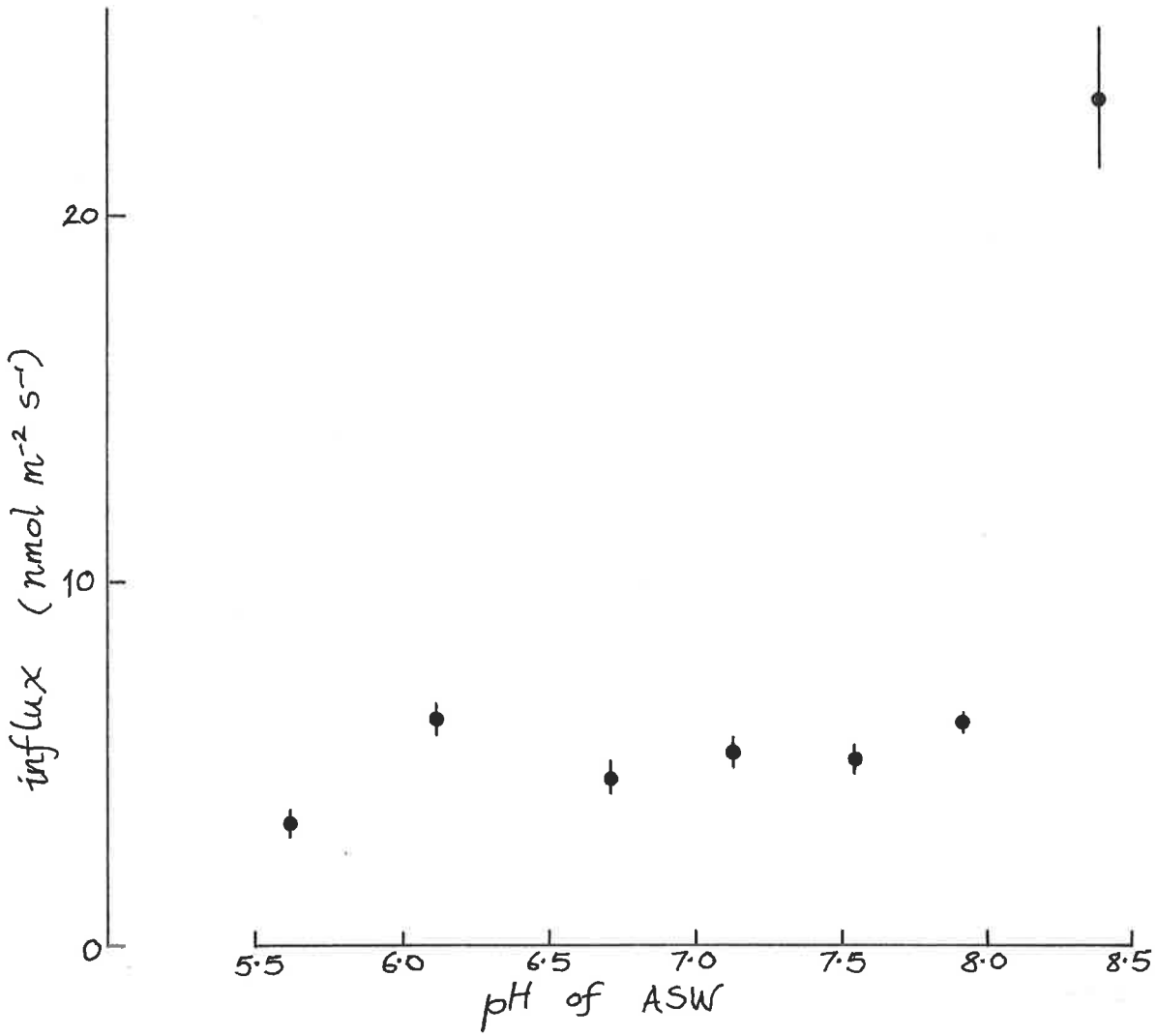

FIGURE 24. Influx of ^{32}P-phosphate at various pH's of ASW (unbuffered) for U.rigida disks (30.9 ± 0.27 g fresh weight m^{-2}) shaken in a shaker bath. Total phosphate concentration = 500 µM, T = 25°C.

correction to k_T is approximately $(6.88 \times 10^{-10}/3.07 \times 10^{-9})^{\frac{2}{3}}$, or 0.369. The diffusion coefficient of $H_2PO_4^-$ is estimated as 6.88×10^{-10} m^2 s^{-1} by multiplying the value at infinite dilution (9.50×10^{-10} m^2 s^{-1}: Gros, Moll, Hoppe and Gros, 1976) by the activity factor $1 + I \frac{d \ln \gamma}{d I}$ (Robinson and Stokes, 1959), where γ is the activity coefficient for $H_2PO_4^-$ and I the ionic strength. The activity factor was estimated as 0.724 at I = 0.7 M (sea water) from the data of Whitfield (1975). (In the same way, the correction for $k_T^{HPO_4^{2-}}$ becomes 0.147).

Since stirring has a relatively slight effect (at least compared with methylamine influx), and ignoring internal diffusion in cell walls, the K_M^{app} for phosphate influx in level 5 ($\sim$1.6 μM) must be close to the true K_M. Using K_M = 1.5 μM(total phosphate), V = 15 nmol m^{-2} s^{-1} and the corrected $k_T^{H_2PO_4^-}$s from the zinc disk experiment, the Briggs-Maskell equation generates the set of curves shown in Fig. 25. $[H_2PO_4^-]$ has been taken at 2.4% of the total phosphate concentration at pH 7.48 using a pK_a' for $H_2PO_4^-$ in sea water of 5.90 (an average value of the measurements quoted in Millero, 1983).

Clearly the theory is inadequate to explain the observed effects of stirring on phosphate influx; influx is grossly underestimated and the differences in influx between the levels of the stirring gradient tower are predicted to be much larger.

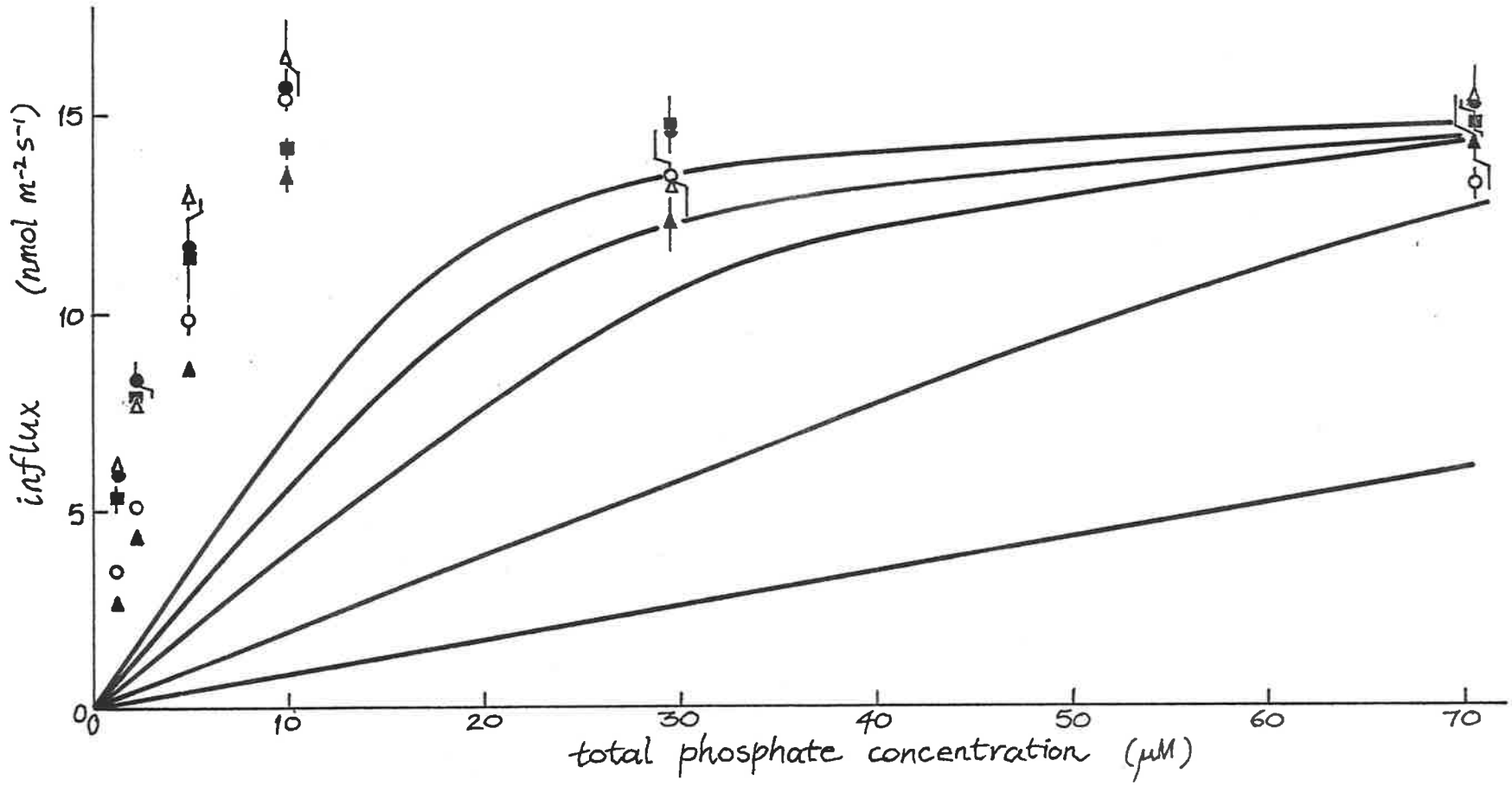

FIGURE 25. Influx versus concentration curves predicted by the Briggs-Maskell equation using k_T's for $H_2PO_4^-$ transport of 3.14, 2.27, 1.60, 0.797 and 0.342 x 10^{-5} m s^{-1} (left to right), K_M (total phosphate) = 1.5 μM and V = 15 nmol m^{-2} s^{-1}. The symbols are those of Fig. 23.

A likely explanation for the discrepancy lies in the fact that most (>97%) of the phosphate at the pH of this experiment is in the form of HPO_4^{2-} or PO_4^{3-}. This will effectively enhance the flux of $H_2PO_4^-$ across the diffusion boundary layer because there are now <u>three</u> species which can carry ^{32}P, not just the one. The flux, J, of $H_2PO_4^-$ through the unstirred layer will be

$$J_{H_2PO_4^-} = k_T^{H_2PO_4^-}(c_b^{H_2PO_4^-} - c_s^{H_2PO_4^-}) + k_T^{HPO_4^{2-}}(c_b^{HPO_4^{2-}} - c_s^{HPO_4^{2-}}) + k_T^{PO_4^{3-}}(c_b^{PO_4^{3-}} - c_s^{PO_4^{3-}}). \quad (30)$$

(This assumes that equilibrium between $H_2PO_4^-$, HPO_4^{2-} and PO_4^{3-} is established rapidly which is true in this case.) The concentrations (c_b and c_s) of HPO_4^{2-} and PO_4^{2-} can be expressed in terms of $H_2PO_4^-$ by $[HPO_4^{2-}] = \frac{K'_{a_2}}{(H^+)}[H_2PO_4^-]$ and $[PO_4^{3-}] = \frac{K'_{a_2}K'_{a_3}}{(H^+)^2}[H_2PO_4^-]$ (Butler, 1964) where K'_{a_2} and K'_{a_3} are the second and the third stoichiometric dissociation constants of H_3PO_4 and (H^+) is the activity of H^+ ions. Equation (30) then becomes

$$J_{H_2PO_4^-} = \left[k_T^{H_2PO_4^-} + k_T^{HPO_4^{2-}}\frac{K'_{a_2}}{(H^+)} + k_T^{PO_4^{3-}}\frac{K'_{a_2}K'_{a_3}}{(H^+)^2}\right](c_b^{H_2PO_4^-} - c_s^{H_2PO_4^-}) \quad (31)$$

which is of the same form as Nernst's expression but with an overall k_T equal to $k_T^{H_2PO_4^-} + k_T^{HPO_4^{2-}}\frac{K'_{a_2}}{(H^+)} + k_T^{PO_4^{3-}}\frac{K'_{a_2}K'_{a_3}}{(H^+)^2}$. Assuming that the pH gradient within the unstirred layer is negligible (i.e. (H^+) is everywhere equal to that in the bulk medium), overall k_T's for the

experiment shown in Fig. 23 can be calculated. These are shown in Table 3. The term due to PO_4^{3-} diffusion is ignored, because the PO_4^{3-} diffusion coefficient is small (in fact the simple formula based on the activity factor predicts a coefficient less than zero), and $[PO_4^{3-}]$ is only 6% of $[HPO_4^{2-}]$.

TABLE 3

Overall k_T's ($\sim k_T^{H_2PO_4^-} + k_T^{HPO_4^{2-}} K'_{a_2}/(H^+)$) for $H_2PO_4^-$ transport in the five levels of the stirring gradient tower, using $K'_{a_2} = 1.26 \times 10^{-6}$ M, $(H^+) = 3.31 \times 10^{-8}$ M (pH 7.48). Units of k_T are m $s^{-1} \times 10^{-5}$.

	Level 1	Level 2	Level 3	Level 4	Level 5
$k_T^{H_2PO_4^-}$	0.342	0.797	1.60	2.27	3.14
$k_T^{HPO_4^{2-}}$	0.136	0.318	0.637	0.904	1.25
overall k_T	5.52	12.9	25.8	36.7	50.7

Fig. 26 shows some plots of the Briggs-Maskell equation using these overall k_T's, together with the data of Fig.23. The agreement between theory and experiment is better, but influx still tends to be underestimated and stirring is still predicted to have a greater effect than it does in practise.

A probable explanation is that the pH within the unstirred layer is not constant. Although the sea water was buffered (10 mM TES) a pH rise close to the surface of the thallus is likely in view of the very rapid

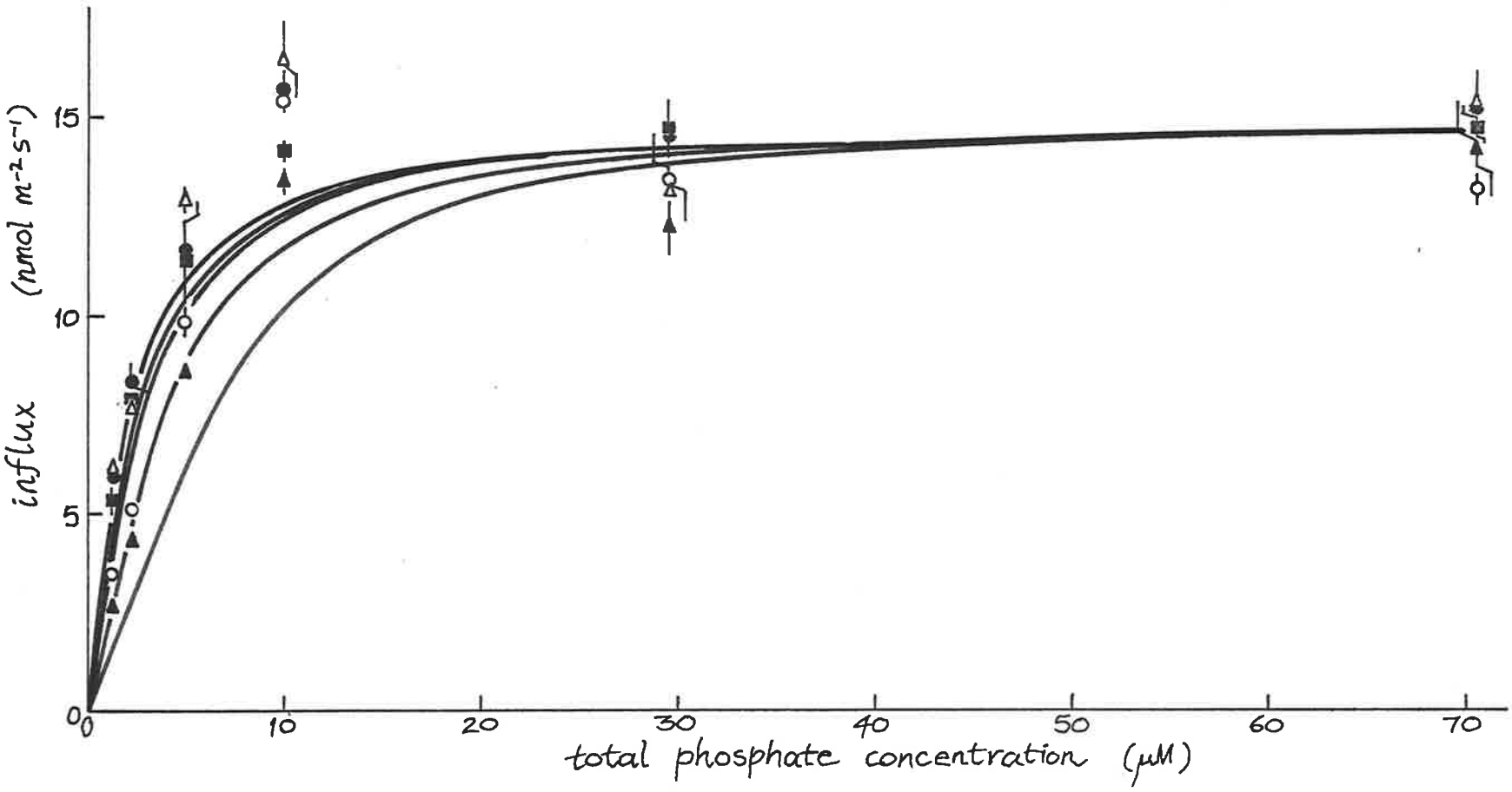

FIGURE 26. Briggs-Maskell concentration curves using $k_T^{H_2PO_4^-}$ = 50.7, 36.7, 25.8, 12.9 or 5.52 x 10^{-5} m s^{-1} (left to right), otherwise as in Fig. 25.

uptake of CO_2 during photosynthesis (see later). This would lead to a greater proportion of HPO_4^{2-} (and PO_4^{3-}) to $H_2PO_4^-$ in the diffusion boundary layer than in the bulk medium and a consequent increase in the overall k_T for $H_2PO_4^-$. Thus, k_T would be a truly "overall" k_T, being the integral of the differential k_T's at each (H^+) of the pH gradient. Qualitatively, however, if the average pH of the unstirred layer could be considered as being 8, the overall k_T's at low rates of stirring would be more than sufficient to account for the data.

There are other lines of enquiry in the interpretation of the results. The first is suggested by the predictions of FVKUP for the data of Fig. 23. These are shown in Table 4. Lines of best fit are obtained with a low K_M for total phosphate

TABLE 4

Parameters in the Briggs-Maskell equation predicted by FVKUP for the data shown in Fig.23, and regression coefficients.

	Level 1	Level 2	Level 3	Level 4	Level 5
V (nmol m^{-2} s^{-1})	14.3	14.0	15.4	15.7	15.9
K_M (μM)	0.447	0.611	0.833	0.821	0.817
k_T (m $s^{-1} \times 10^{-5}$)	0.209	0.279	0.642	0.588	0.851
Reg. coefficient	0.999	0.996	0.996	0.979	0.993

(average 0.77 μM) and with a fairly large diffusion resistance, where this resistance changes relatively little from level 1 to level 5. The suggestion is that the diffusion of phosphate within the thallus (i.e. in the cell walls) is slow enough to make negligible the changes in k_T that occur in the stirring gradient tower. However, using the Blum-Jenden expression for K_M^{app} (see Fig. V.9 and equation V.23) it can be readily shown that even if the true K_M was zero and the internal diffusion resistance ($\frac{1}{3}R/D_{eff}$) was large enough to enable a fit to the data of level 5, the external "resistances" ($1/k_T$'s) would still be large and stirring would be predicted to have much the same effect as shown in Fig. 26.

The second is that HPO_4^{2-} is the species that is transported across the membrane. Allowing for the very slight enhancement due to $H_2PO_4^-$ and PO_4^{3-}, HPO_4^{2-} influx versus concentration curves based on the Briggs-Maskell equation are virtually identical to those shown in Fig. 26. The unstirred layer pH would have to be a good deal larger than 8 for there to be significant enhancement by PO_4^{3-}; the ratio of $[PO_4^{3-}]$ to $[HPO_4^{2-}]$ is $K'_{a_3}/(H^+)$ which is only 0.2 at pH 8 (using $pK'_{a_3} = 8.69$; Millero, 1983). In addition, k_T for PO_4^{3-} is very low because of its very low diffusion coefficient. This further reduces its effectiveness as an "enhancer" of HPO_4^{2-} diffusion.

The third possibility is that of a relatively <u>low</u> pH

in the cell wall, given an equilibrium distribution of H^+ between the Donnan free space (DFS) and the bulk medium. Since $H_2PO_4^-$ and HPO_4^{2-} will always be in equilibrium, the concentration of $H_2PO_4^-$ could be increased in the cell wall relative to $[HPO_4^{2-}]$. Whilst this would lower the effective k_T for $H_2PO_4^-$ transport through the cell wall, it would increase the concentration of $H_2PO_4^-$ on the "unstirred layer" side of the wall, and possibly at the plasmalemma also. Equilibrium between the DFS and the unstirred layer with regard to H^+ is unlikely; even so, the overall, steady-state pH of the wall may still be somewhat lower than in the adjacent unstirred layer and may contribute something towards an increased rate of $H_2PO_4^-$ uptake.

It is reasonable to conclude that U. rigida possesses a membrane porter for $H_2PO_4^-$ ions which, at the pH of this experiment, is prevented from diffusional limitations external to the membrane because of the parallel diffusion of HPO_4^{2-} and PO_4^{3-} and a possible lowering of pH in the cell wall. The K_M for total phosphate (1.5 μM) is quite low; indeed, at zero ionic strength, the K_M could be halved if the activity coefficient for $H_2PO_4^-$ in sea water is 0.5 (Whitfield, 1975; footnote to equation (10)). However, very low K_M's for phosphate uptake have been measured in many marine algae, including the related genus Enteromorpha (Wallentinus, 1984). The deduced K_M for $H_2PO_4^-$ is very

low (0.036 μM in ASW) but again in line with the measurements quoted in Wallentinus (1984) when the pH of the medium is taken into account. At lower pH's, it would be predicted that the K_M^{app} for total phosphate would decrease, but that diffusional limitations would become greater. This would be worth testing in future experiments.

III. Uptake of [^{32}P] phosphate and [^{14}C] methylamine by *Vallisneria spiralis*

(i) Results

Phosphate influx versus phosphate concentration is shown in Fig. 27, at three different stirring rates. It is immediately apparent that stirring has even less of an effect on influx than it does with *Ulva*, and that the apparent K_M is much larger (around 60 μM). This is in spite of the fact that at the pH of this experiment $H_2PO_4^-$ constitutes 74% of the total phosphate, using the pK_a for $H_2PO_4^-$ in distilled water (7.21). The potential for enhancement of $H_2PO_4^-$ fluxes by HPO_4^{2-}, therefore, is not large. In Fig. 28, [^{14}C]methylamine influx is shown as a function of concentration. Although the data are not particularly conclusive, stirring appears to have little effect overall and the observed K_M is comparatively high. In each of these experiments, the stirrer was on its maximum setting. The correction factors for the k_T's measured in the zinc disk

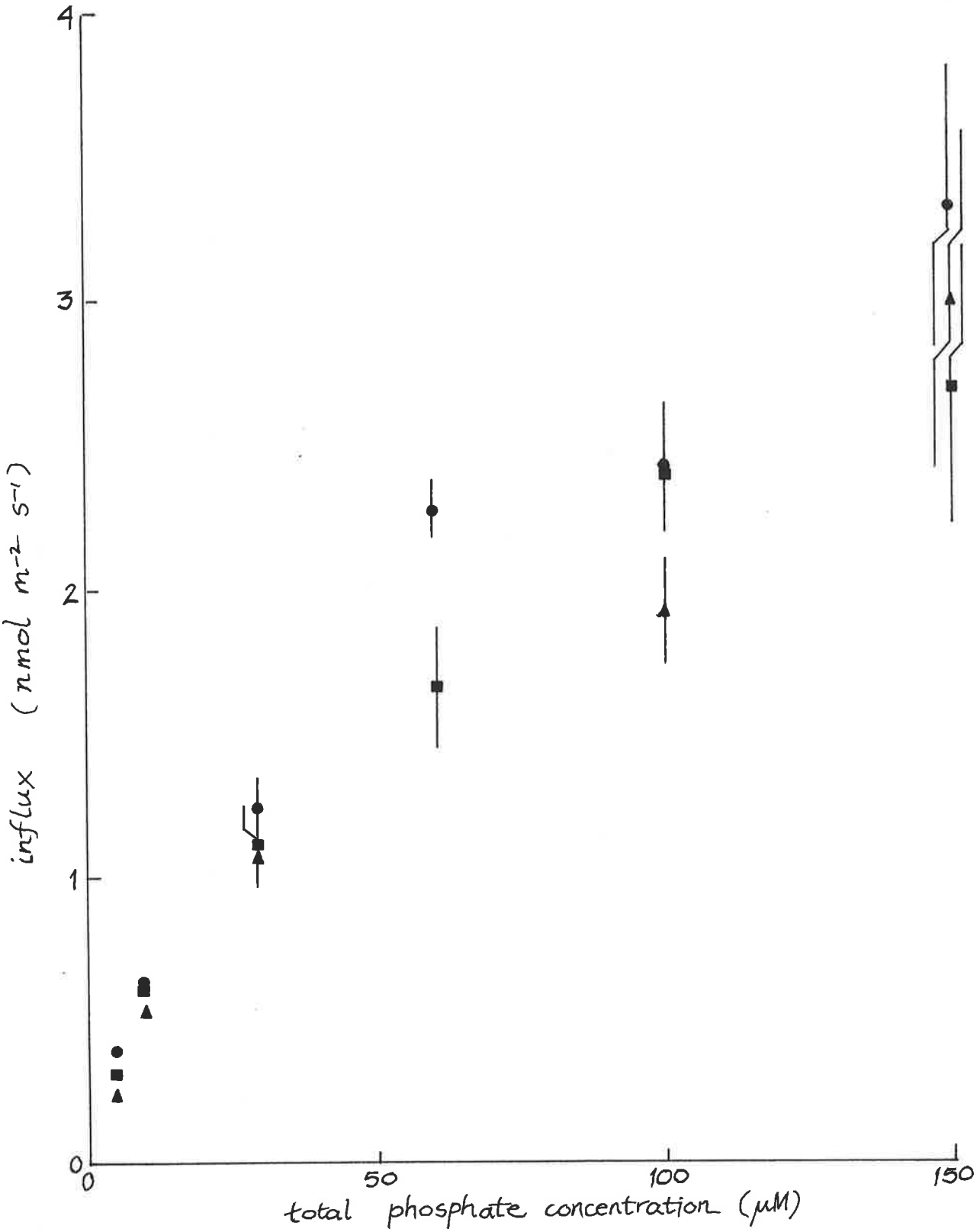

FIGURE 27. $[^{32}P]$phosphate influx against concentration for sections of V.spiralis leaves, in levels 1 (▲), 3 (■) and 5 (●) of the stirring gradient tower. APW + 10 mM MES, pH 6.72 - 6.77, 25°C.

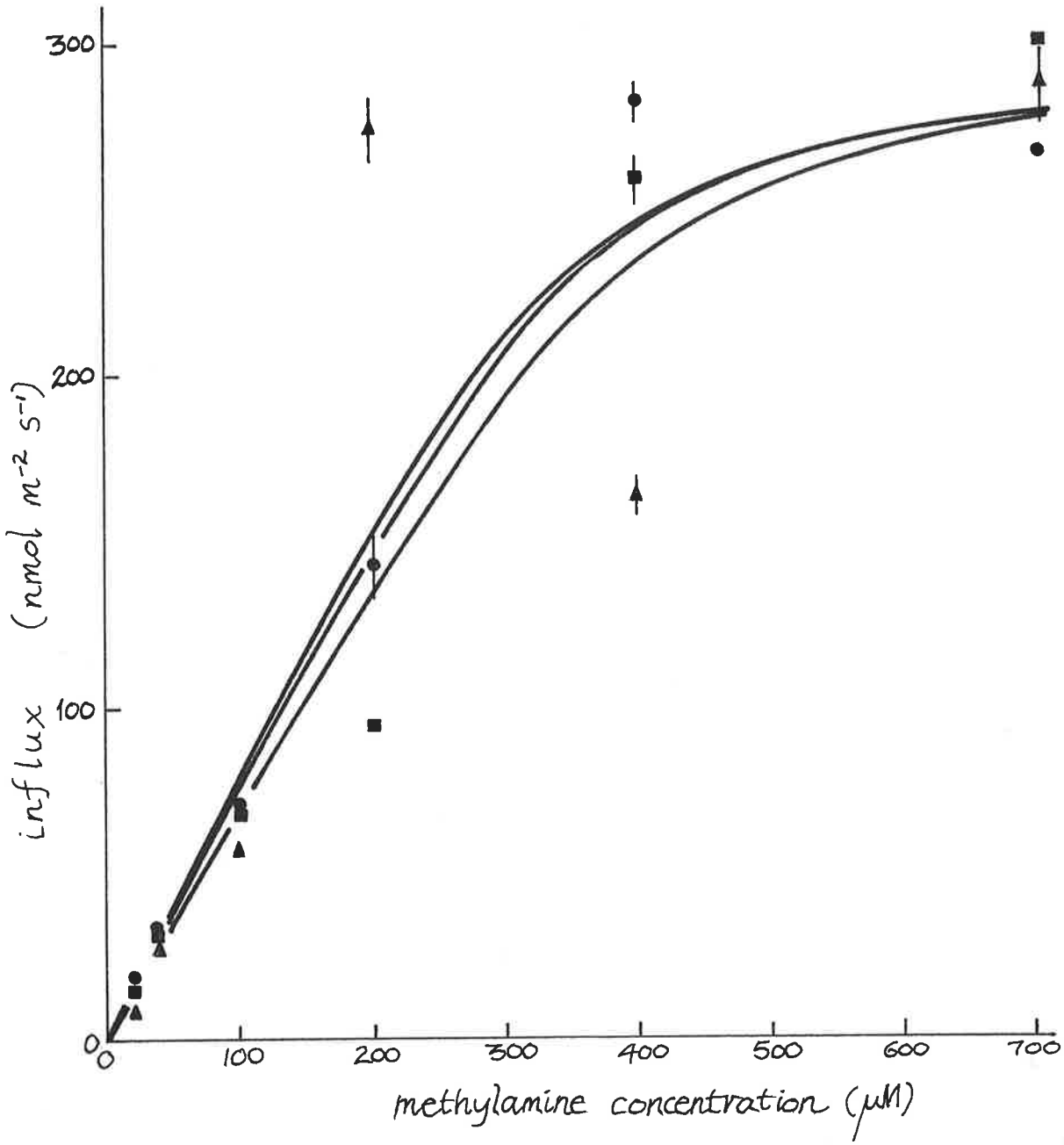

FIGURE 28. [^{14}C]methylamine influx versus concentration for V.spiralis leaf pieces. Symbols as in Fig. 27. APW + 10 mM MES, pH 6.72 - 6.77, 25°C. The lines represent the Briggs-Maskell equation, with K_M = 20 μM, V = 295 nmol m^{-2} s^{-1} and k_T = 8.35, 8.21, and 7.33 x 10^{-7} m s^{-1}.

experiment are thus $(9.5 \times 10^{-10}/3.34 \times 10^{-9})^{\frac{2}{3}}$ = 0.432 for $H_2PO_4^-$, and $(1.46 \times 10^{-9}/3.34 \times 10^{-9})^{\frac{2}{3}}$ = 0.576 for $CH_3NH_3^+$. (All diffusion coefficients are those at infinite dilution and are from Gros et al., 1976, Tanaka and Hashitani, 1971 and Robinson and Stokes, 1959.)

(ii) Discussion

There are basically three possible explanations for the results: (a) the kinetics of uptake are determined by the rate of the membrane transport reaction itself,

(b) internal diffusion resistances are so large (due to the thickness of the leaf) that the diffusion boundary layer constitutes a relatively small resistance, or

(c) the cuticle is the dominant resistance.

The shape of the methylamine concentration curve at the highest rate of stirring (Fig. 28) is immediately suggestive of a large in-series resistance, implicating the cuticle as the culprit. The solid lines shown in Fig. 28 are for a cuticle with a permeability to $CH_3NH_3^+$ of 8.5×10^{-7} m s^{-1}, together with the corrected k_T's for the different levels of the stirring gradient tower and a K_M for $CH_3NH_3^+$ influx of 20 μM. Such a low permeability of the cuticle is not unlikely. McFarlane and Berry (1974) found that isolated apricot cuticles had a permeability to Li^+ of 0.39 - 2.85×10^{-10} m s^{-1}.

$CH_3NH_3^+$ is likely to penetrate more rapidly because of its smaller hydrated radius. Also, the cuticles of aquatic plant leaves are much thinner than those of terrestrial plant leaves (Arber, 1920). Schönherr (1982), for a range of terrestrial plants, showed that the permeability of the cuticle to water is 0.1 - 2.3 x 10^{-9} m s^{-1}, while for the aquatic Potomogeton lucens, it is about 2.55 x 10^{-6} m s^{-1}.

The phosphate concentation curve (Fig. 27) looks like a rectangular hyperbola typical of Michaelis-Menten kinetics; indeed the computer programme FVKUP showed that the data fitted best to an equation of this type, with a K_M of 40 - 80 μM. The other possible explanation is that diffusion in the cell walls is limiting, which can also lead to a reasonably rectangular hyperbola when it is in parallel with reaction (see Fig. 5). With a K_M for $H_2PO_4^-$ as low as Ulva, $D_{eff}^{H_2PO_4^-}$ would need to be of the order of 2 x 10^{-12} m^2 s^{-1}, if phosphate were diffusing through the faces of the Vallisneria leaf pieces. Such a low effective diffusion coefficient is unlikely. However, it may be that the cuticle presents a virtually impenetrable barrier to phosphate ions, in which case they would diffuse chiefly via the cut edges. Such a situation could easily account for the observed uptake kinetics with reasonable values for $D_{eff}^{H_2PO_4^-}$ in the cell walls. That the cuticle, in general, presents more of a barrier

to the passage of anions than of cations was shown by Yamada, Wittwer and Bukovac (1964,1965; see also Wittwer and Teubner, 1959) who suggested that the more rapid penetration of cations was partially due to their greater binding on the inward-facing side of the cuticle (Yamada, Bukovac and Wittwer, 1964). Again, steric effects will also be important (McFarlane and Berry, 1974); $H_2PO_4^-$ will be considerably less mobile in the cuticle than $CH_3NH_3^+$ simply because of its bulk.

RESPIRATION

I. Kinetics of Oxygen Reduction

By far the most important catalyst for the reduction of O_2 in dark respiration is cytochrome oxidase (Beevers, 1961), which resides in the inner membrane of the mitochondrion. In the reaction catalysed by cytochrome oxidase, O_2 acts as the final electron acceptor of the electron transport chain, being reduced to water. Some plants possess an alternate oxidase, insensitive to the normal inhibitors of cytochrome oxidase (e.g. CN^-, CO) which has a lower affinity for O_2 than cytochrome oxidase (Sargent and Taylor, 1972; Solomos, 1977).

The kinetics of oxygen uptake by cells and tissues have been studied by many workers. The rate of uptake is often subject to internal, and sometimes external, diffusion limitations particularly in large cells or groups of cells or thicker tissue sections (Warburg, 1923; Berry and Norris, 1949; Yocum and Hackett, 1957; Longmuir, 1966; Johnson, 1967; Mueller, Boyle,and Lightfoot, 1968; Poole, 1978; Raven, 1984). In other cases the kinetics appear to be Michaelis-Menten (suggesting insignificant transport limitations - Longmuir, 1966) but with unpredictably changeful kinetic parameters, especially K_M (Tang, 1933; Dromgoole, 1978; Morriset, 1978; Kelly, 1983). Some workers have found

that the Michaelis-Menten equation of an arbitrarily modified order fits best with the experimental data. For example, Bänder and Kiese (1955) proposed $v = V\ c^{1.4}/(K_M + c^{1.4})$ while Ivanov and Lyabakh (1982) suggested the equation $v = V\ c^2/(K_M^2 + c^2)$.

The problem is almost certainly related to the complexity of the reaction. The initial reaction of O_2 with cytochrome oxidase (here designated cyt.a_3) can be written

$$\text{cyt.}a_3^{2+} + O_2 \xrightarrow{k+1} \text{cyt.}a_3^{3+}(+ O_2^-) \qquad \text{(i)}$$

($k_{+1} \sim 5 \times 10^7\ M^{-1}\ s^{-1}$ (Chance, 1965) at 25°C). Thus, the rate of O_2 reduction will depend on [cyt.a_3^{2+}] as well as on the concentration of O_2. In the very small volume of the mitochondrion, the concentration of cyt.a_3^{2+} will be a steady-state determined by the rate of its consumption in reaction (i) and of its supply by the reaction (ignoring cytochrome a)

$$\text{cyt.}a_3^{3+} + \text{cyt } c^{2+} \underset{k-2}{\overset{k+2}{\rightleftharpoons}} \text{cyt.}a_3^{2+} + \text{cyt.}c^{3+}. \qquad \text{(ii)}$$

Here again, [cyt.c^{2+}] will be a steady-state concentration which will be determined by the rate of reaction (ii) and a supply reaction of the form

$$AH + \text{cyt.}c^{3+} \xrightarrow{k+3} A + H^+ + \text{cyt.}c^{2+} \qquad \text{(iii)}$$

where AH represents a reducing agent such as NADH or succinate and where other components of the electron transport chain (e.g. cytochrome b, flavoprotein) have been ignored. In general, the volume of the cell accessible to AH includes the cytoplasm, so it is more difficult to disturb the steady-state concentration of AH than that of the oxidized or reduced form of the cytochromes in the mitochondria. There is also a much wider variety of reactions which are capable of supplying AH. [AH], therefore, is a convenient reference on which to base a prediction of the rate of electron transport in the mitochondrion.

From reactions (i), (ii) and (iii), Petersen, Nicholls and Degn (1974) showed that the rate equation

$$v + \frac{A_1 \, v}{c_s^{O_2} \, e} - \frac{A_2 \, v^2}{c_s^{O_2} \, e} = A_3 \qquad (32)$$

can be deduced, where A_1, A_2 and A_3 have the following values:

$$A_1 = \frac{k_{+2} \, k_{+3} \, [AH] \, e}{4k_{+1}(k_{+2} + k_{+3} \, [AH])} \, ,$$

$$A_2 = \frac{k_{+2} - k_{-2}}{4k_{+1}(k_{+2} + k_{+3} \, [AH])} \quad \text{and}$$

$$A_3 = \frac{k_{+2} \, k_{+3} \, [AH] \, e}{k_{+2} + k_{+3} \, [AH]} \, .$$

The symbol "e" represents the total concentration of cytochrome oxidase in the mitochondrion, which is assumed to approximately equal the total concentration of cytochrome c (Chance and Williams, 1955; Lance and Bonner, 1968); $c_s^{O_2}$ is the O_2 concentration at the site of reaction. K_M for O_2 is equal to $A_1/e - A_2A_3/2e$ and the maximum rate of electron transport, V, is equal to A_3. (The maximum rate of the reduction of O_2 to $2H_2O$ is one quarter of V.) Both $K_M^{O_2}$ and V, therefore, will be sensitive to [AH]. $K_M^{O_2}$ will also be sensitive to A_2, which is proportional to the difference between k_{+2} and k_{-2}. This arises from a change in the order of the reaction with A_2, illustrated in Fig. 29 a,b and c. When $A_2 = 0$ ($k_{+2} = k_{-2}$), the kinetics are first-order Michaelis-Menten (Fig. 29b). For k_{-2} smaller than k_{+2} ($A_2 > 0$), the overall reaction order becomes greater than one (Fig. 29a) and the kinetics are of the form of Bänder and Kiese (1955) and Ivanov and Lyabakh (1982). For $k_{-2} > k_{+2}$ ($A_2 < 0$), the reaction order is less than one, which was what Petersen et al. observed for fully energized mitochondria (Fig. 29c). The dependence of the velocity on the O_2 concentration is weakened in this case and saturation is approached quite slowly.

It can be readily shown that if mitochondria displaying these kinetics were constrained in a slab shape (half-thickness = R), in which internal O_2

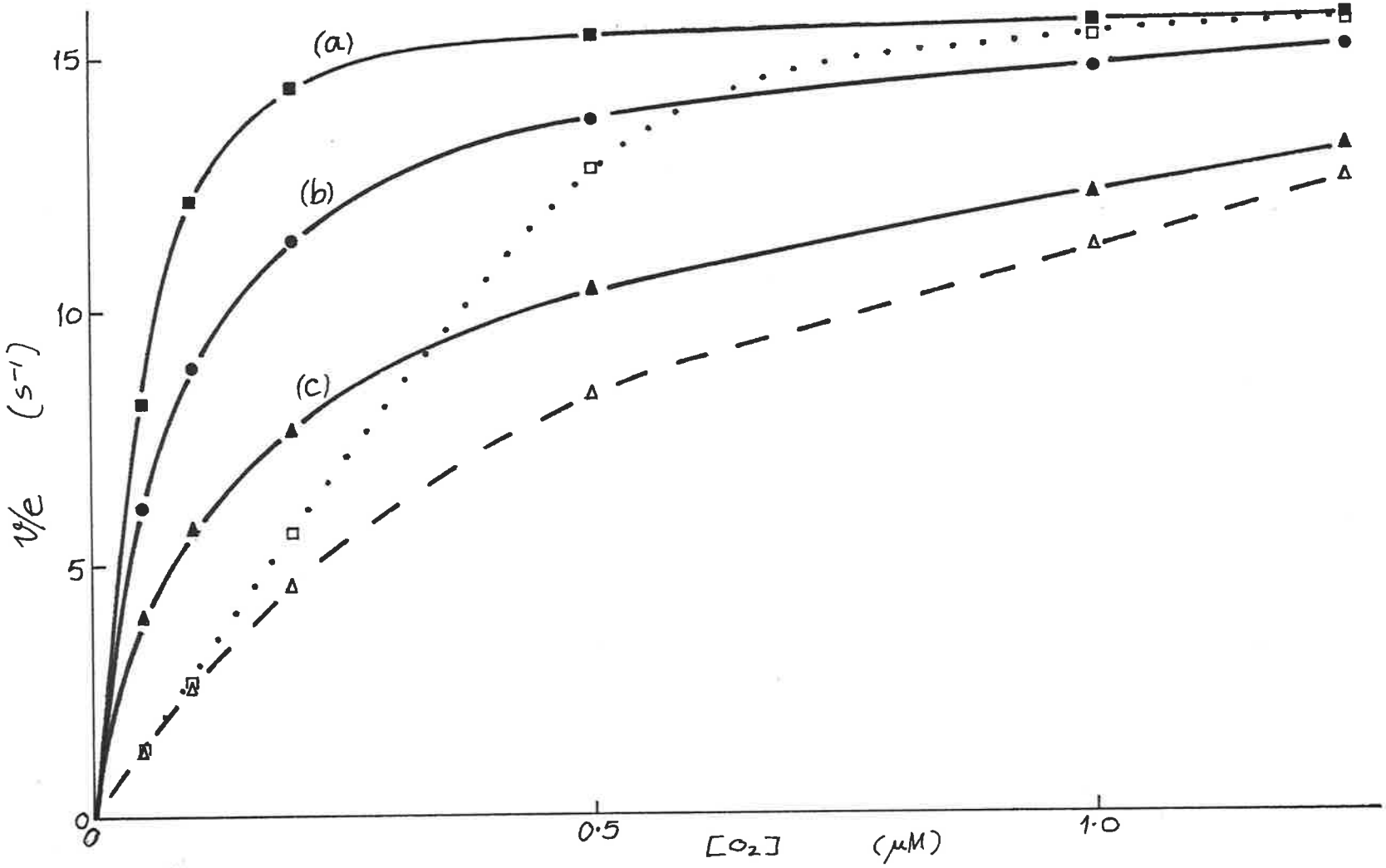

FIGURE 29. Rate of electron transport, v, in mitochondria vs. $[O_2]$ based on equation (32); v/e is plotted as this eliminates e from the rest of the equation. Values of k_{+1}, k_{+2} and $k_{+3}[AH]$ are from Petersen et al.(1974) giving $A_1/e = 0.08\ \mu M$ and $A_3/e = 16\ s^{-1}$. Values of A_2 are (a) 0.004 (b) 0 and (c) - 0.018 μM s. The dotted and dashed lines represent equation (33) with $A_2 = 0.004$ and - 0.018 μM s respectively and $e\,R/k_T = 0.03\ \mu M$ s.

transport was fast, then an external resistance to the transport of O_2 would change equation (32) to

$$v = \frac{e\, c_b^{O_2} k_T + A_1 k_T + e\, A_3 R}{2(A_2 k_T + e\, R)} - \frac{\sqrt{(e\, c_b^{O_2} k_T + A_1 k_T + e\, A_3 R)^2 - 4(A_2 k_T + e\, R) e\, A_3 c_b^{O_2} k_T}}{2(A_2 k_T + e\, R)} \qquad (33)$$

($c_b^{O_2}$ is the oxygen concentration in the bulk phase and k_T the transport coefficient between bulk phase and the surface of the slab). The dotted and dashed lines in Fig. 29 show the effect of an external transport resistance on kinetics of the greater-than-first-order type or less-than-first-order type respectively. (When $A_2 = 0$, equation (33) becomes equivalent to the Briggs-Maskell equation.) Fig. 29 shows that the same transport resistance will have a much larger effect on kinetics of the type shown in curve (a) compared with those shown in curve (c).

The differences in the shapes of the various hyperbolae shown in Fig. 29 are brought out more clearly in the linear transformations of the Michaelis-Menten equation. Fig 30 shows the Woolf plot (c/v against c); the Bänder and Kiese type of kinetics transforms to a curve which is concave upward while the order < 1 type is concave downwards (cf. Petersen et al., 1974). Transport limitations will always tend to force the

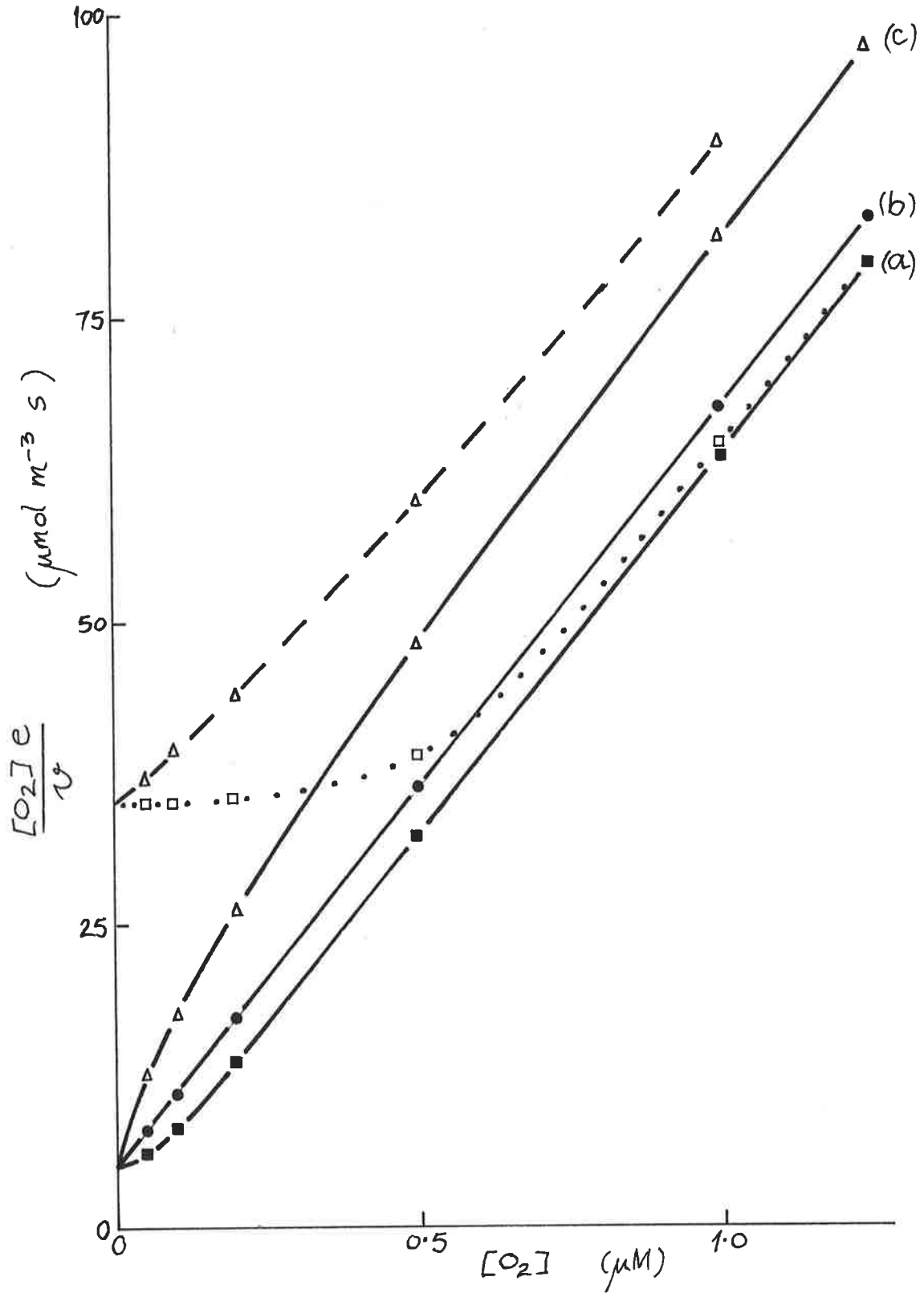

FIGURE 30. Woolf plots of the data of Fig. 29. The slope of the line at large $[O_2]$ is "V^{-1}" $((A_3/e)^{-1})$; the intercept on the ordinate is "K_M/V" (A_1/A_3) with no transport limitations (solid lines) or $A_1/A_3 + e\,R/k_T$ with them (dotted and dashed lines).

concavity upward in plots of this type (cf. Winne, 1973), with the result that the concave-downward curve (c) becomes almost linear (i.e. a rectangular hyperbola for v against c) while the inflection in curve (a) is augmented. However, all the curves tend towards the some slope (1/V) at high substrate concentrations.

II. Respiration in Ulva rigida

(i) Results

Figs. 31 - 36 show a number of experiments on the relationship between O_2 consumption in the dark, the $[O_2]$ of the surrounding sea water ($c_b^{O_2}$) and the thickness of the diffusion boundary layer. Woolf plots of the data are shown as insets. In the presence of the artificial unstirred layers, the response to $c_b^{O_2}$ is atypical of diffusion in series with first-order Michaelis-Menten kinetics because the rate at low $c_b^{O_2}$ is so large and is little affected by an increase in the layer thickness from 0.75 - 1.8 mm (Figs. 32 - 34). Indeed the Woolf plots are all concave downward, the exact opposite of what would be expected for rate limitations by diffusion. In the absence of any artificial unstirred layers, the Woolf plots are mainly straight (Figs. 32, 33, 36), sometimes concave downward (Figs. 31, 35) and in one case slightly concave upward(Fig. 34) indicating Michaelis-Menten kinetics of orders equal to, less than and greater than one

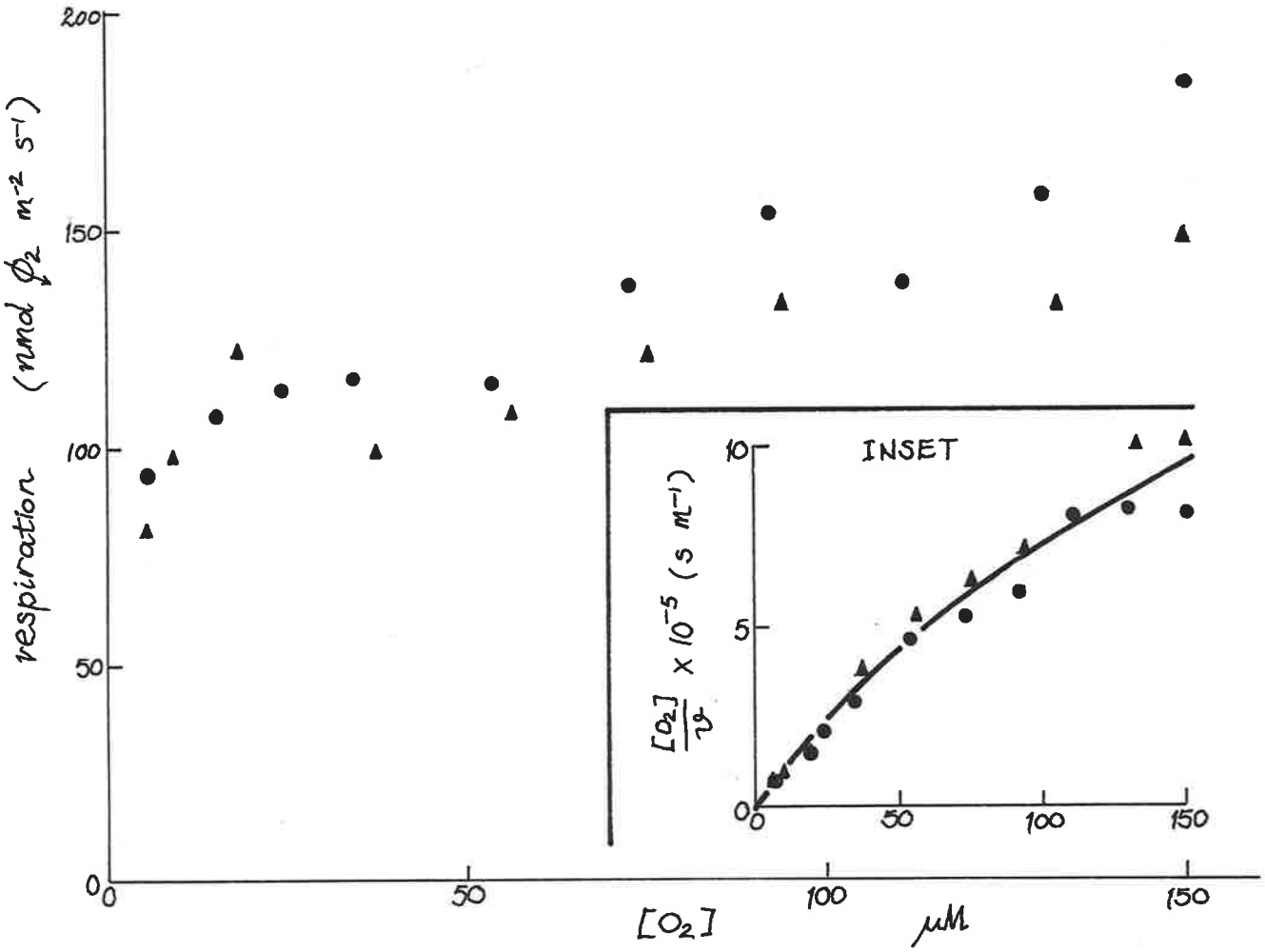

FIGURE 31. Rate of respiratory oxygen uptake as a function of the oxygen concentration for U.rigida (in type A holder) in FSW at 25°C. Inset shows a Woolf plot of the data (v refers to the rate of respiration). Results of two experiments.

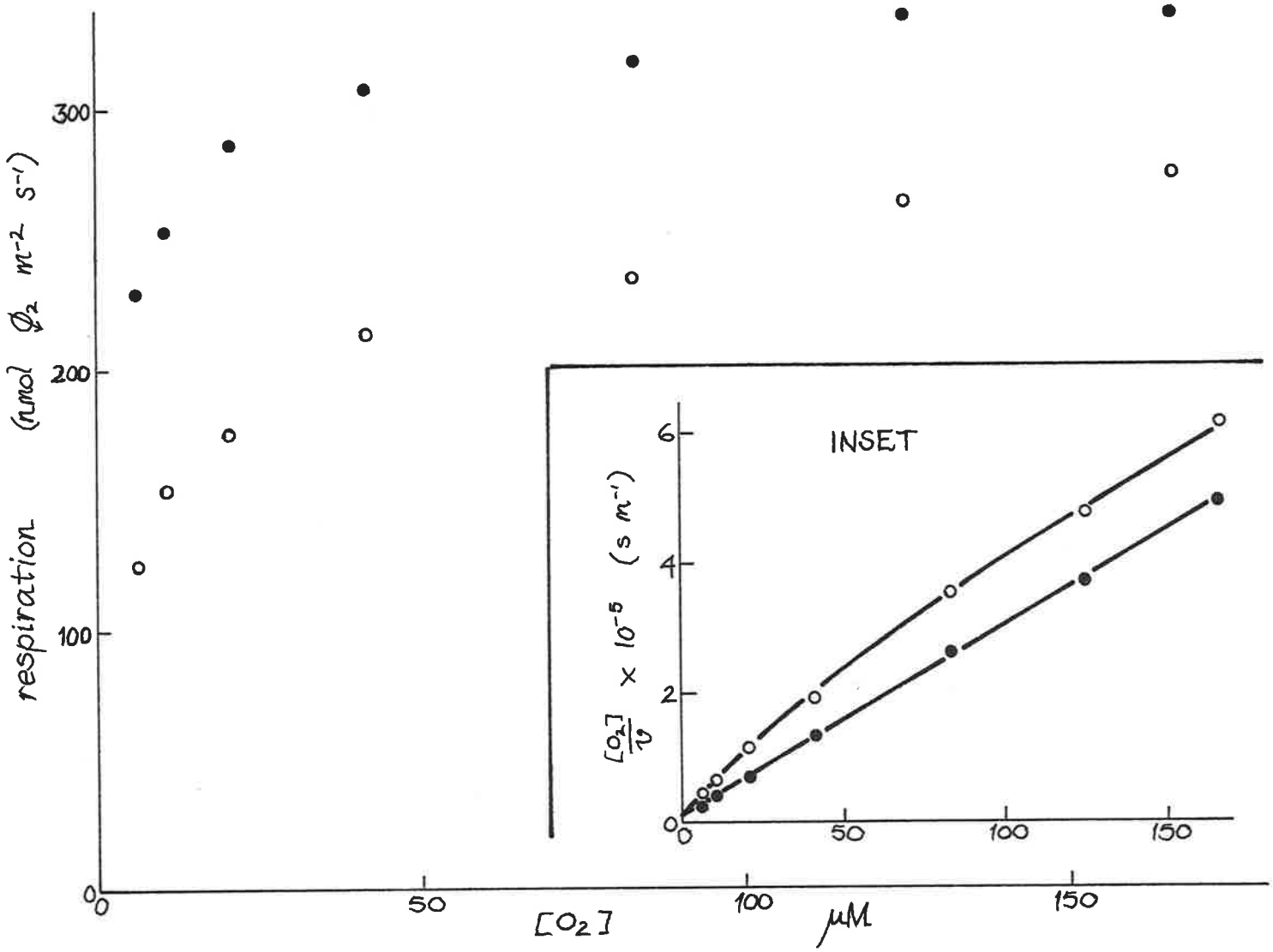

FIGURE 32. As in Fig. 31, for U.rigida in holder B(0) + B(0) with (o) or without (●) 10 layers of lens tissue (both sides), ~0.75 mm thick each side. 20°C.

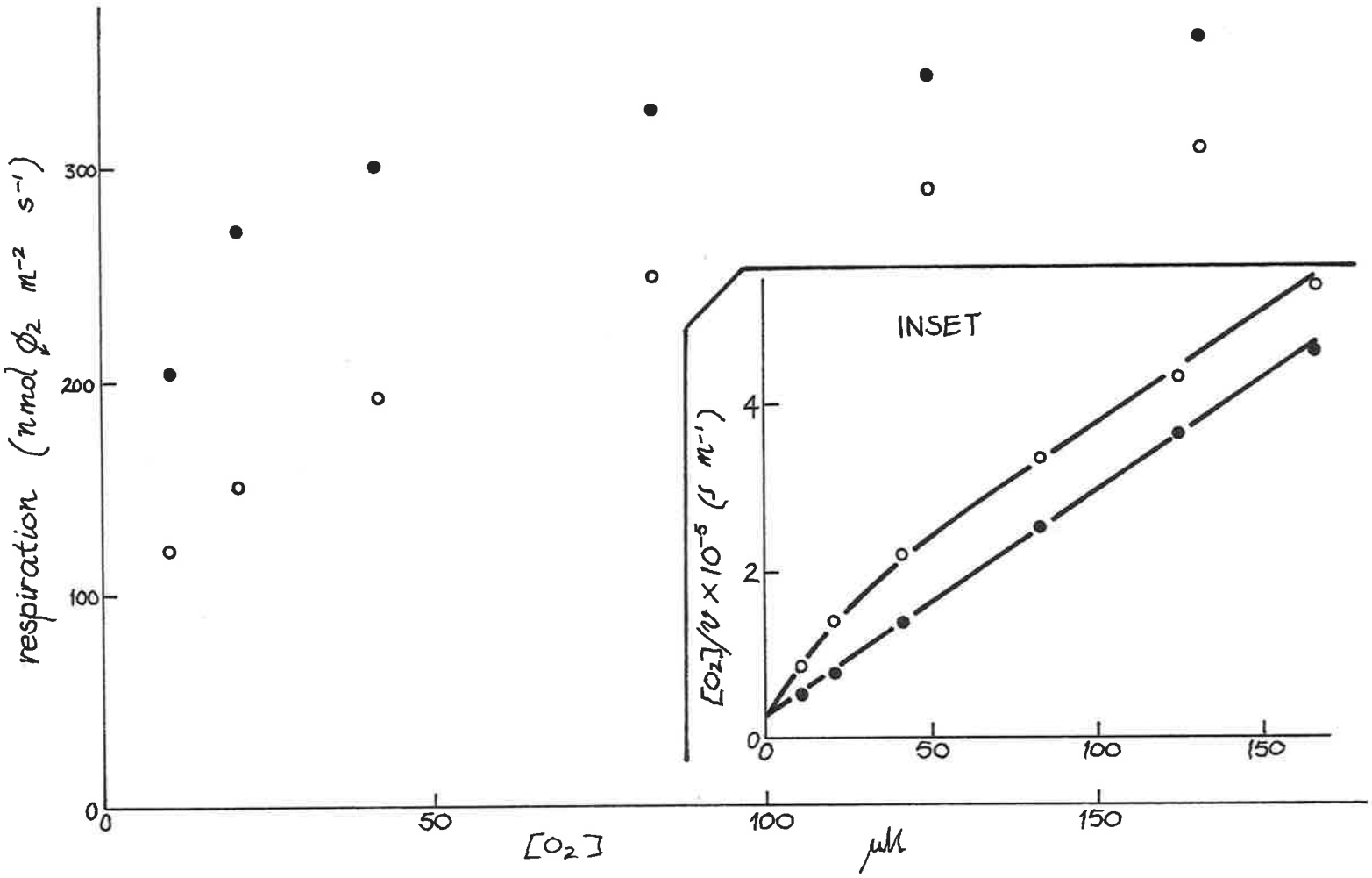

FIGURE 33. As in Fig. 32 with (o) or without (●) 20 layers of lens tissue (both sides), ~1.3 mm thick each side.

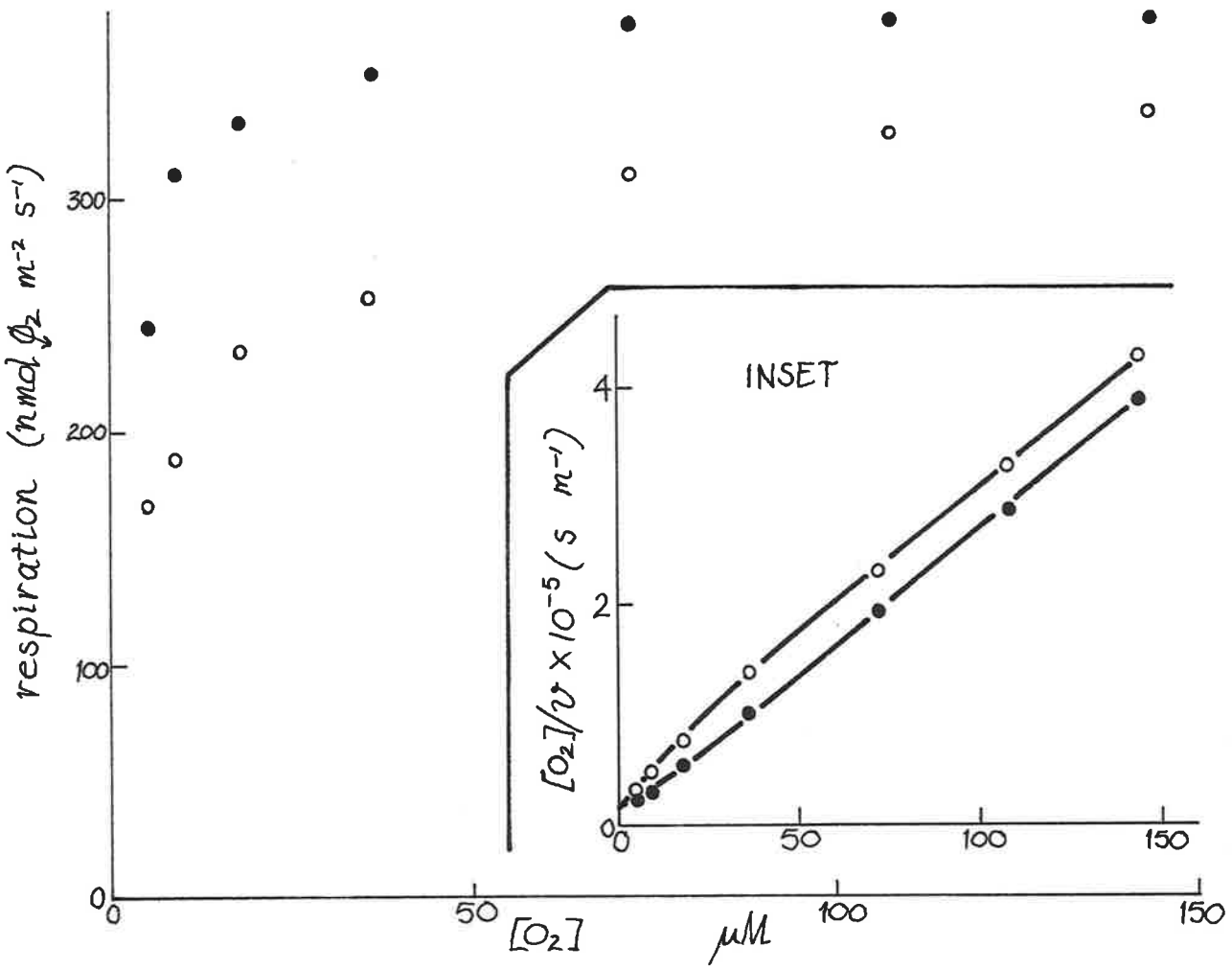

FIGURE 34. As in Fig. 33 with (o) or without (●) 30 layers of lens tissue (both sides), ~ 1.8 mm thick each side, and tissue aged for 22 hours. 27°C.

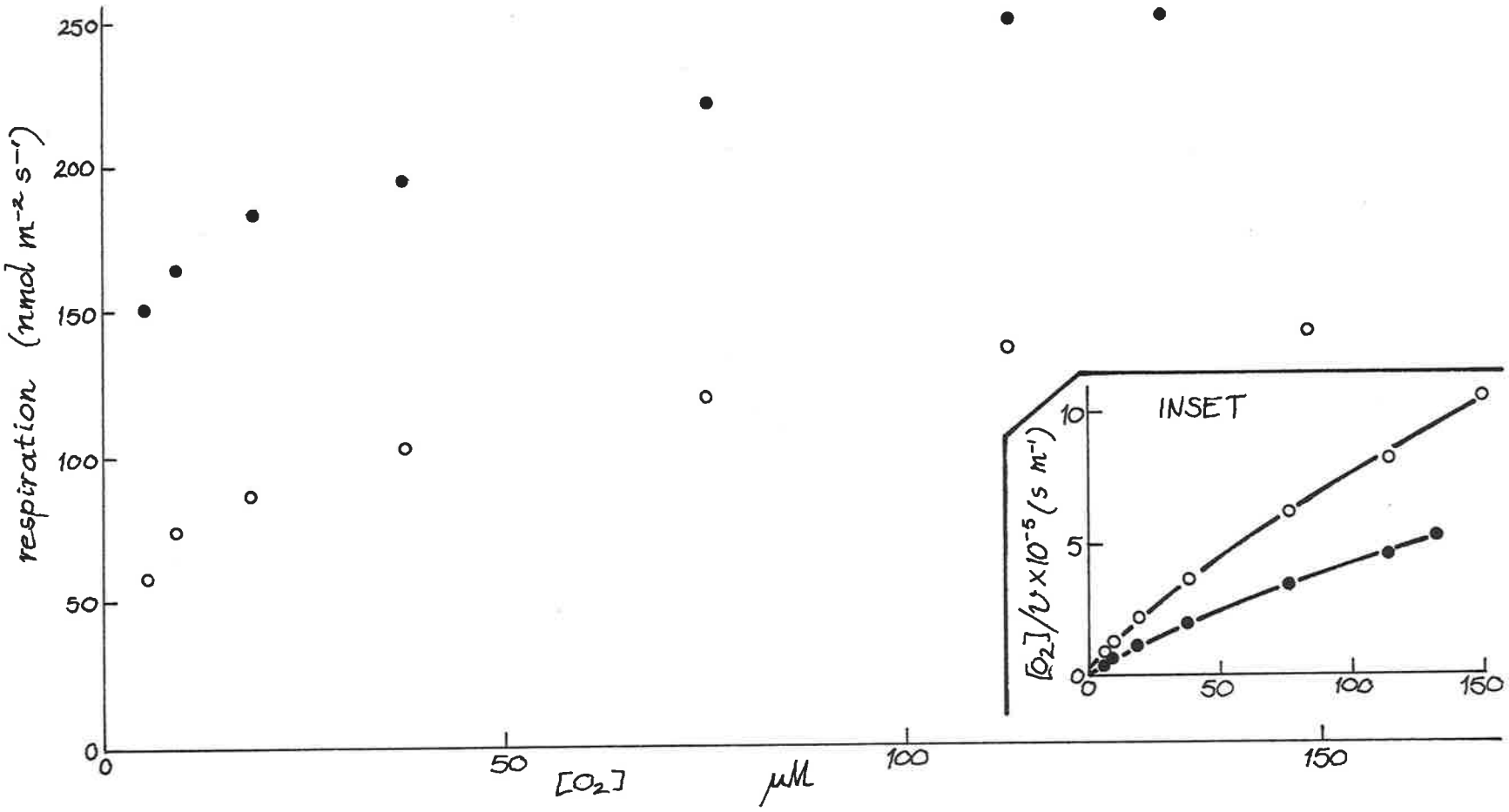

FIGURE 35. As in Fig. 34 with (o) or without (●) 3 layers of Whatman No. 1 filter paper (both sides), ~ 0.8 mm thick each side. 25°C.

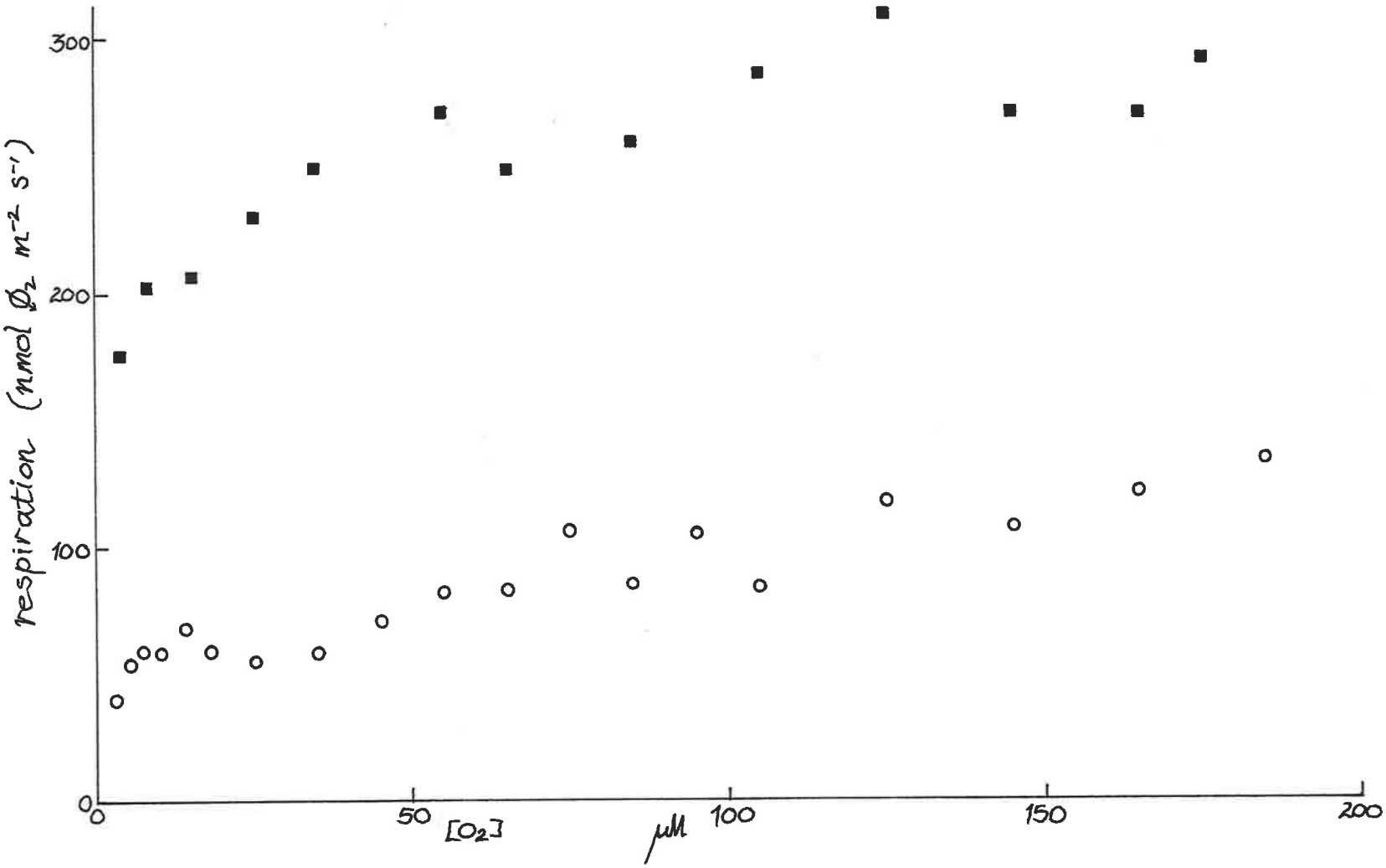

FIGURE 36a. Rate of respiration vs. [O_2] of three small fragments of U.rigida (■) (total surface area = 2.22 cm^2 both sides), and for a piece of thallus (o) in holder B(3). FSW, 25°C.

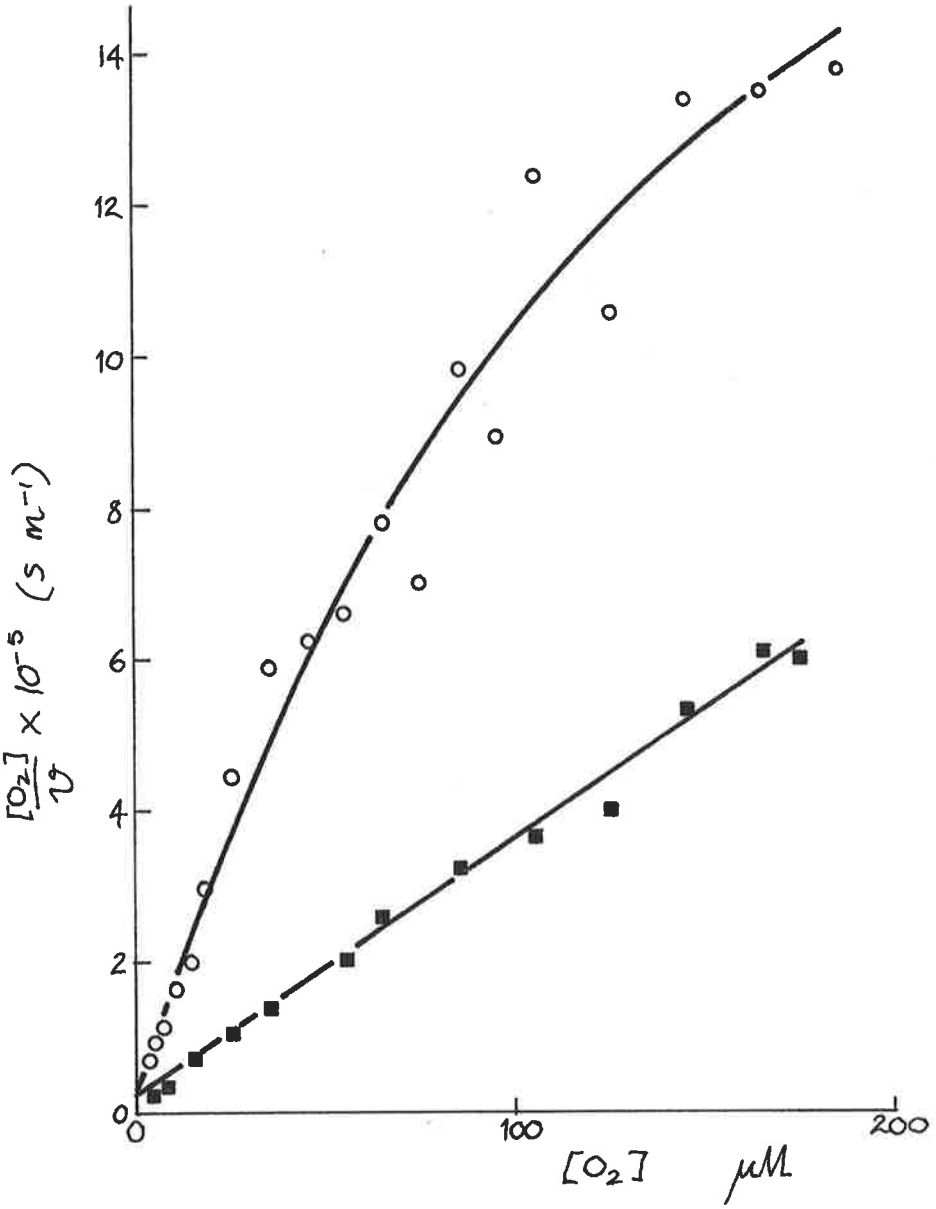

FIGURE 36b. Woolf plot of the data of Fig. 36a.

respectively. In all cases, apart from the results shown in Fig. 35, the maximum rate appears to be the same with or without the artificial unstirred layers. Results for tissue pieces which were aged for 22 hours in aerated FSW after being cut from the thallus are shown in Figs. 34 and 35.

(ii) Discussion

There are a number of snags in the method used to determine the kinetics of O_2 uptake which may run the intrepid experimenter aground. I will begin by identifying some of them, but have more-than-likely missed (and consequently hit) plenty of others.

Dromgoole (1978) pointed out that sections of the thallus of various marine brown algae could display a rate of O_2 uptake that was artefactually large when transferred from sea water with a low $[O_2]$ (72 μM) to sea water at a high $[O_2]$ (307 μM), due to the equilibration of the O_2 outside the tissue and that inside. With $[O_2]$ in the thallus lower than in the bulk medium, there is a net loss of O_2 from the latter which is not associated with respiration.

In my case, the initial $[O_2]$ of the medium was the air-saturated $[O_2]$ ($\sim$200 μM); it is unlikely that the $[O_2]$ in the tissue would have been greatly different since pieces of thallus were always kept in air-

equilibrated seawater prior to an experiment.

Another artefact may appear for green tissue displaying rates of dark respiration which are higher immediately following illumination than after a longer period in darkness. If such tissue was sealed into the darkened O_2 electrode chamber immediately after being in the light, the respiration rate would decline with time which could be falsely interpreted as a decline with decreasing $[O_2]$ (cf. Dromgoole, 1978). Although U. rigida did show an occasionally significant post-illumination respiratory "burst", it was a short-lived event (< 10 min). For the data shown in Figs. 31 - 36, the tissue had been in the dark for at least this period of time before the first measurement of the respiration rate was made. In addition, the alga was previously exposed to only dim laboratory light, leading to relatively low rates of photosynthesis and presumably low rates of whatever process was responsible for the post-illumination burst (possibly photorespiration).

With the artificial unstirred layers, respiration was remarkably fast at low $c_b^{O_2}$; indeed, it would appear, impossibly fast. In Fig. 34, for instance, with an unstirred layer on each face of the tissue of at least 1.8 mm (i.e. without taking tortuosity and porosity into account) the highest possible O_2 flux by diffusion at 10 μM O_2 would be $J = (D/\delta)c_b \sim 10$ nmol m^{-2} s^{-1}; the measured rate was close to 200 nmol m^{-2} s^{-1}. It could

be argued that the cut edges of the tissue, where the boundary layer would be thin, had a very high rate of respiration, in which case virtually all the O_2 uptake at low $c_b^{O_2}$ would be due to the respiration at the edges. Small pieces (Fig. 36) of tissue, however, in which the edge constituted a much bigger proportion of the total surface area, did not respire any faster than larger pieces. Also, in the experiments where the tissue was aged, there were still high rates of respiration at low $c_b^{O_2}$ (Figs. 34, 35), although the period of aging may not have been sufficient to alleviate the effects of cutting (cf. discs of storage tissue; Laties, 1967).

Per unit area of edge rates of respiration would be absurdly large, e.g. 25 μmol m^{-2} s^{-1} in Fig. 35 (5 μM O_2). Edge effects may extend beyond the actual edge of the tissue, however, since the length of the diffusion pathway will be less for those faces of the tissue near the edge. Assuming that for a distance from the edge of the tissue equal to the thickness of the unstirred layer diffusional limitations are negligible, it can again be calculated what the rate of respiration must be to account for virtually all the O_2 uptake at low $c_b^{O_2}$. From Fig. 34, the rate is 450 nmol m^{-2} s^{-1} at 5 μM O_2. This is a much more reasonable number than the one just quoted for the edge alone but it is based on a very generous assumption. It is possible that there is an additional contribution from

the respiration of bacteria on the surface of the thallus with thick unstirred layers, as these experiments were more prolonged.

Another potential difficulty, which may be relevant to the magnitude of the rates of O_2 uptake, is that the O_2 measurements were not made under strictly steady-state conditions. Athough the rate of change of concentration in the bulk medium was not large, it was sufficiently large to be measurable within five minutes; this period of time would probably allow the enzymic reactions of oxygen reduction to come into an approximately steady-state, but may not have been sufficient for steady-state diffusion to be established. This would mean that the concentration gradient would not be fully developed at a particular bulk O_2 concentration, and the unstirred layer thinner than one would have predicted based on the assumption of a steady-state.

A rough indication of the time required to reach steady-state for diffusion in one dimension is given by the equation

$$\tau = 0.257 \frac{\delta^2}{D} \qquad (34)$$

(Sundaram, Tweedale and Laidler, 1970) in which τ is the time at which the concentration gradient is within 10% of the steady-state profile. For an unstirred

layer 1.8 mm thick, τ is about 7 minutes, suggesting that diffusion may have been quite a way from steady-state throughout the course of the experiment shown in Fig. 34, and possibly in the other experiments as well.

Given the complexity of the non-steady-state equations for diffusion, let alone diffusion in series with reaction, as well as the uncertainty even as to the whereabouts of the reaction within (or upon?) the thallus, it is not worthwhile analyzing the absolute rates of O_2 uptake that were found with the thick unstirred layers. Whether any significance can be attached to the shape of the absorption isotherm will be discussed later.

In the belief that the relationships between $[O_2]$ and the rate of O_2 uptake for thallus with no artificial unstirred layers approach reality, it is clear that the kinetics are often first-order Michaelis-Menten but that the order is sometimes greater and sometimes less than one. In terms of the mechanism proposed by Petersen et al. (1974), the forward and backward rate constants for the reduction of cytochrome a_3^{3+} by cytochrome c^{2+} change their relative magnitudes, i.e. the equilibrium constant changes. The unlikelihood of this event suggests that the reaction actually involves more chemical species than just the two cytochromes. Since the reduction of cyt. a_3^{3+} is normally coupled to the phosphorylation of ADP, reaction (ii) could be written

$$ADP + P_i + cyt.c^{2+} + cyt.a_3^{3+} \underset{k_{-2}'}{\overset{k_{+2}'}{\rightleftharpoons}} cyt.c^{3+} + cyt.a_3^{2+} + ATP + H_2O.$$

A change in the ratio of [ATP] to [ADP] and [P_i] would, therefore, appear as an apparent change in the equilibrium constant if adenylates were not taken into account. Specifically, the rate of the back reaction would increase if [ATP] were to build up relative to [ADP] and [P_i], which would account for the order < 1 kinetics obtained by Petersen et al. (1974) in fully energized mitochondria.

A simple explanation, then, for the observed differences in the reaction order is a change in the energy charge of the tissue. A large number of processes contribute to the energy charge of tissue, including photosynthesis, glycolysis, the oxidative pentose phosphate pathway, the Krebs cycle and oxidative phosphorylation itself. In my case, there is a positive correlation between the observed order and the "freshness" of the tissue; the times when reaction orders less than one were found (for tissue with no unstirred layers attached) correspond to fresh tissue (less than 8 days in the laboratory - Figs. 31 and 35) while the tissue which had been kept quite some time in the laboratory (Fig. 34) shows a reaction order greater than one, implying a slow back reaction and a low energy

charge. Kinetics of order one were obtained with tissue of intermediate "freshness".

The addition of an artificial unstirred layer appears to decrease the order of the reaction (in all cases but one - Fig. 35) suggesting that the unstirred layer somehow increases the energy charge. In Fig. 35 (very fresh tissue - only one day in the laboratory) the order is virtually unchanged, but the maximum rate is nearly halved. The latter phenomenon suggests a decrease in the concentration of reductant. It is hard to see how the addition of an unstirred layer could bring about changes like these. The possible immediate effects of the "unstirred layers" (e.g. partial anoxia, partial darkness) would tend to increase the ratio of reduced to total pyridine nucleotides and decrease the ratio of ATP to total adenylate, if they do anything (Kawada and Kanazawa, 1982). It is likely, then, that the shape of the concentration curves, as well as the absolute rate at different concentrations, is altered by the factors previously discussed and that the apparent order < 1 kinetics are artefactual.

With regard to the O_2 transport resistances (internal and external) for U. rigida tissue with no artificial unstirred layers attached, these are difficult to determine because the kinetics of the driving reaction are so complex. If they are first-order "Michaelis-Menten" (i.e. $A_2 = 0$ in Petersen et al.'s(1974)

analysis) then the relationship $K_M = V/(4k_{+1}e)$ holds (cf. Chance, 1965). The maximum rate of electron transport, V, is four times the maximum rate of O_2 reduction, $k_{+1} \sim 5 \times 10\ M^{-1}\ s^{-1}$ (Chance, 1965) while e is uncertain, but probably within the range 10 - 180 nmol cyt.c per g of chlorophyll (Raven, 1984). For the results of Fig. 36, then, with 88 mg chlorophyll m^{-2} in U. rigida (MacFarlane and Smith, 1982), the range of K_M could be 0.3 - 7 μM. For $A_2 < 0$ (i.e. $k_{-2} > k_{+2}$), the apparent K_M would be further increased. Thus, the K_M's for O_2 that were observed (3 - 9 μM) could be easily accounted for by reasonable values of k_{+1}, k_{+2}, k_{-2}, k_{+3}, [AH] and e, without invoking limitations to the transport of O_2 to cytochrome oxidase.

The similarity between the concentration curve for a large piece of Ulva and several much smaller pieces (cf. Fig. 32, for example, and Fig. 36) as far as apparent K_M's are concerned, suggests that transport limitations are indeed small. Internally, this may be brought about by the diffusion path for O_2 not being confined to the cell wall (cf. $CH_3NH_3^+$); a mitochondrion positioned adjacent to the inner periclinal wall of the cell can receive O_2 via cytoplasm and vacuole as well as via the cell wall. Although protein and organelles in the cytoplasm will tend to lower diffusion coefficients (Wang, Anfinsen, and Polestra, 1954; Garrick and

Redwood, 1977), there is also the possibility of enhanced O_2 transport by macromolecular O_2 carriers (Raven, 1977). In addition, if the apparent kinetics of respiration are of the less-than-first-order type (as appears to be the case for fresh U. rigida) the same O_2 transport resistance limits respiration less severely than if the kinetics are first-order or greater-than-first-order Michaelis-Menten. Fig. 29 illustrates this: here the O_2 transport "resistance" (eR/k_T) is 0.03 μM s, corresponding to a k_T for O_2 of 2.9 - 53 x 10^{-5} m s^{-1} depending on the value of e.

III. Respiration of Vallisneria spiralis

In Fig. 37 are shown the results of a number of experiments with V. spiralis under various conditions. Using the thicker, basal part of the leaf, sealing the air lacunae with wax or increasing the thickness of the diffusion boundary layer makes no difference to the initial slope of the respiration versus O_2 concentration curve although the maximum rates vary significantly. This, combined with the fact that the shape of the concentration curve is the same for the different treatments, suggests that something other than the intrinsic kinetic properties of the enzymic reactions is limiting at low $c_b^{O_2}$.

Several facts suggest that this may be O_2 transport through an external resistance. Firstly, the shape of

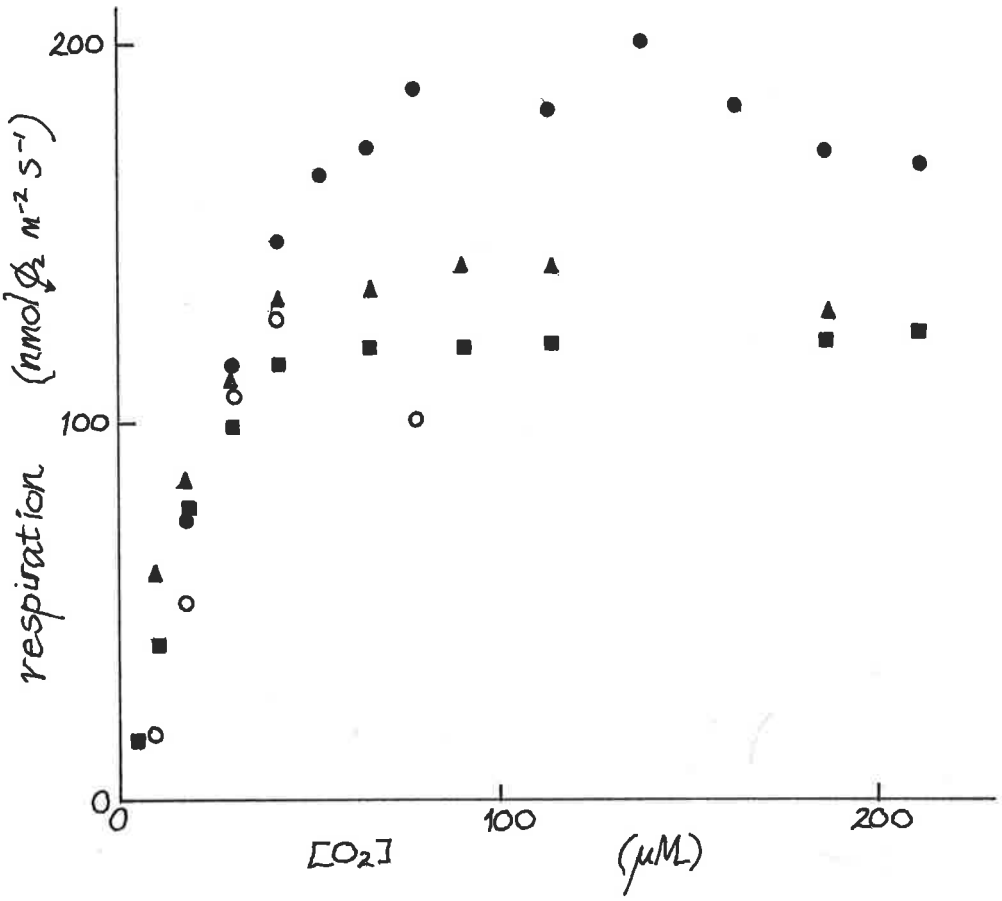

FIGURE 37. Dark respiratory O_2 uptake as a function of O_2 concentration for pieces of V.spiralis leaf. Piece cut from fully expanded region of the leaf (●); section of the basal part (■); piece of fully-expanded leaf with sealed ends (▲) and (○) in holder B(2) + B(2). APW + 10 mM MES, pH 6.6, 25°C, in wire holder (type A) except for (○).

the concentration response curve itself, which shows a very sharp transition to saturation (cf. methylamine influx, Fig. 28). Although such a transition also arises for Michaelis-Menten kinetics of an order greater than one, Fig. 29 shows that these kinetics are very susceptible to limitations by transport. It is odd, then, that the addition of an artificial unstirred layer is without effect. The apparent $K_M^{O_2}$ is also high (15 - 20 μM), whereas with a reaction order > 1, K_M^{app}'s tend to be very low (Fig. 29); the actual value will also depend on [A H], however. Secondly, even though the basal part of the V. spiralis leaf is more than twice as thick as the middle part, the initial slope is the same. If diffusion internally were limiting, the rate should show a strong dependence on the leaf thickness. For a typical thickness of the expanded leaves of V. spiralis of 300 μm, $D_{eff}^{O_2}$ would have to be less than 4×10^{-10} $m^2 s^{-1}$ to produce rates of the order shown in Fig. 37 (using equation (V.22), Fig. V.8 and assuming that $K_M^{O_2}$ is not more than 10 μM). $D_{eff}^{O_2}$, therefore, would need to be less than 17% of its value in the bulk medium (2.42×10^{-9} m^2 s^{-1} at 25°C - Himmelblau, 1964; Hung and Dinius, 1972); such a low D_{eff} is unlikely given that the cytoplasm in the epidermal cells is streaming and much of the diffusion pathway in the mesophyll of the tissue is through vacuolar sap or air spaces. Also, if the distribution of the cytoplasm is a guide, the number of mitochondria may well be greater per unit of volume

of epidermis than per unit volume of mesophyll (Fig. 8c); this would have the effect of decreasing R in the diffusion-reaction equation which would necessitate an even lower $D_{eff}^{O_2}$.

Finally, there remains the possibility that O_2 diffusion within the mitochondria themselves is rate limiting. *In vitro* rates of O_2 uptake by mitochondria can be 3 mmol g^{-1} s^{-1} (3 kmol m^{-3} s^{-1}) or more (J. T. Wiskich, pers. comm.). Assuming that the mitochondrion is a sphere, radius 0.5 μm, and that $D_{eff}^{O_2}$ is the same in the mitochondrion as in the medium, Φ (equation (29)) would then be about 1.7 at $c_b^{O_2}$ = 20 μM. With this value of Φ, even if the kinetics of O_2 uptake were zeroth-order, the mitochondrion would be little more than 70% effective. Having no information about the rate of O_2 uptake of the mitochondria of *V. spiralis* (i.e. *in vivo*) it is impossible to say whether or not intra-mitochondrial diffusion limitations can be significant.

Assuming, albeit teleologically, that mitochondria *are* effective in what they do (i.e. they are not partially anoxic) it is likely that the results of Fig. 37 are due to an external resistance to O_2 diffusion. The respiration experiments were done under well-stirred conditions in the oxygen electrode chamber and the diffusion boundary layer would therefore be thin. That

the boundary layer is an insignificant resistance is confirmed by the experiment (Fig. 37) in which it was artificially increased using holder B(2) (0.2 mm thick). The results plotted as amount of O_2 per m^2 leaf are the same as the other results in Fig. 37 at low $c_b^{O_2}$. This is in spite of the fact that the surface area available for diffusion though the holder was only 31.4% of that of the leaf. That is, calculated on the basis of the surface area available for diffusion in the boundary layer, O_2 uptake would be over 3 times faster with the holder than without. This is unreasonable and supports the notion that whatever is limiting O_2 uptake has to do with the leaf (i.e. cuticle and outer cell wall) and not with the diffusion boundary layer.

Comparison of Figs. 37 and 28 shows that the rate of O_2 transport through the cuticle and outer cell wall must be nearly 5 fold the rate of $CH_3NH_3^+$ transport (limiting slopes are 3.82×10^{-6} m s^{-1} for O_2 and 8.35×10^{-7} m s^{-1} for methylamine at the fastest stirring rate). This is not unlikely in view of the known properties of plant cuticles. Cuticle has a lipid fraction (Martin and Juniper, 1970) and a polymer matrix with fixed charges, negative at pH's above about 3 (Schönherr and Huber, 1977). The penetration of ions through the polymer matrix can be quite rapid, depending upon the ion exchange capacity of the polymer (McFarlane and Berry, 1974; Schönherr and Huber, 1977). The lipid

part of the cuticle, however, constitutes a severe barrier to the movement of ions and polar molecules (Schönherr and Schmidt, 1979). Schönherr (1976) showed that its removal with chloroform increased water permeability by a factor of 300 - 500. More lipid soluble substances, therefore, are likely to penetrate the cuticle much faster than ions, although the difference in permeability will be related to the proportion of lipid in the cuticle. Urea has been found to cross some cuticles more than 10 times faster than Rb^+ ions (Yamada et al., 1965) while Lendzian (1982) showed that the oxygen permeability of isolated cuticles from various terrestrial plants was 44 to nearly 300 times the water permeability. The approximate O_2 permeability of the V. spiralis cuticle postulated here (3.82×10^{-6} m s^{-1}) is considerably higher than the values determined by Lendzian (2.72×10^{-7} - 1.42×10^{-6} m s^{-1}), as would be expected for the thin cuticle of V. spiralis and submerged aquatic angiosperms in general (Arber, 1920; Schönherr, 1982).

PHOTOSYNTHESIS

I. Photosynthesis of Ulva rigida

(i) Results

Photosynthesis was mainly studied as O_2 evolution, using the O_2 electrode. Fig. 38 shows the effect of the pH of the medium (FSW) on the photosynthesis of U. rigida under saturating concentrations of inorganic carbon ($\sim$ 2.2 mM). There is a slight maximum at around the pH of the alga's native sea water (pH 8.3), but photosynthesis is not greatly affected by pH at values lower than this. At higher values there is a fairly steep decline in photosynthesis, although at pH 10.2 the rate is still some 30% of the maximum rate.

In Figs. 39 - 43 are shown the relationship between photosynthesis at 25^{o}C and the calculated concentration of CO_2 in the surrounding sea water, at four different pH's and with various unstirred layer thicknesses or degrees of slicing of the tissue. There is considerable variability in the maximum rates of photosynthesis that are attainable by tissue of fixed surface area. Nevertheless, it is clear that the perspex artificial unstirred layers have a marked effect on photosynthesis at low pH (Fig. 40). Some of this is due to the fact that the surface area available for diffusion in the perspex unstirred layers is around 30% of the surface area available for transport were the

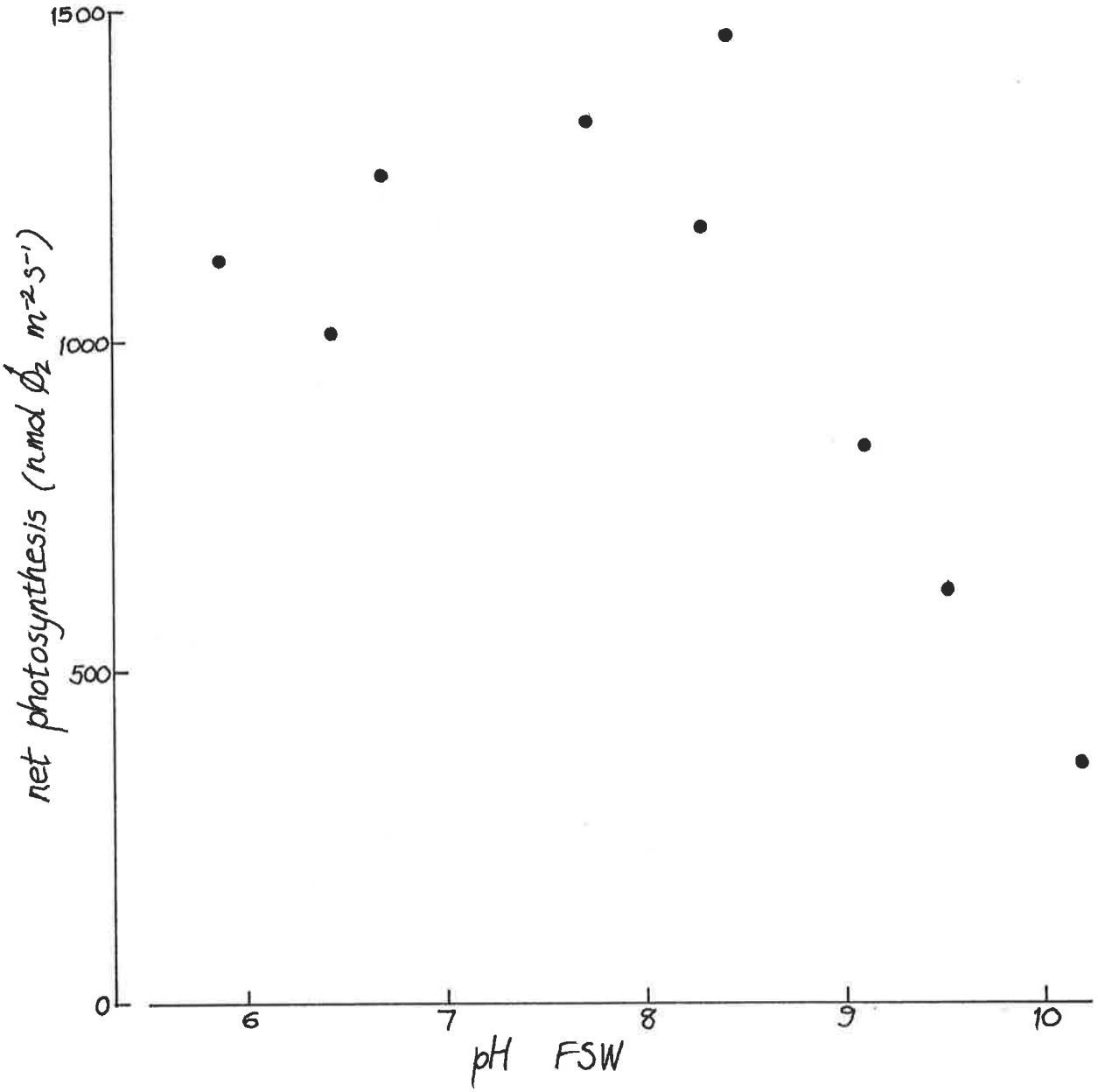

FIGURE 38. Photosynthetic O_2 evolution of U.rigida (two 14 mm diameter discs) at various pH's of FSW. T = 20.5°C.

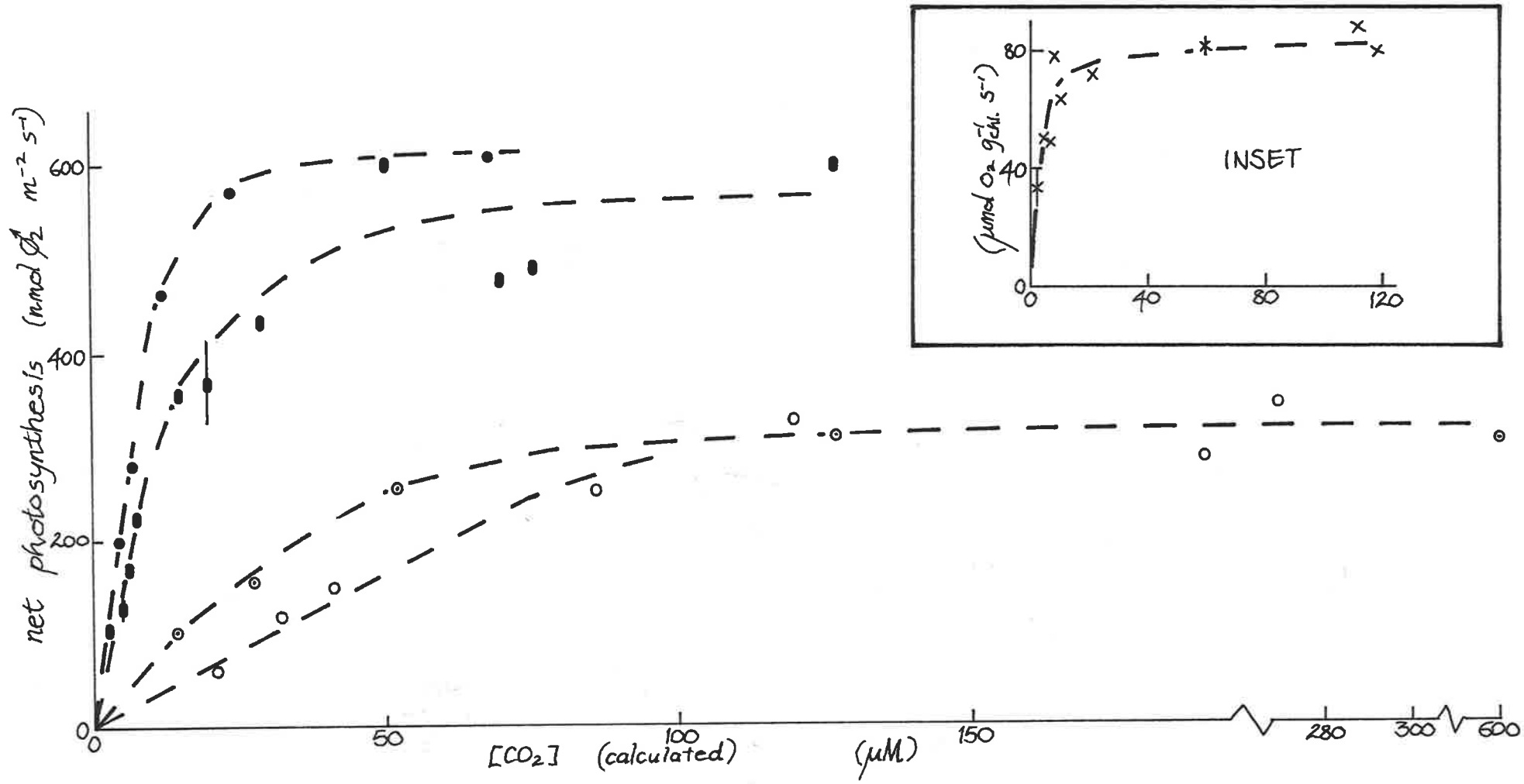

FIGURE 39. Photosynthesis of U.rigida in ASW + 10 mM MES, pH 5.45 - 5.82, at various concentrations of CO_2 for: (o) piece of thallus in B(0) with one side only exposed to solution, (⊙) same with both sides exposed, (▮) slices and (●) fewer slices. Inset shows photosynthesis of Ulva swarmers. T = 25°C.

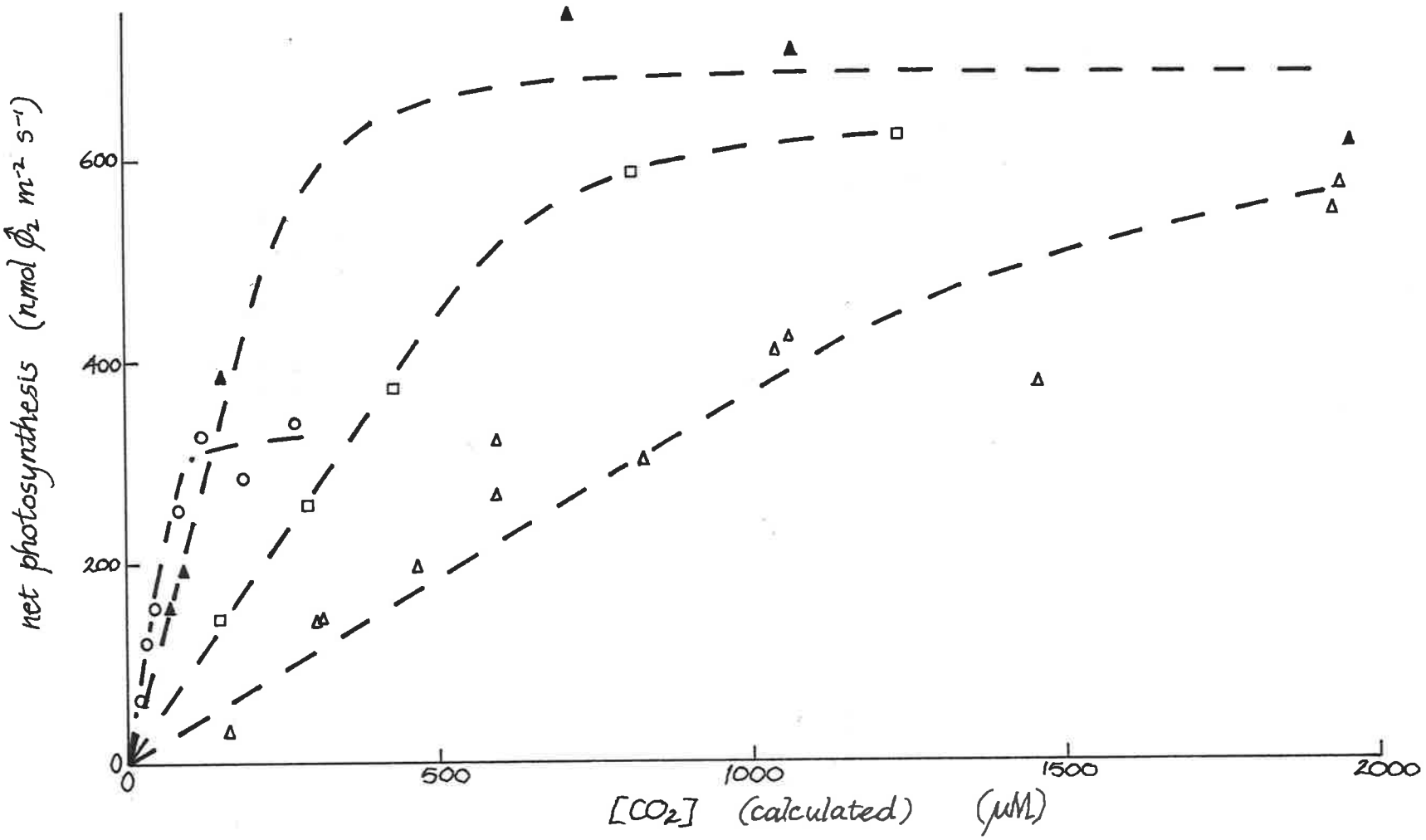

FIGURE 40. Photosynthesis of U.rigida in ASW + 10 mM MES, pH 5.45 - 6.00, at various concentrations of CO_2 for: (o) piece of thallus in B(0), (▲) in B(1), (□) in B(1a), (Δ) in B(2). T = 25°C.

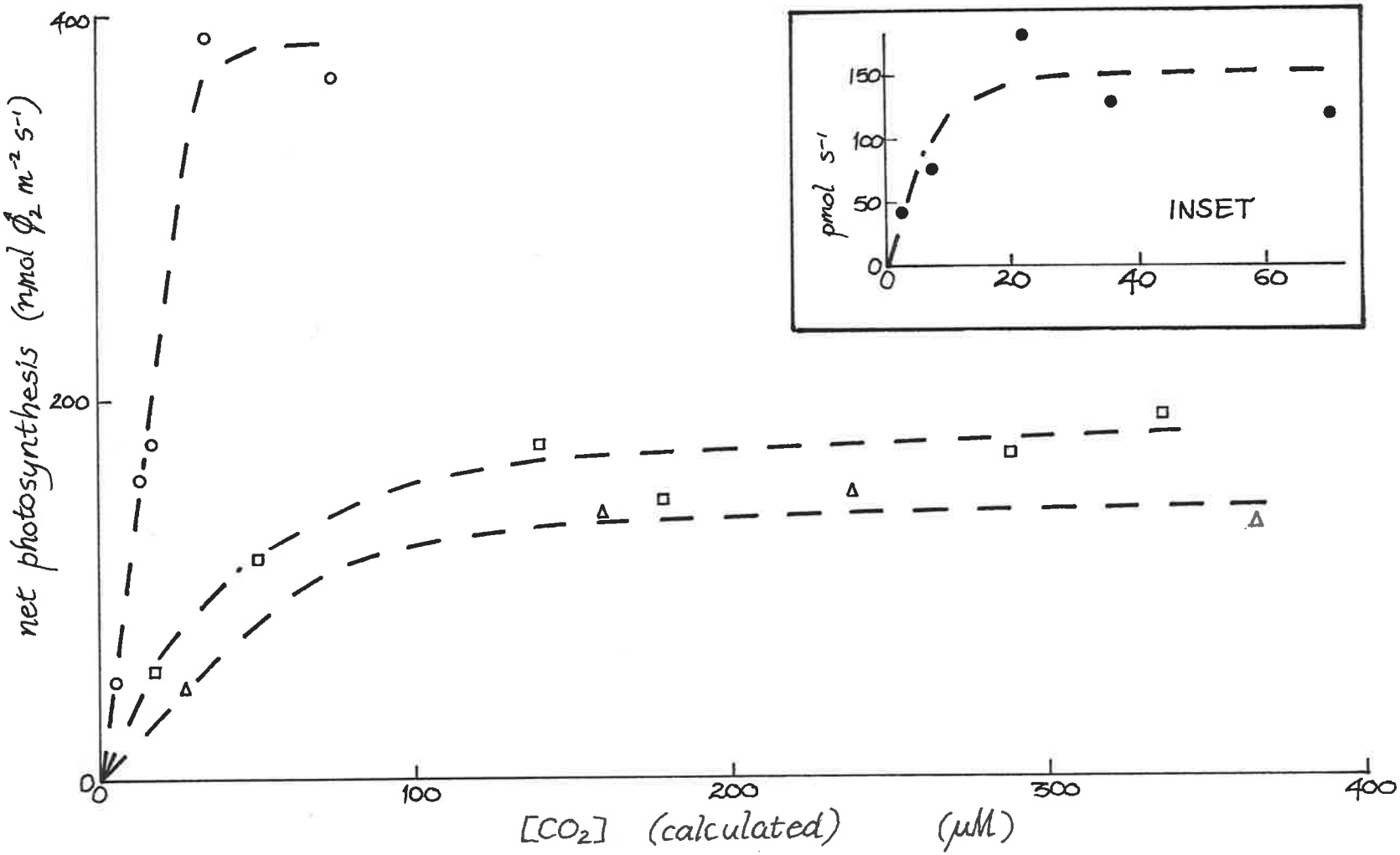

FIGURE 41. Photosynthesis of U.rigida in ASW + 10 mM MES, pH 6.53 - 7.10, at various concentrations of CO_2 for: (o) piece of thallus in B(0), (□) in B(1a) and (Δ) in B(2). Inset shows photosynthesis of slices (surface area not determined). T = 25°C.

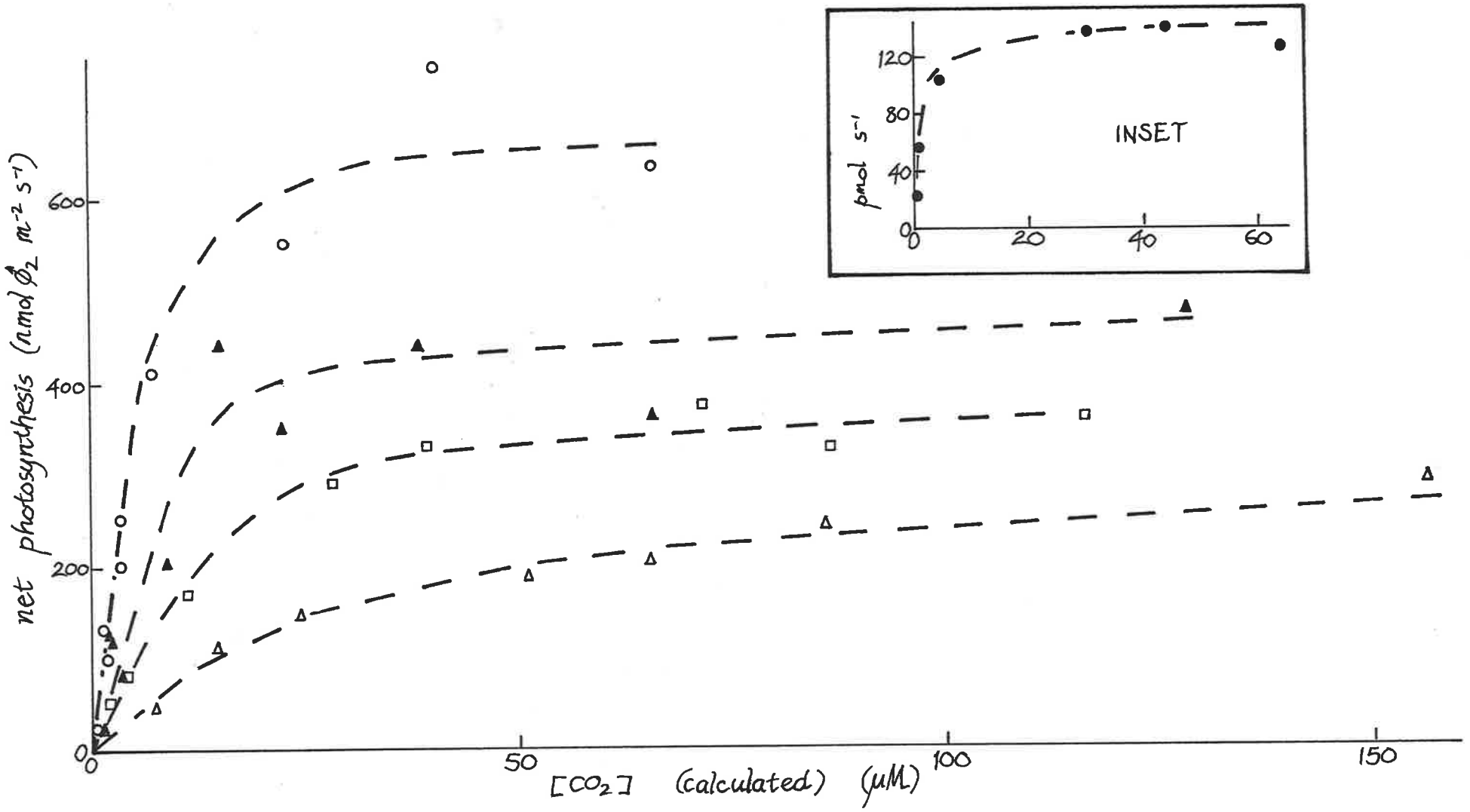

FIGURE 42. Photosynthesis of U.rigida in ASW + 10 mM TES, pH 7.60 - 7.75, at various concentrations of CO_2 for: (○) piece of thallus in B(0), (▲) in B(1), (□) in B(1a) and (Δ) in B(2). Inset - photosynthesis of slices (surface area not determined). T = 25°C.

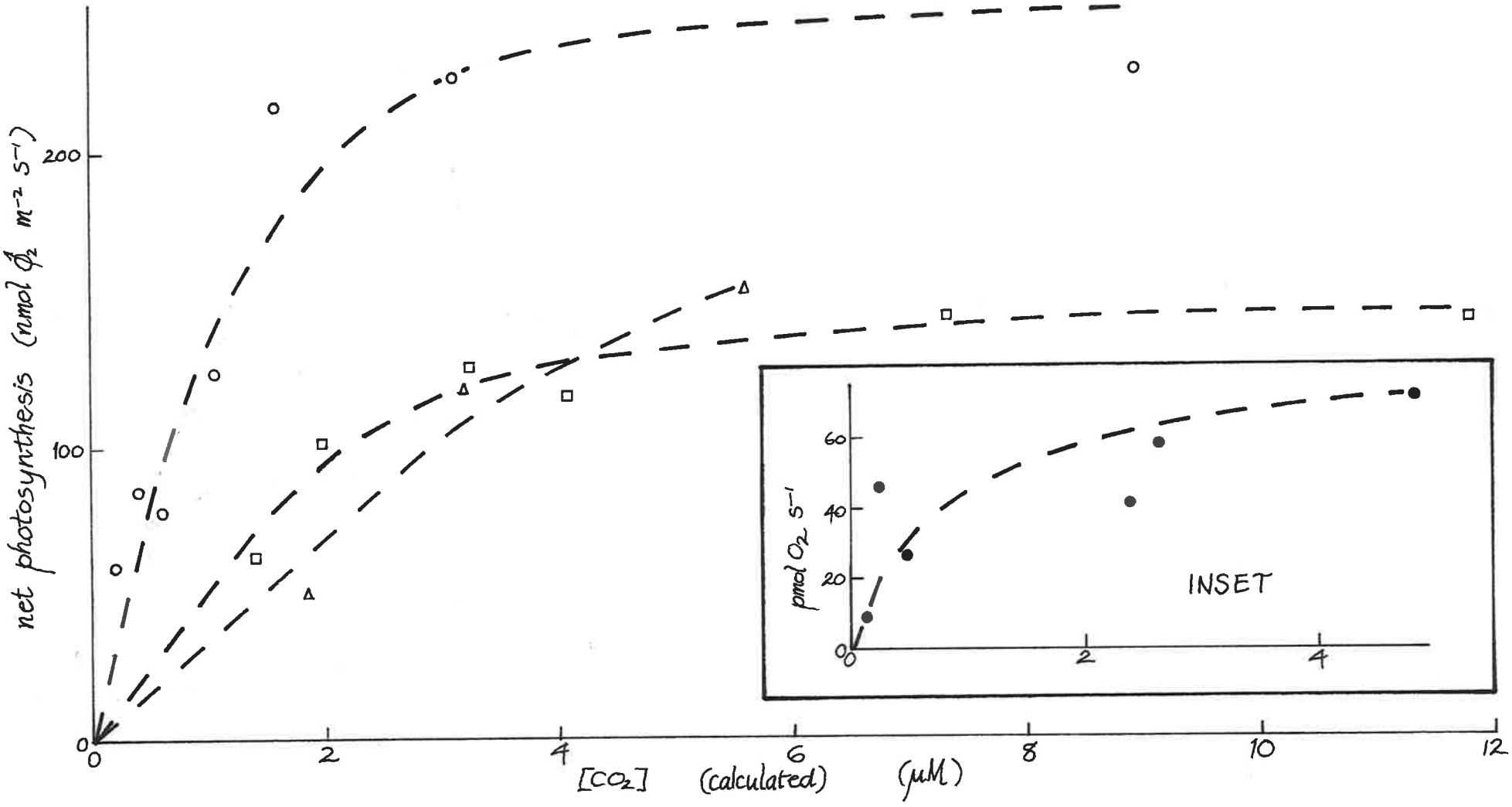

FIGURE 43. Photosynthesis of U.rigida in ASW + 10 mM TAPS, pH 8.40 - 8.65, at various concentrations of CO_2 for: (o) piece of thallus in B(0), (□) in B(1a) and (Δ) in B(2). Inset - photosynthesis of slices (surface area not determined). T = 25°C.

perspex holders not present (i.e. if the piece of thallus were "bare"). In Table 5 the initial slopes of the curves in Figs. 39 - 43 are corrected for surface area effects; when surface area is taken into account, there is little difference between photosynthesis of a piece of Ulva and the same piece in holder B(1) (cf. Figs 40 and 42).

TABLE 5

Initial slopes ($m\ s^{-1} \times 10^{-5}$) of the concentration curves shown in Figs. 39-43, with photosynthesis expressed on the basis of the surface area available for diffusion in the boundary layer.

Holder	pH of ASW			
	5.45-5.82	6.53-7.10	7.60-7.75	8.40-8.65
B(0) (both sides exposed)	1.13	-	-	-
B(0) (one side exposed)	1.14	3.20	22.1	50.7
B(1)	1.33	-	22.0	-
B(1a)	0.491	1.97	10.7	28.4
B(2)	0.222	1.03	4.62	20.9

Because of the complicated geometry of the system, initial slopes of concentration curves for slices or swarmers are less meaningful, or have a less obvious meaning. However, the apparent K_M's for CO_2 can be (see

below) an indication of diffusional limitations and these are shown in Table 6, together with the K_M^{app} for pieces of Ulva thallus. (The K_M^{app} values were obtained by using the V predicted by the computer programme FVKUP, and assuming the rate to be linear with concentration for $[CO_2] < K_M^{app}$.) Here again, surface area must be taken into account for pieces of thallus, since the holders cover a portion thereof (Fig. 9B). The K_M^{app} values shown in Table 6 are derived for the initial, linear part of the concentration curve corrected for surface area, i.e. with photosynthesis expressed on the basis of the surface area available for diffusion in the boundary layer.

TABLE 6

Apparent K_M values (μM CO_2) for photosynthetic O_2 evolution by Ulva in buffered ASW at various pH's

	pH of ASW			
	5.45-5.82	6.53-6.60	7.60-7.75	8.40-8.60
swarmers	3.6	-	-	-
few slices	6.9	-	-	0.35
slices	9.7	5.3	0.98	0.42
piece (both sides exposed)	15	-	-	-
piece (one side only exposed)	15	10 ± 5*	1.5	0.24

*Assuming V could be anywhere between 380 and 700 nmol m^{-2} s^{-1}.

In a number of experiments, I used holder B(1a) with the holes filled with a 2% agar solution of ASW + 10 mM MES; the external diffusion path length is 1.33 mm. Here (Fig. 44) rates of photosynthesis are expressed on the basis of the surface area available for diffusion, i.e. the combined surface area of the holes (97.0 mm^2). If photosynthesis was completely diffusion limited by the unstirred layer, the slope of the line in Fig. 44 would be the unstirred layer permeability (i.e. k_T). Using a diffusion coefficient for CO_2 in sea water of 1.81×10^{-9} m^2 s^{-1} (interpolated from the data of Ratcliff and Holdcroft, 1963), the predicted k_T is 1.36×10^{-6} m s^{-1}, which is in good agreement with the observed slope of the line of best fit (1.30×10^{-6} m s^{-1}).

Fig. 45 shows some results from the stirring gradient tower using ^{14}C-labelled inorganic carbon in ASW at low pH. The predictions of FVKUP for this data are shown in Table 7.

Rates of photosynthesis at high pH in the presence of the carbonic anhydrase inhibitor sulphanilamide (Fig. 46) are markedly decreased at low CO_2 concentrations (cf. Fig. 43). The apparent K_M for CO_2 has increased from 0.24 μM to about 3 μM. This large effect is not immediate; for the experiments shown in Fig. 46 the tissue had already been exposed to 0.5 mM sulphanilamide for two days. The response is similar with or without

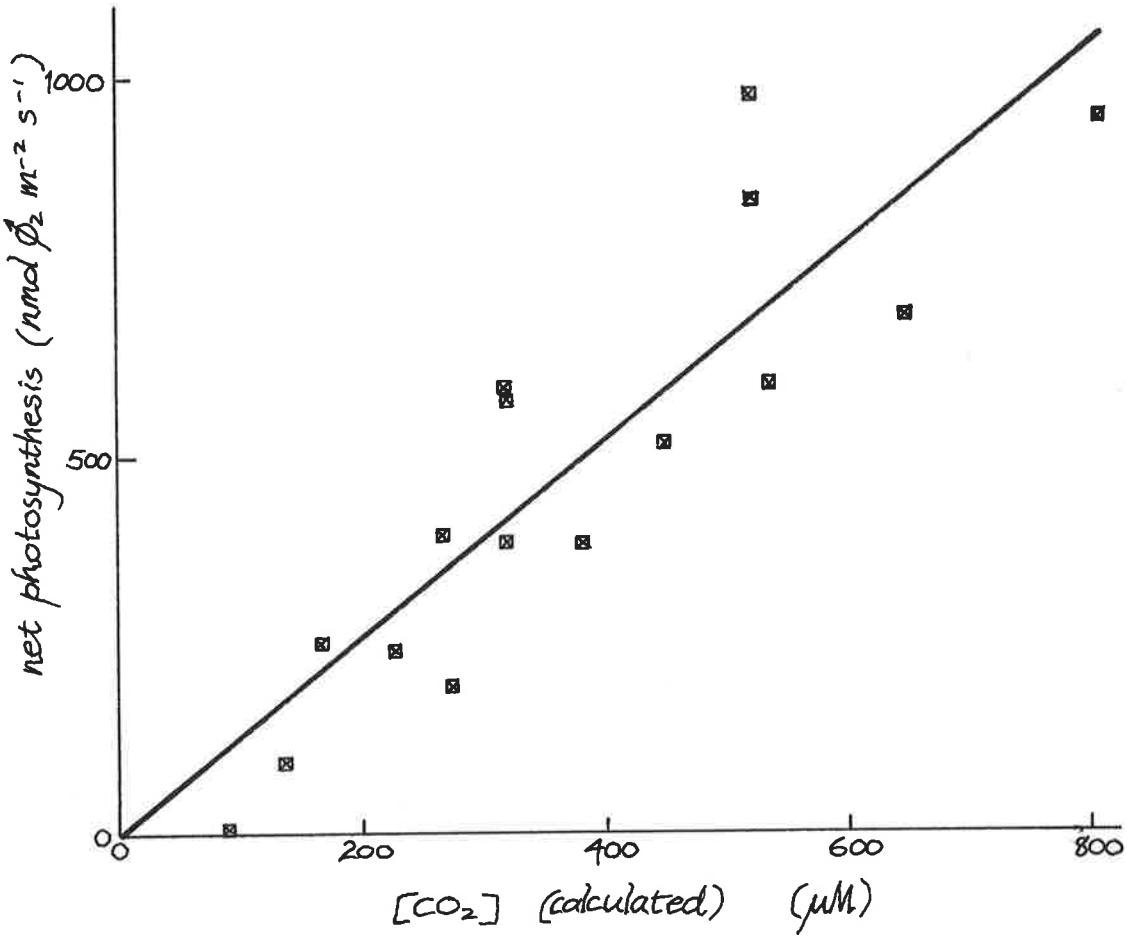

FIGURE 44. Photosynthesis of U.rigida in ASW + 10 mM MES, pH 6.55 - 6.84, 25°C, at various concentrations of CO_2 for a piece of thallus in B(1a). The holes were filled with a 2% agar solution of the bathing medium, giving a diffusion path length of 1.33 mm. The solid line (calculated by linear regression) has a slope of 1.30×10^{-6} m s^{-1} ($r = 0.899$).

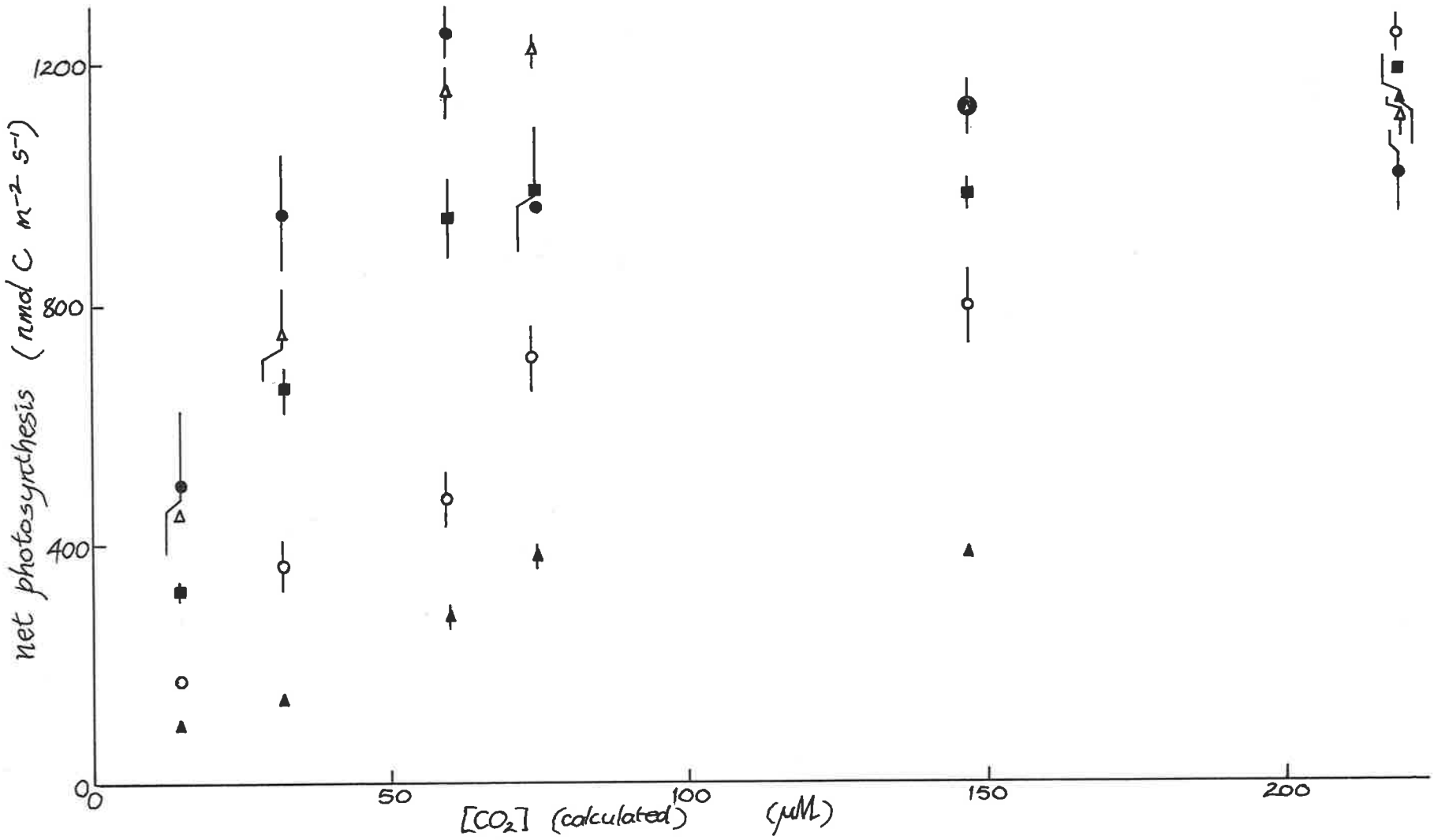

FIGURE 45. Photosynthetic $^{14}CO_2$-fixation in ASW + 10 mM MES, pH 5.19 - 5.40, at various concentrations of CO_2. Measured in stirring gradient tower at levels 1 (▲), 2 (o), 3 (■), 4 (▲) and 5 (●). T = 25°C.

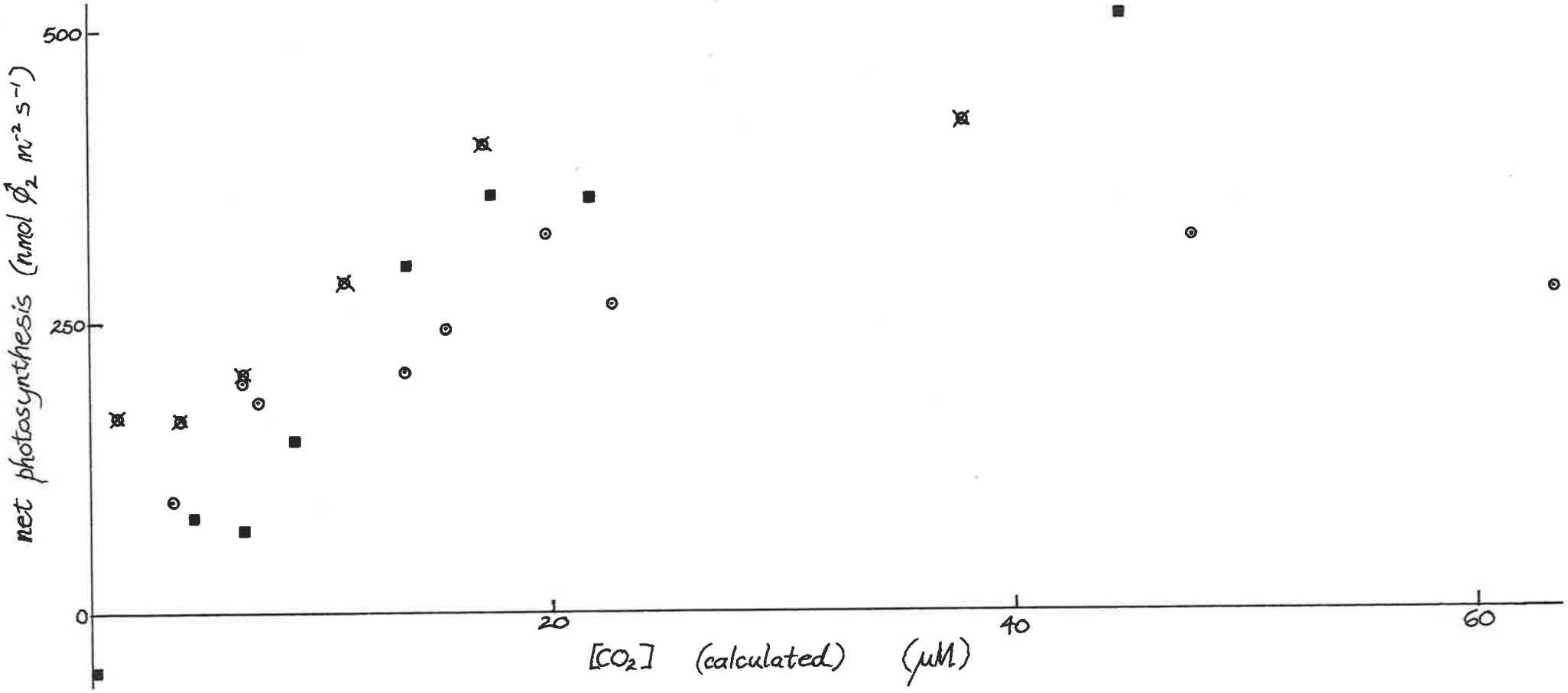

FIGURE 46. Photosynthesis of U.rigida in ASW + 10 mM TAPS + 0.5 mM sulphanilamide, pH 8.32 - 8.66, at various concentrations of CO_2. Piece of thallus in B(0) with both sides of the thallus exposed to the solution; (■) + 5 μM PABA. (⊙) and (⊠) are two different experiments. T = 25°C.

PABA which suggests that the effect of sulphanilamide is not associated with one-carbon transfer reactions (Scheffrahn, 1966). The rate of penetration of (completely dissociated) PABA, however, may have been slower than that of (mainly neutral) sulphanilamide. In the presence of both sulphanilamide and PABA there was the rare occurrence of net O_2 uptake in the light.

TABLE 7

Predicted values of V, K_M and k_T for the data shown in Fig. 45*, from the programme FVKUP.

	Level 1	Level 2	Level 3	Level 4	Level 5
V (nmol m^{-2} s^{-1})	2190	2170	1230	1180	1080
K_M (μM CO_2)	947	158	7.11	0.394	5.50
$k_T \times 10^5$ (m s^{-1})	0.631	19.6	2.67	3.03	361
regression coefficient	0.997	1.000	1.000	0.997	0.569

* Rates of photosynthesis corresponding to [CO_2] = 147 μM were omitted by mistake in these calculations.

(ii) A note on the meaning of K_M for photosynthetic CO_2 fixation

The reduction of CO_2 in photosynthesis, as catalysed by ribulose bisphosphate (RuBP) carboxylase, is a two substrate (excluding water) reaction:

$$CO_2 + H_2O + RuBP \longrightarrow 2PGA \text{ (phosphoglyceric acid)}$$

The K_M of RuBP carboxylase for CO_2, therefore, will be affected by [RuBP], as will the maximum rate (cf. the reduction of O_2). Farquhar and co-workers (Farquhar, 1979; Farquhar, von Caemmerer and Berry, 1980; Farquhar and von Caemmerer, 1982) have suggested that the binding of RuBP is so rapid that it is the rate of the supply of RuBP rather than its concentration which is important and that the former process governs the maximum rate of photosynthesis at saturating [CO_2] while at low (sub-saturating) [CO_2], the enzyme can be regarded as saturated with respect to RuBP.

On a surface area basis, the maximum rate of photosynthesis of U. rigida is very variable (Figs. 39 - 45; cf. Beer and Eshel, 1983); if the variations are due to changes in [RuBP] or the rate of supply of RuBP then there will be large changes in the apparent K_M of ribulose bisphosphate carboxylase for CO_2. Thus, a low V may lead to a low estimate of K_M; however, since the maximum (i.e. CO_2- and RuBP-saturated) rate of RuBP carboxylase sets an upper limit on the rate of CO_2

fixation, a high V will not lead to a high estimate of K_M, CO_2 transport limitations aside. For the K_M values in Table 6, all of the maximum rates at high pH (8.40 - 8.60; Fig. 43) were particularly low. This does not seem to be a direct effect of pH (Fig. 38). It may be that the observed K_M values are underestimates in this case.

(iii) Photosynthesis at low pH

The most extensive data are for photosynthesis at low pH (Figs. 39, 40 and 45) where diffusional limitations are very significant for the photosynthesis of U. rigida. This is true even for a bare piece of thallus, (Fig. 39) with the result that the apparent K_M for CO_2 decreases from about 15 μM to less than 7 μM in slices, to less than 4 μM in swarmers (Table 6). Maximum rates of photosynthesis were reasonably similar, so this comparison is probably meaningful. Indeed, on a chlorophyll basis, the rate of photosynthesis of the swarmers was higher than for slices or a more intact piece of tissue.

For the latter, the internal diffusion pathway might constitute an important part of the diffusional path length for CO_2 transport. Internal diffusion includes both diffusion in cell walls, and diffusion across membranes, cytoplasm and within the chloroplast. Because of their thinness and typical composition, CO_2 transport across membranes is likely to be fast

UNIVERSITY OF ADELAIDE LIBRARY

(Forster, 1969; Gutnecht, Bisson and Tosteson, 1977; Gros and Bartag, 1979); the cytoplasmic diffusion pathway, too, is relatively short because the chloroplasts tend to cup the inside of the cell close to the outside surface. The single chloroplast in each cell is large, however, and it might be possible for CO_2 transport within the chloroplast to become a limiting factor. At 5 μM CO_2, the rate of photosynthesis of the swarmers is about 50 μmol (g chl)$^{-1}$ s^{-1} (Fig.39) which is about 2.7 x 10^{-11} μmol s^{-1} for each swarmer (based on 60 mg chl m^{-2}, 1.4 x 10^{10} cells m^{-2} and assuming (Haxo and Clendenning, 1953) eight swarmers per "body" cell of the thallus. It is difficult to estimate the volume of the chloroplast because it is highly convoluted. Assuming it is spherical with a diameter half that of the swarmer cell ($\sim$10 μm), the volume is about 6.5 x 10^{-17} m^3; photosynthesis per unit volume of chloroplast would then be 420 mmol m^{-3} s^{-1} at 5 μM CO_2. By this same analysis, the maximum rate of photosynthesis of the swarmers would be 750 mmol m^{-3} s^{-1}. This compares reasonably well with maximum rates of photosynthesis in chloroplasts isolated from other plants; an average value would be 150 μmol (mg chl)$^{-1}$ h^{-1} or about 1600 mmol m^{-3} s^{-1} (Hall, 1976). Based on the above estimate, the modulus Φ (equation (29)) for swarmer chloroplasts is about 0.32 at c_b = 5 μM CO_2. This assumes that transport limitations external to the

chloroplast envelope are negligible and that the CO_2 diffusion coefficient is reduced 10-fold within the chloroplast - this is probably a low estimate based on some of the diffusion coefficients which have been measured in cytoplasm (Caillé and Hinke, 1974)

If Φ = 0.32, the chloroplast will be 82 - 100% "effective", depending upon the value chosen for K_M, so it is likely that 3.6 μM is a good estimate of the true K_M for CO_2 fixation i.e. CO_2 diffusion within the chloroplast is not severely rate limiting. For a piece of Ulva, internal diffusion limitations will be somewhat larger because the CO_2 supply to the chloroplasts is only from the two outer surfaces of the thallus (cf. swarmers, which are surrounded by the bathing medium) and because of the tortuosity and solid bulk of the cell walls. There are also the additional, external ("in-series") resistances of the outer cell wall (with its thin, mucilaginous cuticle) and a thicker unstirred layer due to the increase in the size of the body - pp. 16,20). These effects may combine to increase the observed K_M for CO_2-fixation to about 15 μM (Table 6, Fig 39).

The external unstirred layers imposed by the perspex holders also have a marked effect at this pH (Fig. 40). With due allowance for surface area affects, Table 5 shows that initial velocities are decreased more than 2 and more than 5 fold by holders B(1a) and B(2)

respectively.

The results shown in Fig. 45 can be compared with results from the zinc disk experiment. The stirrer was on "7" (420 r.p.m.), so k_T's must be multiplied by 0.878 (see p 57). Using D^{CO_2} (in seawater) equal to 1.81 x 10^{-9} m^2 s^{-1} (Ratcliff and Holdcroft, 1963), k_T will be futher reduced by $\{(1.81 \times 10^{-9})/(3.07 \times 10^{-9})\}^{2/3}$, or 0.703 (cf. p 57). With predicted k_T's of 0.573, 1.33, 2.67, 3.80 and 5.25 x 10^{-5} m s^{-1} (levels 1 to 5 respectively), K_M (CO_2) = 3.6 μM and V = 1150 nmol m^{-2} s^{-1}, the set of curves shown in Fig. 47 is generated by the Briggs-Maskell equation.

Taking internal diffusion into account, by using R = 5 μm (roughly the thickness of the chloroplast "layer" in U. rigida) and D_{eff} for CO_2 within the chloroplast layer of 0.603 x 10^{-9} m^2 s^{-1} (i.e. one third of D^{CO_2} in sea water), produces the curves shown in Fig. 48. The fit of the latter set of curves is only a slight improvement on that of the former at low [CO_2].

Table 7 shows, and it can be seen by inspection, that the very best fit to the data of Fig. 45 is obtained with K_M, on the whole, increasing going from level 5 to 1. Such an event would be inexplicable in terms of a simple first-order enzymic reaction, coupled with diffusional limitations. A possible recourse is to the oxygen inhibition of photosynthesis; this will be

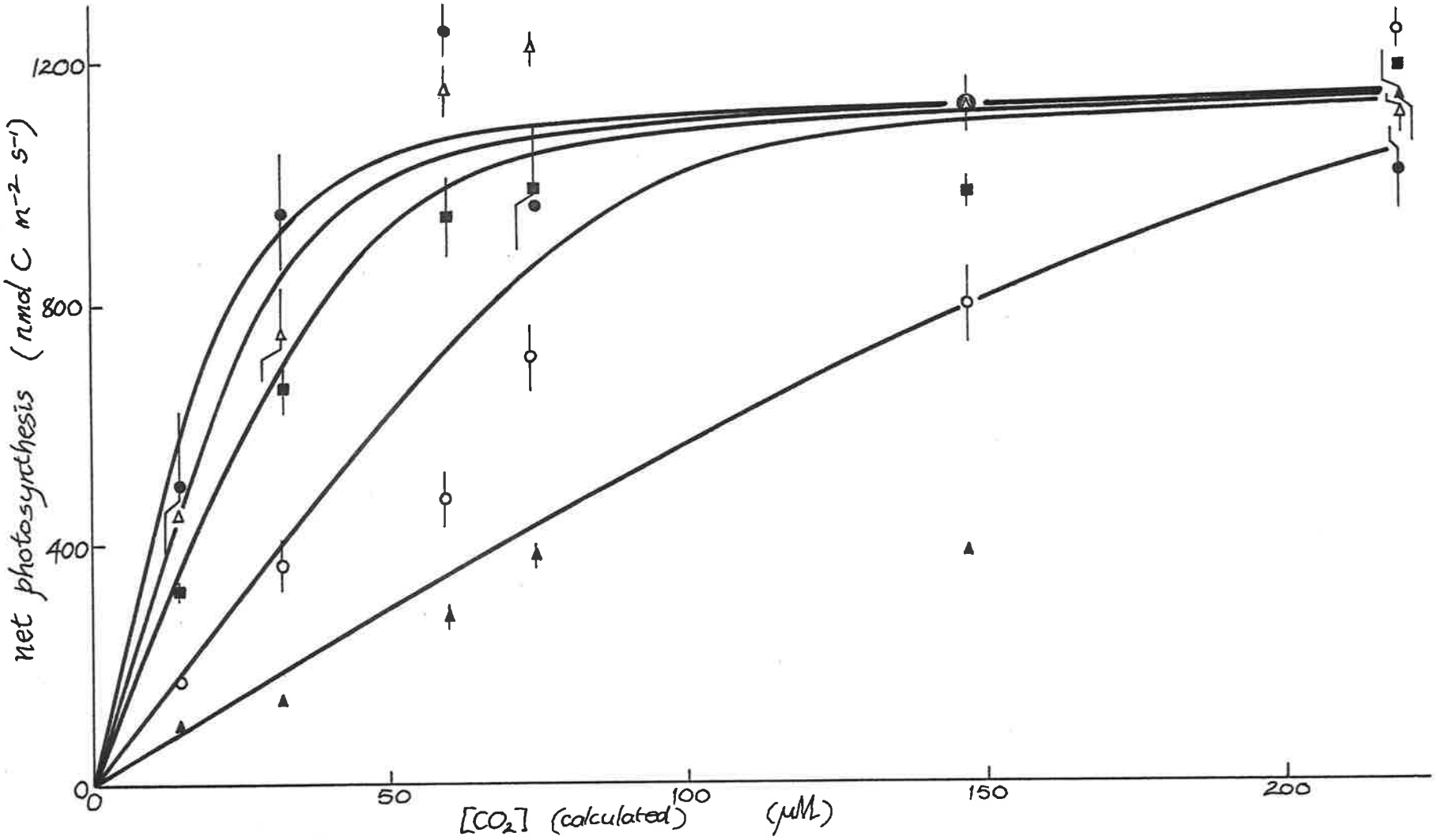

FIGURE 47. Briggs-Maskell equation, with the data of Fig. 45. See text for values of the parameters.

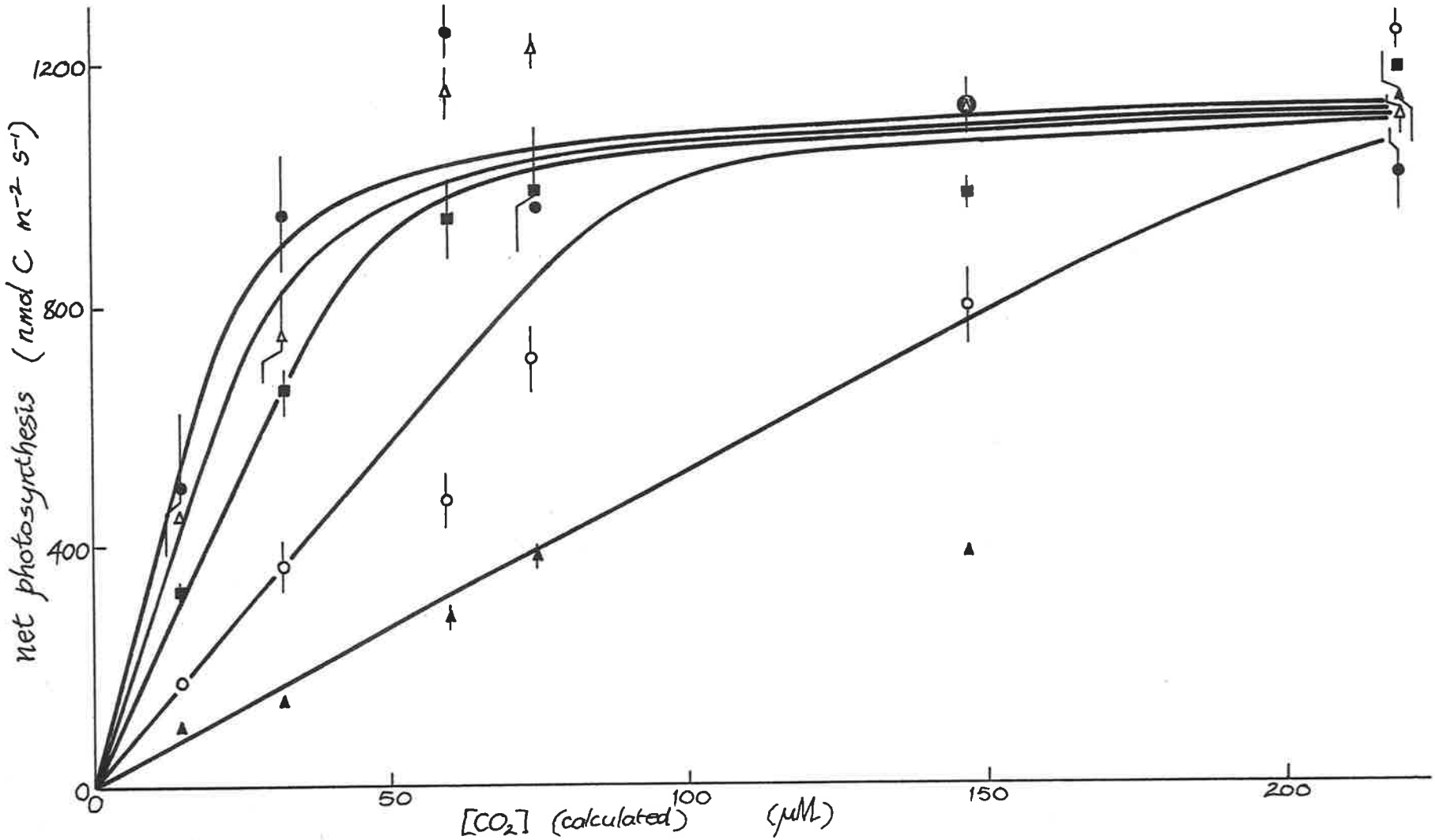

FIGURE 48. Photosynthesis-$[CO_2]$ curves based on the Yamané equation (equation (V.21)), with the data of Fig. 45. See text for values of the parameters.

discussed in the next section. Whatever the predictions of FVKUP might mean, it is interesting to note that the predicted, true K_M's for the three most well-stirred levels of the tower are still very low (5.33, 0.394 and 7.11 μM) compared with the apparent K_M's (~18, 24 and 29 μM), i.e. diffusional limitations are significant even at high rates of stirring.

(iv) Oxygen inhibition of photosynthesis

In most marine Chlorophyceae, including Ulva lactuca,L., the major enzyme catalyzing carbon fixation is ribulose-1,5-bisphosphate carboxylase (Kremer and Küppers, 1977; Colman, 1984). This enzyme is also an oxygenase, catalysing the reaction of ribulose bisphosphate with oxygen to form phosphoglycerate and phosphoglycollate. The overall kinetics of carbon fixation can be regarded as Michaelis-Menten with competitive inhibition by O_2, the overall K_M being given by

$$K_M = K_M^{CO_2}\left(1 + \frac{c_i^{O_2}}{K_M^{O_2}}\right) \qquad (35)$$

(Laing, Ogren and Hageman, 1974). $K_M^{CO_2}$ and $K_M^{O_2}$ are the K_M's of RuBP carboxylase/oxygenase for CO_2 and O_2 respectively and $c_i^{O_2}$ is the oxygen concentration at the active sites of the enzyme. With CO_2 transport limitations, the rate equation for CO_2 fixation will

then be

$$v_{CO_2} = \tfrac{1}{2}\{(K_M^{CO_2}[1 + \frac{c_i^{O_2}}{K_M^{O_2}}]k_T^{CO_2} + c_b^{CO_2}k_T^{CO_2} + V) - \sqrt{(K_M^{CO_2}[1 + \frac{c_i^{O_2}}{K_M^{O_2}}]k_T^{CO_2} + c_b^{CO_2}k_T^{CO_2} + V)^2 - 4c_b^{CO_2}k_T^{CO_2}V}\} \quad (36)$$

by substituting equation (35) into the Briggs-Maskell equation. If the rate of O_2 transport away from its place of generation is slow compared with rates of photosynthesis, then $c_i^{O_2}$ will also be a "steady-state concentration", as we have assumed is the case for $c_i^{CO_2}$. The rate of O_2 transport can be written

$$v_{O_2} = k_T^{O_2}(c_i^{O_2} - c_o^{O_2}) \quad (37)$$

based on the simple Nernst description (i.e. ignoring simultaneous diffusion and reaction, or at least partially incorporating it into k_T). In the steady state, and with a photosynthetic quotient of one, the rate of photosynthesis, v, is the rate of CO_2 fixation (v_{CO_2}, equation (36)) which will equal the rate of O_2 evolution. (v_{O_2}, equation (37)). Substituting the expression for $c_i^{O_2}$ from equation (37) into equation (36) generates a quadratic equation in v; it can be shown that the solution is

$$V = \left\{2\left(1 - \frac{K_M^{CO}\, k_T^{CO}}{K_M^{O}\, k_T^{O}}\right)\right\}^{-1} \left\{K_M^{CO_2} k_T^{CO_2} \left(1 + \frac{c_b^{O_2}}{K_M^{O_2}}\right) + c_b^{CO_2} k_T^{CO_2} + V - \sqrt{\left(K_M^{CO_2} k_T^{CO_2}\left[1 + \frac{c_b^{O_2}}{K_M^{O_2}}\right] + c_b^{CO_2} k_T^{CO_2} + V\right)^2 - 4\left[1 - \frac{K_M^{CO_2} k_T^{CO_2}}{K_M^{O_2} k_T^{O_2}}\right] c_b^{CO_2} V}\right\}. \quad (38)$$

If $c_b^{O_2} = 0$ and $k_T^{O_2}$ tends to infinity, this equation reduces to the Briggs-Maskell equation. If $c_b^{O_2} = 0$ but $k_T^{O_2}$ is finite, v will still be less than predicted with no oxygen inhibition, because $c_i^{O_2}$ will be greater than zero (see Fig. 49).

To get an idea of the importance of oxygen inhibition of photosynthesis, a knowledge of $K_M^{O_2}$ and the relative magnitude of $k_T^{O_2}$ and $k_T^{CO_2}$ is required. If it is assumed that the two transport coefficients are roughly the same and that $K_M^{O_2}$ is about 200 μM (Tolbert, 1980), then oxygen inhibition can be quite significant at high values of $c_b^{O_2}$ and low values of k_T (Fig. 49b). When $c_b^{O_2}$ is low, the effect is minor because of the low affinity of the enzyme for O_2 compared with CO_2 (i.e. the factor $K_M^{CO_2}/K_M^{O_2}$ is small).

In my experiments using the O_2 electrode, $c_b^{O_2}$ was never greater than 120 μM and estimates of k_T range from 0.2 to 1.3 x 10^{-5} m s^{-1} (Table 5). For the thicker unstirred layers, therefore, photosynthesis may have been slightly lowered by oxygen inhibition, compared with the rates which would have been expected were O_2 transport infinitely fast. Based on a fit to the

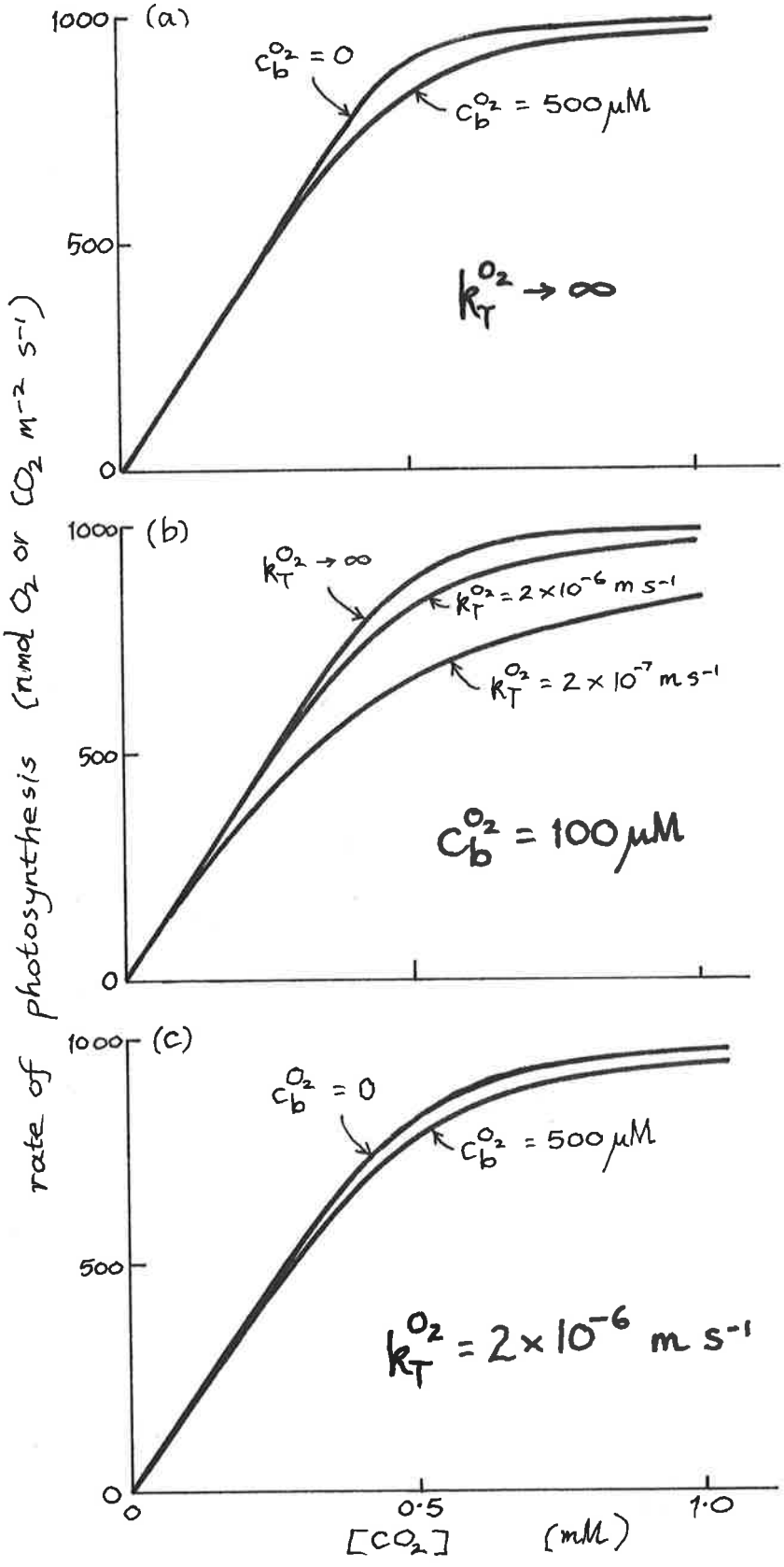

FIGURE 49. O_2 inhibition of photosynthesis, i.e. equation (38) with K_M for CO_2 = 5 μM, K_M for O_2 = 200 μM, V = 1 000 nmol m^{-2} s^{-1} and k_T for CO_2 = 2 x 10^{-6} m s^{-1}.

Briggs-Maskell equation, values for $k_T^{CO_2}$ would be slightly underestimated, i.e. the predicted unstirred layer thicknesses would be too large. The effect might be more important for the experiment shown in Fig. 45, in which $c_b^{O_2}$ was not measured but may have been close to air-equilibrium ($\sim$ 200 μM); then "K_M" would indeed have been increasing with increasing δ, if "K_M" is given by equation (35), as FVKUP predicted.

It should be added that the diffusion of O_2, compared to CO_2, is likely to be faster for the same diffusion path length because of the ratio of the diffusion coefficients (D^{O_2}/D^{CO_2} = 1.29 at 25°C in pure water; Himmelblau, 1964). O_2 transport, therefore, may impose smaller limitations than CO_2 transport on photosynthesis. However, there can be facilitation of CO_2 transport by HCO_3^- ions (see next sub-section), just as there can be facilitation of O_2 transport by macromolecular carriers (Raven, 1977). In the diffusion boundary layer, k_T has weaker dependence on the diffusion coefficient than in a strictly unstirred solution (i.e. compared with transport <u>within</u> the thallus).

(v) <u>Photosynthesis at higher pH's</u>

In ASW of higher pH (6.5 or more), it is immediately apparent that, for the same [CO_2], rates of photosynthesis are considerably increased (Figs. 41, 42,

43; Table 5). This is the typical response of a "HCO_3^- - user" and can be taken as evidence of HCO_3^- "use" (Raven, 1970). What is the nature of this HCO_3^- use in U. rigida?

The simplest explanation would be that HCO_3^- ions enhance CO_2 transport across the boundary layer in the same way as HPO_4^{2-} ions can enhance $H_2PO_4^-$ transport. A direct prediction of this mechanism is that the constraints on photosynthesis due to diffusion of CO_2 across the boundary layer should become progressively less significant as $[HCO_3^-]$ and $[CO_3^{2-}]$ increase relative to $[CO_2]$ (i.e. as the pH increases).

On the whole, this prediction is not fulfilled. At pH 6.55 - 6.84 (Fig. 44) the predicted k_T for CO_2 is very close to that observed, i.e. there is little if any enhancement of the CO_2 flux even though $[HCO_3^-]$ is more than five times $[CO_2]$ at the pH of the experiment and the unstirred layer is very thick. Similarly, at pH 7.6 - 7.75 (Fig. 42), the initial slopes of the photosynthesis - $[CO_2]$ curves for various thicknesses of the unstirred layer are in roughly the same proportions as they are at pH 5.45 - 5.82 (Table 5). This is despite the fact that $[CO_2]$ is less than 2% of the total inorganic carbon at pH 7.6 (cf. $\sim$ 70% at pH 5.6).

At pH 8.4 - 8.65 (Fig. 43), where $[CO_2]$ is only 0.12 - 0.25% of the total concentration of inorganic carbon,

there is some evidence for HCO_3^- enhancement since the CO_2-response curve for tissue in holder B(1a) is close to that in B(2). Table 5 shows that the initial slope of the "B(1a)" curve is still about half that of a piece of thallus in B(0) when this initial slope is based on the surface area directly exposed to the solution. If the flux of CO_2 to those portions of the thallus beneath the vinyl of holder B(0) was greatly enhanced, then a better basis for the calculation of the initial slope would be the total surface area of one face. The slope would then be 31.8×10^{-5} m s^{-1} in B(0), i.e. much the same as the initial slope of photosynthesis vs. $[CO_2]$ in holder B(1a), and close to that in holder B(2). There is, therefore, a case for HCO_3^- enhancenent of the CO_2 flux at pH 8.4 - 8.65. Weakening the argument, however, is the fact that, if there is strong enhancement, <u>all</u> the initial slopes, whatever the type of holder, should be calculated on the basis of the surface area of one face (even both faces?) of the tissue since the diffusion of CO_2 within tissue not directly beneath a hole will be fast. The initial slopes would then have just the proportions shown in Fig. 43. Moreover, the maximum rates of photosynthesis are quite low (160 - 260 nmol m^{-2} s^{-1}, cf. 300 - 1500 nmol m^{-2} s^{-1} from Figs.38, 39,40,42 and 45) which would lead to a lessening of diffusion restraints not necessarily associated with HCO_3^- enhancement. Indeed, at pH 6.53 - 7.10 (Fig. 42),

TABLE 8

Reactions involving CO_2, and some values of rate constants, equilibrium constants and diffusion coefficients in sea water of the chlorinity of ASW (20‰) at 25°C (from Buch, 1960; Edsall, 1969; Johnson, 1982).

Reactions	Relevant rate constants	Equilibrium constants
1. $HCO_3^- + H^+ \underset{k_{-1}}{\overset{K_{H_2CO_3}}{\rightleftharpoons}} H_2CO_3$ $H_2CO_3 \underset{k_{-2}}{\overset{k_2}{\rightleftharpoons}} CO_2 + H_2O$	$k_{CO_2} = k_1 + k_2$ $= 3.62\times10^{-2}\ s^{-1}$	$K_A' = \frac{[H_2CO_3]}{[CO_2]}$ $= 2.57\times10^{-3}$
	$k_{H_2CO_3} = k_{-1} + k_{-2}K_{H_2CO_3}'$ $= 14.2\ s^{-1}$	$K_{H_2CO_3}' = \frac{(H^+)[HCO_3^-]}{[H_2CO_3]}$ $= 4.02\times10^{-4}$ M
		$K_1'\ (\sim K_A' K_{H_2CO_3}')$ $= \frac{(H^+)[HCO_3^-]}{[CO_2]+[H_2CO_3]}$ $= 1.04\times10^{-6}$ M
2. $CO_2 + OH^- \underset{k_{HCO_3^-}}{\overset{k_{CO_2}'}{\rightleftharpoons}} HCO_3^-$	$k_{CO_2}' = 1.3\times10^{-4}\ M^{-1}\ s^{-1}$ $k_{HCO_3^-} = 1.17\times10^{-4}\ s^{-1}$	$K_{HCO_3^-}'\ (\sim K_1'/K_W')$ $= \frac{[HCO_3^-]}{[CO_2][OH^-]}$ $= 1\times10^{8}\ M^{-1}$
3. $HCO_3^- \rightleftharpoons CO_3^{2-} + H^+$		$K_2' = \frac{(H^+)[CO_3^{2-}]}{[HCO_3^-]}$ $= 1.14\times10^{-9}$ M
4. $H_2O \rightleftharpoons H^+ + OH^-$		$K_W' = (H^+)[OH^-]$ $= 1.03\times10^{-14}\ M^2$

Diffusion coefficients ($m^2\ s^{-1} \times 10^{-9}$)

CO_2	1.81	a
H_2CO_3	1.52	b
HCO_3^-	0.822	c,d
CO_3^{2-}	0.523	c,e

a. From Ratcliff and Holdcroft, 1963.
b. From D for CO_2 using Stokes' law.
c. From Kigoshi and Hashitani, 1963.
d. Corrected for ionic strength using the activity coefficients of Pytkowicz, 1975.
e. Estimate by analogy with the effect of ionic strength on D for SO_4^{2-} - Robinson and Stokes, 1959.

photosynthesis in holders B(1a) and B(2) is also low and the initial slopes are again similar.

The data over the pH range 5.5 - 8.5 do not allow a firm conclusion as to the importance of HCO_3^- enhancement for the CO_2 flux through the boundary layer and cell walls. It is worthwhile to consider whether any theoretical predictions can be made. The uncatalysed rates of the reactions between CO_2 and HCO_3^- are relatively slow (cf. the dissociation of $H_2PO_4^-$) which means that the diffusion of CO_2 also needs to be slow if the reactions are to keep pace with diffusion and influence it in any way. Friedlander and Keller (1965), showed that chemical reactions within the diffusion boundary layer have a significant effect on the flux of a particular solute only if the thickness of the Nernst layer, δ , is much greater than a "characteristic length" for the reactions involving the solute. The relevant reactions of CO_2, together with equilibrium and/or rate constants, are shown in Table 8. An initial estimate of the "characteristic length" is simply $\sqrt{D^{CO_2}/k_{CO_2}}$ which is 224 μm. This would be the value if the rate of the hydroxylation reaction $CO_2 + OH^- \longrightarrow HCO_3^-$ was negligible. At pH 8.4, the rate of this reaction is significant. The "characteristic length", based on both the hydration and hydroxylation reactions is given by Meldon, Stroeve and Gregoire (1982):

$$\left\{\left[\frac{1}{D^{CO_2}} + \frac{4K_2'\overline{[HCO_3^-]}(2A - \overline{[HCO_3^-]})}{K_1'\,\bar{D}\,(A - \overline{[HCO_3^-]})^2}\right]\right.$$
$$\left.\left[k_{CO_2} + \frac{k_{HCO_3^-}\,K_1'(A - \overline{[HCO_3^-]})}{2K_2'\overline{[HCO_3^-]}}\right]\right\}^{-\frac{1}{2}}$$

in which $\overline{[HCO_3^-]}$ is a mean $[HCO_3^-]$ throughout the Nernst layer, $\bar{D}$ is a mean diffusion coefficient for HCO_3^- and CO_3^{2-} ions and A is equal to $[HCO_3^-] + 2[CO_3^{2-}]$. Assuming that $\overline{[HCO_3^-]}$ is approximately $[HCO_3^-]$ in the bulk solution (this gives a maximum value of the "characteristic length") and that $\bar{D}$ is midway between $D^{HCO_3^-}$ and D^{CO_2}, the "characteristic length" is 159 μm at pH 8.4. By comparison, the thickness of the unstirred layer is about 815 μm for holder B(2) and about 370 μm for holder B(1a). (These values are obtained from the initial slopes at low pH (Table 5). They are good estimates in that the apparent K_M for CO_2 is so far removed from the "true" K_M, and the effect of oxygen inhibition (Fig. 49) is probably small.)

For the thick unstirred layer then (holder B(2)), some enhancement of CO_2 transport through it is expected since the "characteristic length" for the uncatalysed reactions of CO_2 is less than one fifth of the unstirred layer thickness. Calculation of the degree of enhancement is greatly simplified if it is assumed that the pH gradient across the diffusion boundary layer is negligible, although given the relatively mild buffering used (10 mM TAPS) this is probably not a good

assumption. In any case, the constant pH assumption gives the maximum enhancement possible based on the uncatalysed hydration and hydroxylation of CO_2. Using the solution of Hoover and Berkshire (1969), the predicted enhancement is 5.45 times the CO_2 flux in the absence of chemical reactions in the diffusion boundary layer. In the calculation, I have used a mean diffusion coefficient for CO_2/HCO_3^-; this is more realistic than assuming (as Hoover and Berkshire did) that the diffusion coefficients of the inorganic carbon species are equal (see Quinn and Otto, 1971). If there were no buffering at all in the unstirred layer, apart from the CO_2-HCO_3^--CO_3^{2-} system, the predicted enhancement would be something more than 20% lower (Quinn and Otto, 1971).

In Fig. 43, then, the similarity in the two CO_2 response curves for U. rigida in holders B(1a) and B(2) may well be due to HCO_3^- enhancement of the rate of CO_2 diffusion through B(2), and there may also be a small enhancement of diffusion through B(1a). However, such a mechanism still cannot account for the "use" of HCO_3^- by U. rigida since, even if the transport of CO_2 to the plasmalemma were infinitely fast, its equilibrium concentration at the plasmalemma would not be sufficient to support the observed rates of O_2 evolution. From the experiments at low pH, the half saturation concentration of CO_2 with negligible transport limitations is about

3.6 μM. At pH 8.4 - 8.65, however, (Fig. 43, Table 6), the calculated K_M for CO_2 is one tenth of this value - 0.24 - 0.42 μM.

It is possible that the pH of the cell wall is lower than that of the bulk medium, given a Donnan distribution of H^+ ions. Then, at equilibrium,* $[CO_2]$ would be higher in the cell wall than in the bulk solution or the unstirred layer. However, equilibrium would never be approached in the cell wall: the thickness of the outer cell wall is only about 2 μm at the most, so that, unless diffusion coefficients were reduced 80 fold or more, the diffusion of CO_2 across the wall would be rapid compared with the rate of transformation of HCO_3^- into CO_2 in the wall. The effective $[CO_2]$ at the plasmalemma,therefore, would not be affected by the wall pH, unless the wall pH was very low (cf. Walker, Smith and Cathers, 1980). This may not be the case if there was a powerful catalyst in the cell wall. There are a number of substances that are known to be CO_2-hydration catalysts (e.g. oxyanions of weak acids, such as arsenite ion, hypochlorite ion). The most powerful catalyst is the enzyme carbonic anhydrase. If the cell wall was catalytic, then equilibrium between CO_2 and HCO_3^- might be approached even for short diffusion times. The experiments with sulphanilamide (Fig. 46) suggest that carbonic anhydrase is involved in photosynthesis, but the lengthy pre-treatment that is

---

* That is, the equilibrium between CO_2 and $HCO_3^-/CO_3^=$ <u>in the cell wall</u>, <u>not</u> the equilibrium $CO_{2(wall)} \rightleftharpoons CO_{2(bulk)}$.

required for a significant effect implies that the enzyme is not located in the cell wall, which should be readily accessible to the inhibitor.

Even if equilibrium was approached in the cell wall, for there to be a ten fold decrease in the apparent K_M for CO_2 at pH 8.4, the pH in the cell wall would need to be about 7.5. This seems unlikely, particularly since there is a net influx of H^+ ions during the photosynthesis of at least two Ulva species which increases the pH of the boundary layer above that of the bulk solution (Cummins, Strand and Vaughan, 1969).

(vi) Mechanisms of HCO_3^- use

Given that an enhanced CO_2 flux across an unstirred layer, due to the presence of HCO_3^-, cannot solely account for the observed use of HCO_3^- ions by U. rigida, the next (in order of decreasing economy) additional postulate is that the cell membrane is sufficiently permeable to HCO_3^- ions to allow a significant flux of the ion across the plasmalemma. If there were no catalyst for converting HCO_3^- to CO_2, the cell would be no better off in this situation. With a catalyst, at a pH of 7 in the cytoplasm and using an estimated pK'_a for HCO_3^- of 5.98 (i.e. the same as in sea water), HCO_3^- would be in equilibrium with about 8% as much CO_2. The required steady-state $[HCO_3^-]$ needed to account for the rates of O_2 evolution that are observed can be

calculated, therefore. For instance, at pH ~8.4, 0.5 μM CO_2 in the bulk phase gave a rate of O_2 evolution of about 80 nmol m^{-2} s^{-1} (piece of thallus in B(0), Fig. 43). At pH ~5.5 (Fig. 39) the comparable rate is only 5.8 nmol m^{-2} s^{-1} at 0.5 μM CO_2. This low rate, however, is partly because of the limitations imposed by the transport of CO_2 upto the plasmalemma. The results with swarmers (Fig. 39, Table 6) imply that the rate can be increased more than four times at low [CO_2] if the rate of transport of CO_2 up to the plasmalemma is increased. Per unit area of thallus, the rate of O_2 evolution would be 24 nmol m^{-2} s^{-1} at 0.5 μM CO_2 if CO_2 transport upto the plasmalemma were as fast as it is in a well-stirred suspension of swarmers. The rate could be even higher if transport limitations up to the chloroplast envelope were entirely removed. (This would approximate the situation for cells with an 'inside'(i.e. cytoplasmic) source of CO_2 from equilibration with HCO_3^- in the cytoplasm.) So cytoplasmic HCO_3^- would need to supply a sufficient [CO_2] to give a rate of photosynthesis of (80 - 24) = 56 nmol O_2 m^{-2} s^{-1} i.e. about 1.2 μM CO_2 at most by analogy with swarmers. [HCO_3^-], therefore, would need to be 15 μM, or possibly less, in the cytoplasm. In the bulk phase, [HCO_3^-] is about 200 μM at pH 8.4, 0.5 μM CO_2, so the required [HCO_3^-] could be achieved within the cytoplasm provided the electrical potential difference (P.D.) across the plasmalemma were not too much more negative than -66 mV. This value of the

membrane P.D. is plausible; West and Pitman (1967) quote a value of -60 mV for U. lactuca while Black and Weeks (1972) found only -42 mV in a species of the related genus Enteromorpha.

Thus, by this equilibrium argument, the scheme outlined above could work. The problem is that $[HCO_3^-]$ is not an equilibrium concentration but a steady-state one. The CO_2 formed from HCO_3^- is continually removed not just by the diffusion of CO_2 back into the bulk medium but also in photosynthesis itself. Ignoring the latter for the moment, it is clear that the influx of HCO_3^- must far exceed the efflux of CO_2, since the tendency is for $[CO_2]$ to equalize on either side of the plasmalemma. It could be argued that diffusion limitations, both internal and external, could lead to a decrease in the efflux of CO_2 formed from HCO_3^- in the cytoplasm, i.e. CO_2 "trapping". The results shown in Fig. 39 (low pH) imply that diffusion resistances for CO_2 between the plasmalemma and the bulk medium are significant, so that transport between these two could be rate limiting for CO_2 efflux. This may not be the case for HCO_3^- influx, where the potential concentration gradients (and therefore rates of transport) are much larger (at high pH). In this situation, therefore, a thick Nernst layer may be an advantage provided the influx of HCO_3^- is not too greatly affected. The results at high pH (Fig. 43) provide some support, since in this

case slicing is detrimental from the point of view of the half-saturation concentration of CO_2 needed for photosynthesis; the apparent K_M <u>increases</u> upon slicing (Table 6).

The extent of diffusion limitations to the membrane transport of HCO_3^- will depend on the kinetics of the influx. Assuming they are Michaelis-Menten, an influx as large as that required for CO_2 fixation could occur even if the K_M of the porter was quite high, because of the high concentration of HCO_3^-. Transport (bulk phase to plasmalemma) restrictions would then be much less severe than those that exist for CO_2 fixation at low pH. (It is also possible that the <u>maximum</u> HCO_3^- influx determines the maximum rate of phtosynthesis. This would explain why the maximum rates at high pH are low and would also lead to an underestimate of the "true K_M" for CO_2 of the carboxylase. No firm conclusions can be drawn from the measured values of the maximum rates, however, given their variability.)

It is possible, then, to obtain a higher steady-state concentration of CO_2 in the cytoplasm than in the bulk medium provided the influx of HCO_3^- is rapid compared with the efflux of CO_2. The work done to maintain the dis-equilibrium would be the work required to maintain the pH gradient across the plasmalemma (i.e. to keep the cytoplasmic pH low in comparison with the bulk medium in

the face of a rapid influx of base), and to maintain a constant electrical potential difference across the plasmalemma.

It is also necessary that CO_2 is formed rapidly enough from HCO_3^- to keep up with the rate of its assimilation in photosynthesis. The presence of the enzyme carbonic anhydrase in moderate amounts would ensure that HCO_3^- and CO_2 are always virtually in equilibrium. The effects of sulphanilamide (Fig. 46) are not immediately consistent with the inhibition of carbonic anhydrase. The prolonged pretreatment that is required is puzzling, because even intra-cellular carbonic anhydrase should be reasonably accessible to sulphanilamide; Geers and Gros (1984), for example, give a value of 30 minutes for the penetration of another sulphonamide (acetazolamide, 10 μM) into skeletal muscle cells and the work of Holder and Hayes (1965) suggests that sulphanilamide would penetrate considerably faster. It is possible that U. rigida contains an iso-enzyme of carbonic anhydrase which is more insensitive to sulphanilamide than most animal enzymes (Everson, 1970; Graham, Reed, Patterson and Hockley, 1984). In that case, relatively large amounts of sulphanilamide would be needed within the cell for significant inhibition of the enzyme. A concentration higher than that in the bulk medium could be achieved by an accumulation mechanism analogous to the classical model for ammonia

accumulation by plant cells, i.e. diffusion across the membrane as the neutral base and trapping in the more acid cytoplasm (and even more acid vacuole) as NH_3^+  SO_2NH_2; however, there is then some uncertainty as to whether electron transport in the chloroplasts remains unaffected (Stern, 1963; Swader and Jacobson, 1972). It would be worthwhile to study the effects of more powerful inhibitors of the plant enzyme at high pH.

The uptake of O_2 in the light (no CO_2) that was observed following treatment with sulphanilamide plus PABA is interesting from the point of view of the trapping and subsequent (re) fixation of respiratory and photorespiratory CO_2. With carbonic anhydrase present, the cytoplasm would form an effective CO_2 trap since most of the CO_2 would be immediately converted to HCO_3^- ions; this could explain why, in general, O_2 uptake (CO_2 evolution) was not observed in the light. Inhibiting the carbonic anhydrase with sulphanilamide in the presence of PABA has the predicted effect, but not in its absence. One or other of sulphanilamide or PABA, therefore, might have other effects on mitochondrial respiration or photorespiration; it was observed, for example, that rates of dark respiration were much (up to five times) higher in the sulphanilamide plus PABA treated tissue than for tissue treated with sulphanilamide alone. High rates of dark respiration do

not necessarily give rise to the uptake of O_2 in the light - U. rigida swarmers had extremely high rates of dark respiration, but O_2 uptake in the light was not observed.

II. Photosynthesis of Amphibolis antarctica and Vallisneria spiralis

(i) Results

Fig. 50 shows the photosynthesis - CO_2 curve of A. antarctica leaf pieces at low pH; CO_2 seems to inhibit photosynthesis at high concentrations. Some data at high pH, again obtained with the O_2 electrode, are shown in Fig. 51.

Using ^{14}C-fixation, the response to [CO_2] (low pH) of sections of V. spiralis leaf in the stirring gradient tower does not have any relationship with the degree of stirring of the bulk solution (Fig. 52a). If the rates of ^{14}C fixation at each concentration are lumped (Fig. 52b), the Briggs-Maskell curve of best fit (FVKUP) is obtained with a K_M (293 μM CO_2) virtually the same as the apparent K_M (V equal to 675 nmol m^{-2} s^{-1}). A reasonable fit can also be obtained if k_T is small (as it is for O_2) and K_M quite low; the solid line in Fig. 52b, for example, represents the Briggs-Maskell equation with K_M = 30 μM and k_T = 1.3 x 10^{-6} m s^{-1}. Again, CO_2 is possibly inhibitory at the highest concentration.

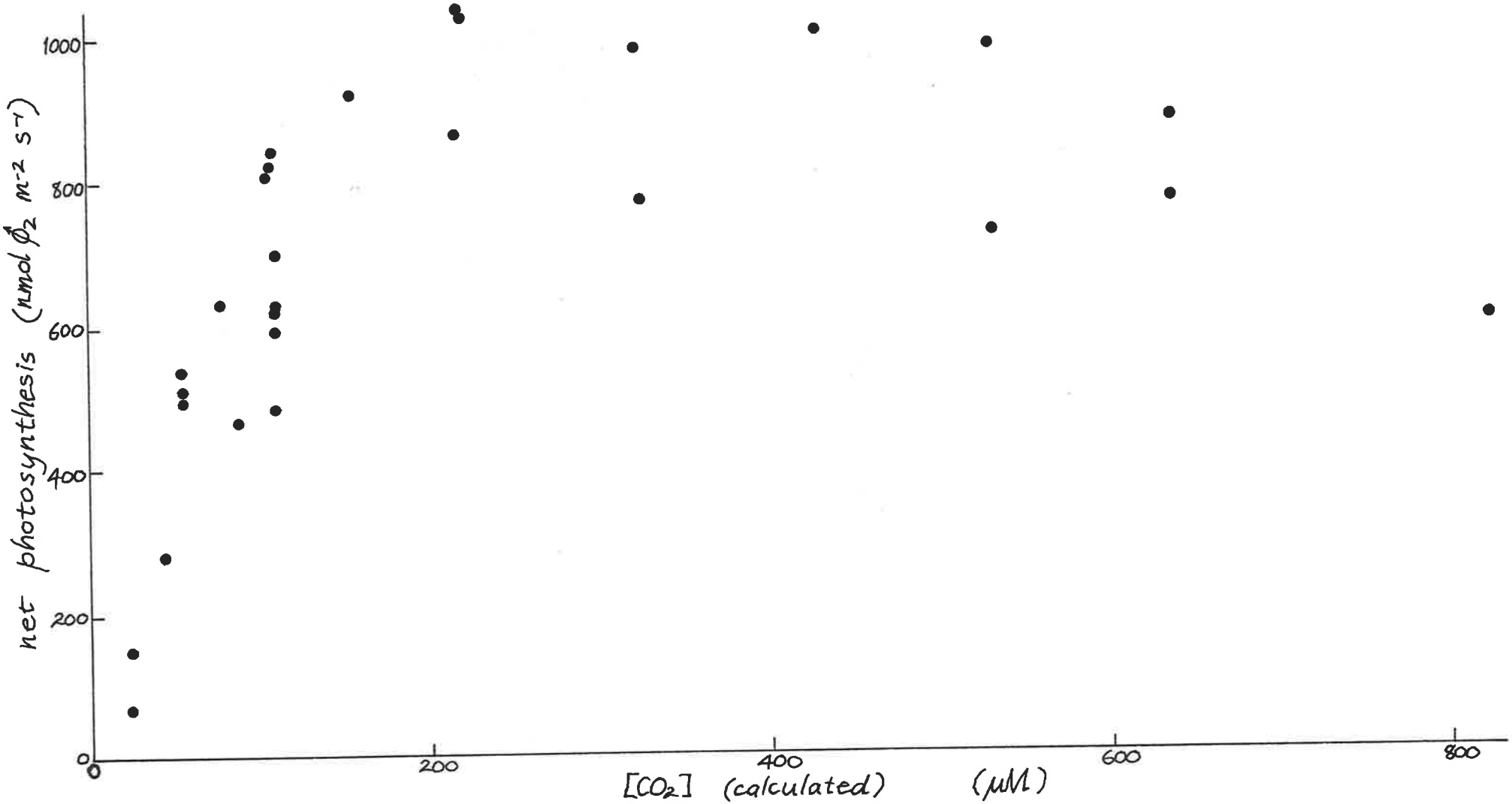

FIGURE 50. Net photosynthetic O_2 evolution against [CO_2] of A.antarctica leaves, in ASW + 50 mM MES, pH 5.01 - 5.20, 20°C.

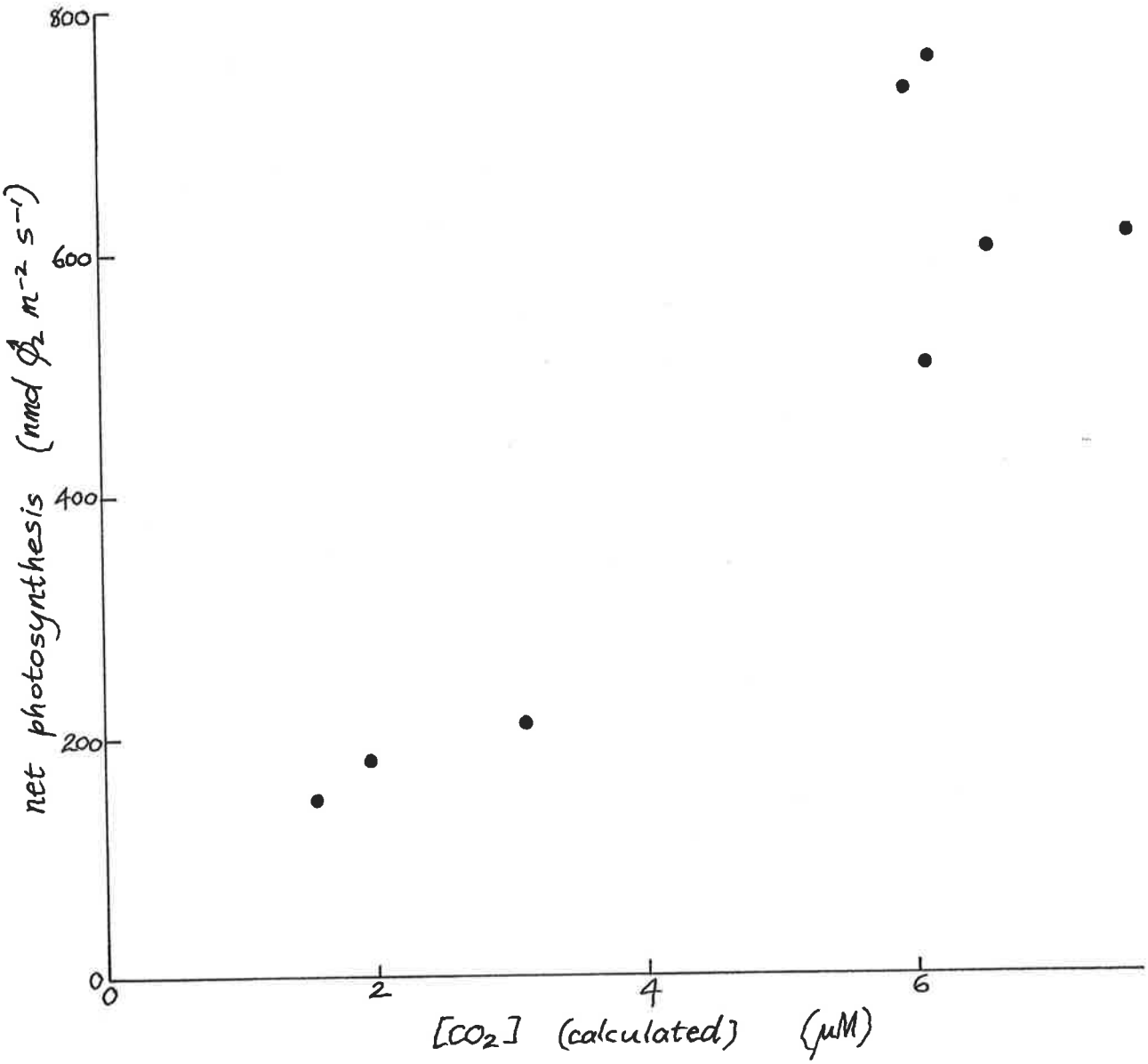

FIGURE 51. Photosynthesis of A.antarctica leaves in ASW + 50 mM TAPS, pH 8.45 - 8.80, 20°C.

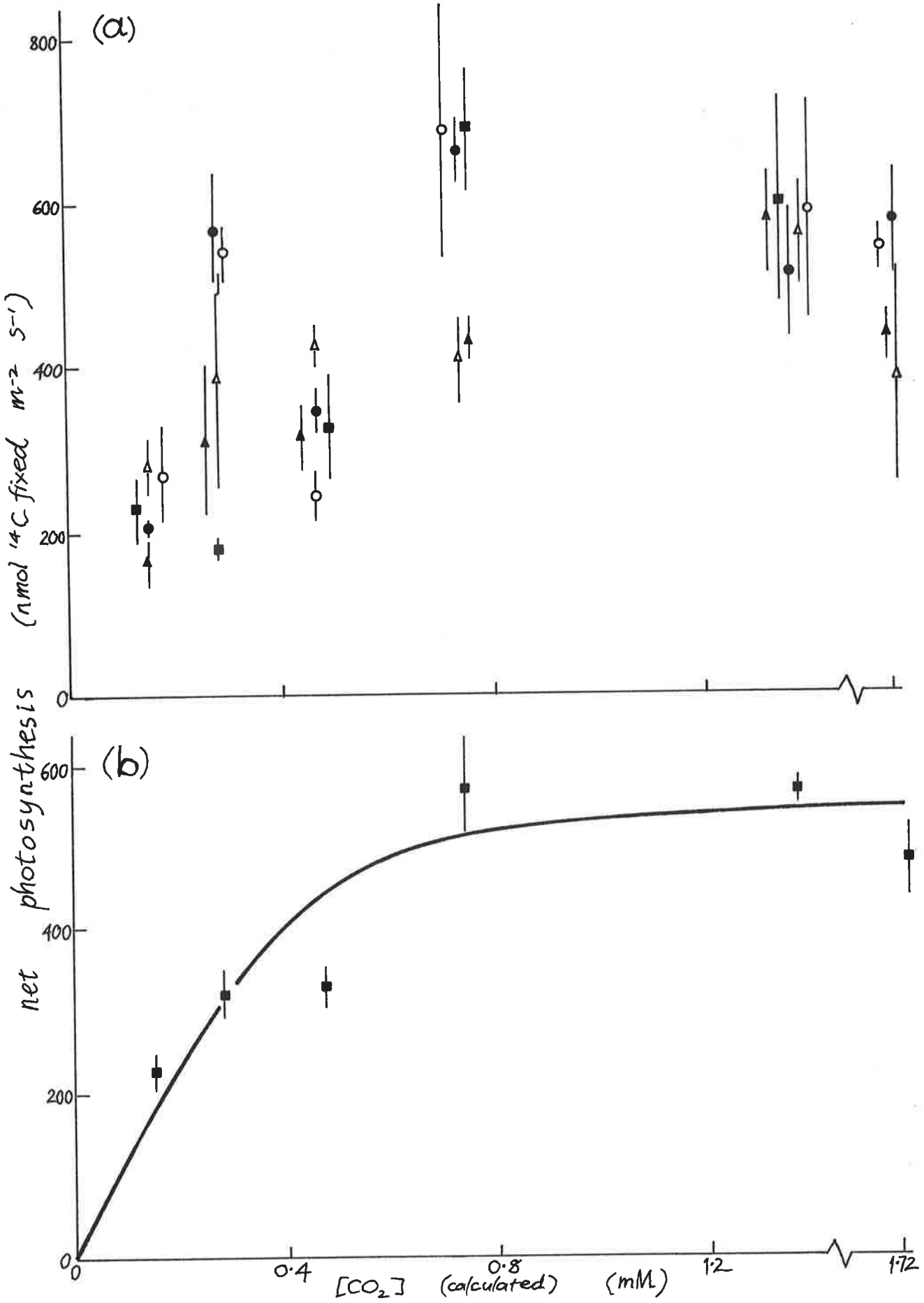

FIGURE 52a. Photosynthetic $^{14}CO_2$ fixation of V.spiralis (292 g fresh wt. m^{-2}) in the stirring gradient tower (symbols as in Fig. 15); pH 5.7 - 6.0, 25°C.
b. Data at each concentration lumped.

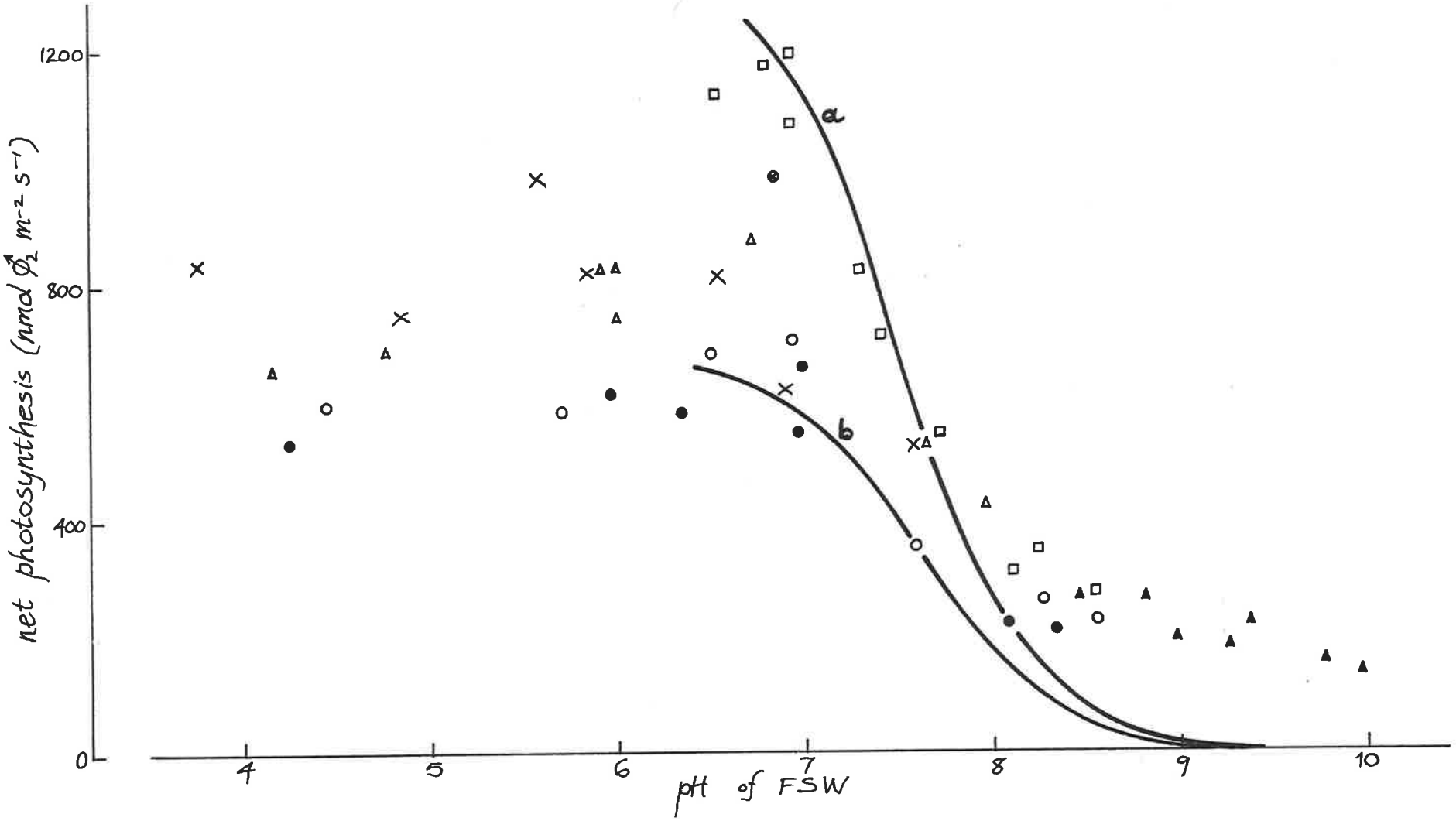

FIGURE 53. Photosynthesis vs. pH profile for A.antarctica in FSW (inorganic carbon concentration = 2.22 mM). Results of a number of experiments shown; 51.7 ± 1.2 g fresh weight m^{-2}, 1.18 ± 0.052 mg chlorophyll (g fresh weight)$^{-1}$. 20°C. Curve a: pH response predicted by Briggs-Maskell equation with V = 1400 nmol m^{-2} s^{-1}, K_M = 30 μM, k_T = 3 x 10^{-5} m s. Curve b: Same as "a" but with V = 700 nmol m^{-2} s^{-1}.

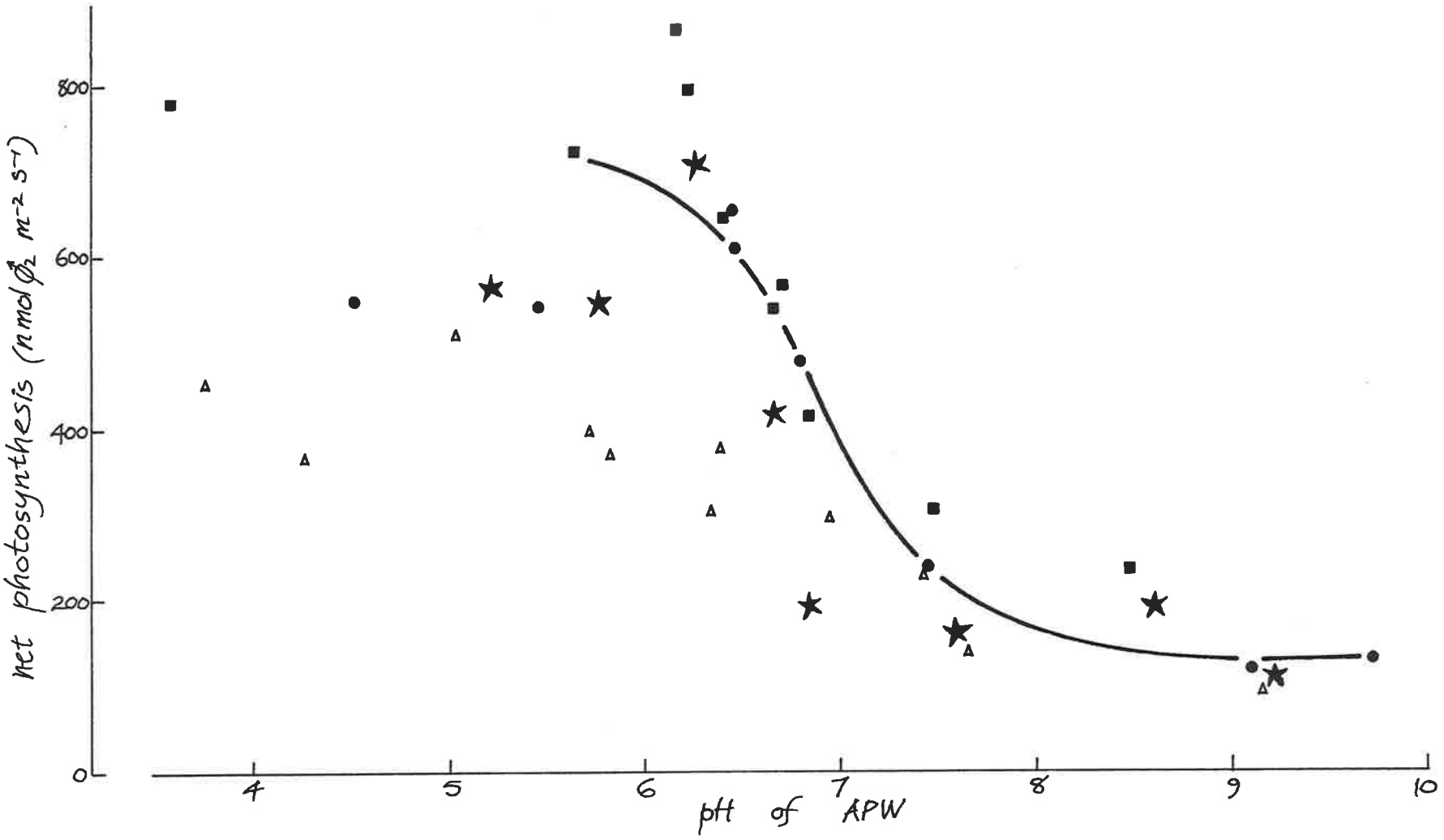

FIGURE 54. Photosynthesis of sections of V.spiralis leaf (■,●): in the presence of carbonic anhydrase (★), and in holder B(2) (Δ). Inorganic carbon concentration: 1.64 mM (■), 1.19 mM (●,★), 1.87 mM (Δ). T = 20°C (■) or 25°C (●,★,Δ).

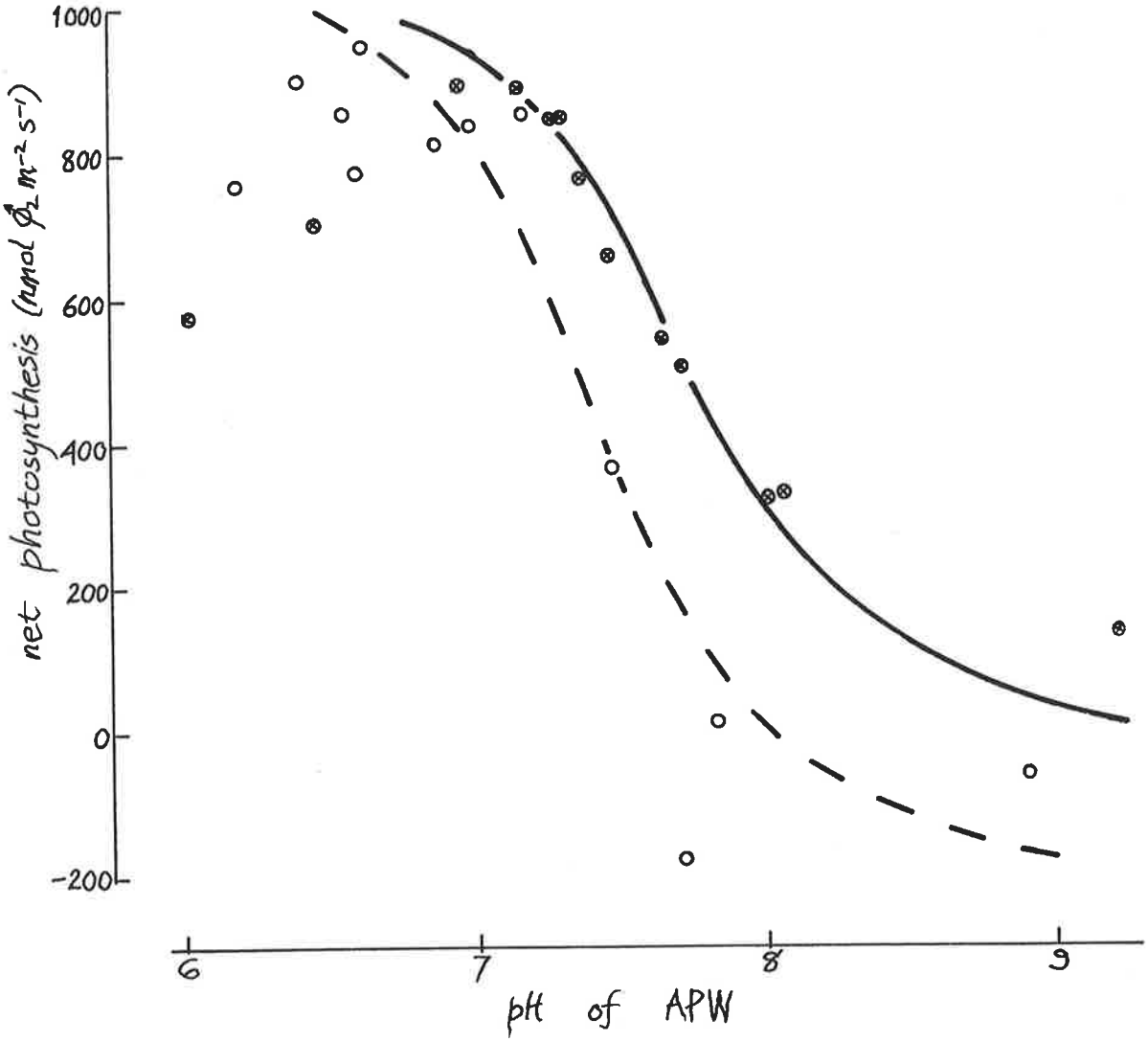

FIGURE 55. Photosynthesis of "epidermal" pieces of V.spiralis; inorganic carbon concentration is 1.17 mM (o) or 1.96 mM (⊗). T = 25°C. Broken line is a fit (Briggs-Maskell equation) to (o), with V (minus respiration = - 200 nmol m^{-2} s^{-1}) equal to 1100 nmol m^{-2} s^{-1}. Solid line is a fit to (⊗) with V equal to 1050 nmol m^{-2} s^{-1} (respiration equal to zero). K_M = 30 μM CO_2, k_T = 1 x 10^{-5} m s^{-1} in both cases.

The results of a number of experiments on the response of photosynthetic O_2 evolution to the pH of the bulk medium are shown in Fig. 53 (A. antarctica) and Fig. 54 (V. spiralis). For the sea grass, the maximum rate of photosynthesis occurred at about pH 6.8 (total inorganic carbon concentration = 2.22 mM). The optimum pH for V. spiralis (1.2 - 1.6 mM total inorganic carbon) was about 6. The optimum pH's correspond to $[CO_2]$'s of about 240 μM and 1 mM respectively. In both plants, photosynthesis declined below, as well as above, this pH. The addition of an artificial unstirred layer (B(2)) to a section of V. spiralis leaf (open triangles, Fig. 54), with cut ends sealed with dental wax, resulted in a lower pH optimum, even though the total inorganic carbon concentration was higher in this case (1.87 mM) than for the experiments with "bare" leaf sections; the maximum rate of photosynthesis was also comparatively low. In the presence of carbonic anhydrase (1900 Wilbur-Andersen units ml^{-1}), there was a very steep decline in the rate of photosynthesis between pH 6.2 and 6.8 but the rate was more or less constant from pH 6.8 - 8.6, at 180 nmol m^{-2} s^{-1} (Fig. 54,stars).

The photosynthesis of pieces of epidermis of V. spiralis (with, at the most, 3 underlying layers of mesophyll) also decreased comparatively sharply, although this began at the higher pH of 7 (Fig. 55). Photosynthesis also decreased dramatically at pH less

than 7 in the presence of 1.96 mM inorganic carbon; the effect was less pronounced at the lower inorganic carbon concentration of 1.17 mM (cf. Fig. 54).

As mentioned in the "Materials and Methods", O_2 evolution in V. spiralis continues all day in the absence of exogenous inorganic carbon. Table 9 shows results from experiments in which O_2 evolution and ^{14}C fixation were measured simultaneously in the O_2 electrode chamber, at high pH. The amount of carbon fixed was a very small proportion of the O_2 evolved, i.e. O_2 evolution was not linked with exogenous C fixation at this pH.

TABLE 9

Net photosynthetic oxygen evolution and ^{14}C fixation for a section of the leaf of V. spiralis, 25°C, total inorganic carbon concentration = 1.20 mM.

pH	net photosynthesis	
	nmol $O_2\uparrow$ m^{-2} s^{-1}	nmol C$\downarrow$ m^{-2} s^{-1}
9.36	198	0.80
8.97	175	22.7
8.63	138	7.91

Table 10 shows some $\delta^{13}C$ values (relative to the Pee Dee Belemnite standard) for entire V. spiralis leaves grown under stirred and unstirred conditions. The values were kindly obtained by C.B.Osmond: for methods,

see Osmond, Valaane, Haslam, Uotila and Roksandic (1981). The two cultures were identical in every way except that in one tank the water was vigorously stirred and pumped using the stirrer/impeller sections of two immersion circulators (as used in constant temperature baths). The $\delta^{13}C$ values for the two cultures were not significantly different; the overall value was 19.79 ± 0.19‰ .

TABLE 10

$\delta^{13}C$ values (relative to the Pee Dee Belemnite standard) for V. spiralis leaves grown in stirred or unstirred water.

Sample	$\delta^{13}C$ ‰ (±.1)
12.11.80 stirred	-19.93
12.11.80 unstirred	-19.55
5.2.81 unstirred	-20.10
2.6.81 stirred	-19.18
2.6.81 unstirred	-20.21

(ii) C supply for photosynthesis of A. antarctica

A. antarctica appears to be a "bicarbonate user" in that about 200 μM CO_2 is required to saturate photosynthesis at low pH (Fig. 50) whereas less than one twentieth the CO_2 concentration is needed at high pH

(Fig. 51). FVKUP predicted that photosynthesis is strongly diffusion limited at low pH, low [CO_2] (k_T = 7 x 10^{-6} m s^{-1}, $K_M^{CO_2}$ = 2.5 μM) and so HCO_3^- enhancement of CO_2 transport, potentially, could explain the observed effect. However, at pH 8.5, the "characteristic length" of the uncatalysed CO_2 hydration/dehydration and hydroxylation/dehydroxylation reactions is about 150 μm. This compares with an effective diffusion path length of 246 μm (from k_T above, D^{CO_2} = 1.72 x 10^{-9} m^2 s^{-1}). Although the reaction "length" is shorter than the diffusion length, the difference between the two is small, and so the CO_2 reactions in the unstirred layer would have to be catalysed to account for the 14-fold increase in the rate that is observed at high pH cf. low pH at the same (low) [CO_2]. Further, it may be that photosynthesis at low pH is not as diffusion-limited as FVKUP supposed. The computer chose a mean maximum rate of 886 nmol m^{-2} s^{-1} for the data of Fig. 50; however, if there was substrate (CO_2) inhibition of photosynthesis, the maximum rate would be considerably higher and a good fit to the data would be obtained with a more Michaelis-Menten response to CO_2, together with inhibition at higher concentrations.

Inhibition by the substrate is also a plausible explanation for the decline in photosynthesis (Fig. 53) when the pH is less than optimal. The optimum pH is

about 6.8, i.e. 240 μM CO_2, and this [CO_2] agrees well with the optimum CO_2 concentration from Fig. 50. Higher concentrations of CO_2 would be present at lower pH's leading to greater narcosis. Inhibition of photosynthesis at high [CO_2] or low pH is not uncommon in water plants. Van Lookeren Campagne (1955) observed it in his experiments with V. spiralis (cf. Figs. 52, 54 and 54), as did Talling (1976) in phytoplankton, Weber, Tenhunen, Yocum and Gates (1979) in Elodea, and MacFarlane and Raven (1985) in Lemanea. High [CO_2] might acidify the cytoplasm. In some of the experiments shown in Fig. 53, however, low pH has little or no effect on the rate of photosynthesis.

At supra-optimal pH's, photosynthesis again decreases and this presumably reflects the decrease in [CO_2]. The lines in Fig. 53 represent the way in which the rate would decline if the response to CO_2 were of the Briggs-Maskell form. Here k_T has been assigned the nominal value of 3×10^{-5} m s^{-1} (an effective δ of 57 μm). The Briggs-Maskell equation successfully predicts the shape of the initial decline of photosynthesis with pH for reasonable values of its parameters; however, it fails miserably in predicting the rates of photosynthesis that occur at high pH (> 8). Indeed, to obtain rates of the observed magnitude, $K_M^{CO_2}$ would have to be exceedingly low (< 1 μM) and even then it would be impossible to fit the data over the whole pH range, or even from pH 9

- 10. It can be concluded that either (a) the plant is able to take up HCO_3^- directly from the solution, or (b) there is external (to the plasmalemma) acidification with catalysis of the CO_2 hydration/dehydration reactions.

(iii) C supply for photosynthesis of V. spiralis

The continual evolution of O_2 in the light in the absence of exogenous C, together with the data of Table 9, imply that V. spiralis has access to an internal source of oxidant. The most likely contender is CO_2, particularly in the light of Helder and van Harmelen's (1982) findings that V. spiralis accumulates large quantities of malate (in the vacuoles of mesophyll cells?) which can be decarboxylated when the external supply of CO_2 is limited (cf. Beer and Wetzel, 1981). In this respect, V. spiralis has some of the characteristics of CAM even though it is a C_3 plant. Indeed, the $\delta^{13}C$ values (Table 10) are not unexpected for fractionation by CAM although the $\delta^{13}C$ of the inorganic carbon supply is not known (Raven, Griffiths and MacFarlane, 1985).

The dependence of photosynthesis upon exogenous CO_2 is seen most clearly for pieces of (mainly) epidermal tissue (Fig. 55) and, for more intact leaf sections, in short-term $^{14}CO_2$ fixation studies (Fig. 52). In the former, there does not seem to be any significant inside

source of CO_2 (immediately implying that this source is in the mesophyll of the leaf) and transport limitations on the supply of exogenous CO_2 will be much less important than for the intact leaf. The response to pH can be modelled using the Briggs-Maskell equation and the calculated [CO_2] at various pH's; the broken and solid lines represent fits to the data with K_M for CO_2 equal to 30 μM and k_T for CO_2 equal to 1×10^{-5} m s^{-1}. V's have been taken as higher than the maximum rates that were observed because it seems likely that there is inhibition of photosynthesis at high concentrations of CO_2, i.e. at low pH in this case (Van Lookeren Campagne, 1955). The value of the transport coefficient, k_T, has been assigned arbitrarily; transport from the bulk phase will be much faster than in the intact leaf but, nevertheless, not unimportant due to the remaining underlying mesophyll cells. There may even be some HCO_3^- enhancement of CO_2 transport at pH 9, perhaps accounting for the underestimate of the rate of photosynthesis there.

For more intact sections of leaves at low pH (Fig. 52b), the Briggs-Maskell equation is again quite a good fit to the data but with the much lower k_T of 1.3×10^{-6} m s^{-1}. The value is about one third of k_T for oxygen in V. spiralis. Such a proportion is unexpected, since organic polymers generally have a higher permeability to CO_2 than to O_2 (Barrer, 1941, ch.9). I do not know of

any measurements on the relative rates of penetration of the two gases through plant cuticles, although if a solution/ diffusion mechanism is operating then the oil/water partition coefficient (5 for O_2, only 1.6 for CO_2 - Forster, 1969) might be relevant. If the penetration of CO_2 through the plant cuticle is slow, an important pathway for the diffusion of the gas might be via the cut edges of the leaf section.

The pH response of O_2 evolution of V. spiralis (Fig. 54) is complicated because CO_2 can be supplied from two sources, within and outwith the leaf. At high pH, the outside source will be negligible and O_2 evolution probably reflects the fixation of CO_2 generated internally. The Briggs-Maskell equation has been fitted to the data of Fig. 54 (total inorganic carbon concentration = 1.19 mM) by taking a contribution of 120 nmol m^{-2} s^{-1} to O_2 evolution from endogenous CO_2 fixation. K_M (30 μM) and k_T (1.3×10^{-6} m s^{-1}) are the same as for the line in Fig. 52b and V has been taken as 600 nmol m^{-2} s^{-1}. The fit to the data is good. The same cannot be said, however, for photosynthesis in the presence of carbonic anhydrase nor for the photosynthesis of a leaf section in B(2) even using a lower value for V.

In the presence of the enzyme, O_2 evolution declines much more sharply after pH 6.2 than the Briggs-Maskell equation, with the above values of the parameters, would

predict. This is (and was!) a puzzling result; the enzyme causes a decrease in the rate of photosynthesis over the pH range that it has an effect, whereas carbonic anhydrase should always enhance the exogenous CO_2 supply (if the supply is enhanceable). With the weight of evidence suggesting that all the significant transport barriers to the supply of nutrients are within the V. spiralis leaf itself, the result is even more of a puzzle since then the added enzyme should have no effect at all on the CO_2 supply - it is unlikely that the enzyme would penetrate the cuticle, or even the cell wall (Carpita, Sabularse, Montezianos and Delmer, 1979; Tepfer and Taylor, 1981). Perhaps the most likely site of action for the added enzyme is in the small volume of solution which infiltrates the ends of the air lacunae, where they are cut. (Although leaf sections showing obvious infiltration, i.e. almost along the entire length, of the lacunae were discarded, there was always some infiltration.) If the permeability of the cuticle to CO_2 is low, then an important pathway for CO_2 diffusion would probably be through the lacunal tunnels and thence to the epidermal cells (via, in most cases, the mesophyll). Diffusion along a lacuna would be very rapid (1 cm of stagnant gas is equivalent to about 1 μm of stagnant water, diffusion-wise) so the major diffusion barriers in this pathway are the mesophyll and the infiltrated water at the cut ends of the lacunae.

With carbonic anhydrase present in the latter, it at least has the potential to have an effect; its effect, however, still remains opposite to what one might have reasonably expected. A possible explanation is that the enzyme enhances the efflux of endogenous CO_2, with a subsequent loss in the efficiency of fixation of that CO_2. The effect must work both ways, i.e. exogenous CO_2 influx must be enhanced as well, but this may be a quantitatively less important source of CO_2 over the pH range being considered than the "inside" source. Further, even if the CO_2 supplies were initially of similar importance, the two fluxes may not be enhanced to the same extent : when carbonic anhydrase occupies only a portion of a diffusion pathway, its effect (as a CO_2-flux enhancer) is greater when it is located downstream rather than upstream, with respect to the direction of the flux (Schulz, 1980).

The addition of the artificial unstirred layer (Fig. 54), with cut lacunae sealed with wax, significantly lowers the pH optimum for photosynthesis (i.e. the $[CO_2]$ required for the attainment of the maximum rate is increased). Thus, for a fit to the data using the Briggs-Maskell equation as before, the effective k_T needs to be small. (The main reason is probably the sealing of the lacunae; holder B(2) had no effect on rates of O_2 transport - Fig. 37). However, O_2 evolution is then predicted to decrease quite sharply beyond the

optimum pH, whereas the decline is gradual. As before, there may be complications due to the internal CO_2 source ; the fixation of this CO_2 is potentially more efficient with the unstirred layer, and the lacunae sealed, than with out. Again, therefore, there is the suggestion that endogenous CO_2 fixation makes a significant contribution to O_2 evolution even at near-neutral pH's.

In all of the foregoing there are numerous complications which might occur, although I have tended to side with William of Occam in discussing possible explanations for my results. It has been assumed, for example, that endogenous CO_2 is supplied at a constant rate regardless of the exogenous CO_2 supply : it is possible that at high bulk CO_2 concentrations the internal CO_2 supply is shut off. Similarly, pH changes within the leaf accompanying net malate(?) decarboxylation or synthesis will affect the rate of transport of CO_2 through mesophyll cells (which are mainly vacuole) and the tissue apoplast. This will be very important in the intact leaf, but for the leaf sections which I used the somewhat artificial transport barrier of infiltrated water in cut lacunae would appear to be the dominant resistance.

Finally, the intracacies of (symplastic ?) malate(?) transport from the vacuoles of mesphyll cells into the chloroplasts of epidermal cells, and its subsequent

decarboxylation, have not been discussed at all. If carbonic anhydrase is present in the chloroplasts, most of the CO_2 from the decarboxylation will be immediately converted to HCO_3^- which raises the possibility of net HCO_3^- efflux from epidermal cells. It seems unlikely that HCO_3^- ions would cross the cuticle at a great rate (see discussion on phosphate influx, pp 73-74), but they may carry most of the inorganic carbon flux between epidermis and lacunae - even if they are not transported across the plasmalemma of epidermal cells as such.

CONCLUSIONS

The main objective of this work was to quantify the limitations due to diffusion, particularly diffusion across the boundary layer, on the uptake of nutrients by some aquatic macrophytes. This requires a knowledge of the rate of diffusion, and of the intrinsic rate of the nutrient-utilizing "reaction"; it is the relative rate of diffusion which determines whether or not it imposes any limitation on the rate of the reaction, and modifies the kinetics.

For the membrane transport of ^{14}C-methylamine in Ulva, the intrinsic kinetics of influx do appear to be first-order Michaelis-Menten, and so in series with diffusion, influx should be given by the Briggs-Maskell equation. This was found to be the case, with the value of the transport coefficient, k_T, being derived independently from the dissolution of zinc in acid. Occasionally, there is an additional burden on reaction due to diffusion in parts of the tissue where diffusion and reaction proceed simultaneously. The Briggs-Maskell equation is not valid under these conditions, but the quasi-empirical equation of Yamané can be used. Using reasonable estimates of the two additional parameters, the thickness of the zone wherein the reaction is occurring and the effective diffusion coefficient there, the Yamané equation describes the data quite well. At high rates of stirring, and for fast reactions, internal

diffusion can be a major transport limitation even in tissue as thin as the Ulva thallus. For thicker tissues, with reaction sites distributed evenly throughout the thickness, the boundary layer may be a relatively minor diffusion resistance. The diffusion boundary layer thickness is also almost irrelevant for nutrient uptake by Vallisneria leaf sections, because of the cuticle. It is dangerous, therefore, to generalize about the importance of the unstirred layer for aquatic plants as a class.

Even general statements about the nutrients themselves, with regard to their rate of transport across the unstirred layer, can be dangerous. For the uptake of solutes such as phosphate and inorganic carbon, which exist in various forms in solution, chemical transformations along the length of the diffusion pathway can, effectively, increase k_T (or D_{eff}). The magnitude of the increase depends upon the relative rate of the diffusion of the species in question and the rate of its chemical transformation into other "carrier" species. Because the interconversion of dihydrogen phosphate and monohydrogen phosphate ions is so rapid, the uptake of $H_2PO_4^-$ will be significantly enhanced in the presence of HPO_4^{2-} even when the diffusion pathway is quite short. However, in the case of CO_2 uptake, very thick unstirred layers are required for enhancement by HCO_3^- ions to be significant,

unless the rate of the normally slow interconversion is increased by catalysis.

The degree of enhancement can be quantified if the "characteristic length" of the chemical reaction is known, compared with the diffusion path length. For analytical calculations, however, it must be assumed that H^+ and OH^- transport is very fast, i.e. that there is no pH gradient along the diffusion pathway. This in itself, can constitute an important difference among aquatic plants, because there may be net fluxes of H^+ across the plasmalemma. For the same unstirred layer thickness, variations in the magnitude of the H^+ flux will give rise to different pH gradients, and similarly for equal H^+ fluxes but different thicknesses of the unstirred layer. Concerning the CO_2 supply for photosynthesis, net H^+ influx (or OH^- efflux) will give rise to a somewhat alkaline boundary layer, which will tend to increase the rate of the reaction $CO_2 + OH^- \rightarrow HCO_3^-$ and enhance rates of CO_2 diffusion by HCO_3^- "carriage". On the other hand, net H^+ efflux will tend to acidify the boundary layer which will not lead to any enhancement of CO_2 diffusion but will tend to increase its concentration near the plasmalemma.

The Briggs-Maskell equation is derived on the assumption of first-order Michaelis-Menten kinetics for the nutrient-utilizing reaction. In a number of cases, the assumption is not good, The outstanding example is

O_2 uptake in dark respiration. Here, the reaction involves two substrates (O_2 and reduced cytochrome oxidase) which means that the $K_M^{O_2}$ of cytochrome oxidase is a variable dependent upon the degree of reduction of itself. Even the apparent order of the reaction can change if the rate of electron transfer to (oxidized) cytochrome oxidase is very slow or very fast compared with the rate of reaction with O_2. It is possible, therefore, to obtain apparent first-order Michaelis-Menten kinetics even if there are significant diffusion limitations (e.g. if the reaction order is less than one) and conversly, if the reaction order is greater than one, a strongly oblique hyperbola may be obtained when diffusion limitations are negligible. Under these circumstances, making predictions from fits to the Briggs-Maskell equation with no prior knowledge of the intrinsic reaction kinetics is extremely hazardous.

These problems, and more, also occur for photosynthetic CO_2 fixation. The driving reaction catalysed by RuBP carboxylase is again a two substrate reaction but with the added complication of O_2 inhibition. The observed K_M for CO_2 of RuBP carboxylase is a variable depending on the concentrations of RuBP and O_2, and the order of the reaction can also change depending on the rate of RuBP supply. In addition, high [CO_2] can be inhibitory. The complexity of the intrinsic kinetics can be reduced by conducting

experiments at low bulk O_2 concentrations and CO_2 concentrations that are not inhibitory, and in many cases the response of photosynthesis to $[CO_2]$ has the Briggs-Maskell form. There is always doubt, however, as to the meaning of the "true K_M for CO_2" that is predicted by, or that one uses in, the equation - this quantity may be less than the K_M for CO_2 of the RuBP-saturated enzyme if RuBP is less than saturating in vivo. Further, unless rates of CO_2 transport are known independently, the value of k_T predicted by the Briggs-Maskell equation is also in doubt since the intrinsic kinetics of CO_2 fixation may themselves describe an oblique hyperbola with $[CO_2]$. Nevertheless, photosynthesis of U. rigida is clearly affected by stirring, especially at low pH, and independent measurements of k_T describe the response quite well (Fig. 45).

At high (sea water) pH's, both in U. rigida and A. antarctica, the membrane transport of HCO_3^- ions is likely to contribute to the supply of CO_2 within the cells. Because $[HCO_3^-]$ is high, and because the rate of uptake is low, diffusion in the bulk medium and within the tissue is unlikely to be rate-limiting for HCO_3^- uptake although it may yet be for CO_2. Thus, the transport limitations that exist for CO_2 influx can be turned to advantage at high pH by the plant since they will limit CO_2 (derived from HCO_3^-) efflux. In V.

spiralis, the cuticle will be very effective at preventing the loss of CO_2 from endogenous sources. This plant grows in culture in a solution of pH 9 or more, so $[CO_2]$ will probably be negligible. Even floating leaves will be exposed to only about 14 μM CO_2 in air, which is again a negligible $[CO_2]$ for V. spiralis photosynthesis. It is possible that a major source of CO_2 for the leaves is the sediment, with transport via the air lacunae. A cuticle with a permeability to CO_2 of 1.3×10^{-6} m s^{-1} is equivalent to a diffusion path length in air of more than 10 m(!) which is much longer than a V. spiralis leaf. The sediment may also be an important source of mineral nutrients (e.g. phosphate) for the leaves (Denny, 1980), given the relative impermeability of the cuticle.

Table 11 summarizes the results for the plants and processes which I studied. The maximum values of the transport coefficient (k_T) are for well-stirred conditions and small sections of tissue. They are equivalent to unstirred layers 30 - 60 μm thick. For comparison with k_T, I have included an estimate of $V/2K_M$ which is a measure of the intrinsic rate of the process (i.e. in the absence of transport limitations); unless this ratio is much smaller than k_T, the transport limitations imposed by the boundary layer should significantly modify the response of influx or net influx to concentration.

TABLE 11

Summary of plants and processes studied and the effect of stirring and the validity or otherwise of the Briggs-Maskell equation.

Plant	Effect of Stirring	Range of k_T predicted for unstirred layer ($m\ s^{-1} \times 10^{-5}$)	$V/2K_M$ ($m\ s^{-1} \times 10^{-5}$)	Validity of Briggs-Maskell equation	Comments
		$CH_3NH_3^+$ Influx			
U.rigida	Yes	0.36-3.9	1.2-1.87	Yes	-
V.spiralis	No	0.53-4.9	0.7 ?	Yes	Cuticle!
		$H_2PO_4^-$ Influx			
U.rigida	Weak	0.34-3.1	21	Yes	Transport enhanced by HPO_4^{2-}
V.spiralis	No	0.40-3.7	5?	No?	Cell Walls?
		O_2 Uptake (Dark Respiration)			
U.rigida	Weak	0.1-3.3	-	No	Complex kinetics
V.spiralis	No	0.25-3.5	-	Yes?	Cuticle
		CO_2 Uptake (Photosynthesis)			
U.rigida	Yes (low pH)	0.22-3.2	2.1-21	Yes (low pH, low O_2) and No (high pH)	Membrane HCO_3^- transport
V.spiralis	No	0.23-3.3	1.7?	Yes (but not for O_2 evolution)	Endogenous CO_2
A.antarctica	Yes (low pH)	~3.2	12?	No (high pH)	Membrane HCO_3^- transport? Acid zones?

Often, however, this is not the case, because of the complications just discussed. In Vallisneria, for example, $V/2K_M$ (estimated) for $CH_3NH_3^+$ influx and photosynthetic CO_2 uptake, is (somewhat) lower than the maximum k_T but the reactions are still very diffusion limited by the cuticle. In Ulva, $V/2K_M$ for $H_2PO_4^-$ influx and CO_2 fixation can be quite high compared with k_T, and yet the effect of stirring on $H_2PO_4^-$ influx or CO_2 uptake at high pH is slight.

It can be concluded, then, that besides a knowledge of the unstirred layer thickness and the intrinsic rate of nutrient uptake, a considerable amount of information must be known about the plant (and nutrient) concerned before anything definite can be said regarding the rôle of the boundary layer as a (rate) limiting factor. Nevertheless, when the boundary layer is an important transport barrier, its rôle can be crucial.

Appendix I: Fick's Laws

Fick (1855) was the first to describe mathematically the process of diffusion under the influence of a concentration gradient.

If diffusion in only one dimension is considered, we may write Fick's first law of diffusion:

$$J_j = - D_j \frac{\partial c_j}{\partial x} \qquad (I.1)$$

where J_j is the flux of the diffusing species j (amount of j which crosses a plane of unit area per unit time), caused by a gradient in the concentration of j in the x direction, $\frac{\partial c_j}{\partial x}$. The minus sign indicates that the direction of the flux (with respect to x) is opposite to the way in which the concentration changes with respect to x. D_j is the diffusion coefficient of species j. Partial derivatives are written because the concentration gradient itself changes with time.

The time dependence of the concentration gradient is described by the continuity equation

$$- \frac{\partial J_j}{\partial x} = \frac{\partial c_j}{\partial t} \quad . \qquad (I.2)$$

This equation simply means that if the flux of j is faster at x than at x + dx (i.e. $\frac{\partial J_j}{\partial x}$ is negative), then the local concentration of j (i.e. in the volume element

enclosed by x and x + dx) must be increasing with time - more j is coming in than going out.

By substituting Fick's first law into the continuity equation, and assuming D_j constant, Fick's second law is obtained:

$$\frac{\partial c_j}{\partial t} = - \frac{\partial}{\partial x}(-D_j \frac{\partial c_j}{\partial x}) = D_j \frac{\partial^2 c_j}{\partial x^2} \cdot \qquad (I.3)$$

The equation can be solved for c_j in a number of specific cases (see Crank, 1957).

It should be noted that Fick's laws do not include a term for any electrical potential gradient and so may not hold for the movement of ions. Later equations, due to Nernst and Planck, include a term for the electrical potential.

Appendix II: Origin of the Quadratic Describing an Enzyme-Catalysed Reaction in Series with a Diffusion Resistance

In a letter to the late Professor G.E.Briggs (12th Nov.1981), F.A. Smith and N.A. Walker enquired about the origin of equation (12), which they had previously referred to as the Hill-Whittingham equation (after Hill and Whittingham, 1955, in which the equation appears). Part of Professor Briggs's reply is reproduced below:

Dear Smith & Walker,

Thank you for your letter. Although (1935-60) it is 21+ yrs since I lectured on phs, I did it for 25 yrs & my memory of it is good.

I developed the quadratic for R as $f(c_e)$ from

$$R = \frac{R_\infty c_i}{c_i + k_e} = \frac{D}{l}(c_e - c_i)$$

an equation to an oblique hyperbola - limits

$$R \to \frac{R_\infty c_e}{(c_e + k_e)} \quad \text{when } l \to 0 \qquad R.H.$$

& $R = \frac{D}{l} c_e$ or $R = R_\infty$ as $l \to \infty$

I provided notes to this effect.

Whittingham attended the lectures, I was his supervisor when he was an undergraduate & when a Res. Stud.

We used what I taught him when he wrote the book as he had a right to do.

I have no access to my scientific books & cannot remember H & W's acknowledgements, apparently they forgot the source of the quadratic.

It was a bread

[illegible]

G.E.Briggs

In fact, in the Preface to their monograph, Hill and Whittingham acknowledge the teaching of Professor Briggs in chapters 2 and 4, and state that he allowed them free access to his unpublished lecture notes. They also acknowledge the criticism of Professor E. J. Maskell. Maskell (1928) did not explicitly solve the quadratic for v (R in Briggs' terminology), but he published its limits and its behaviour for various values of k_T ($D/\mathcal{L}$). I shall refer to it as the Briggs-Maskell equation.

Appendix III: The Meaning of the Apparent K_M for an Enzyme-Catalysed Reaction in Series with a Transport Process

The apparent K_M, K_M^{app}, is found by putting $v = V/2$ in the Briggs-Maskell equation

$$v = \tfrac{1}{2}\{K_M k_T + c_b k_T + V - \sqrt{(K_M k_T + c_b k_T + V)^2 - 4c_b k_T V}\}$$

and solving for c_b. Thus,

$$\tfrac{1}{2}V = \tfrac{1}{2}\{K_M k_T + c_b k_T + V - \sqrt{(K_M k_T + c_b k_T + V)^2 - 4c_b k_T V}\}$$

i.e. $(K_M k_T + c_b k_T)^2 = (K_M k_T + c_b k_T + V)^2 - 4c_b k_T V,$

$$\therefore k_T^2(K_M + c_b)^2 = k_T^2 (K_M + c_b)^2 + V^2 + 2k_T(K_M + c_b)V - 4c_b k_T V,$$

or $V^2 + 2k_T(K_M + c_b)V - 4c_b k_T V = 0,$

i.e. $V\{V + 2k_T(K_M - c_b)\} = 0.$

For $V \neq 0$, $V + 2k_T(K_M - c_b) = 0$

and $\therefore c_b = K_M + \frac{V}{2k_T}$.

Thus $K_M^{app} = K_M + \frac{V}{2k_T}$. (III.1)

1. When $K_M >> V/2k_T$ (i.e. when $k_T >> V/2K_M$), $K_M^{app} \sim K_M$ and the kinetics are determined by the enzymic reaction.

2. Equation (III.1) is the equation of a straight line. If K_M^{app} is determined at various values of k_T, and the results plotted with K_M^{app} on the ordinate and $1/k_T$

(proportional to the unstirred layer thickness) on the abscissa, the slope should be V/2 and the intercept on the ordinate should be K_M (cf. Thomson and Dietschy, 1977). Similarly, if K_M^{app} is plotted against V, the predicted slope is $1/(2k_T)$, with the true K_M again being given by the intercept on the ordinate (cf. Lívanský, 1982).

Appendix IV: Relaxation of Diffusion to a Flat Plate

Consider a solution in laminar flow (bulk velocity, U) passing over a flat plate of length X and breadth Z as shown in Fig. IV. 1. A component of the solution (concentration in the bulk phase = c_b) reacts with the plate.

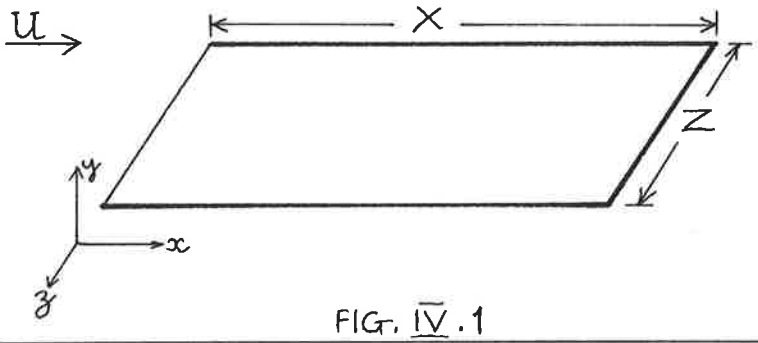

FIG. IV.1

At any point on the plate, the limiting flux of the reactant (i.e. the maximum possible flux normal to the plate's surface) is given by

$$J_{lim} = B \frac{c_b}{\sqrt{x}}$$

in which, provided the diffusion coefficient of the reactant, the kinematic viscosity of the solution and U are constant, B is a constant (equation (18)). The total diffusional flow, I_{lim}, over the entire plate is then

$$I_{lim} = \int_0^x J_{lim}\, dx\, dz = 2\ Z.B\ c_b \sqrt{X}$$

and therefore the average flux to the whole plate is

$$\bar{J}_l = \frac{I_{lim}}{Z.X} = 2\ B\ c_b \frac{\sqrt{X}}{X} \quad .$$

Now, upto $x = X_o$, the plate is coated so that it can no longer react (Fig. IV. 2). The flux at any point

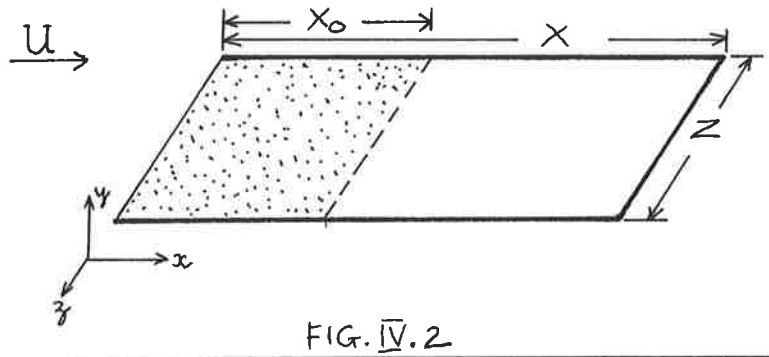

FIG. IV. 2

($x > X_o$) is given by (Levich, 1962, p106)

$$J(x,0) = B \frac{c_b}{\sqrt{x}[1 - (X_o/x)^{3/4}]^{1/3}}$$

and so the total diffusional flow to the uncoated portion of the plate is

$$I = \int_{X_o}^{X} J(x,0)dx\ dz = Z.B\ c_b \int_{X_o}^{X} \frac{dx}{\sqrt{x}[1 - X_o^{\frac{3}{4}}.x^{-\frac{3}{4}}]^{\frac{1}{3}}}$$

which has the solution (cf. Petit-Bois, 1961, p95)

$$I = Z.B\ c_b \left[2\sqrt{x}\left(1 - \left(\frac{X_o}{x}\right)^{3/4}\right)^{2/3}\right]_{X_o}^{X}$$

or $$I = 2Z.B\ c_b \sqrt{X} \left[1 - \left(\frac{X_o}{X}\right)^{3/4}\right]^{2/3}.$$

The average flux to the uncoated portion of the plate is

therefore

$$\bar{J}_2 = \frac{I}{Z(X - X_o)} = 2B\, c_b \frac{\sqrt{X}}{X - X_o} \left[1 - \left(\frac{X_o}{X}\right)^{3/4}\right]^{2/3} .$$

Hence,

$$\frac{\bar{J}_2}{\bar{J}_1} = \frac{X}{X - X_o} \left[1 - \left(\frac{X_o}{X}\right)^{3/4}\right]^{2/3} . \qquad (13)$$

Appendix V: Diffusion and Reaction in Parallel

(i) The diffusion-reaction equation

Consider a plant cell or a piece of plant tissue in the shape of a slab, cylinder or sphere (Fig. V.1). The first two either have their edges (or ends) sealed, or the edges or ends are such a small proportion of the total surface area that they can be ignored. Substrate, B, surrounds the cell or tissue at a bulk concentration of c_b and at a surface concentration of c_s. The interior of the cell or piece of tissue will be considered as an homogeneous enzyme suspension, which is at a constant temperature throughout and which can be regarded as being in direct contact with the bathing medium - i.e. the permeability of any cell membrane is very large.

The basic equation of diffusion and chemical reaction within the body is given by the Poisson equation

$$\frac{\partial c}{\partial t} = D_{eff} \nabla^2 c - v \qquad (V.1)$$

where D_{eff} is the effective diffusion coefficient inside the plant, ∇^2 the Laplacian operator ($\nabla^2 c = \frac{\partial^2 c}{\partial x^2} + \frac{\partial^2 c}{\partial y^2} + \frac{\partial^2 c}{\partial z^2}$ in Cartesian coordinates) and v the rate of consumption of substrate by chemical reaction. This equation follows directly from Fick's second law (see Appendix I) applied to the three dimensional case, and

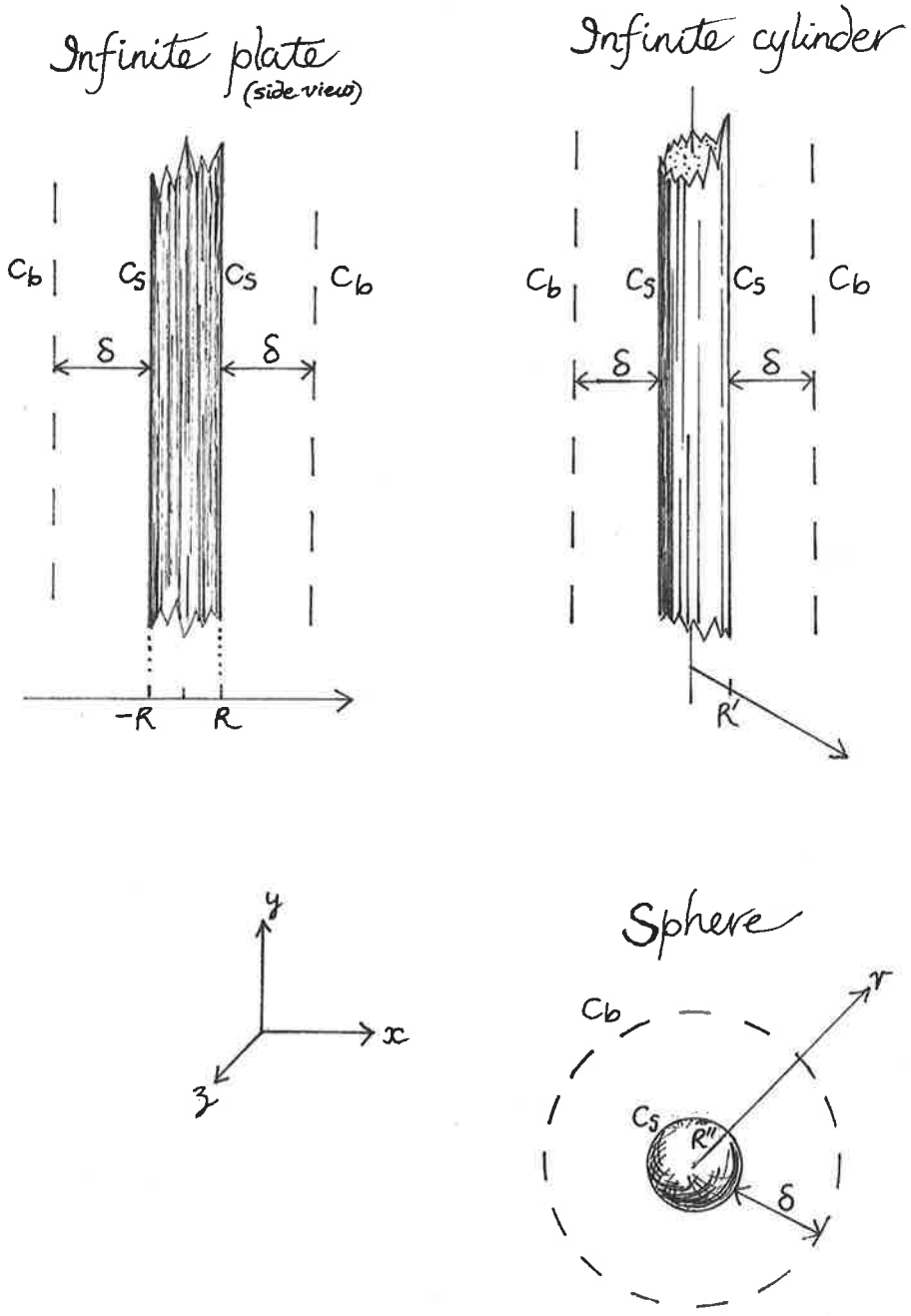

FIGURE V.1. The reacting plate, cylinder and sphere. The thickness of the Nernst layer is denoted by δ.

the law of conservation of matter, provided that electrical interactions can be ignored.

I will assume that within the plant the enzyme-catalysed reaction of B $\rightarrow$ products follows first-order Michaelis-Menten (Briggs-Haldane) kinetics, i.e. equation (10). (In form, these kinetics are the same as those known to physical chemists as Langmuir-Hinshelwood for adsorption and subsequent chemical reaction on a surface: $v = \frac{k' c_s}{1 + K c_s}$ in which k' is the rate constant for the chemical reaction and K is an adsorption constant.)

With Michaelis-Menten kinetics, and in the steady state ($\frac{\partial c}{\partial t} = 0$), equation (V.1) becomes

$$D_{eff} \left[\frac{d^2c}{dr^2} + \left(\frac{P + 1}{r}\right) \frac{dc}{dr}\right] = V \frac{c}{K_M + c} \qquad (V.2)$$

in which the Laplacian has been expressed in terms of r (see Fig. V.1), and p is -1 for the slab, 0 for the cylinder and +1 for a sphere (e.g. Bland, 1961).

Equation (V.2) is non-linear and the exact solution can only be obtain by numerical methods. However, Michaelis-Menten kinetics simplifies to first-order or zeroth-order kinetics when c is very low or very high and so it is worthwhile exploring equation (V.2) in these two limiting situations. Equation (V.2) is also simplified for the slab because it represents the one

dimensional case and the equation becomes

$$D_{eff} \left(\frac{d^2c}{dr^2}\right) = V \frac{c}{K_M + c} \quad . \qquad (V.3)$$

The solutions for the other shapes are not greatly different as will be shown later.

(ii) First-order kinetics

For $c << K_M$, equation (V.3) becomes

$$D_{eff} \frac{d^2c}{dr^2} = \left(\frac{V}{K_M}\right) c \qquad (V.4)$$

or $$\frac{d^2c}{dr^2} = \left(\frac{\phi}{R}\right)^2 c$$

where $$\phi = R\sqrt{\frac{V}{K_M . D_{eff}}} \quad .$$

Here V is taken to be expressed per unit volume (e.g. mol m^{-3} s^{-1}) which renders ϕ dimensionless. The general solution is

$$c = A \sinh \left[\left(\frac{\phi}{R}\right) r\right] + B \cosh \left[\left(\frac{\phi}{R}\right) r\right] \qquad (V.5)$$

where A and B are integration constants. A is quickly eliminated since at $r = 0$, $\frac{dc}{dr} = 0$, i.e. $\left(A \frac{\phi}{R} \cosh \left[\left(\frac{\phi}{R}\right) r\right] + B \frac{\phi}{R} \sinh \left[\left(\frac{\phi}{R}\right) r\right]\right)_{r=0} = 0$. Because $\sinh \phi = 0$ and $\cosh \phi = 1$, $A = 0$. Equation (V.5) is now

$$c = B \cosh \left[\left(\frac{\phi}{R} \right) r \right] \quad . \qquad (V.6)$$

At $r = R$, $c = c_s$, so we can write

$$c_s = B \cosh \phi$$

whence $$B = \frac{c_s}{\cosh \phi}$$

and substituting back into equation (V.6),

$$c = \left(\frac{c_s}{\cosh \phi} \right) \cosh \left[\left(\frac{\phi}{R} \right) r \right] \quad . \qquad (V.7)$$

The concentration of substrate at the surface is usually unknown, but we can express it in terms of the bulk concentration using Nernst's theory (Introduction, section I). Thus, at the surface, the flux is $D_{eff} \left(\frac{dc}{dr}\right)_{r=R}$ which is equal to $k_T(c_b - c_s)$ where k_T is the velocity constant for external mass transport. From equation (V.7),

$$D_{eff} \left(\frac{dc}{dr} \right)_{r=R} = D_{eff} \frac{c_s \ (\phi/R)}{\cosh \phi} \sinh \phi = k_T(c_b - c_s)$$

and so $$c_s = \frac{k_T c_b}{k_T + \dfrac{D_{eff} \ (\phi/R) \sinh \phi}{\cosh \phi}}$$

and substituting into equation (V.7) yields

$$c = \frac{k_T\, c_b \cosh\,[(\phi/R)\, r]}{k_T \cosh \phi + D_{eff}\, (\phi/R) \sinh \phi} \quad . \qquad (V.8)$$

The flux of B into the plant through each face of the slab is

$$J = D_{eff} \left(\frac{dc}{dr}\right)_{r=R} = D_{eff}\, \left(\frac{k_T\, c_b\, (\phi/R) \sinh \phi}{k_T \cosh \phi + D_{eff}\, (\phi/R) \sinh \phi}\right) \qquad (V.9)$$

$$\text{or} \qquad \frac{1}{J} = \frac{1}{c_b}\, \left(\frac{\cosh \phi}{D_{eff}\, (\phi/R) \sinh \phi} + \frac{1}{k_T}\right) \quad . \qquad (V.10)$$

In this last equation, the term $\frac{\cosh \phi}{D_{eff}\, (\phi/R) \sinh \phi . c_b}$ is simply the inverse of the flux that would occur if there were no external diffusion boundary layer. The other term, $\frac{1}{c_b\, k_T}$, is the inverse of the maximum flux through the diffusion boundary layer. In fact, the two terms within the brackets have the units of a resistance (s m^{-1}, say) and the overall resistance is simply the sum of the resistances internally and externally. This additivity of resistances is a property of the symmetry of the system and holds for infinite cylinders and spheres as well (Aris, 1975).

The rate of uptake of substrate into the plant per unit volume, v, is J/R

$$\text{i.e.} \qquad \frac{1}{v} = \frac{1}{c_b}\, \left(\frac{R^2 \cosh \phi}{D_{eff}\, \phi \sinh \phi} + \frac{R}{k_T}\right) \quad . \qquad (V.11)$$

If there were no external resistance, v would be given by $c_b\, \left(\frac{D_{eff}\, \phi \sinh \phi}{R^2 \cosh \phi}\right)$ which can be rearranged to give

$$v = c_b \left(\frac{V}{K_M}\right)\left(\frac{\tanh \phi}{\phi}\right) \quad . \qquad (V.12)$$

The overall velocity falls below its maximum value ($c_b \frac{V}{K_M}$) by the factor $\frac{\tanh \phi}{\phi}$. This factor is the effectiveness factor, η , used by chemical engineers. (Briggs and Robertson, 1948, also made use of a similar term in their experiments with carrot disks.) Equation (V.12) is quite general and holds for any first order reaction in a slab, with the rate constant replacing the term $\frac{V}{K_M}$.

Fig. V.2 shows some plots of η against the Thiele modulus, ϕ, for various shapes. It can be seen that all the curves are similar, with the sphere being the least effective shape and the slab the most effective. The difference is really only significant at ϕ values of 1 or 2, where the slab is 10 - 15% more effective than the sphere.

Fig. V.2 shows that for small values of ϕ (less than, say, 0.2) η is virtually 1 and the rate of consumption of substrate is determined by the chemical reaction. This corresponds to a situation where the reaction rate is very much slower than the rate of diffusion. Throughout the solid body, c is practically equal to c_s. For values of ϕ larger than, say, 2, catalyst effectiveness is low (in fact $\eta \rightarrow \frac{1}{\phi}$ as $\phi \rightarrow \infty$) and

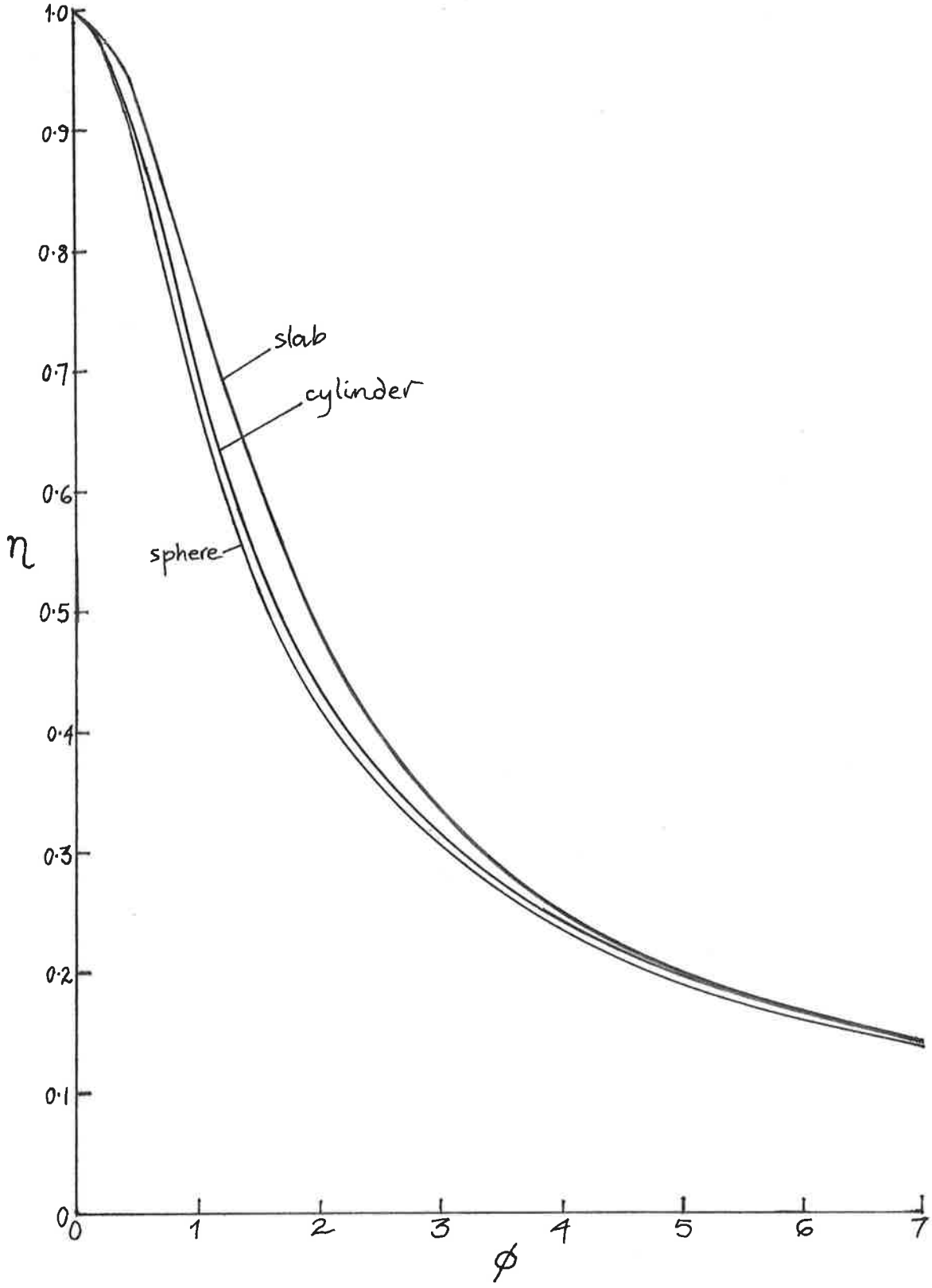

FIGURE V.2. Effectiveness factor, η, against the Thiele modulus, ϕ, for a sphere, a cylinder and a slab (adapted from Aris, 1957 and Aris, 1975, Fig. 3.7). ϕ is based on a characteristic dimension which is the ratio of the volume to the surface area of the body. For the slab this is simply the half-thickness, R (Fig. V.1), while for the cylinder and sphere it is $\frac{1}{2}$ the radius and $\frac{1}{3}$ the radius respectively (Aris, 1957; Roberts and Satterfield, 1965).

the overall consumption of B is constrained by the rate of diffusion; for much of the slab, $c << c_s$. Fig.V.3 illustrates the concentration gradients that form within a slab for various values of ϕ.

When an external mass-transfer resistance is present, it can be shown from equation (V.11) that

$$\frac{1}{\eta} = \frac{\phi}{\tanh \phi} + \frac{\phi^2}{Bi} \qquad (V.13)$$

where Bi is the dimensionless Biot number, $\frac{R\ k_T}{D_{eff}}$. Bi can be seen as a ratio of external (k_T) to internal (D_{eff}/R) rates of mass transport.

Fig.V.4 shows the effectiveness factor as a function of ϕ for various values of the Biot number. For a particular value of the Thiele modulus, catalyst-effectiveness gets progressively lower as Bi decreases (i.e. as k_T decreases). For spheres, it can be shown that k_T approaches a limiting value of D/R as the thickness of the Nernst diffusion layer increases (see Langmuir, 1918). The Biot number, therefore, cannot be less than $\frac{D}{D_{eff}}$. Generally, D_{eff} is less than D and so Bi for spheres will usually be more than 1. For infinite plates and cylinders there is no such restriction on k_T (and Bi) which continues to decrease as δ increases (Satterfield, 1981, p 112).

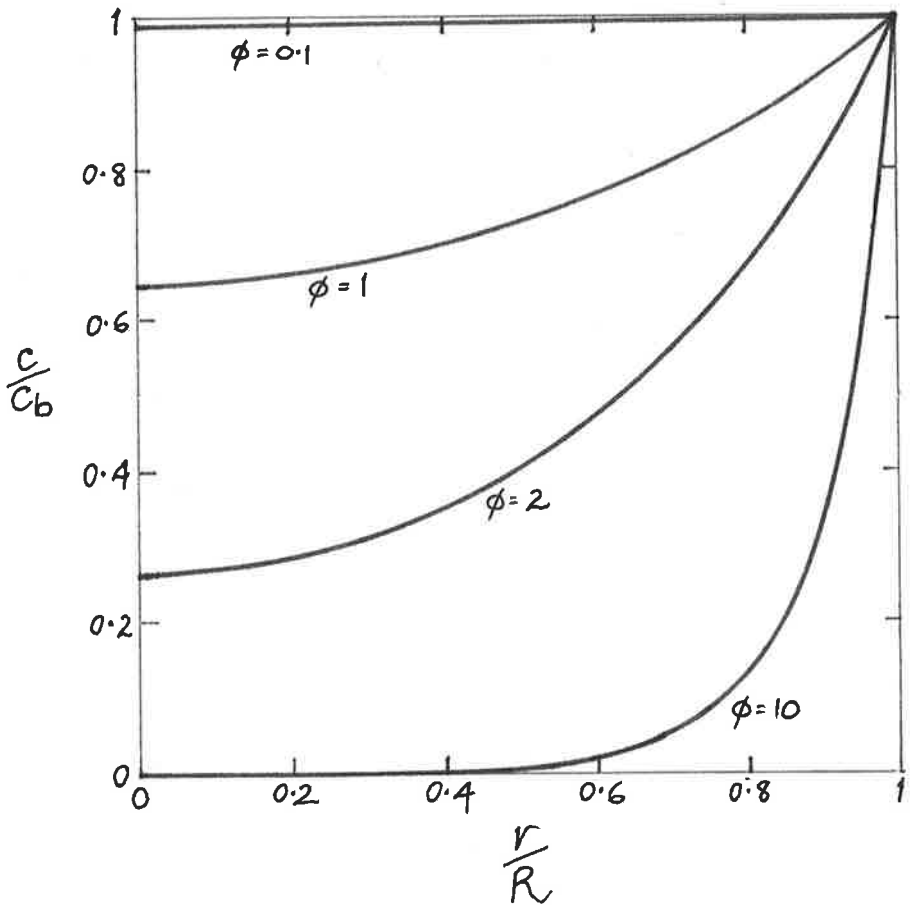

FIGURE V.3. Profiles of concentration in one half of a reacting slab (first-order kinetics) for various values of the Thiele modulus, ϕ.

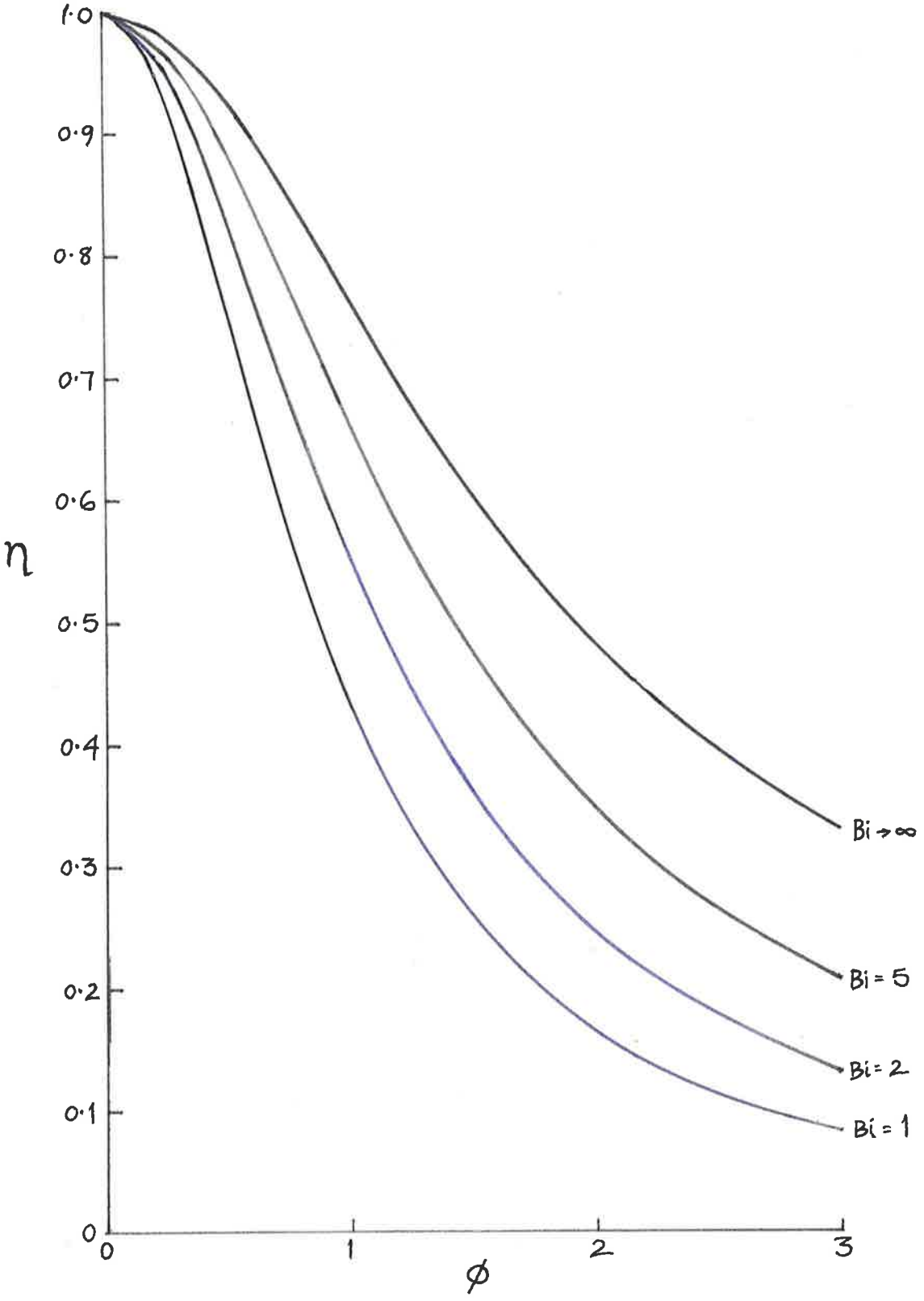

FIGURE V.4. Effectiveness factor, η, versus ϕ for various Biot numbers (Bi $\propto k_T$).

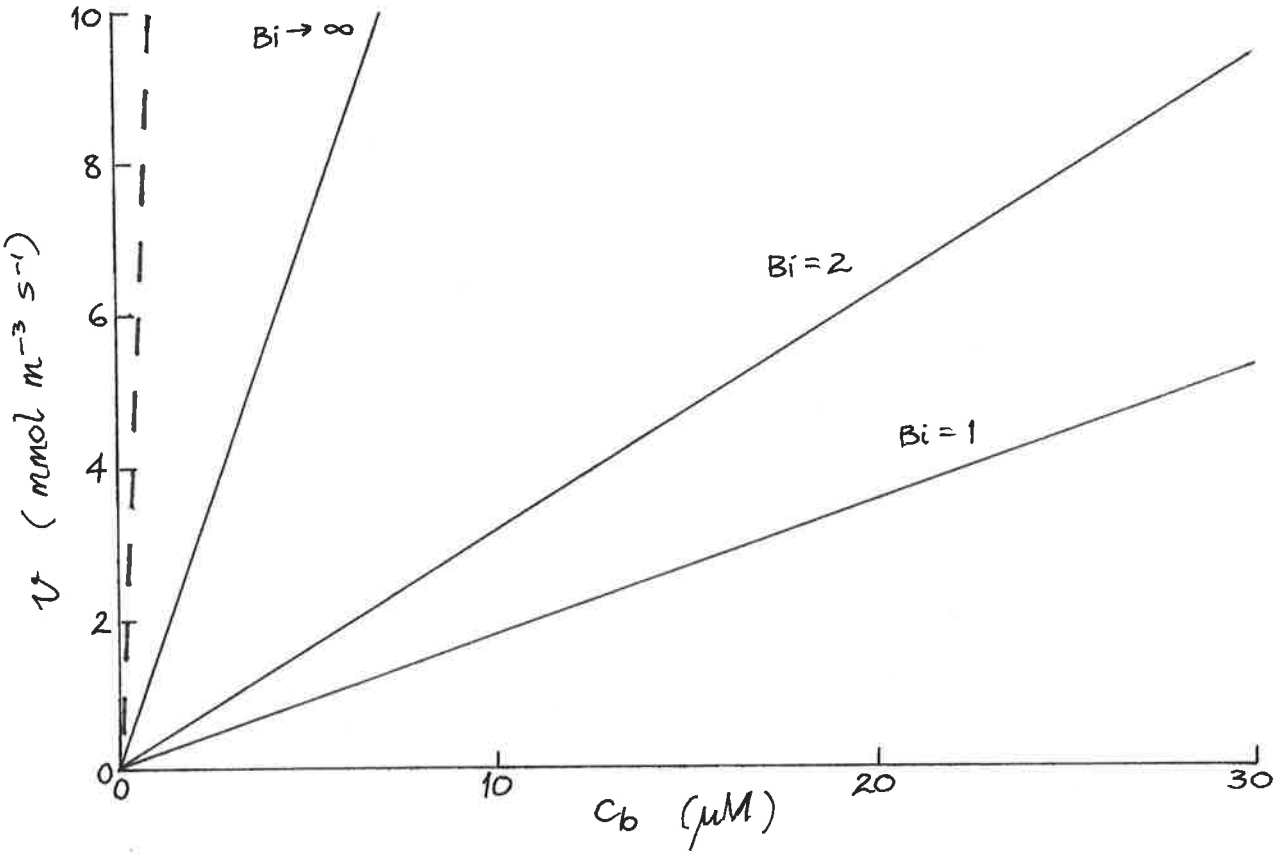

FIGURE V.5. Relationship between the reaction velocity and the bulk concentration of reactant, c_b, for a first-order reaction within a slab 100 μm thick, $D_{eff} = 5 \times 10^{-10}$ m^2 s^{-1}. The rate equation is taken to be $v = (V/K_M) \cdot c_b$, with $K_M = 1\ \mu M$ and $V = 10$ mmol m^{-3} s^{-1}; thus $\phi = 7.071$. Bi = 1 corresponds to $k_T = 1 \times 10^{-5}$ m s^{-1}; for Bi = 2, $k_T = 2 \times 10^{-5}$ m s^{-1}. The dashed line represents the kinetics in the complete absence of transport limitations (i.e. D_{eff}, $k_T \rightarrow \infty$).

The actual uptake rate, v, will be given by $v = c_b(\frac{V}{K_M})\eta$ which is equivalent to equation (V.11). Fig.V.5 shows the v versus c_b curve based on this equation, compared with the kinetics if there were (a) no external resistance and (b) if there were no resistance at all, either external or internal.

(iii) Zeroth-order kinetics

For $c >> K_M$, equation (V.3) becomes $D_{eff} \frac{d^2c}{dr^2} = V$ which has the solution (Blum and Jenden, 1957)

$$c = c_b - V \left(\frac{R}{k_T} + \frac{R^2 - r^2}{2 D_{eff}}\right) . \qquad (V.14)$$

This function is discontinuous at $c = V \left(\frac{R}{k_T} + \frac{R^2 - r^2}{2 D_{eff}}\right)$ because c cannot be negative. This is clearly seen in Fig.V.6, where concentration profiles in a slab are sketched for various values of c_b ($k_T \rightarrow \infty$). Due to the nature of the kinetics, for those regions of the tissue where $c > 0$, the local rate of reaction will be V. Overall, the reaction velocity will be $V \frac{R'}{R}$ and the influx into the slab will be $V\ 2R'$, where R' is the depth to which substrate penetrates (see Fig.V.6). There will be a critical c_b, c_b', above which R' is simply R (Fig.V.6b). c_b' occurs when the concentration of substrate in the middle of the slice just equals zero. From equation (V.14), putting $r = 0$,

$$c_{middle} = c_b - V \left(\frac{R}{k_T} + \frac{R^2}{2 D_{eff}}\right)$$

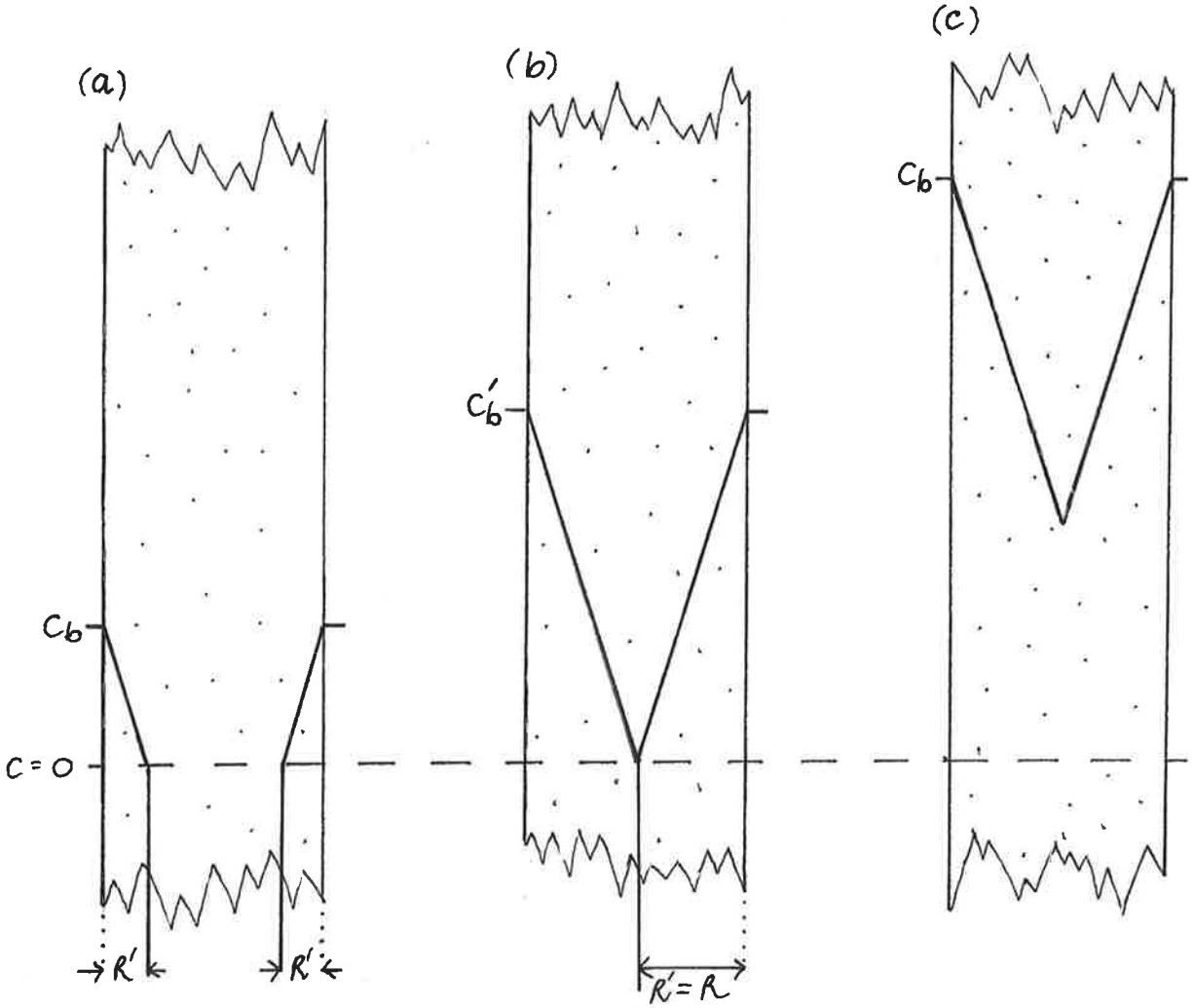

FIGURE V.6. Concentration profiles within a reacting slab (zeroth-order reaction kinetics). For low c_b, reactant only penetrates part way into the slab (a); at $c_b = c_b'$, reactant just penetrates to the middle (b); for all $c_b > c_b'$, c is everywhere greater than zero (c).

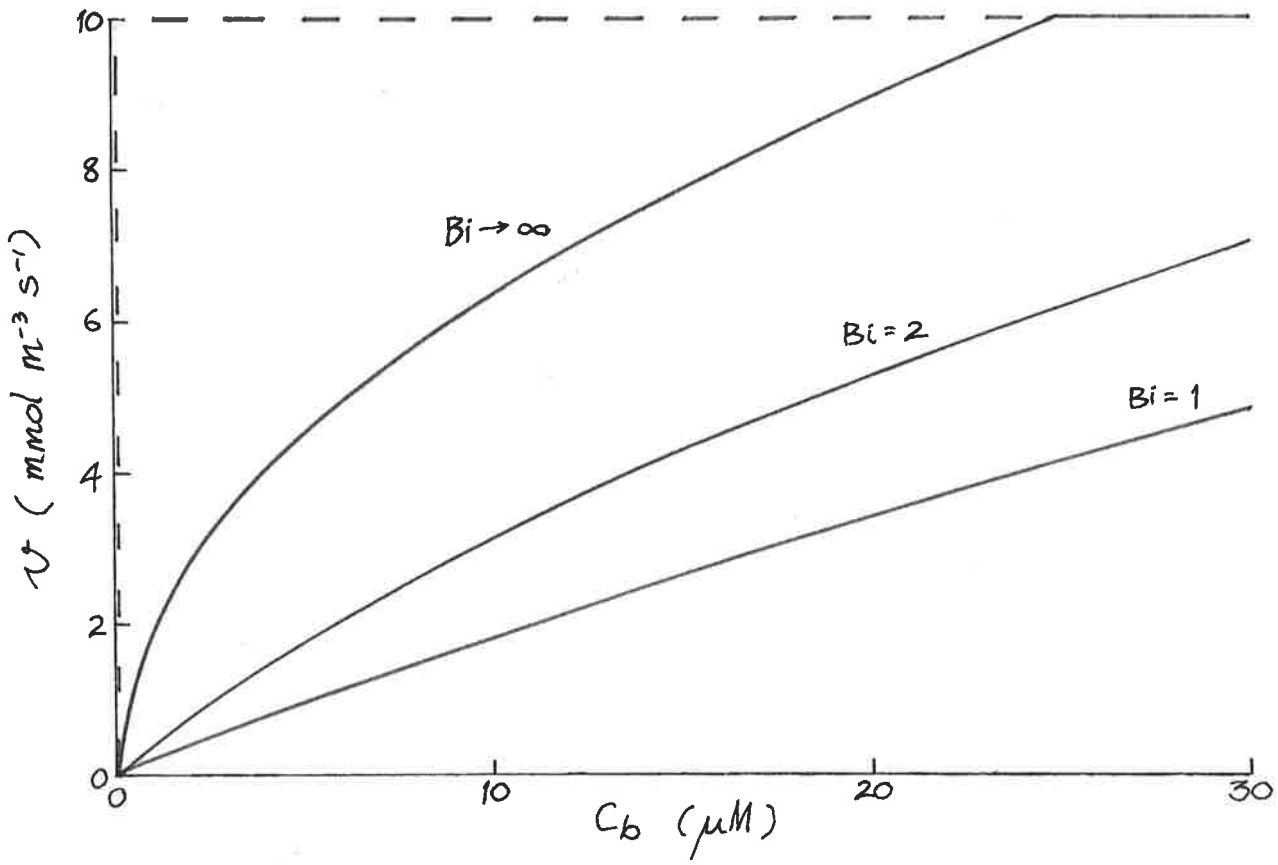

FIGURE V.7. Velocity versus concentration curves for a zeroth-order reaction within a slab 100 μm thick, $D_{eff} = 5 \times 10^{-10}$ m^2 s^{-1}. The reaction rate equation is $v = V$ $(c > 0)$ or $v = 0$ $(c = 0)$, represented by the dashed line. $V = 10$ mmol m^{-3} s^{-1}. Biot numbers of 1 and 2 correspond to k_T's of 1×10^{-5} and 2×10^{-5} m s^{-1} respectively.

therefore

$$c_b' = V \left(\frac{R}{k_T} + \frac{R^2}{2\, D_{eff}} \right) \qquad (V.15)$$

and correspondingly solving for R,

$$R' = \sqrt{\left(\frac{D_{eff}}{k_T} \right)^2 + \frac{2\, D_{eff}\, c_b}{V}} - \frac{D_{eff}}{k_T} \quad . \qquad (V.16)$$

Equation (V.16) agrees with the equation of Kidder (1970), which was based on Warburg's (1923) equations but with an additional external resistance. Fig. V.7, which can be compared to Fig. V.5, shows the uptake kinetics based on equation (V.16).*

The complete solution of the diffusion-reaction equation (equation (V.3)) will approach the solutions shown in Fig.V.5 and V.7 at low and high c_b respectively. An analytical expression for the flux over the entire range of c_b will be necessarily approximate; the accuracy

---

*In terms of Thiele moduli and effectiveness factors, with ϕ defined as $R\sqrt{V/(D_{eff} \cdot c_b)}$ and $\eta = R'/R$, then for no external mass-transfer resistance

$$\eta = \begin{cases} 1 & (\phi \leqslant \sqrt{2}) \\ \frac{\sqrt{2}}{\phi} & (\phi \geqslant \sqrt{2}) \end{cases} \qquad (V.17)$$

while with an external resistance,

$$\eta = \begin{cases} 1 & \left(\phi \leqslant \sqrt{\frac{2}{1 + 2/Bi}}\right) \\ \sqrt{\frac{1}{Bi^2} + \frac{2}{\phi^2}} - \frac{1}{Bi} & \left(\phi \geqslant \sqrt{\frac{2}{1 + 2/Bi}}\right) \end{cases} \qquad (V.18)$$

.

can be checked by comparing the approximate solution with the exact, numerically calculated one.

(iv) Approximate solutions of the equation

The Briggs-Maskell equation (p 8) holds if the reaction takes place only on the surface of the plant cell or tissue, or if mass transfer in the interior of the plant is fast due, for instance, to cytoplasmic streaming. It holds, therefore, for small values of Bi.

Where these conditions are not met, i.e. where there are significant internal mass transfer resistances, the diffusion-reaction equation is non-linear. Blum and Jenden (1957) approximated it to linearity by a Taylor series expansion. They derived the equation

$$\frac{c_b}{v} = \frac{K_M}{V - v} + \frac{R^2}{(p + 2)(p + 4)\, D_{eff}} + \frac{R}{(p + 2)\, k_T}$$

which for a plate ($p = -1$) becomes

$$\frac{c_b}{v} = \frac{K_M}{V - v} + \frac{R^2}{3\, D_{eff}} + \frac{R}{k_T} \quad . \qquad (V.19)$$

This is a quadratic in v, and solving gives

$$v = \frac{(c_b + K_M + aV - \sqrt{(c_b + K_M + aV)^2 - 4a\, c_b\, V}\,)}{2a} \qquad (V.20)$$

in which $a = \frac{R^2}{3\, D_{eff}} + \frac{R}{k_T}$. When $\frac{R}{k_T}$ is large compared

with $\frac{R^2}{3\,D_{eff}}$ (e.g. if D_{eff} were large), $a \sim \frac{R}{k_T}$ and equation (V.20) reduces to the Briggs-Maskell equation.

Murray (1968) used the mathematical technique of singular perturbation to obtain solutions to the diffusion-reaction equation. His method, however, is only valid when the dimensionless parameter $\frac{D\,c_b}{V\,R^2}$ is small (certainly less than 0.1); this is often not the case for the plants studied in this project.

Other approximations rely on empirically-derived equations, obtained by adjusting parameters until the derived equation produces values close to those obtained numerically (Atkinson and Daoud, 1968; Kobayashi, Ohmiya and Shimizu, 1976). These expressions (which are in terms of the effectiveness factor) do not consider an external mass-transfer resistance. Recently, Yamané (1981) modified the equations of Kobayashi et al. (1976) to rectify this. His equation is

$$\eta = \frac{\eta_0 + (2.6\kappa^{0.8})\eta_1}{1 + (2.6\kappa^{0.8})} \qquad (V.21)$$

where κ is the dimensionless Michaelis constant, $\frac{K_M}{c_b}$. The effectiveness factors η_0 and η_1 are those for a zeroth-order and first-order reaction, based on an "overall" Thiele modulus

$$\phi = R\sqrt{\frac{V}{D_{eff}\,(K_M + c_b)}} \quad . \qquad (V.22)$$

Using this value of ϕ, η_o is given by equation (V.18) and η_1 by equation (V.13) for a slab. The overall η is simply the arithmetic mean of these two, with the weighting factor $2.6\kappa^{0.8}$ determined empirically so as to minimize the difference between the calculated and the true effectiveness factor. This difference is generally slight (<4%); over a very limited range of ϕ ($0.4 < \phi < 0.8$) and with $0.1 < \kappa < 1$, the difference may be 6% or more at small Biot numbers (Yamané, 1981). Yamané's effectiveness factor is shown as a function of ϕ in Fig.V.8 for various values of κ, with Bi (and therefore k_T) $\rightarrow \infty$.

Fig.V.9 shows some graphs of v versus c_b based on equations (V.20) and (V.21) for various values of k_T.

For the values of K_M, V, R and D_{eff} used in Fig.V.9, Yamané's equation is in virtual agreement with the numerical result because the Thiele modulus is large, particularly at low c_b's ($\kappa \geqslant 0.1$). Blum and Jenden's equation, which is the simplest , tends to straighten the curve but still shows reasonable agreement with it; at a velocity of half V, the agreement is very close which makes the equation useful for predicting (and describing) apparent K_M's. In fact, K_M^{app} from the Blum-Jenden equation is

$$K_M^{app} = K_M + a\,\frac{V}{2} \qquad (V.23)$$

(cf. Appendix III).

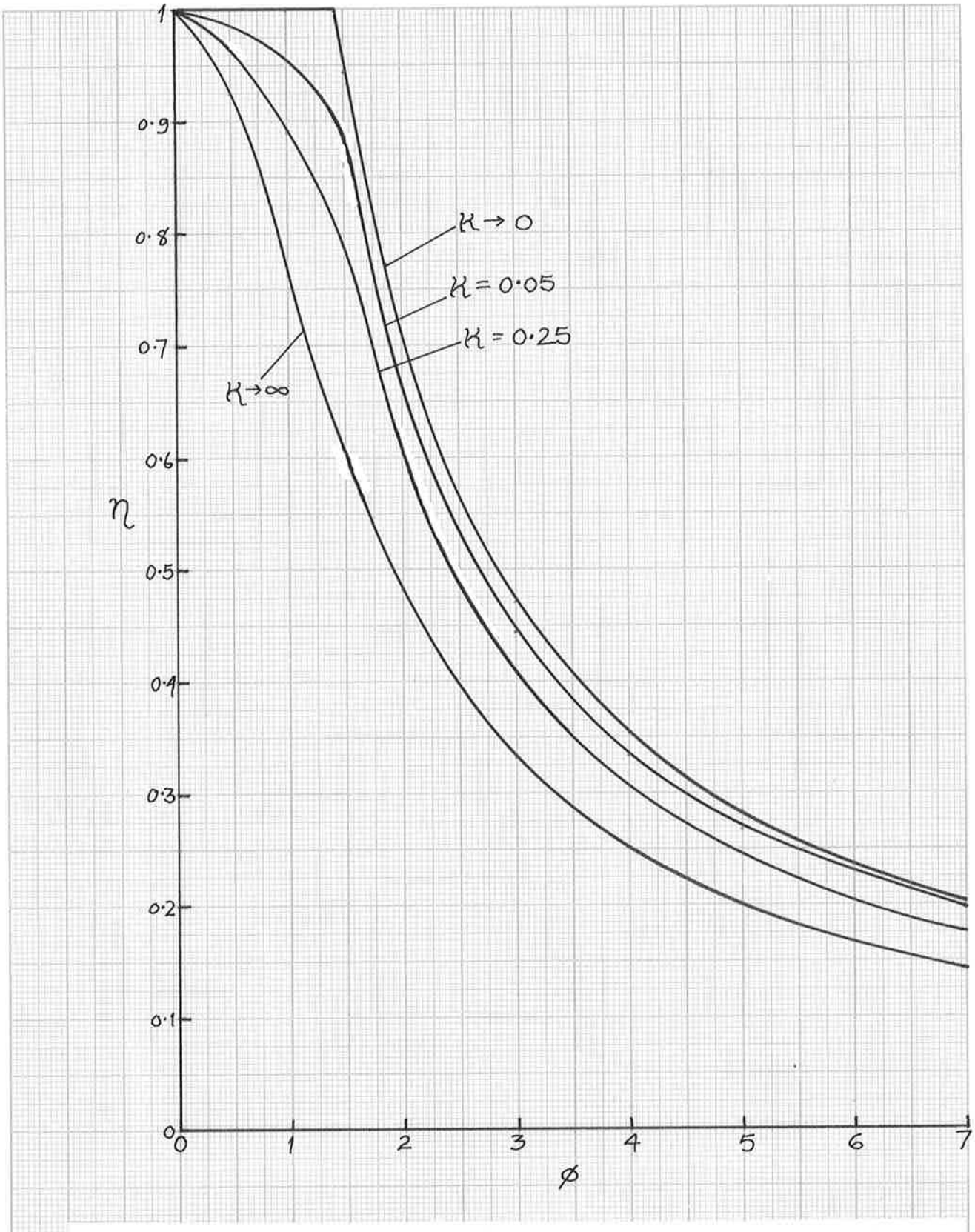

FIGURE V.8. Yamane's effectiveness factor, η, against ϕ for various values of κ (K_M/c_b) and Bi $\rightarrow \infty$.

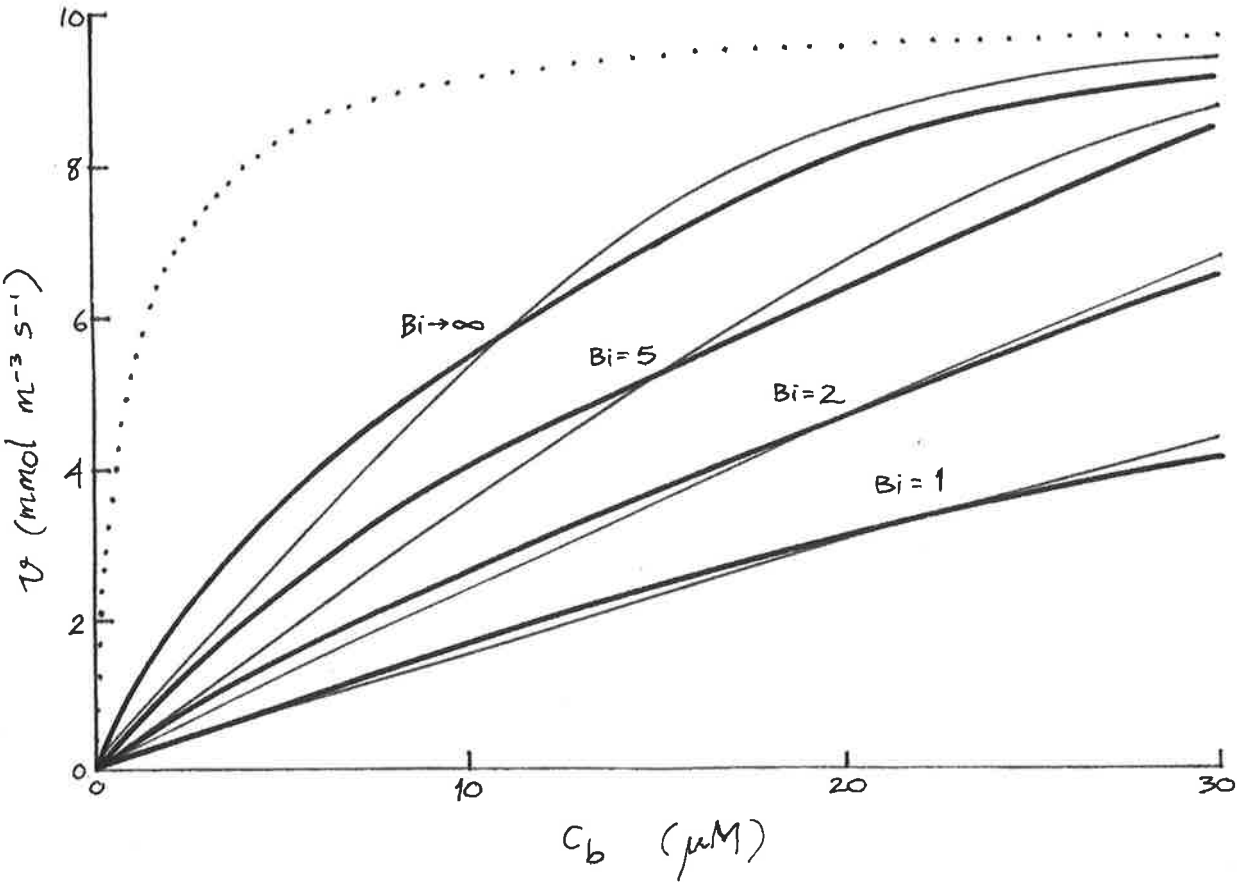

FIGURE V.9. Concentration curves for the rate of an enzyme-catalysed reaction in a slab, 100 μm thick. $D_{eff} = 5 \times 10^{-10}$ m^2 s^{-1}, $K_M = 1$ μM and $V = 10$ mmol m^{-3} s^{-1}.
Thick lines - Yamané's equation (equation V.21).
Thin lines - Blum-Jenden equation (equation V.20).
Dotted line - Michaelis-Menten equation with no transport limitations (i.e. D_{eff}, $k_T \rightarrow \infty$).

Appendix VI: List of Symbols and their Usual Units

A	surface area; m^2
A_1, A_2, A_3	parameters used in equation (32), p 77; μM^2, μM s, μM s^{-1}
B	a number; dimensionless
Bi	Biot number (=R k_T/D_{eff}); dimensionless
c	concentration; μM (μmol dm^{-3} = mmol m^{-3})
D	diffusion coefficient; m^2 s^{-1}
e	total concentration of cytochrome oxidase in mitochondrion; μM
g	acceleration due to gravity; m s^{-2}
J	flux; nmol m^{-2} s^{-1}
k	velocity constant; nmol s^{-1}
k'	rate constant; s^{-1}
$k_{+1}, k_{+2}, k_{+3}, k_{-2}$	rate constants for electron transfer reactions (p 76); M^{-1} s^{-1} or s^{-1}
K	equilibrium constant; dimensionless, M or M^2
K_M	Michaelis constant; μM
Pr	Prandtl number (= ν/D); dimensionless
R	characteristic dimension; m
t	time; s
u	local fluid velocity; m s^{-1}
U	fluid velocity in bulk medium; m s^{-1}
v	velocity in reference to an enzyme-catalyzed reaction; nmol m^{-2} s^{-1} or mol m^{-3} s^{-1}
V	maximum velocity of an enzyme-catalyzed reaction; nmol m^{-2} s^{-1} or mol m^{-3} s^{-1}
vol	volume; m^3
x	distance in x direction (e.g. along flat plate from leading edge); m
X	length of flat plate; m
X_o	length of coated section of plate (p 148); m
y	molar activity coefficient; dimensionless

Greek letters

α	density coefficient (= $\frac{1}{\rho}\frac{\partial \rho}{\partial c}$); m^3 mol^{-1}
δ	thickness of diffusion boundary layer; μm
δ_o	thickness of hydrodynamic boundary layer; μm
η	effectiveness factor; dimensionless
$\varkappa$	dimensionless Michaelis constant (= K_M/c_b)

ν	kinematic viscosity; $m^2\ s^{-1}$
ρ	density; $g\ m^{-3}$
τ	approximate time to reach steady state (Eqn 34); s
ϕ	Thiele modulus (= $R\sqrt{k'/D_{eff}}$); dimensionless
Φ	Thiele modulus based on observed reaction rate (Eqn 29); dimensionless
ω	angular velocity; s^{-1}

Subscripts

app	apparent
ave	average
b	bulk medium
C	chemical process
cut	cuticle
dbl	diffusion boundary layer
eff	effective
i	enzyme active site
lim	limiting
s	surface of reacting body
T	transport process
wall	plant outer cell wall

Superscripts

app	apparent
n,p,q, r,s,t	exponents

Overbar (e.g. $\bar{J}$) indicates a mean value

[ ] refers to concentration

( ) refers to activity

Literature Cited

ARBER, A., 1920. Water Plants (First edition). University Press, Cambridge.

ARNON, D. I., 1949. Copper enzymes in isolated chloroplasts. Polyphenoloxidase in Beta vulgaris. Plant Physiology, **24**, 1-15.

ARIS, R., 1957. On shape factors for irregular particles - I. The steady state problem. Diffusion and reaction. Chemical Engineering Science, **6**, 262-8.

____ 1975. The Mathematical Theory of Diffusion and Reaction in Permeable Catalysts. Volume I. The Theory of the Steady State. Clarendon Press, Oxford.

ATKINSON, B., and DAOUD, I. S., 1968. The analogy between microbiological 'reactions' and heterogeneous catalysis. Transactions of the Institution of Chemical Engineers, **46**, T19-T24.

BAIN, J. T., 1982. Unpublished experiments in Proctor, M. C. F., Physiological ecology : water relations, light and temperature responses, carbon balance. In Bryophyte Ecology. Ed. A.J.E. Smith. Chapman and Hall, London. P. 375.

BÄNDER, A., and KIESE, M., 1955. Die Wirkung des sauerstoffubertragenden Ferments in Mitochondrien aus Rattenlebern bei niedrigen Sauerstoffdrucken. Naunyn - Schmiedebergs Archiv für Experimentelle Pathologie und Pharmakologie, **224**, 312-21.

BARBER, D. A., 1972. 'Dual isotherms' for the absorption of ions by plant tissues. New Phytologist, **71**, 255-62.

BARRER, R. M., 1941. Diffusion in and through solids. Cambridge University Press, London.

BARRY, P. H., and DIAMOND, J. M., 1984. Effects of unstirred layers on membrane phenomena. Physiological Reviews, **64**, 763-872.

BEER, S., and ESHEL, A., 1983. Photosynthesis of Ulva sp. II. Utilization of CO_2 and HCO_3^- when submerged. Journal of Experimental Marine Biology and Ecology, **70**, 99-106.

____and WETZEL, R. G., 1981. Photosynthetic carbon metabolism in the submerged aquatic angiosperm Scirpus subterminalis. Plant Science Letters, **21**, 199-207.

BEEVERS, H., 1961. Respiratory metabolism in plants. Row, Peterson and Co., Evanston, Illanois; White Plains, New York.

BERRY, L. J., and NORRIS, W. E., 1949. Studies of onion root respiration. I. Velocity of oxygen consumption in different segments of root at different temperatures as a function of partial pressure of oxygen. Biochimica et Biophysica Acta, **3**, 593-606

BIELESKI, R. L., 1973. Phosphate pools, phosphate transport, and phosphate availability. Annual Review of Plant Physiology, **24**, 225-52.

BIRCUMSHAW, L. L., and RIDDIFORD, A. C., 1952. Transport control in heterogeneous reactions. Quarterly Reviews, **6**, 157-85.

BIRD, R. B., STEWART, W. E., and LIGHTFOOT, E. N., 1960. Transport Phenomena. Wiley, New York.

BLACK, D. R., and WEEKS, D. C., 1972. Ionic relations of Enteromorpha intestinalis. New Phytologist, **71**, 119-27.

BLAND, D. R., 1961. Solution of Laplace's equation "Library of Mathematics" Series. Ed. W. Ledermann. Routledge and Kegan Paul Ltd., London.

BLASIUS, H., 1908. Grenzschichten in Flüssigkeiten mit kleiner Reibung. Zeitschrift für Mathematik und Physik, **56**, 1-36.

BLUM, J. J., and JENDEN, D. J., 1957. Rate behavior and concentration profiles in geometrically constrained enzyme systems. Archives of Biochemistry and Biophysics, **66**, 316-32.

BRIGGS, G. E., 1959. Bicarbonate ions as a source of carbon dioxide in photosynthesis. Journal of Experimental Botany, **10**, 90-2.

____ and ROBERTSON, R. N., 1948. Diffusion and absorption in discs of plant tissue. New Phytologist, **47**, 265-83.

BRUNER, L., and ST. TOLLOCZKO, 1900. Über die Auflösungsgeschwindigkeit fester Körper. Zeitschrift für Physikalische Chemie, **35**, 283-90.

BUCH, K., 1960. Dissoziation der Kohlensaure, Gleichgewichte und Puffersysteme. In Handbuch der Pflanzenphysiologie. Vol. 5, No. 1. Ed. W. Ruhland. Springer-Verlag, Berlin. Pp. 1-11.

BUESA, R. J., 1977. Photosynthesis and respiration of some tropical marine plants. Aquatic Botany, 3, 203-16.

BUTLER, J. N., 1964. Solubility and pH calculations. Addison-Wesley Publishing Co. Inc. (Principles of Chemistry Series), Reading, Massechusetts.

CAILLÉ, J. P., and HINKE, J. A. M., 1974. The volume available to diffusion in the muscle fibre. Canadian Journal of Physiology and Pharmacology, **52**, 814-828.

CARPITA, N., SABULARSE, D., MONTEZIANOS, D., and DELMER, D. P., 1979. Determination of the pore size of cell walls of living plant cells. Science, **205**, 1144-7.

CHANCE, B., 1965. Reaction of oxygen with the respiratory chain in cells and tissues. Journal of General Physiology, **49**, 163-95.

____ and WILLIAMS, G. R., 1955. Respiratory enzymes in oxidative phosphorylation. II. Difference spectra. The Journal of Biological Chemistry, **217**, 395-407.

COCHRAN, W. G., 1934. The flow due to a rotating disk. Proceedings of the Cambridge Philosophical Society, **30**, 365-75.

COLMAN, B., 1984. The effect of temperature and oxygen on the CO_2 compensation point of the marine alga Ulva lactuca. Plant, Cell and Environment, **7**, 619-21.

CONOVER, J. T., 1968. The importance of natural diffusion gradients and transport of substances related to benthic marine plant metabolism. Botanica Marina, 11, 1-9.

CRANK, J., 1957. The mathematics of diffusion. Clarendon Press, Oxford.

CUMMINS, J. T., STRAND, J. A. and VAUGHAN, B. E., 1969. The movement of H^+ and other ions at the onset of photosynthesis in Ulva. Biochimica et Biophysica Acta, 173, 198-205.

DAINTY, J., 1963. Water relations of plant cells. In Advances in Botanical Research. Ed. R.D. Preston. Academic Press, London. Pp 276-326.

DARWIN, F., and PERTZ, D. F. M., 1896. On the effect of water currents on the assimilation of aquatic plants. Cambridge Philosophical Society Proceedings, 9, 76-90.

DENNY, P., 1980. Solute movement in submerged angiosperms. Biological Reviews, 55, 65-92.

DOTY, M. S., 1971. Physical factors in the production of tropical benthic marine algae. In Fertility of the sea, Vol.1. Ed. J.D. Costlow. Gordon and Breach Science Publishers, New York. Pp.99-121.

DROMGOOLE, F. I., 1978. The effects of oxygen on dark respiration and apparent photosynthesis of marine macro-algae. Aquatic Botany, 4, 281-97.

EDSALL, J. T., 1969. Carbon dioxide, carbonic acid, and bicarbonate ion : physical properties and kinetics of interconversion. In CO_2: Chemical Biochemical and Physiological Aspects. Eds R.E. Forster, J.T. Edsall, A.B. Otis, and F.J.W. Roughton. NASA, Washington DC. Pp 15-27.

EDWARDS, D. G., 1970. Phosphate absorption and long-distance transport in wheat seedlings. Australian Journal of Biological Sciences, **23**, 255-64.

EUCKEN, A., 1932. Die Ermittelung der absoluten grösse des Diffusionsstromes in bewegten Elektrolyten. Zeitschrift für Elektrochemie, **38**, 341-5.

EVERSON, R. G., 1970. Carbonic anhydrase and CO_2 fixation in isolated chloroplasts. Phytochemistry, **9**, 25-32.

FAGE, A., and TOWNEND, H. C. H., 1932. An examination of turbulent flow with an ultramicroscope. Proceedings of the Royal Society, Series A, **135**, 656-77.

FALCO, J. W., KERR, P. C., BARRON, M. B., and BROCKWAY, D. L., 1975. The effect of mass transport on biostimulation of algal growth. Ecological Modelling, **1**, 117-31.

FALKNER, G., HORNER, F., and SIMONIS, W., 1980. The regulation of the energy-dependent phosphate uptake by the blue-green alga Anacystis nidulans. Planta, **149**, 138-43.

____ WERDAN, K., HORNER, F., and HELDT, H. W., 1974. Energieabhängige Phosphataufnahme der Blaualge Anacystis nidulans. Berichte der Deutschen Botanischen Gesellschaft, **87**, 263-6.

FARQUHAR, G. D., 1979. Model describing the kinetics of ribulose biphosphate carboxylase-oxygenase. Archives of Biochemistry and Biophysics, **193**, 456-68.

____ and VON CAEMMERER, S., 1982. Modelling of photosynthetic response to environmental conditions. In Encyclopedia of Plant Physiology, New series, Vol. 12 B. Eds O.L. Lange, P.S. Nobel, C.B. Osmond, and H. Ziegler. Springer-Verlag, Berlin, Heidelberg. Pp 549-87.

____ ____ and BERRY, J. A., 1980. A biochemical model of photosynthetic CO_2 assimilation in leaves of C_3 species. Planta, **149**, 78-90.

FENN, W. O., 1927. The oxygen consumption of frog nerve during stimulation. Journal of General Physiology, **10**, 767-79.

FICK, A., 1855. On liquid diffusion. Philosophical Magazine (Fourth Series), **10**, 30-9.

FINDLAY, G. P., HOPE, A. B., PITMAN, M. G., SMITH, F.A., and WALKER, N. A., 1971. Ionic relations of marine algae. III. Chaetomorpha: membrane electrical properties and Cl fluxes. Australian Journal of Biological Sciences, **24**, 731-46.

FORSTER, R. E., 1969. The rate of CO_2 equilibration between red cells and plasma. In CO_2: Chemical Biochemical and Physiological Aspects. Eds R.E. Forster, J.T. Edsall, A.B. Otis, and F.J.W. Roughton. NASA, Washington DC. Pp 275-84.

FRIEDLANDER, S. K., and KELLER, K. H., 1965. Mass transfer in reacting systems near equilibrium. Use of the affinity function. Chemical Engineering Science, **20**, 121-29.

GAASTRA, P., 1959. Photosynthesis of crop plants as influenced by light, carbon dioxide, temperature and stomatal diffusion resistance. Mededelingen van de Landbouwhogeschool te Wageningen, **59**, 1-68.

GAINS, N., 1980. The determination of the kinetic parameters of a carrier mediated transport process in the presence of an unstirred water layer. Journal of Theoretical Biology, **87**, 559-68.

GARRICK, R. A., and REDWOOD, W. R., 1977. Membrane permeability of isolated lung cells to nonelectrolytes. American Journal of Physiology, **233**, C104-C110.

GEERS, C., and GROS, G., 1984. Inhibition properties and inhibition kinetics of an extracellular carbonic anhydrase in perfused skeletal muscle. Respiration Physiology, **56**, 269-87.

GERARD, R. W., 1927. Respiration in oxygen and nitrogen. American Journal of Physiology, **82**, 381-404.

____ 1931. Oxygen diffusion into cells. Biological Bulletin, **60**, 245-68.

GERARD, V. A. , 1982. In situ water motion and nutrient uptake by the giant kelp Macrocystis pyrifera. Marine Biology, **69**, 51-4.

GESSNER, F., 1938. Die Beziehung zwischen Lichtintensität und Assimilation bei submersen Wasserpflanzen. Jahrbücher für Wissenschaftliche Botanik, **86**, 491-526.

____ 1940. Die Bedeutung der Wasserbewegung für die Atmung und Assimilation der Meersalgen. Ibid. **89**, 1-12.

____ and PANNIER, F., 1958a. Der Sauerstoffverbrauch der Wasserpflanzen bei verschiedenen Sauerstoffspannungen. Hydrobiologia, **10**, 323-51.

____ ____ 1958b. Influence of oxygen tension on respiration of phytoplankton. Limnology and Oceanography, **3**, 478-80.

GRAHAM, D., 1979. Effects of light on "dark" respiration. In The Biochemistry of Plants. A Comprehensive Treatise. Volume 2. Metabolism and Respiration. Ed. D.D. Davies. Academic Press, London. Ch. 13.

____ REED, M. L., PATTERSON, B. D., and HOCKLEY, D. G., 1984. Chemical properties, distribution and physiology of plant and algal carbonic anhydrases. Annals of the New York Academy of Sciences, **429**, 222-37.

GREGORY, D. P., RIDDIFORD, A. C., 1956. Transport to the surface of a rotating disc. Journal of the Chemical Society, 3756-64.

GROS, G., and BARTAG, I., 1979. Permeability of the red cell membrane for CO_2 and O_2. Pflügers Archiv, supplement, **382**, R21.

____ MOLL, W., HOPPE, H., and GROS, H., 1976. Proton transport by phosphate diffusion - a mechanism of facilitated CO_2 transfer. Journal of General Physiology, **67**, 773-90.

GUTNECHT, J., BISSON, M. A., and TOSTESON, D. C., 1977. Diffusion of carbon dioxide across lipid bilayer membranes. Ibid. **69**, 779-94.

HALL, D. O., 1976. The coupling of photophosphorylation to electron transport in isolated chloroplasts. In The Intact Chloroplast. Ed. J. Barber. Elsevier, Amsterdam. Pp 135-70.

HANISAK M. D. and HARLIN M. M., 1978. Uptake of inorganic nitrogen by Codium fragile subsp. tomentosoides (Chlorophyta). Journal of Phycology, **14**, 450-54.

HARTMANN, L., 1967. Influence of turbulence on the activity of bacterial slimes. Journal of the Water Pollution Control Federation, **39**, 958-64.

HAXO, F. T., and CLENDENNING, K. A., 1953. Photosynthesis and phototaxis in Ulva lactuca gametes. Biological Bulletin, **105**, 103-14.

HELDER, R. J., and VAN HARMELEN, M., 1982. Carbon assimilation pattern in the submerged leaves of the aquatic angiosperm :Vallisneria spiralis. Acta Botanica Neerlandica, 31, 281-95.

HERBERG, R. J., 1965. Channels ratio method of quench correction in liquid scintillation counting. Packard Technical Bulletin no.15.

HIMMELBLAU, D. M., 1964. Diffusion of dissolved gases in liquids. Chemical Reviews, 64, 527-50.

HILL, A. V., 1929. The diffusion of oxygen and lactic acid through tissues. Proceedings of the Royal Society of London, Series B, 104, 39-96.

HILL, R., and WHITTINGHAM, C. P., 1955. Photosynthesis. Methuen & Co. Ltd., London.

HOGGE, E. A., and KRAICHMAN, M. B. 1954. The limiting current on a rotating disc electrode in potassium iodide-potassium triiodide solutions. Journal of the American Chemical Society, 76, 1431-3.

HOLDER, L. B., and HAYES, S. L., 1965. Diffusion of sulfonamides in aqueous buffers and into red cells. Molecular Pharmacology, 1, 266-79.

HOOVER, T. E., and BERKSHIRE, D. C., 1969. Effects of hydration on carbon dioxide exchange across an air-water interface. Journal of Geophysical Research, 74, 456-64.

HUNG, G. W., and DINIUS, R. H., 1972. Diffusivity of oxygen in electrolyte solutions. Journal of Chemical and Engineering Data, 17, 449-51.

HUTCHINSON, G. E., 1975. A Treatise on Limnology, Vol. III. Limnological Botany. John Wiley and Sons, New York, London and Sydney.

IBL, N., BARRADA, Y., and TRÜMPLER, G., 1954. Zur Kenntnis der natürlichen Konvektion bis der Elektrolyse: Interferometrische Untersuchungen der Diffusionsschicht I. Helvetica Chimica Acta, **37**, 583-97.

____ and MULLER, R., 1955. Optische Untersuchungen der Diffusionsschicht und der hydrodynamischen Grenzschicht an belasteten Elektroden. Zeitschrift für Eletrochemie, **59**, 671-76.

IVANOV, K. P., and LYABAKH, E. G., 1982. Change in affinity of receptor enzymes for oxygen as a factor in the physiological regulation of the oxygen supply of tissues. Doklady Biological Sciences, **267**, 632-5.

JAMES, W. O., 1928. Experimental researches on vegetable assimilation and respiration. XIX. The effect of variations of carbon dioxide supply upon the rate of assimilation of submerged water plants. Proceedings of the Royal Society, Series B, **103**, 1-42.

JENSEN, R. G., and BAHR, J. T., 1977. Ribulose 1,5 - bisphosphate carboxylase-oxygenase. Annual Review of Plant Physiology, **28**, 379-400.

JESCHKE, W. D., and SIMONIS, W., 1965. Über die Aufnahme von Phosphat und Sulfationen durch Blätter von Elodea densa und ihre Beeinflussung durch Licht, Temperatur und Aussenkonzentration. Planta, **67**, 6-32.

JOHNSON, K. S., 1982. Carbon dioxide hydration and dehydration kinetics in seawater. Limnology and Oceanography, **27**, 849-55.

JOHNSON, M. J., 1967. Aerobic microbial growth at low O_2 concentrations. Journal of Bacteriology, **94**, 101-8.

JONES, H. G., and SLATYER, R. O., 1972. Estimation of the transport and carboxylation components of the intracellular limitation to leaf photosynthesis. Plant Physiology, **50**, 283-88.

JONES, W. E., 1959. Experiments on some effects of certain environmental factors on Gracilaria verrucosa (Hudson) Papenfuss. Journal of the Marine Biological Association, U.K., **38**, 153-67.

KARAOGLANOFF, Z., 1906. Über oxydations - und Reduktionsvorgänge bei der Elektrolyse von Eisensalzlösungen II. Teil. Diffusion und Konvektion. Zeitschrift für Elektrochemie, **12**, 5-16.

KAUTSKY, L., 1982. Primary production and uptake kinetics of ammonium and phosphate by Enteromorpha compressa in an ammonium sulfate industry outlet area. Aquatic Botany, **12**, 23-40.

KAWADA, E., and KANAZAWA, T., 1982. Transient changes in the energy state of adenylates and the redox states of pyridine nucleotides in Chlorella cells induced by environmental changes. Plant and Cell Physiology, **23**, 775-83.

KELLY, B. M., 1983. Role of O_2 and mitochondrial respiration in a photosynthetic stimulation of oat protoplast acidification of a surrounding medium. Plant Physiology, 72, 356-61.

KIDDER III, G., 1970. Unstirred layers in tissue respiration: application to studies of frog gastric mucosa. American Journal of Physiology, 219, 1789-95.

KIGOSHI, K., and HASHITANI, T., 1963. The self-diffusion coefficients of carbon dioxide, hydrogen carbonate ions and carbonate ions in aqueous solutions. Bulletin of the Chemical Society of Japan, 36, 1372.

KING, C. V., 1948. The rate of dissolution of metals in aqueous reagents. Transactions of the New York Academy of Sciences, II, 10, 262-7.

____ and BRAVERMAN, M. M., 1932. The rate of solution of zinc in acids. Journal of the American Chemical Society, 54, 1744-57.

____ and CATHCART, W. H., 1937. The rate of dissolution of magnesium in acids. Ibid. 59, 63-7.

KNUDSEN, C. W., ROBERTS, G. W., and SATTERFIELD, C. N., 1966. Effect of geometry on catalyst effectiveness factor. Industrial and Engineering Chemistry, Fundamentals, 5, 325-6.

KOBAYASHI, T., OHMIYA, K., and SHIMIZU, S., 1976. Approximate expression of effectiveness factor for immobilized enzymes with Michaelis-Menten kinetics. Journal of Fermentation Technology, **54**, 260-3.

KOHN, P. G., and DAINTY, J., 1966. The measurement of permeability to water in disks of storage tissues. Journal of Experimental Botany, **17**, 809-21.

KRAICHMAN, M. B., and HOGGE, E. A., 1955. The limiting current on a rotating disc electrode in silver nitrate - potassium nitrate solutions. The diffusion coefficient of silver ion. Journal of Physical Chemistry, **59**, 986-7.

KREMER, B. P. and KÜPPERS, U., 1977. Carboxylating enzymes and pathway of photosynthetic carbon assimilation in different marine algae - evidence for the C_4 pathway? Planta, **133**, 191-6.

KROGH, A., 1919. The number and distribution of capillaries in muscles with calculations of the oxygen pressure head necessary for supplying the tissue. Journal of Physiology, 409-15.

LAING, W. A., OGREN, W. L., and HAGEMAN, R. H., 1974. Regulation of soybean net photosynthetic CO_2 fixation by the interaction of CO_2, O_2, and ribulose 1,5 - diphosphate carboxylase. Plant Physiology, **54**, 678-85.

LANCE, C. and BONNER, W. D. Jr, 1968. The respiratory chain components of higher plant mitochondria. Plant Physiology, **43**, 756-66.

LANGMUIR, I., 1918. Evaporation of small spheres. Physical Review, **12**, 368-70.

LATIES G. G., 1967. Metabolic and physiological development in plant tissues. Australian Journal of Science, **30**, 193-203.

LENDZIAN, K. J., 1982. Gas permeability of plant cuticles. Oxygen permeability. Planta, **155**, 310-5.

LEVICH, V. G., 1942. The Theory of Concentration Polarization. Acta Physicochimica U.R.S.S., **17**, 257-307.

____ 1962. Physicochemical hydrodynamics. Prentice Hall, Englewood Cliffs, New Jersey.

LITTLER, M. M., 1979. The effects of bottle volume, thallus weight, oxygen saturation levels, and water movement on apparent photosynthetic rates in marine algae. Aquatic Botany, **7**, 21-34.

LÍVANSKÝ, K., 1982. CO_2 transport in cultures of autotrophic algae. Archiv für Hydrobiologie, SUPPLEMENT, **63 (1)**, 101-9.

LOMMEN, P. W., SCHWINTZER, C. R., YOCUM, C. S., and GATES, D. M., 1971. A model describing photosynthesis in terms of gas diffusion and enzyme kinetics. Planta, **98**, 195-220.

LONERAGAN, J. F., and ASHER, C. J., 1967. Response of plants to phosphate concentration in solution culture. II. Rate of phosphate absorption and its relation to growth. Soil Science, **103**, 311-8.

LONGMUIR, I. S., 1966. Tissue Oxygen transport. In Proceedings of the Third International Conference on Hyperbaric Medicine. Eds I. E. Brown and B. G. Cox. National Academy of Sciences, National Research Council, Washington. Pp 46-51.

MACFARLANE, J. J., 1979. Uptake of Ammonia and Methylamine by Ulva. B.Sc. Honours Thesis, The University of Adelaide.

____ and SMITH, F. A., 1982. Uptake of methylamine by Ulva rigida: transport of cations and diffusion of free base. Journal of Experimental Botany, **33**, 195-207.

____ ____ 1984. Limitations of membrane transport in Ulva by unstirred layers. In Membrane Transport in Plants. Eds W.J. Cram, K. Janacek, R. Rybova, and K. Sigler. Academia, Praha, Czechoslovakia. Pp 333-4.

____ and RAVEN, J. A., 1985. External and internal CO_2 transport in Lemanea :interactions with the kinetics of ribulose bisphosphate carboxylase. Journal of Experimental Botany, **36**, 610-22.

MADSEN, T. V., 1984. Resistance to CO_2 fixation in the submerged aquatic macrophyte Callitriche stagnalis Scop. Ibid. **35**, 338-47.

____ and SØNDERGAARD, M., 1983. The effects of current velocity on the photosynthesis of Callitriche stagnalis Scop. Aquatic Botany, **15**, 187-93.

MANN, T. and KEILIN, D., 1940. Sulphanilamide as a specific inhibitor of carbonic anhydrase. Nature, **146**, 164-5.

MÄRKL, H., 1977. CO_2 transport and photosynthetic productivity of a continuous culture of algae. Biotechnology and Bioengineering, **19**, 1851-62.

MARTIN, J. T., and JUNIPER, B. E., 1970. The Cuticles of Plants. Edward Arnold Ltd., Great Britain.

MASKELL, E. J., 1928. Experimental researches on vegetable assimilation and respiration. XVII.-The relation between stomatal opening and assimilation. - A critical study of assimilation rates and porometer rates in leaves of Cherry Laurel. Proceedings of the Royal Society of London, Series B, **102**, 488-533.

MATSUMOTO, F., 1959. Studies on the effect of environmental factors on the growth of "Nori" (Porhyra tenera KJELLM.), with special reference to the water current. Journal of the Faculty of Fisheries and Animal Husbandry, Hiroshima University, 2, 249-333.

MAYNARD, J. W., and LUCAS, W. J., 1982. A reanalysis of the two-component phloem loading system in Beta vulgaris. Plant Physiology, **69**, 734-9.

McFARLANE, J. C., and BERRY, W. L., 1974. Cation penetration through isolated leaf cuticles. Plant Physiology, 53, 723-7.

McINTIRE, C. D., 1966a. Some factors affecting respiration of periphyton communities in lotic environments. Ecology, **47**, 918-30.

____ 1966b. Some effects of current velocity on periphyton communities in laboratory streams. Hydrobiologia, **27**, 559-70.

____ and PHINNEY, H. K., 1965. Laboratory studies of periphyton production and community metabolism in lotic environments. Ecological Monographs, **35**, 237-58.

MELDON, J. H., STROEVE, P., and GREGOIRE, C. E., 1982. Facilitated transport of carbon dioxide: a review. Chemical Engineering Communications, **16**, 263-300.

MILLERO, F. J., 1983. The estimation of pK^*_{HA} of acids in sea water using the Pitzer equations. Geochimica et Cosmochimica Acta, **47**, 2121-29.

MORRISET, C., 1978. Structural and cytoenzymological aspects of the mitochondria in excised roots of oxygen-deprived Lycopersicum cultivated in vitro. In Plant Life in Anaerobic Environments. Ed. D. D. Hook. Ann Arbor Science, Ann Arbor, MI. Pp 497-537.

MUELLER, J. A., BOYLE, W. C., and LIGHTFOOT, E. N., 1968. Oxygen diffusion through zoogloeal flocs. Biotechnology and Bioengineering, **X**, 331-58.

MUNK, W. H., and RILEY, G. A., 1952. Absorption of nutrients by aquatic plants. Journal of Marine Research, **11**, 215-40.

MURRAY, J. D., 1968. A simple method for obtaining approximate solutions for a class of diffusion-kinetics enzyme problems: I. General class and illustrative examples. Mathematical Biosciences, **2**, 379-411.

MYERS, J. 1944. The growth of Chlorella pyrenoidosa under various culture conditions. Plant Physiology, **19**, 576-89.

NERNST, W. 1904. Theorie der Reaktionsgeschwindigkeit in heterogenen Systemen. Zeitschrift für Physikalische Chemie, **47**, 52-5.

____ 1916. Theoretical Chemistry. 4th English Edition. MacMillan, London.

NOYES, A. A. and WHITNEY, W. R., 1897. Ueber die Auflösungsgeschwindigkeit von festen Stoffen in ihren eigenen Lösungen. Zeitschrift für Physikalische Chemie, **23**, 689-92.

OSMOND, C. B., VALAANE, N., HASLAM, S. M., UOTILA, P., and ROKSANDIC, Z., 1981. Comparisons of $\delta^{13}C$ values in leaves of aquatic macrophytes from different habitats in Britain and Finland; some implications for photosynthetic processes in aquatic plants. Oecologia, **50**, 117-24.

OWENS, M., and MARIS, P. J., 1964. Some factors affecting the respiration of some aquatic plants. Hydrobiologia, **23**, 533-43.

PARKER, H. S., 1981. Influence of relative water motion on the growth, ammonium uptake, and carbon and nitrogen composition of Ulva lactuca (Chlorophyta). Marine Biology, **63**, 309-18.

PARKHURST, D. F., 1977. A three-dimensional model for CO_2 uptake by continuously distributed mesophyll in leaves. Journal of Theoretical Biology, **67**, 471-88.

PASCIAK, W. J.,and GAVIS, J., 1974. Transport limitation of nutrient uptake in phytoplankton. Limnology and Oceanography, **19**, 881-8.

____ ____ 1975. Transport limited nutrient uptake rates in Ditylum brightwellii. Ibid.**20**, 604-17.

PETERSEN, L. P., NICHOLLS, P., and DEGN, H., 1974. The effect of energization on the apparent Michaelis-Menten constant for oxygen in mitochondrial respiration. Biochemical Journal, **142**, 247-52.

PETIT-BOIS, G., 1961. Tables of indefinite integrals. Dover.

PFEIFER, R. F., and McDIFFETT, W. F., 1975. Some factors affecting primary productivity of stream riffle communities. Archiv für Hydrobiologie, **75**, 306-17.

PITMAN, M. G., LÜTTGE, U., KRAMER, D., and BALL, E., 1974. Free space characteristics of barley leaf slices. Australian Journal of Plant Physiology, 1, 65-75.

POOLE, R. J., 1978. Energy coupling for membrane transport. Annual Review of Plant Physiology, **29**, 437-60.

PRINTZ, H., 1942. Algenphysiologische Untersuchungen. Skrifter utgitt av Det Norske Vindenskap-Akademi i Oslo, **1**, 1-35.

PYTKOWICZ, R. M., 1975. Activity cefficients of bicarbonates and carbonates in sea water. Limnology and Oceanography, **20**, 971-5.

QUINN, J. A., and OTTO, N. C., 1971. Carbon dioxide exchange at the air-sea interface: flux augmentation by chemical reaction. Journal of Geophysical Research, **76**, 1539-49.

RATCLIFF, G. A., and HOLDCROFT, J. G., 1963. Diffusivities of gases in aqueous electrolyte solutions. Transactions of the Institution of Chemical Engineers, **41**, 315-9.

RAVEN J. A., 1970. Exogenous inorganic carbon sources in plant photosynthesis. Biological Reviews, **45**, 167-221.

____ 1977. Ribulose Bisphosphate carboxylase activity in terrestrial plants : significance of O_2 and CO_2 diffusion. Current Advances in Plant Science, **9**, 579-90.

____ 1980. Nutrient transport in microalgae. Advances in Microbial Physiology, **21**, 47-226.

____ 1984. Energetics and Transport in Aquatic Plants. A.R. Liss, Inc, New York.

____ GRIFFITHS, H. and MACFARLANE, J. J., 1985. The application of carbon isotope discrimination techniques. In Physiological Ecology of Amphibious and Intertidal Plants. Eds D.H.N. Spence and R.M.M. Crawford, in press. Blackwell Scientific Publications, Oxford.

RILEY, J. P., and SKIRROW, G., 1975. Chemical Oceanography, Second Edition, Volume 2. Academic Press, London, New York.

ROBERTS, G.W., and SATTERFIELD, C.N., 1965. Effectiveness factor for porous catalysts. Langmuir-Hinshelwood kinetic expressions. Industrial and Engineering Chemistry,Fundamentals, **41**, 288-93.

ROBINSON, R. A., and STOKES, R. H., 1959. Electrolyte Solutions. Butterworths, London.

ROFF, P. A., ROUGH, G. E., CUMMINS, K. W., and COFFMAN, W. P., 1966. A method for measuring carbon fixation of attached stream algae. Journal of Phycology (supplement), **2**, 3.

ROLLER, P.S.1935. The physical and chemical relations in fluid phase heterogeneous reaction. Journal of Physical Chemistry, **39**, 221-237.

SACKUR, O., 1906. Die anodische Auflösung von Wasserstoff und seine Passivität. Zeitschrift für Physikalische Chemie, **54**, 641-64.

SARGENT, D. F., and TAYLOR, C. P. S., 1972. Terminal oxidases of Chlorella pyrenoidosa. Plant Physiology, **49**, 775-8.

SATTERFIELD, C.N. 1981. Mass Transfer in Heterogeneous Catalysts. Robert. E. Krieger Publishing Company, Huntington, New York.

SCHEFFRAHN, H., 1966. Untersuchungen zur Rolle der Follsäure im Stoffwechsel autotropher Zellen. Planta, **71**, 140-59.

SCHLICHTING, H., 1968. Boundary layer theory (Sixth Edition). McGraw Hill, New York.

SCHÖNHERR, J., 1976. Water permeability of isolated cuticular membranes : the effect of cuticular waxes on diffusion of water. Planta, **131**,159-64.

____ 1982. Resistances of plant surfaces to water loss: transport properties of cutin, suberin and associated lipids. In Encyclopedia of Plant Physiology (New Series), Volume 12B. Eds O.L.Lange, P.S. Nobel, C.B. Osmond and H. Ziegler. Springer-Verlag, Berlin. Pp 153-79.

____ and HUBER, R., 1977. Plant cuticles are polyelectrolytes with isoelectric points around 3. Plant Physiology, **59**, 145-50.

____ and SCHMIDT, H. W., 1979. Water permeability of plant cuticles. Dependence of permeability coefficients of cuticular transpiration on vapour pressure saturation deficit. Planta, **144**, 391-400.

SCHÜKAREV, A. 1891. Reaktionsgeschwindigkeiten zwischen Metallen und Haloiden. Zeitschrift für Physikalische Chemie, **8**, 76-82.

SCHULTZ, J. S., 1980. Facilitation of CO_2 through layers with a spatial distribution of carbonic anhydrase. In Biophysics and Physiology of Carbon Dioxide. Eds C. Bauer, G. Gros, and H. Bartels. Springer-Verlag, Berlin. Pp 15-22.

SCHUMACHER, G. J., and WHITFORD, L. A., 1965. Respiration and ^{32}P uptake in various species of freshwater algae as affected by current. Journal of Phycology, 1, 78-80.

SCHWOERBEL, J., and TILLMANNS, G. C., 1964. Konzentrationsabhängige Aufnahme von wasserlöslichen Phosphaten bei submersen Wasserplanzen. Naturwissenschaften, 51, 319-22.

SINGH, P., and NAIK, M. S., 1984. Effect of phtosynthesis on dark mitochondrial respiration in green cells. FEBS letters, **165**, 145-50.

SKELLAND, A.H.P. 1974. Diffusional Mass Transfer. John Wiley & Sons, New York.

SMITH, F. A., 1980. Amine transport in Elodea leaves. In Plant Membrane Transport : Current Conceptual Issues. Eds R.M. Spanswick, W.J. Lucas, and J. Dainty. Elsevier/North Holland Biomedical Press. Pp 627-8.

____ and FOX, A. L., 1975. The free space of Citrus leaf slices. Australian Journal of Plant Physiology, **2**, 441-6.

____ and WALKER, N. A., 1980. Photosynthesis by aquatic plants: effects of unstirred layers in relation to assimilation of CO_2 and HCO_3^-, and to carbon isotopic discrimination. New Phytologist, **86**, 245-59.

SOLOMOS, T., 1977. Cyanide-resistant respiration in higher plants. Annual Review of Plant Physiology, **28**, 279-97.

SPERLING, J. A., and GRUNEWALD, R., 1969. Batch culturing of thermophilic benthic algae and phosphorus uptake in a laboratory stream model. Limnology and Oceanography, **14**, 944-9.

____ and HALE, G. M., 1973. Patterns of radiocarbon uptake by a thermophilic blue-green alga under varying conditions of incubation. Limnology and Oceanography, **18**, 658-62.

STEIN, W. D., 1981. Concepts in mediated transport. In Membrane transport. Eds S.L. Bonting and J.J.H.H.M. de Pont. Elsevier/North-Holland Biomedical press, Amsterdam. Pp 123-57.

STERN, B. K., 1963. The effect of sulfonamides on ferricyanide reduction by illuminated spinach chloroplasts. Biochimica et Biophysica Acta, **71**, 727-9.

STRICKLAND, J. D. A., and PARSONS, T. R., 1965. A manual of sea-water analysis. Fisheries Research Board of Canada, Bulletin no. **125** (Second Edition). Pp 1-203.

SUNDARAM, P. V., TWEEDALE, A., and LAIDLER, K. J., 1970. Kinetic laws for solid-supported enzymes. Canadian Journal of Chemistry, **48**, 1498-1504.

SWADER, J. A., and JACOBSON, B. S., 1972. Acetazolamide inhibition of photosystem II in isolated spinach chloroplasts. Phytochemistry, 11, 65-70.

TALLING J. F.,1976. The depletion of carbon dioxide from lake water by phytoplankton. Journal of Ecology, **64**, 79-121.

TANAKA, K., and HASHITANI, T., 1971. Measurements of self-diffusion coefficients of ammonium ion in aqueous solutions. Transactions of the Faraday Society, **67**, 2314-17.

TANG, P.-S., 1933. On the rate of oxygen consumption by tissues and lower organisms as a function of oxygen tension. The Quarterly Review of Biology, **8**, 260-74.

TEPFER, M., and TAYLOR, I. E. P., 1981. The permeability of plant cell walls as measured by gel filtration chromatography. Science, 213, 761-3.

THIELE, E.W., 1939. Relation between catalytic activity and size of particle. Industrial and Engineering Chemistry, **31**, 916-20.

THIRB, H. H., and BENSON-EVANS, K., 1982. The effect of different current velocities on the red alga Lemanea in a laboratory stream. Archiv für Hydrobiologie, **96**, 65-72.

THOM, A. S., 1968. The exchange of momentum, mass and heat between an artificial leaf and the airflow in a wind-tunnel. Quarterly Journal of the Royal Meteorological Society, **94**, 44-55.

THOMSON, A. B. R., 1979a. Limitations of the Eadie-Hofstee plot to estimate kinetic parameters of intestinal transport in the presence of an unstirred water layer. Journal of Membrane Biology, **47**, 39-57.

____ 1979b. Kinetic constants for intestinal transport of four monosaccharides determined under conditions of variable effective resistance of the unstirred water layer. Ibid. **50**, 141-63.

____ and DIETSCHY, J. M., 1977. Derivation of the equations that describe the effects of unstirred water layers on the kinetic parameters of active transport in the intestine. Journal of Theoretical Biology, **64**, 277-94.

TOLBERT, N. E., 1980. Photorespiration. In The Biochemistry of Plants; A Comprehensive Treatise. Vol 2. Metabolism and Respiration. Ed D. D. Davies. Academic Press, New York. Pp 487-523.

TRÜMPLER, G., and ZELLER, H., 1951. Zur Strömungsabhängigkeit von Grenzströmen. Helvetica Chimica Acta, **34**, 952-8.

TYREE, M. T., 1968. Determination of transport constants of isolated Nitella cell walls. Canadian Journal of Botany, **46**, 317-27.

VAN LOOKEREN CAMPAGNE, R. N., 1955. On the influence of carbon dioxide and bicarbonate on the photosynthesis in Vallisneria spiralis. Proceedings of the Koninklijke Nederlandse Akademie Van Wentenschappen, Series C, **58**, 548-53.

VETTER, K.J., 1967. Electrochemical Kinetics. Academic Press, New York.

VIELSTICH, W., 1953. Der Zusammenhang zwischen Nernstscher Diffusionschicht und Prandtlscher Strömungsgrenzschicht. Zeitschrift für Elektrochemie, **57** 646-55.

WAGNER, C., 1943. Über das Zussammenwirken von Strömung, Diffusion und chemischer Reaktion bei der heterogenen Katalyse. Zeitschrift für Physikalische Chemie, **193**, 1-15.

WALKER, N. A., and PITMAN, M. G., 1976.Measurement of fluxes across membranes. In Encyclopedia of Plant Physiology (New Series) Volume 2A. Eds U. Lüttge and M.G. Pitman. Springer-Verlag, Berlin. Pp 93-126.

____ SMITH, F. A., and CATHERS, I. R., 1980. Bicarbonate assimilation by freshwater charophytes and higher plants: I. Membranes transport of bicarbonate ions is not proven. Journal of Membrane Biology, **57**, 51-8.

WALLENTINUS, I., 1984. Comparisons of nutrient uptake rates for Baltic macroalgae with different thallus morphologies. Marine Biology, **80**, 215-25.

WANG, J. H., ANFINSEN, C. B. and POLESTRA, F. M., 1954. The self-diffusion coefficient of water and ovalbumin in aqueous ovalbumin solutions at 10°C. Journal of the American Chemical Society, **76**, 4763-5.

WARBURG, O., 1923. Versuche an überlebendem Carcinomgewebe. Biochemische Zeitschrift, **142**, 317-33.

WEBER, J. A., TENHUNEN, J. D., YOCUM, D. S., and GATES, D. M., 1979. Variation of photosynthesis in Elodea densa with pH and/or high CO_2 concentrations. Photosynthetica, **13**, 454-8.

WEISZ, P.B., 1973. Diffusion and chemical transformation - an interdisciplinary excursion. Science, **179**, 433-40.

—— and HICKS, J.S., 1962. The behaviour of porous catalyst particles in view of internal mass and heat diffusion effects. Chemical Engineering Science, **17**, 265-275.

WERNER, I., and WEISE, G., 1982. Biomass production of submerged macrophytes in a selected stretch of the River Zschopan (South GDR) with special regard to orthophosphate incorporation. Internationale Revue gesamten Hydrobiologie, **67**, 45-62.

WEST, K. R., and PITMAN, M. G., 1967. Ionic relations and ultrastructure in Ulva lactuca. Australian Journal of Biological Sciences, **20**, 901-14.

WESTLAKE, D. F., 1967. Some effects of low-velocity currents on the metabolism of aquatic macrophytes. Journal of Experimental Botany, **18**, 187-205.

WHEELER, W.N., 1980. Effect of boundary layer transport on the fixation of carbon by the giant kelp Macrocystis pyrifera. Marine Biology, **56**, 103-110.

WHITFIELD, M., 1975. Extension of chemical models for sea water to include trace components at 25°C and 1 atm. pressure. Geochimica et Cosmochimica Acta, **39**, 1545-57.

WHITFORD, L. A., and SCHUMACHER, G. J., 1961. Effect of current on mineral uptake and respiration by a fresh-water alga. Limnology and Oceanography, **6**, 423-5.

____ ____ 1964. Effect of a current on respiration and mineral uptake in Spirogyra and Oedogonium. Ecology, **45**, 168-70.

WILSON, F.A., and DIETSCHY, J.M.,1974. The intestinal unstirred layer: its surface area and effect on active transport kinetics. Biochimica et Biophysica Acta, 363, 112-126.

WINNE, D., 1973. Unstirred layer, source of biased Michaelis constant in membrane transport. Ibid. **298**, 27-31.

WITTWER, S. H., amd TEUBNER, F. G., 1959. Foliar absorption of mineral nutrients. Annual Review of Plant Physiology, **10**, 13-32.

YAMADA, Y., WITTWER, S. H., and BUKOVAC, M. J., 1964. Penetration of ions through isolated cuticles. Plant Physiology, **39**, 28-32.

____ ____ ____ 1965. Penetration of organic compounds through isolated cuticular membranes with special reference to C^{14} urea. Ibid. **40**, 170-5.

YAMANÉ, T., 1981. On approximate expressions of effectiveness factors for immobilized biocatalysts. Journal of Fermentation Technology, 59, 375-381.

YOCUM, C. S., and HACKETT, D. P., 1957. Participation of cytochromes in the respiration of the aroid spadix. Plant Physiology, **32**, 186-91.

MacFarlane, J.J., and Smith, F.A., (1982) Uptake of methylamine by *ulva rigida*: transport of cations and diffusion of free base.
Journal of Experimental Botany, v. 33 (2), pp. 195-207.

NOTE:
This publication is included in the print copy of the thesis held in the University of Adelaide Library.

It is also available online to authorised users at:

http://dx.doi.org/10.1093/jxb/33.2.195